Cell-free synthesis and characterisation of catecholamine and Endothelin receptors:

A case study to obtain G-protein coupled receptors in defined lipid bilayers for functional and structural analysis

Dissertation
zur Erlangung des Doktorgrades
der Naturwissenschaften

vorgelegt beim Fachbereich
Biochemie, Chemie und Pharmazie (FB 14)
der Goethe-Universität
in Frankfurt am Main

von
Ralf-Bernhardt Rues
aus Cuxhaven

Frankfurt am Main 2017
(D30)

Vom Fachbereich Biochemie, Chemie und Pharmazie (FB14)
der Goethe-Universität als Dissertation angenommen.

Dekan:	Prof. Dr. Clemens Glaubitz
Gutachter:	Prof. Dr. Volker Dötsch PD Dr. Rupert Abele

Datum der Disputation:

„Il faut imaginer Sisyphe heureux.”

Albert Camus

Eidesstattliche Erklärung

Ich erkläre hiermit an Eides statt, dass ich die vorgelegte Dissertation mit dem Titel „Cell-free synthesis and characterisation of catecholamine and Endothelin receptors: A case study to obtain G-protein coupled receptors in defined lipid bilayers for functional and structural analysis“ selbständig angefertigt und mich anderer Hilfsmittel als der in ihr angegebenen nicht bedient habe. Ich erkläre weiterhin, dass Entlehnungen aus Schriften, soweit sie in der Dissertation nicht ausdrücklich als solche bezeichnet sind, nicht stattgefunden haben. Ich habe bisher an keiner anderen Universität ein Gesuch um Zulassung zur Promotion eingereicht oder die vorliegende oder eine andere Arbeit als Dissertation vorgelegt.

Frankfurt am Main, den 18.12.2017

_____

Ralf-Bernhardt Rues

Table of contents

List of figures

List of tables

Units and abbreviations

°C	Degree celsius
AcP	Acetylphosphate
AR	Adrenergic receptor
AsoPC	L-α–phosphocholine
CE	Continuous exchange
CF	Cell-free
CHS	Cholesterylhemisuccinate
Da	Dalton
DE(lipid)	1,2-dielaidoyl-sn-glycero-
DDM	n-dodecyl-β-D-maltoside
DH_7PC	1,2-diheptanoyl-sn-glycero-3-phosphocholine
DM (lipid)	1,2-dimyristoyl-sn-glycero-
DO (lipid)	1,2-dioleoyl-sn-glycero-
DP (lipid)	1,2-dipalmitoyl-sn-glycero-
DTT	Dithiotreitol
ECL	Extracellular loop
E. coli	Escherichia coli
EDTA	Ethylenediaminetetraacetic acid
ET-1	Endothelin-1
ETA	Endothelin receptor type A
ETB	Endothelin receptor type B
Fig.	Figure
FM	Feeding mixture
Fos-16	N-hexadecylphosphocholine
Fos-12	N-dodecylphosphocholine
g	Gram
GPCR	G-protein coupled receptor
GSH	Reduced glutathione
GSSG	Oxidised glutathione
h	Hour
HEPES	4-(2-hydroxyethyl)-1-piperazineethanesulfonic acid
HRP	Horse radish peroxidase
ICL	Intracellular loop
IMAC	Immobilized metal ion affinity chromatography
K_D	Dissociation constante
l	Liter
LAC	Ligand affinity chromatography
LM	Myristoyl-2-hydroxy-sn-glycero-3-

LP	Liposome
m	Meter
M	Molar
min	Minute
MP	Membrane protein
MSP	Membrane scaffold protein
MWCO	Molecular weight cut off
ND	Nanodisc
OD	Optical density
PCR	polymerase chain reaction
PEP	Phosphoenolpyruvate
PA	Phosphatic acid
PE	Phosphoethanolamine
PC	Phosphocholine
PG	Phospho-(1'-rac-glycerol)
PO (lipid)	1-palmitoyl-2-oleoyl-sn-glycero-
PS	Phospho-L-serine
rHDL	Reconstituted high density lipoprotein
RM	Reaction mixture
rpm	Rounds per minute
s	Second
SD	Standard deviation
SDS	Sodium-dodecyl-sulfate
SEC	Size exclusion chromatography
Sf	Spodoptera frugiperda
sfGFP	Superfolder green fluorescent protein
SMALP	Styrene maleic acid lipid particles
SO (lipid)	1-stearoyl-2-oleoyl-sn-glycero-
T7RNAP	T7-RNA polymerase
Tab.	Table
TCEP	Tris(2-carboxyethyl)phosphine
T_M	Melting temperature
Tni	Trichoplusia ni
TRIS	(Tris(hydroxymethyl)aminomethane
ts	Thermostabilised
x g	Times gravity

Summary

G-protein coupled receptors (GPCRs) are a predominant class of cell-surface receptors in eukaryotic life. They are responsible for the perception of a broad range of ligands and involved in a multitude of physiological functions. GPCRs are therefore of crucial interest for biological and pharmaceutical research. Molecular analysis and functional characterisation of GPCRs is frequently hampered by challenges in efficient large-scale production, non-destructive purification and long-term stability of these highly dynamic membrane proteins.

Cell-free protein synthesis (CFPS) provides new production platforms for GPCRs by extracting the protein synthesis machinery of the cell in an open system that allows target-oriented modulations of the synthesis process and direct access to the nascent polypeptide chain. CFPS is fast, reliable and highly adaptable. Unfortunately, highly productive cell-free synthesis of GPCRs is often opposed by low product quality. This thesis was aimed to adapt and improve some of the new possibilities for the cell-free production of GPCRs in high yield and quality for structural and pharmaceutical analysis.

An *E. coli* based CFPS system was applied to synthesise various turkey and human β-adrenergic receptor (β1AR) derivatives as well as human Endothelin receptors type A and B (ETA and ETB) constructs. βARs are mediating the cardiovascular functions of the symphatic nervous system. The Endothelin system is responsible for the strongest vasoconstriction effects found so far in humans and other mammals. Both receptor families are important drug targets and pharmacologically addressed in the treatment of several cardiovascular diseases.

CF-synthesis was mainly performed in presence of nanodiscs (ND), which are reconstituted high density lipoprotein particles forming discoidal bilayer patches with a diameter varyring from 6 to approx. 15 nm. The supplementation of ND in the CF-synthesis reaction caused the co-translational solubilisation of the freshly synthesised GPCRs. The fraction of the solubilised GPCR that was correctly folded was analysed by the competence to bind its ligand alprenolol or Endothelin-1, respectively. Both the solubilisation efficiency and the ability to fold in a ligand binding competent state was strongly affected by the lipid composition of the supplied ND. Best results were generally achieved with lipids having phosphoglycerol headgroups and unsaturated fatty acid chains with 18 carbon atoms. Furthermore, thermostabilisation by introduction of point mutations had a large positive impact on the folding efficiency of both β1AR and ETB receptor. Formation of a conserved disulphide bridge in the extracellular region was additionally found to be crucial for the function of the ETB receptor. Disulphide bridge formation could be enhanced by applying a glutathione-based redox system in the CFPS. Further improvements in the quality of ETB receptor could be made by the enrichment of heat-shock chaperones in the CF-reaction.

Depending on the receptor type and DNA-template, roughly 10 – 30 nmol (350 – 1500 µg) of protein could be synthesised in 1 ml of CF-reaction mixture. After the applied optimisation steps, the fractions of correctly folded receptor could be improved by several orders of magnitude and were finally in between 35% for the thermostabilised turkey β1AR, 9% for the thermostabilised ETB receptor, 6.5% for the non-stabilised ETB receptor, 1 - 5% for non-stabilised turkey β1AR and for human β1AR isoforms and 0.1% for ETA receptor. Therefore, between 2 and 120 µg of GPCR could be synthesised in a ligand binding competent form, depending on the receptor and its modifications. Correctly folded

turkey β1AR and ETB receptors were thermostable at 30°C and could be stored at 4°C for several weeks after purification.

Yields of the thermostabilised turkey β1AR were sufficient to purify the receptor in a two-step process by ligand-binding chromatography to obtain pure and correctly folded receptor in the lipid bilayer of a ND. Furthermore, a lipid dependent ligand screen could be demonstrated with the turkey β1AR and significant alterations in binding affinities to currently in-use pharmaceuticals were found. The established protocols are therefore suitable and highly competetive for a variety of applications such as screening of GPCR ligands, analysis of lipid effects on GPCR function or for the systematical biochemical characterisation of GPCRs.

There is still a high optimisation potential to further improve the folding of cell-free synthesised GPCRs, as for all targets the majority of the synthesised protein remains non-functional in ligand binding. Most promising for future approaches appreas to address the suspected bottlenecks of intial insertion of the GPCR-polypeptide chain in the ND bilayer and the thermal stability of the receptors. Nevertheless, the estabilised protocols for the analysed targets in this thesis are already highly competitive to previously published production protocols either in cell-based or cell-free systems with regard to yield of functional protein, speediness and costs. Moreover, the direct accessibility and other general characteristics of cell-free synthesis open a large variety of possible applications and this work can therefore contribute to the molecular characterisation of this important receptor type and to the development of new pharmaceuticals.

Zusammenfassung

Mit mehr als 800 kodierten Genen stellen G-protein gekoppelte Rezeptoren (*G-protein coupled receptors* - GPCRs) die drittgrößte Genfamilie im menschlichen Genom. Sie sind eine Hauptklasse von Zell-Oberflächenrezeptoren und von enormer physiologischer Bedeutung (Fredriksson et al. 2003). GPCRs vermitteln die Perzeption einer großen Vielzahl natürlicher Liganden und ihre physiologischen Funktionen umfassen neuronale Signalwege, die neuroendokrine Kontrolle der physiologischen Homöostase, Regulation des Blutflusses und von Stoffwechselwegen sowie Zellwachstum, -Proliferation, Differentiation und Apoptose (Luttrell 2008). Prinzipielle Gemeinsamkeiten aller GPCRs ist ihr Aufbau in sieben membranständige Bereiche und die G-protein-gekoppelte Signaltransduktion. Allerdings konnte letztere bisher nicht für alle GPCRs belegt werden und einige Rezeptorklassen, die zur GPCR-Superfamilie gezählt werden, sprechen im Allgemeinen andere Signalwege an (Fredriksson et al. 2003).

Aufgrund ihres ubiquitären Vorkommens und ihrer physiologischen Bedeutung haben sich GPCRs zu Hauptadressaten der konservativen Medizin entwickelt und etwa 34% aller aktuell von der US Food and Drug Administration (FDA) zugelassen Medikamente wirken direkt auf GPCRs (Hauser et al. 2017). Sie stehen somit im Fokus biomedizinischer Forschung. Ihre molekulare Analyse und funktionelle Charakterisierung wird jedoch häufig beeinträchtig durch die geringe Stabilität von GPCRs, welche Probleme in ihrer Überexpression und Aufreinigung in Detergenzien verursacht (Milić and Veprintsev 2015).

Die zell-freie Proteinsynthese (*Cell-free protein synthesis* - CFPS) bietet neue Möglichkeiten zur Herstellung und zum Zugang zu GPCRs, da sie die molekulare Proteinsynthesemaschinerie der Zelle extrahiert und in eine offene, leicht zugängliche Umgebung einbettet. Dies erlaubt zielgerichtete Modifikationen des Transkriptions- und Translationsprozess und bietet direkten Zugang zur frisch-synthetisierten Polypeptidkette. Durch die Zugabe von Detergenzien, hydrophoben Substanzen oder künstlichen Lipidmembranen können die CF-synthetisierten GPCRs kotranslational in einer definierten hydrophoben Umgebung solubilisiert werden. Die CFPS ist schnell, robust und vielfältig adaptierbar und ermöglicht hohe Syntheseraten. Leider stehen dem häufig nur geringe Raten an korrekt gefaltetem Rezeptor entgegen, was die Anwendbarkeit dieser Systeme bisher einschränkt.

Ziel dieser Arbeit war die Weiterentwicklung von Wegen zur Synthese von funktionell aktiven GPCRs in einem *Escherichia coli (E. coli)* basierten CFPS-System. Zur Herstellung des CFPS-Systems wurden *E. coli* Zellen mechanisch aufgeschlossen und störende Proteine im Zytosol durch Präzipitation nach Salz- und Hitzeeinwirkung grob entfernt. Niedermolekulare Bestandteile wurden durch Dialyse abgetrennt. Der Zellextrakt wurde mit für die CFPS notwendigen Bestandteilen angereichert: Nukleotidtriphosphate (NTPs), Aminosäuren und Folinsäure sowie tRNAs und RNA-Polymerase für die Translation und Transkription und die Energiebereitstellung, einem auf Phosphoenolpyruvat und Acetylphosphat beruhendes Regenerationssystem für die NTPs, Konservierungsstoffe um das Wachstum von Mikroorganismen auszuschließen, Proteaseinhibitoren um den Proteinabbau zu verhindern und Puffer, reduzierende Agenzien sowie Polyethylenglykol mit einer durchschnittlichen Molmasse von 8 kDa um die natürliche Zellzusammensetzung zu simulieren (Schwarz et al. 2007). Die Proteinsynthese wurde durch Zugabe einer DNA-Matrize eingeleitet, in der das zu synthetisierende

GPCR-Konstrukt unter Kontrolle eines T7-Promotors kodiert war. Zur Erhöhung der Syntheserate wurde ein partitioniertes CPFS-System eingesetzt, in dem der Reaktionsmix (RM) durch eine Dialysemembran mit einem größeren Reservoir an niedermolekularen Bestandteilen verbunden war (*feeding mixture* - FM). Hierdurch wurden toxische Nebenprodukte verdünnt und weitere Ressourcen zur Energieregeneration und Proteinsynthese bereitgestellt. Da es sich bei GPCRs um Membranproteine handelt, ist eine lösliche Synthese nur durch Zugabe von hydrophoben Substanzen erreichbar, andernfalls präzipitiert die synthetisierte Polypeptidkette im RM (Schwarz et al. 2007). Zur Solubilisierung wurden vor allem Nanodiscs (ND) eingesetzt. Dies sind rekonstituierte *high density lipoprotein* (rHDL) Partikel welche eine Lipiddoppelschicht mit diskoidaler Form und einem Durchmesser von etwa 6-15 nm ausbilden (Bibow et al. 2017). Die Zugabe der ND zur CFPS ermöglichte die kotranslationale Solubilisierung der gebildeten GPCRs. Von der Gesamtmenge an synthetisiertem und solubilisiertem Rezeptor wurde die Fraktion mit korrekter Faltung anhand von Ligandbindungseperimenten bestimmt.

Verschiedene Rezeptortypen wurden in der vorliegenden Arbeit verwendet. Der Katecholamin bindende Adrenozeptor des Typs β1 (β1AR) in verschiedenen Modifikationen vom Truthahn und vom Menschen sowie die Rezeptoren Typ A und Typ B des humanen Endothelin-Systems (ETA und ETB). Adrenozeptoren vermitteln unter anderem die kardiovaskulären Funktionen des sympathischen Nervensystems, während das Endothelin-System starke vasokontraktive Effekte vermittelt. Beide Rezeptorfamilien sind wichtige Medikamentenziele und werden für die Behandlung verschiedener kardiovaskulärer Erkrankungen pharmakologisch adressiert. Insbesondere der humane β1AR konnte bisher mit konventionellen zell-basierten Produktionssystem aufgrund seiner hohen Empfindlichkeit gegenüber Detergenzien nicht rekombinant hergestellt und aufgreinigt werden.

Je nach DNA-Matrize und synthetisiertem GPCR-Konstrukt konnten Gesamtsyntheseraten von etwa 10 - 30 nmol pro ml RM erreicht werden. Je nach Molmasse entspricht dies etwa 350 - 1500 µg. Die Faltungseffizienzen unterschieden sich jedoch beträchtlich. Die größten Anteile an korrekt gefaltetem GPCR konnten mit einer Variante des β1AR aus dem Truthahn erreicht werden, welche durch Insertion von 11 Punktmutationen thermisch stabilisiert war. Hier konnten Faltungseffizienzen von etwa 35 - 50% gemessen werden. Die Gesamtsyntheserate lag hier bei etwa 350 µg pro ml RM, entsprechend also ~120 µg an korrekt gefaltetem Rezeptor. Interessanterweise waren sowohl die Löslichkeit des GPCRs wie auch dessen Faltungseffizienz stark abhängig von der Lipidzusammensetzung der verwendeten ND. Es wurden Lipide mit unterschiedlicher Kopfgruppe und Fettsäurekettenzusammensetzung getestet und die höchsten Solubilisierungsraten wurden mit Phosphoglycerolkopfgruppen (PG) erreicht. Phosphoserin (PS) und Phosphocholinkopfgruppen (PC) bewirken ebenfalls hohe Solubilisierungsraten des β1AR, während Phosphoethanolamin (PE) und Phosphatsäurekopfgruppen (PA) nur geringe Effizienzen aufwiesen. Die Faltungseffizienz war sowohl abhängig von der Kopfgruppenart als auch vom Aufbau der Fettsäureseitenketten der verwendeten Lipide. Dabei war, wie auch bei Solubilisierung, ein deutlicher Trend zu PG-Kopfgruppen erkennbar. Desweiteren waren längerkettige, ungesättigte Fettsäuren mit etwa 18 Kohlenstoffatomen scheinbar am besten zur Faltung des thermostabilisierten β1AR geeignet, während mit kürzerkettigen Lipiden mit PC Kopfgruppen nur etwa ein 12-tel der Faltungseffizienz erreicht werden konnte.

In einem weiteren Schritt wurden die Versuche auf eine nicht-thermostabilisierte Variante des Truthahn-β1AR sowie thermostabilisierte und nicht-stabilisierte Varianten des humanen β1AR ausgedehnt. Hierbei wurden ND mit anscheinend optimaler Lipidzusammensetzung verwendet. Es konnten Faltungseffizienzen von etwa 1 - 5% gemessen werden, wobei die thermostabilisierte Varianten in allen Fällen höhere Faltungseffizienzen zeigten. Die Gesamtsyntheseraten waren dabei vergleichbar mit denen des thermostabilisierten β1AR aus dem Truthahn. Insgesamt konnten pro ml RM etwa 4 µg vom nicht-stabilisierten Truthahn-β1AR, 15 - 30 µg vom thermostabilisierten humanen β1AR und etwa 2 µg vom nicht-stabilisierten humanen β1AR in ligandenbindungsfähiger Form synthetisiert werden. Die Fraktionen an korrekt gefaltetem Rezeptor zeigten dabei in allen Fällen eine hohe Affinität zum Liganden mit Dissoziationskonstanten im niedrigen nanomolaren Bereich und Werten die weitestgehend den Literaturangaben entsprachen.

In einem nächsten Schritt wurden die Versuche auf die Endothelin Rezeptoren ETA und ETB ausgedehnt. Diese wurden schon in vorherigen Studien dieses Arbeitskreises zell-frei exprimiert und charakterisiert (Junge et al. 2010, Proverbio et al. 2013). Dabei konnte unter Zugabe von ND in die CF-Reaktion in beiden Fällen ligandenbindungsaktiver Rezeptor hergestellt werden. Allerdings lag die Rate an funktionell gefaltetem ETB Rezeptor bei deutlich unter einem Prozent und war sogar noch geringer für den ETA Rezeptor, bei dem auch nur geringe Solubilierungseffizienzen auftraten. In diesen Versuchen wurde allerdings nur ein PC-Kopfgruppenlipid mit kurzkettigen und gesättigten Fettsäuren (14 Kohlenstoffatome) verwendet. In der vorliegenden Arbeit wurden, analog und aufbauend auf den Ansätzen mit dem β1AR, ND mit verschiedener Lipidzusammensetzung getestet. Für den ETB Rezeptor konnte auch hier eine deutliche Lipidabhängigkeit in der Faltungseffizienz gezeigt werden. Höchste Faltungserfolge wurden hier ebenfalls mit PG-Kopfgruppenlipiden mit längerkettigen, ungesättigten Fettsäuren erreicht, wobei die Faltungseffizienz nochmals deutlich gesteigert werden konnte, wenn die Doppelbindung der Fettsäurekette in einer irregulären Transanordnung vorlag. Hier konnten Faltungseffizienzen bis 3.5% gemessen werden. Die Gesamtmenge an solubilisiertem ETB Rezeptor lag im Schnitt bei etwa 20 nmol (1700 µg) pro ml RM und ca. 0.76 nmol (60 µg) an korrekt gefaltetem ETB Rezeptor konnte mit optimaler Lipidzusammensetzung der ND erreicht werden. Der korrekt gefaltete Rezeptor zeigte dabei eine hohe Affinität zu seinem Liganden im pikomolaren Bereich und die Werte entsprachen weitgehend den allgemeinen Literaturangaben.

Aufgrund der relativ geringen Faltungseffizienz wurde vermutet, dass der ETB Rezeptor aufgrund thermischer Instabilität während der Synthesereaktion degradiert, da diese für etwa 12 - 17 h bei 30°C stattfindet. Mit dem Ziel einer höheren Ausbeute an aktivem Rezeptor wurde deshalb die Reaktionszeit verkürzt. Dabei stellte sich jedoch heraus, dass der frisch synthetisierte Rezeptor in den ersten ca. 10 h fast keine Ligandenbindungskompetenz aufwies. Diese trat erst im Rahmen eines posttranslationalen Faltungsprozesses auf, der erst nach etwa 24 h abgeschlossen war. Bei weiteren Untersuchungen stellte sich heraus, das die Maturation des Rezeptors die Bildung einer Disulfidbrücke benötigt, welche ein konserviertes Charakteristikum aller GPCR-Klassen ist (Fredriksson et al. 2003). Die Bildung der Disulfidbrücke war in den ersten Stunden der Zellfreisynthese aufgrund von zugegebenen Reduktionsmitteln blockiert und konnte erst nach, vermutlich thermischer, Degradation dieser Reduktionsmittel ablaufen. Die Zugabe von Reduktionsmittel war allerdings notwendig zur Aufrechterhaltung der Proteinsynthese. Durch Modulation des Reduktionsmittels und Anwendung eines

glutathionbasierten Redoxsystemes konnte der posttranslationalen Faltungseffekt beseitigt werden und eine sofortige Disulfidbrückenbildung bei gleichzeitig nicht-beeinträchtigter Syntheseleistung wurde erreicht. Hierdurch wurde auch die Faltungseffizienz des Rezeptors in etwa verdoppelt.

Ein weiterer Anstieg der Faltungseffizienz des ETB Rezeptors konnte erreicht werden, indem *E. coli* Zellextrakt verwendet wurde, der mit Hitzeschockproteinen angereichert war. Durch Einsatz des Hitzeschock-Extraktes in einem Verhältnis von 3/7 mit normalem Zellextrakt konnte die Faltungseffizienz nochmals in etwa verdoppelt werden, bei gleichzeitig nur geringer Abnahme der Gesamtsyntheserate.

Eine weitere deutliche Verbesserung sowohl in der Gesamtsyntheserate als auch in der Faltungseffizienz konnte erreicht werden, indem eine für *E. coli* kodonoptimierte DNA-Matrize eingesetzt wurde, die für ein modifiziertes ETB-Konstrukt mit abgeschnittenem C-terminus und thermostabilisierenden Punktmutationen kodierte. Hiermit konnte etwa 50% mehr Rezeptor hergestellt werden, bei gleichzeitiger Erhöhung der Faltungseffizienz. In einem direkten Vergleich konnten unter optimierten Bedingungen pro ml RM etwa 1.6 nmol (125 µg) an thermostabilisiertem ETB und 0.8 nmol (65 µg) an nicht-stabilisiertem ETB synthetisiert werden, mit Faltungseffizienzen von 9 bzw. 6.6%. Im Vergleich zur Ausgangslage entspricht dies einer 1500- bzw. 880-fachen Steigerung an korrekt gefaltetem ETB Rezeptor.

Das optimierte CFPS-System wurde im Weiteren zur Synthese des ETA-Rezeptors verwendet. Im Gegensatz zum ETB- zeigte der ETA-Rezeptor in vorherigen Studien nur geringe Solubilisierungseffizienzen mit ND (Proverbio et al. 2013). Durch Modulation der Lipidumgebung und Verwendung von PG-Kopfgruppenlipiden mit langkettiger, ungesättigter Fettsäurezusammensetzung konnte die Solubilisation des ETA-Rezeptors deutlich erhöht werden. Pro ml RM konnte etwa 8 nmol (400 µg) löslicher ETA-Rezeptor hergestellt werden. Allerdings lag die Fraktion an ligandenbindungsaktiv gefaltetem ETA-Rezeptor selbst unter Einsatz des optimierten CFPS Systems bei nur etwa 0.1%. Vorläufige Ergebnisse mit drastisch reduzierter Reaktionsdauer deuteten auf Probleme mit der Stabilität für diesen Rezeptor hin, da die Fraktion an korrekt gefaltetem Protein bei längerer Reaktionszeit scheinbar abnahm.

Zusammenfassend konnten sowohl Quantität als auch Qualität der zell-frei synthetisierten GPCRs verbessert werden, wenn auch mit unterschiedlicher Maße für die einzelnen Rezeptoren. Anhand der Optimisierungschritte lassen sich einige Rückschlüsse auf weitere Maßnahmen ziehen: i) die Löslichkeit und Faltungseffizienz einiger GPCRs kann durch Modulation der Lipidzusammensetzung der zugegebenen ND erhöht werden. Die Lipidzusammensetzung sollte dabei im Optimalfall den Anforderungen des jeweiligen Rezeptors entsprechen. ii) Die Bildung von wichtigen Disulfidbrücken im GPCR kann durch Anwendung eines Redox-Systems verbessert werden. iii) Thermische Stabilität scheint eine Grundvoraussetzung für die Bildung von ligandenbindungskompetenten GPCRs im CFPS-System zu sein, da die CF-Reaktionen im Normalfall für mehrere Stunden bei 30°C andauern. Versuche zur weiteren Qualitätssteigerung sollten daher vor allem Punkte adressieren, die die Insertionseffizienz der frisch gebildeten GPCR-Polypeptidkette in die Lipidmembran der zugegebenen ND erhöhen und die Lipidumgebung weiter optimieren. Dies könnte durch weitere Modulation der Lipidzusammensetzung gelingen oder durch anderweitige Modifikation der ND. Desweiteren sollten

Optimierungsschritte die Thermostabilität der Rezeptoren erhöhen oder das Problem durch Modulation der Reaktionsbedingungen umgehen.

Generell war für alle getesteten GPCRs selbst unter optimalen Bedingungen nur ein Teil des synthetisierten Proteins ligandenbindungsaktiv. Trotz dieser Einschränkung bietet die CFPS Vorteile zur *in vitro* Analyse von GPCRs, da sie außergewöhnlich schnell, zuverlässig und hoch adaptierbar ist. Die Rezeptoren können in einer definierten Lipidumgebung synthetisiert werden und sind ohne Einsatz von Detergenzien und Zelldisruptionstechniken zugänglich für Ligandenbindungsstudien und zur Aufreinigung für weitergehende Zwecke.

Um die Möglichkeiten des CFPS-Systems zu evaluieren wurde die Affinität der Truthahn-β1ARs zu verschiedenen aktuellen Pharmazeutika in verschiedenen Lipidumgebungen getestet. Dazu wurden die Rezeptoren in Gegenwart von ND mit unterschiedlicher Lipidzusammensetzung synthetisiert und Ligandenbindungsscreens direkt im Reaktionsmix durchgeführt. Dabei wurden signifikante Änderungen im Ligandenbindungsverhalten festgestellt. Obwohl weitere Tests notwendig sind um spezifische Muster zu determinieren, standen die Ergebnisse dieses Tests weitgehend in Einklang mit einer vorherigen Studie (Dawaliby et al. 2016). Wie im vorliegenden Fall konnten Dawaliby et al. eine signifikante Steigerung der Affinität des getesteten Ligandentyps zum Rezeptor ermitteln, wenn dieser in Lipiden mit PG-Kopfgruppen vorlag.

Die größten Ausbeuten an funktionell synthetisiertem GPCR und die höchste Faltungseffizienz konnte für den thermostabilisierten β1AR aus dem Truthahn erreicht werden. Im Rahmen einer Pilotstudie wurde dieser Rezeptortyp in einem zweistufigen Prozess in den ND aufgereinigt um sowohl kontaminierende Proteine aus dem RM als auch leere ND und inaktiven Rezeptor abzutrennen. Nach der Synthese des thermostabilisierten Truthahn-β1AR in Gegenwart von ND wurden diese dafür zuerst über eine immobilisierte Metallaffinitätschromatographie (*ion metal affinity chromatography* - IMAC) aufgereinigt. Dabei konnten erste Verunreinigungen aus dem RM abgetrennt werden. In einem zweiten Schritt wurde der ligandenbindungsaktive Rezeptor über eine Ligandenaffinitätschromatographie (LAC) aufgereinigt. Dazu wurde der Alprenololligand des Rezeptors zuerst mit einem *cross-linking* Verfahren kovalent an eine Agarosematrix gebunden. Der IMAC-aufgereinigte Rezeptor-ND Komplex wurde dann über die Interaktion des β1AR mit seinem Liganden an die Säule gebunden und leere ND sowie falsch-gefalteter Rezeptor ausgewaschen. Um den aufgereinigten GPCR-ND Komplex von der LAC-Säule zu eluieren wurde dann nicht gebundener Alprenolol-Ligand in starkem Überschuss zugegeben, was eine Verdrängungsreaktion des kovalent-gebunden Liganden verursachte und somit zu einer Elution des GPCR-ND Komplexes führte. Sämtliche Aufreinigungschritte wurden durch SDS-gebundene Polyacrylamid-Gelelektrophorese (SDS-PAGE) und größenaussschlusschromatographische Methoden (*size exclusion chromatography* - SEC) analysiert. Die Abtrennung der Verunreinigungen von Proteinen aus dem RM und der leeren ND konnte so nachvollzogen werden. Desweiteren zeigte sich eine deutliche Zunahme des Stokes-Durchmessers der β1AR-ND Komplexe im Vergleich zu den leeren ND. Die Ligandenbindungsaktivität des GPCRs konnte somit auch in einem alternativen Ansatz gezeigt werden und weiterhin die Möglichkeit zur Aufreinigung des Rezeptors in einer Lipidumgebung, deren Größe und Zusammensetzung definiert ist.

Nur Teile der in dieser Studie CF-synthetisierten GPCRs wiesen Ligandenbindungsaktivität auf und weitere Optimierungsschritte sind somit naheliegend. Dabei scheint die Addressierung von Problemen

mit der Membraninsertion und der thermischen Stabilit ät der synthetisierten GPCRs vielversprechend. Dennoch konnten bereits immense Fortschritte zum Erhalt von GPCRs in definierten Lipidumgebungen gemacht werden und mit Hinblick auf Kosteneffizienz, Schnelligkeit und funktioneller Ausbeute ist das hier vorgestellte CF-Proteinsynthesesystem für die getesteten GPCRs bereits jetzt hoch kompetitiv zu anderen Systemen. Die direkte Zugänglichkeit und die allgemeinen Vorteile der zell-freien Proteinsynthese eröffnen eine Vielzahl von Anwendungsmöglichkeiten und die vorliegende Arbeit leistet somit einen Beitrag zur molekularen Charakterisierung von GPCRs und zur Entwicklung neuer Medikamente.

1 Introduction

With more than 800 encoded genes, G-protein coupled receptors (GPCRs) represent the third-largest gene family in the human genome (Fredriksson et al. 2003). They are a major class of cell-surface receptors and of eminent physiological and biomedical importance, with 475 drugs targeting 108 unique GPCRs, corresponding to ~34% of all drugs approved by the US Food and Drug Administration (FDA) by mid of 2017 (Hauser et al. 2017). GPCRs are responsible for the perception of a large variety of ligands, including photons of light, odorants, neurotransmitters and peptide hormones. Their physiological functions are related to neurotransmission, neuroendocrine control of physiologic homeostasis and reproduction, regulation of hemodynamics and intermediary metabolism as well cell growth, proliferation, differentiation and apoptosis (Luttrell 2008).

The past decade has seen major breakthroughs in the structural and functional understanding of G-protein coupled receptors (GPCR), largely founded on the progress made in protein engineering, production and crystallisation. However, remaining challenges exist in the large-scale production of GPCRs and isotopical labelling as well as long-term stability are still issues for many GPCR targets (Milić and Veprintsev 2015).

Cell-free protein synthesis (CFPS) is fast, reliable and relatively target independent and enables the production of membrane proteins with strategies that are mainly inaccessible in other production pipelines. This thesis aims to adapt and improve some of these new possibilities to improve the cell-free production of GPCRs in high quality for structural and pharmaceutical analysis. This paragraph will first give an introduction on GPCRs, provide an overview of CFPS techniques and progress made in the field of CFPS of GPCRs and will last explain the strategies for CFPS applied in this thesis.

1.1 G-protein coupled receptors

1.1.1 Classification

Several classification systems for GPCRs exist, based on sequence homology, phylogenetic origin and pharmacological relevance. The frequently used A-F class system is based on sequence homology covering all GPCRs in vertebrates and invertebrates and classifies rhodopsin-like (A), secretin-family (B), metabotropic glutamate (C), fungal mating pheromone (D), cyclic AMP and frizzled/smoothened (F) receptors (Kolakowski 1994). Class D and E are not found in vertebrates. Another frequently used categorisation is the GRAFS system, which is based on phylogenetic analysis in vertebrates and classifies most of the 802 GPCR genes found in the human genome in five main families: The Glutamate, Rhodopsin, Adhesion, Frizzled and Secretin receptor families (Fredriksson et al. 2003). The GRAFS system partly overlaps with the A-F system: The rhodopsin family corresponds to class a, secretin to class B, glutamate to class C and frizzled to class F. The fast majority of 701 GPCRs (including 460 olfactory receptors) belong to the rhodopsin class, which can be further categorised in four main groups: α, β, δ and γ. The α-group branches in five clusters of amine, prostaglandin, opsin, melatonin and MECA receptors. The amine cluster contains the β1AR analysed in this thesis. The β-group has no branches and contains i.a. the Endothelin-related receptors analysed in this thesis. The γ group contains three main

branches, i.a. the chemokine receptors and the δ-group four main branches, including the olfactory receptor cluster. While principal characteristics of GPCRs are the existence of 7 transmembrane segments and coupling to G-protein signalling pathways, it should be noted that G-protein coupling has not yet been demonstrated for all GPCRs and some members of the GPCR superfamily proposed by Fredriksson et al. are not generally thought to signal via heterotrimeric G-proteins, e.g. the frizzled receptors. Furthermore, a group of so-called "orphan receptors" exist for which no physiological ligand is known so far (Alexander et al. 2015).

1.1.2 GPCR signalling

Classically, GPCR signalling happens in a tripartite signalling cascade that involves the GPCR itself, a heterotrimeric G-protein and enzymatically active downstream effectors (Luttrell 2008). The G-protein is composed of each one α-, β- and γ-subunit, with the α-subunit having GTPase activity. The ligand binds as a first messenger to the extracellular or transmembrane domain of the receptor, which transmits the signal via conformational rearrangements to the interior of the cell. The structural changes promote coupling of the GDP-bound heterotrimeric G-protein at the intracellular side of the receptor, which acts as a Guanine-nucleotide Exchange Factor (GEF) on the G_α subunit. Exchange of GDP for GTP activates the subunit and causes dissociation from the $G_{\beta\gamma}$ subunits. Dissociated G_α and $G_{\beta\gamma}$ subunits then regulate the activity of enzymatic effector proteins like adenylate cyclases or phospholipase C to generate small molecule second messengers (i.e. cyclic AMP and inositol-1,4,5-triphosphate) for downstream signalling events like activation of cAMP dependent protein kinases (PKA) and GEFs or inositol triphosphate mediated calcium efflux. The process is cascadic as many second messenger molecules can be generated from one first messenger signal, due to the prolonged effector activity of the signalling components. Inactivation of GPCR signalling is regulated through phosphorylation of the receptor by G-protein coupled receptor kinases (GRK). β-Arrestins recognise and bind the phosphorylated intracellular side of the GPCR and displace the G-protein (Scheerer and Sommer 2017). Clathrin is then engaged to the GPCR-β-Arrestin complex, causing the agonist-occupied receptor to cluster in Clathrin-coated pits and undergo Dynamin-dependent endocytosis. The internalised receptor traffics to early endosomes where it is recycled or degraded (Luttrell 2008).

Besides its effect as negative regulators, β-Arrestin binding can also trigger signalling events distinct from the classical G-protein dependent pathways, a mechanism called "biased signalling" (Shenoy and Lefkowitz 2011). Due to its selective physiological responses, biased signalling by β-Arrestins and other effector molecules has gained more and more attention for pharmaceutical purposes (Rajagopal et al. 2005, Hauser et al. 2017).

For many GPCRs, signalling is not a simple on-off mechanism but a gradual process that can lead to distinct levels of physiological response. GPCRs can also possess constitutive or basal signalling activity that is ligand-binding independent (Rosenbaum et al. 2009). From a pharmaceutical perspective, GPCR ligands are categorised in terms of their efficacy and physiological effect. Inverse agonist inhibit potential basal activity of GPCRs and stabilise an inactive state. Agonists and partial agonists stabilise active states of GPCRs and stimulate biological responses above the basal activity. Neutral antagonist have no effect on the GPCR basal activity but are occupying the ligand binding site and are thus

preventing GPCR activation or deactivation by inverse agonists or agonists (Rosenbaum et al. 2009). Furthermore, biased agonists are ligands that are capable of favouring the activation of one GPCR-associated signalling pathway over another, causing selective physiological responses (Zhou and Bohn 2014, Martí-Solano et al. 2016).

GPCR signalling is tightly regulated and happens on every level of the tripartite cascade (Luttrell 2008). On the GPCR level, regulation and modulation can happen i.a. by phosphorylation through PKA (Luttrell 2008), allosteric modulators like Receptor Activity Modifying Proteins (RAMPs) (Gentry et al. 2015), homo- and heterodimerization (Gahbauer and Böckmann 2016) and interaction with scaffold proteins that regulate GPCR trafficking, localization and signal specificity (Magalhaes et al. 2012). Recently, the membrane lipid environment itself is getting in focus as a modulator of GPCR signalling activity (Oates and Watts 2011, Villar, Van Anthony M et al. 2016).

1.1.3 Structural characteristics of rhodopsin-class GPCRs

Common structural features of all GPCRs are the seven α-helical transmembrane segments (TMS 1-7) which show a relatively high sequence identity, an extracellular N-terminal region (N-term), an intracellular C-terminal region (C-term) and three extracellular as well as three intracellular loops (ECL 1 – 3, ICL 1 – 3). Besides that, sequence identities between the five GRAFS families are relatively low (Fredriksson et al. 2003). This subsection will focus on the rhodopsin-class GPCRs, as they have by far the highest number of family members and are most well understood. Common features in this family include a D/ERY motif at the border between TMS 3 and ICL 2, a NPxxY motif in TMS 7 and two conserved Cys that are intended to form a disulphide bridge in the extracellular region between the end of ECL 1 and ECL 2. N-termini are relatively short in most members of the rhodopsin family and, with some important exceptions, ligand binding usually happens in a cavity between the TMS regions (Fredriksson et al. 2003).

After ligand binding, GPCRs undergo some global structural rearrangements in order to transmit the signal across the membrane to the receiving G-protein. Current models of this signal transduction involve the existence of key intermediate states, as depicted in Fig. 1.1.

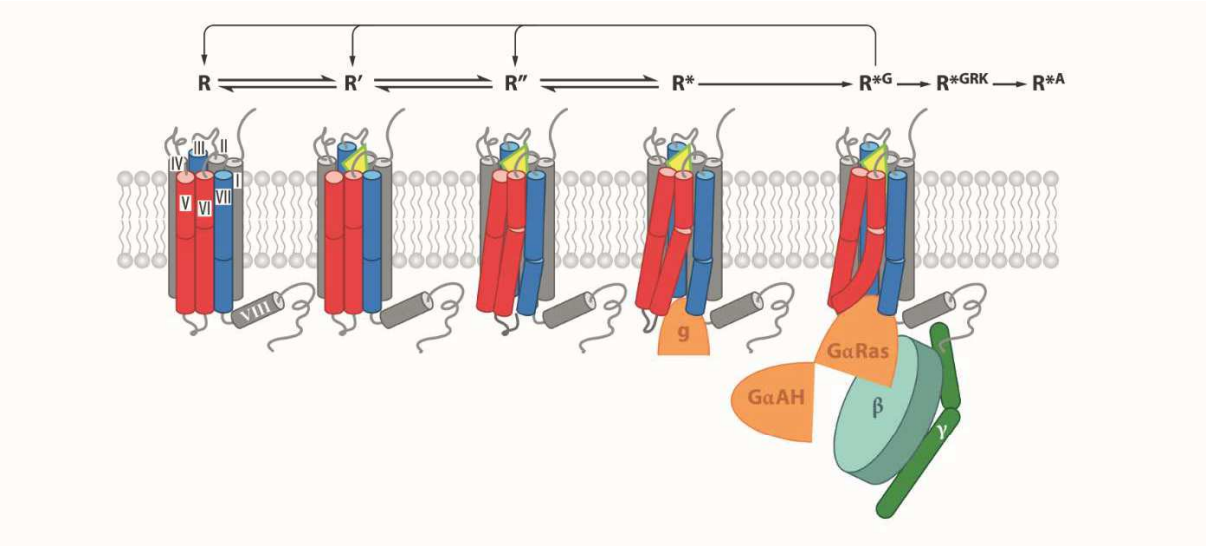

Fig. 1.1 Key intermediate states in GPCR signal transduction.

Highly dynamic GPCRs are in an equilibrium of several inactive (R), active (R*) and intermediate (R' + R'') states. Binding of a ligand (yellow) stabilizes the active state, which can bind and activate the G-protein signalling complex (R*GRK). Stabilisation through ligand binding thus increases the fraction of GPCR molecules in the R* state and the probability of signalling events. Inactivation of the GPCR is then achieved by binding of Arrestin (R*A). Adapted from Katritch et al. 2013.

In the ground state (R), no ligand is bound to the receptor, which is in a complete inactive state in terms of signal transduction. After ligand binding (R'), substantial global rearrangements of the helices and sidechain microswitches lead to a partial exposure of the G-protein binding crevice in the intracellular region (R''). The G_{α}-subunit of the heterotrimeric G-protein recognizes and binds to the binding crevice (R*), causing some further structural rearrangements at the intracellular sides of the receptor that lead to the formation of the distinct G-protein signalling conformation (R*G) (Katritch et al. 2013). Importantly, this mechanism cannot be seen as a consecutive process with distinct receptor states that only exist after ligand and G-protein interaction. On the contrary, most GPCRs are highly dynamic and in equilibrium of a multitude of partly active and inactive states. Ligand binding does not induce a particular active state but rather stabilises it, leading to a change in the equilibrium and an increased probability for G-protein binding and subsequent activation of the signalling cascade (Kobilka and Deupi 2007). This model gives an explanation for the basal or ground-state activity found in many GPCRs (see 1.1.2) and further explains difficulties in the *in vitro* handling and crystallisation of these proteins, that are largely caused by their intrinsic flexibility (Maeda and Schertler 2013)

Nevertheless, recent progress in the fields of membrane protein engineering and crystallisation led to major breakthroughs in the structural characterisation of GPCRs and by late 2017, a total of 218 high resolution structures from 46 distinct GPCRs were openly available (Isberg et al. 2016). Structural data exist for the inactive, active and intermediate states for several GPCRs. This has deepened our understanding of the activation process (Katritch et al. 2013, Venkatakrishnan et al. 2013, Carpenter and Tate 2017).

In brief, GPCRs can be seen in three functional parts, the extracellular- , the TMS and the intracellular region. The extracellular part modulates access for the ligand. This part shows highest

variety in the extracellular loop region, corresponding to the variety of ligands Katritch et al. 2013. In most GPCRs, ECL 2 is the largest ECL, contains α-helical or β-sheet structures and is considered to be most important for ligand recognition and selectivity (Venkatakrishnan et al. 2013). The TMS region forms the structural core that binds ligands and undergoes conformational changes. Ligands often bind in a "ligand binding cradle" that is formed by the TMS bundle and is more or less submerged in the receptor (Venkatakrishnan et al. 2013). Degree of sequence conservation is higher than in the extracellular region, but key alterations and specifications are found, primarily in the ligand binding region (Katritch et al. 2013). A conserved disulphide bond between the end of ECL 1 and ECL 2 anchors the extracellular site of helix 3 near the ligand binding site and is thus important for the formation of the ligand binding site in many GPCRs (Venkatakrishnan et al. 2013). A consensus network of 24 inter-TMS contacts brings receptor in shape and appears to be evolutionary conserved, with TMS 3 serving as a "structural hub" for the receptor (Venkatakrishnan et al. 2013). After ligand binding, a rearrangement of conserved residues Tyr 5.58 and Tyr 7.53 from the NPxxY motif and Arg 3.50 (Ballesteros-Weinstein numbering, Ballesteros and Weinstein 1998) from the DRY motif happens with an outward movement and rotation of helix 6 that is stabilised by the interaction of the above-mentioned residues. The helix motion, which also involves helix 5, is also known as rotamer toggle switch (Rosenbaum et al. 2009). It opens a cavity at the cytoplasmic side that engages the α-5 helix of G_α. Binding of the heterotrimeric G-protein further stabilises the outward formation of helix 6, which shows a total movement of 6 to 17 Å in the active conformation (Carpenter and Tate 2017). Formation of the GPCR-G-protein complex causes an improved packing in the core of the transmembrane bundle that tightens the ligand binding pocket, which goes in hand with higher affinity to the agonist after G-protein binding (Carpenter and Tate 2017). GPCR inactivation by β-Arrestin might then be a process driven by competitive binding of β-Arrestin to the intracellular side, as suggested based on recent negative stain electron microscopy data from a GPCR-β-Arrestin-complex (Ranjan et al. 2017, Carpenter and Tate 2017).

At the moment, question marks exist on the structural reasons for G-protein specificity and on the mechanisms of biased signalling. Furthermore, crystallography can only provide structural snapshots on specific receptor states. Based on the insights provided by crystallography, techniques like NMR- (Kofuku et al. 2014, Isogai et al. 2016, Ye et al. 2016) and DEER-spectroscopy (Manglik et al. 2015) as well as computational approaches (Rosenbaum et al. 2011, Martí-Solano et al. 2014, Martí-Solano et al. 2016) might provide more details in the dynamic process of GPCR signal transduction and are currently getting in focus.

1.1.4 Classical ways to obtain GPCR samples

Classical systems for recombinant expression of proteins include mammalian and insect cells as well as yeast and *Escherichia coli (E. coli)*. Mammalian cell lines appear to be the optimal tool for overexpression of GPCRs as the lipidic content of mammalian cell membrane provides the most native environment and cells have all the necessary machinery for correct membrane insertion, folding, and post translational modification. However, mammalian cells tend to be fragile and extensive overexpression often leads to heterogeneous post-translational modifications and missfolding (Milić and

Veprintsev 2015). Additionally, recombinant overexpression based on either transient expression or transfection methods is relatively time consuming and labour intense and media and antibiotics used for GPCR production in mammalian cells are among the most expensive ones (Milić and Veprintsev 2015). Besides its obvious advantages, crystal structures resolved from GPCRs produced in mammalian cell lines are rare.

The most common recombinant expression system for GPCRs is based on insect cell lines, i.e. *Spodoptera frugiperda* (*Sf*9) and *Trichoplusia ni* (*Tni*) High five cells, with synthesis rates up to milligrams per litre of cell culture (Milić and Veprintsev 2015). Transfection and recombinant gene expression in insect cell based systems require production and handling of baculovirus making the process time consuming and relatively expensive. The altered lipid composition of the insect cell membrane might cause additional problems in overexpression and, as for mammalian cell lines, heterogeneity in folding and post-translational modifications can appear (Thomas and Tate 2014). Compared to insect and mammalian cell lines, yeast grow fast, are easy to handle and culture medium is inexpensive.

Several structures from receptors produced in yeast *Pichia pastoris* are openly available, while *Saccharomyces cerevisiae* is more suitable for cloning and rapid screening of the protein construct (Milić and Veprintsev 2015). Drawbacks are their different glycosylation pattern and the altered lipid content in the membrane. Additionally, the cell wall needs to be removed to gain excess to the target protein (Lundstrom et al. 2006).

Like yeast, *E. coli* have a fast grow rate, are easy to handle and do not need expensive supplies. However, as a prokaryotic system, they are missing the eukaryotic machinery for membrane insertion, folding and post-translational modifications. Additionally, their are high differences in the lipid content of the bacterial inner membrane. Soluble expression is possible in some cases but usually requires N-terminal insertion tags like β-galactosidase or maltose binding protein (MBP) (Milić and Veprintsev 2015). Soluble expression in the *E. coli* inner membrane is frequently used in small-scales for the analysis of mutants in GPCR engineering approaches (Schlinkmann et al. 2012, Maeda and Schertler 2013, Magnani et al. 2016). Some of these engineering approaches resulted in the first high-resolution crystal structure of a mammalian GPCR produced in *E. coli* (Egloff et al. 2014). Strategies for expression as inclusion bodies and subsequent refolding have also been published for the large-scale production of GPCRs in *E. coli* (Schmidt et al. 2010, Michalke et al. 2009).

1.2 Cell-free protein synthesis

1.2.1 When and why to choose cell-free protein synthesis

In contrast to classical cell-based expression systems, cell-free protein synthesis (CFPS) can be optimised for the exclusive production of a single protein without the need for compromises to cell viability. There is no need for background expression of non-target proteins and common issues with cell based expression systems like variable transfection efficiencies, slow grow rates and the need to operate in sterile conditions are not longer present. CF-reaction is set-up by simply mixing individual stock solutions, which can largely be prepared in advance and stored for many month (Schwarz et al. 2007). Synthesis starts just after addition of the DNA template, which can even be provided as a PCR product (Haberstock et al. 2012). Reactions can be scaled from a few microlitres to several millilitres. Synthesis is usually performed in less than 24 h and result in yield up to several mg of target protein per ml of CF-reaction mixture in an optimised CFPS system (Bernhard and Tozawa 2013), making the CFPS attractive for both screening and large-scale production purposes (Carlson et al. 2012). The open nature of CFPS is highly suited for combination with other fields of synthetic biology like incorporation of non-natural amino acids or construction of protein micro arrays (Stoevesandt et al. 2011, Hodgman and Jewett 2012, Lee and Kim 2013, Smith et al. 2014b).

1.2.2 Extract sources and hardware set-up strategies

CFPS systems are often based on crude extracts from *E. coli* cells. Derivatives from expression strains like BL21 or A19 are frequently used for extract preparation (Schwarz et al. 2007). Genetically engineered strains for specific protein requirements, e.g. disulphide bridge formation, have been developed as well as new techniques for cell grow and extract preparation (Knapp et al. 2007, Foshag et al. 2017). *E. coli* based CFPS systems give high expression yields and extract preparation is fast and inexpensive. However, post-translational modifications like glycosylation are usually not addressed, due to prokaryotic origin of the system. Wheat germ based CFPS-extract offer comparable yields and might be more suitable for some applications (Bernhard and Tozawa 2013). On the other hand, extract preparation is relatively time consuming and labour intense, as it requires removal of the endosperm containing enzymatic inhibitors and neat washing procedures of the embryo parts (germ) (Bernhard and Tozawa 2013). Other systems are based on extracts derived from insect cells or lysates made from rabbit reticulocytes (Carlson et al. 2012), are made with extract from mammalian CHO cells (Thoring et al. 2016) and from the purified and reconstituted *E. coli* protein synthesis machinery itself (Shimizu and Ueda 2010). Production efficiency in these systems are usually lower than in *E. coli* or wheat germ based extract and most of them have been developed for analytical purposes.

CPFS systems derived from different cell sources have distinct advantages and drawbacks (Carlson et al. 2012) and require basic considerations on the template design. For example, buffer requirements for DNA transcription and mRNA translation are different in wheat germ CFPS systems and usually require their local or temporal separation (Endo and Sawasaki 2006). On the other hand, *E. coli* based CFPS systems are coupled transcription/translation reactions and frequently based on the transcription

by highly processive T7 RNA polymerase that can be addressed by introduction of respective regulatory elements in the DNA template production (Schwarz et al. 2007).

In the most simple batch configuration of *E. coli* based CF-reaction set-up, DNA templates are mixed with CF-extracts and supplemented with components required for transcription, translation and energy regeneration (for a an exemplary description see 3.2). Protein synthesis reaction prolongs until shortage of precursors or toxic concentrations of inhibitory by-products in the CF-reaction mixture appear (Fig. 1.2). While advances have been made in batch-mode reaction set-up (Carlson et al. 2012) and up-scaling resulted in reaction volumes up to even 100 l for soluble proteins (Zawada et al. 2011), this configuration is naturally well suited for screening approaches, as it can be performed in small volumes and 96- or 384-well plates and yield optimum is usually achieved after 2 – 3 h. Prolonged reactions resulting in higher protein yields are feasible in the continuous exchange cell-free (CECF) configuration, where the reaction mixture (RM) is coupled with the larger feeding mixture (FM) by a dialysis membrane, providing a reservoir for additional small molecular mass precursors and dilution of inhibitory by-products (Bernhard and Tozawa 2013).

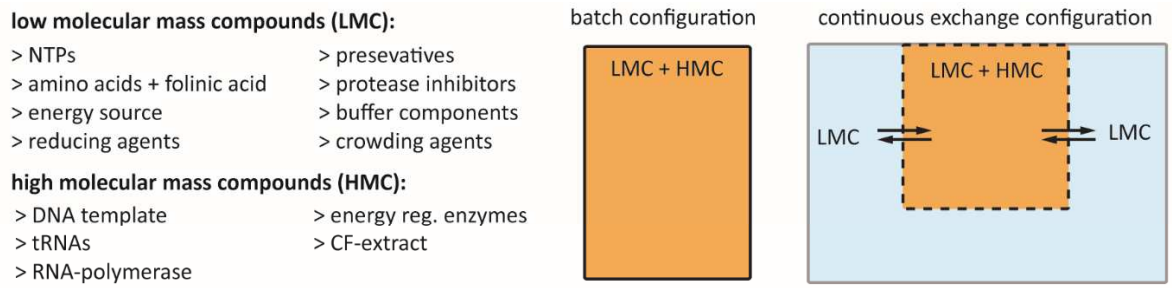

Fig. 1.2 Set-up modes for *E. coli* based cell-free protein synthesis.

CFPS systems consist of both low and high molecular mass compounds. In the batch configuration, only one compartment exist containing the reaction mixture (orange) with both low and high molecular mass components. In continuous exchange configuration, a feeding mixture compartment (blue) contains additional low molecular mass compounds and is connect with the reaction mixture by a semipermeable membrane.

1.2.3 Cell-free protein synthesis of GPCRs

To keep GPCRs and other membrane proteins (MP) soluble in aqueous solution, amphipathic agents need to be applied that shield the otherwise exposed hydrophobic patches that are *in vivo* spanning the membrane lipid bilayer in the cell. Detergents are frequently used for extraction of MPs after in cell production and for further *in vitro* processing. However, use of detergents can have some major drawbacks, e.g. denaturating effects on the MP and the necessity to work with an excess of detergent for critical micelle formation (Seddon et al. 2004). Alternative amphipathic agents like Amphipols and fluorinated surfactants (Popot 2010) or lipid-like peptides (Zhang 2012) and small-diameter membrane mimetics like bicelles (Dürr, Ulrich H N et al. 2013), Membrane Scaffold Protein (MSP) nanodiscs (Borch and Hamann 2009), Styrene Maleic Acid Lipid Particles (SMALP) (Esmaili and Overduin 2017) and Saposin-lipoprotein particles (Frauenfeld et al. 2016) have been developed to circumvent common issues with classical detergents.

In contrast to in cell expression, the open nature of CFPS principally allows the co-translational addition of nearly all of these detergents, amphipathic agents and membrane mimetics, with the sole respect to potentially inhibitory effects on the protein synthesis system. CF-expression strategies are routinely categorised in P-CF modes where no solubilising agent is added and MPs instantly precipitate after synthesis, D-CF modes where detergents in non-inhibitory concentrations are supplied and solubilise the nascent MP and L-CF modes with supplemented lipid environments like liposomal vesicles or nanodiscs, where the MP is co-translationally associated with or inserted in a lipid environment (Bernhard and Tozawa 2013). Addition of multiple detergents and combinations of D- and L-CF modes are also conceivable.

In the past decade, CFPS of GPCRs has been performed with a variety of expression strategies, including P-, D- and L-CF-modes as well as more unconventional approaches and in expression systems with both pro- and eukaryotic origin (Tab. 1.1).

Tab. 1.1 Overview on CFPS strategies from the past 12 years.

GPCR[1]	Co-translational solubilisation	Post-translational solubilisation	Extract source[2]	Quality control[3]	Reference
ADRB2, ACHR, NTSR	Brij35, digitonin	Lipid vesicles	E. coli	RLB	Ishihara et al. 2005
MTNR1B, EDNRB, AVPR2, NPY4R, CRHR	Brij 58 + 78	LMPG	E. coli	EM, TIRFS	Klammt et al. 2007
OFR	Tethered lipid membrane		RRL	SPFS, SEIRAS	Robelek et al. 2007
OFR	Digitonin + Brij 58		WG	SEC, CD, SPR	Kaiser et al. 2008
OFR	Tethered lipid membrane		RRL	TIRFS, FCS, FRAP	Leutenegger et al. 2008
HRH1	n.d.	DDM	E. coli	RLB, MS	Sansuk et al. 2008
EDNRA/B	Digitonin, Brij 35 + 78	LPPG	E. coli	SEC, MALS, CD, EM, LAC, RLB	Junge et al. 2010
EDNRB , NPY2R/4R, NPY4R, MTNR1A/B, SSTR1/2, AVPR1B/2, HRH1, CRHR	n.d.	LMPG	E. coli	SDS-PAGE	Schneider et al. 2010
OFR, TAAR, FPR	Brij 35 + peptide surfactants	Fos-14	E. coli	CD, MST	Corin et al. 2011b, Corin et al. 2011a, Wang et al. 2011
CRHR1/2B	fructose-based polymer (Nvoy10)	LMPG	E. coli	SEC, EM, NMR, RLB	Klammt et al. 2011
ADRB2	Nanodiscs		E. coli	RLB	Yang et al. 2011
NK1R, ADRA2, DRD1	Nanodiscs		E. coli	EPR, FCS, LBA	Gao et al. 2012
ADRB2, ACHRM1 SSTR5	n.d.	SDS	E. coli	CD	Lyukmanova et al. 2012
DRD2	n.d.	SDS	E. coli + WG	RLB	Basu et al. 2013
DRD2	Block copolymer vesicles		RRL	FC, LBA	May et al. 2013
EDNRA/B	Brij-78 + nanodiscs	LMPG	E. coli	RLB, SPR, LBA	Proverbio et al. 2013
OFR	Lipid vesicles		*E. coli*, WG, IC, MC	SEC, CD	Ritz et al. 2013
RXFP3	n.d.	LMPG	E. coli	SDS-PAGE, EM	Shilling et al. 2013
TAAR, FPR	n.d.	Brij-35	E. coli	SEC, CD	Wang et al. 2013a, Wang et al. 2013b
EDNRB, CXCR4	Microsomes	Giant vesicles	IC	SMFM	Fenz et al. 2014
CXCR4/5	Brij35		E. coli	PD, QMB	Chi et al. 2015, Chi et al. 2016
EDNRA/B, GNRHR	Microsomes		IC	RLB	Merk et al. 2015
ADRB1	Nanodiscs		E. coli	SEC, RLB, LAC	Rues et al. 2016
NTSR1	Nanodiscs, Brij-35 + 58	DDM	E. coli	SEC, CD, LPD, NMR	Shilling et al. 2017
OPRM, EDNRB	Microsomes		IC	PD, FM, RLB	Sonnabend et al. 2017, Zemella et al. 2017

1; gene names are given, OFR = olfactory receptors

2; RRL = rabbit reticulocyte lysate, WG = wheat germ, IC = insect cell, MC = mammalian cell

3; CD = circular dichroism, EM = electron microscopy, FCS = fluorescence correlation spectroscopy, FM = fluorescence microscopy, FRAP = fluorescence recovery after photo bleaching, LAC = ligand affinity chromatography, LBA = ligand binding assay, LPD = ligand pulldown, MALS = multi angle light scattering, MS = mass spectrometry, MST = microscale thermophoresis, NMR = nuclear magnetic resonance, PD = proteolytic digestion, QMB = quartz microbalance, RLB = radioligand binding assay, SEC = size exclusion chromatography, SEIRAS = surface infrared reflection absorption spectroscopy, SMFM = single molecule fluorescence microscopy, SPFS = surface plasmon fluorescence microscopy, SPR = surface plasmon

Adapted from Rues et al. 2014.

P-CF synthesis could be used successfully for the high quality production of several MPs even without the need of extensive refolding steps (Maslennikov et al. 2010, Boland et al. 2014). Post-translational solubilisation of P-CF synthesised GPCRs is often performed with lyso-phosphoglycerol derivatives, SDS, Fos-14 or DDM, which might be subsequently exchanged to milder detergents or receptors might be reconstituted into liposomes for functional analyses. For example, human histamine H1 receptor (HRH1) was P-CF-synthesised in an *E. coli* based CF-system, post-translationally solubilised in DDM and reconstituted in asolectin liposomes and ligand binding selectivity was similar to samples obtained from insect cells, despite a somewhat decreased affinity (Sansuk et al. 2008). From an extensive P- and D-CF expression screen, solubilisation of P-CF synthesised Endothelin receptor type A (EDNRA or ETA) in LPPG and subsequent exchange to milder Brij-35 or Fos-16 detergent was found to give best results for homogeneity and ligand binding characteristics of this receptor (Junge et al. 2010).

Mild Brij-detergents and digitonin in a final concentration of 0.1 – 1% have most frequently been used for the D-CF synthesis of GPCRs (Tab. 1.1). Detergents can have inhibitory effects on parts of the protein synthesis machinery and therefore both its type and concentration is often a balance between solubilisation efficiency and tolerance of the translation machinery (Klammt et al. 2005). Besides detergents, surfactants composed of lipid-like peptides (Corin et al. 2011b) or fructose-based polymers (Klammt et al. 2011) have been used for the soluble CF-synthesis of several GPCRs and the optimisation of co-translational expression environments resulted in several cases in GPCRs with binding characteristics similar to corresponding samples derived from insect or mammalian cell overexpression (Ishihara et al. 2005, Corin et al. 2011a, Wang et al. 2011).

Lipids can have essential effects on the folding, function and stability of GPCRs (Yao and Kobilka 2005) and can be added to CF-reactions either as additives in detergent-based expression systems resulting in lipid-enriched proteomicelles or as lipid bilayer in form of e.g. bicelles, nanodiscs, preformed liposomes or lipid microsomes extracted from insect cells. Several approaches have been made for the L-CF synthesis of GPCRs in the past years. For example, several olfactory receptors were co-translational inserted into phosphocholine liposomes and insertion was found to be unidirectional (Ritz et al. 2013). In another study, unidirectional insertion was observed for olfactory receptors CF-synthesised in presence of surface coupled planar lipid bilayers (Robelek et al. 2007). Approaches to closely mimic the natural insertion mechanism were described with insect cell based CF-expression systems with microsomal vesicles derived from the endoplasmatic reticulum that still contained natural insertion machineries (Fenz et al. 2014, Merk et al. 2015). In combination with a glutathione based redox system for disulphide bridge formation, this approach resulted in the production of ligand binding competent Endothelin receptor type B (EDNRB or ETB). The receptor showed high affinity to its natural ligand Endothelin-1, despite low insertion and folding efficiencies, that were judged partly to limited efficiency and saturation of the insertion machinery (Merk et al. 2015). MSP-nanodiscs (ND) are small and homogeneous membrane lipid patches (see 1.3.3 for a more detailed description) and combine both easy handling and membrane mimicry characteristics. Several studies have been performed with CFPS of GPCRs in presence of pre-assembled ND and ligand binding competent receptor could be produced in case of engineered β2-adrenergic receptor (ADRB2) (Yang et al. 2011) and ETB receptor (Proverbio et al. 2013). However, folding efficiencies were low in both cases, with yields of <1% ligand binding competent receptor.

For several cases, ligand binding affinity appeared to be similar with data from *in cell* derived sources, as for Histamine H1 receptor HRH1 (Sansuk et al. 2008), β-adrenergic receptors ADRB(Ishihara et al. 2005, Yang et al. 2011) , Dopamine D2 receptor DRD2 (Basu et al. 2013) , Neurokinin type 1 receptor NK1R (Gao et al. 2012) as well as ETA and ETB receptors EDRNA/B(Junge et al. 2010, Proverbio et al. 2013). This indicated the feasibility of drug screening approach with CF-derived GPCR samples in the future and is particular interesting in respect to the progress made with addition of highly soluble nanodiscs (Proverbio et al. 2013), synthetic membrane mimetics (May et al. 2013) or tethered lipid bilayers (Leutenegger et al. 2008). On the other hand, quantitative studies revealed mostly still rather low folding efficiencies for CF-produced GPCRs in a range of approx. 0.05% to 5% (Yang et al. 2011, Basu et al. 2013, Proverbio et al. 2013), leaving plenty of room for improvements.

1.3 The strategy for cell-free synthesis of GPCRs applied in this study

1.3.1 The Cell-free protein synthesis system

In this study, an *E. coli* strain A19 based CECF system was used which was previously described in Schwarz et al. 2007 and Schneider et al. 2010. Expression was based on T7 RNA polymerase (T7RNAP) under T7 promotor and construct templates were therefore inserted in a pET-21a vector. The extract was prepared as S30-extract (i.e. sedimentation at 30,000 x g) and contained essential components like ribosomes, aminoacyl-tRNA, synthetases and translation factors. A so-called "run-off" step was performed to release stalled ribosomes and reduce the background protein and mRNA content. Usually, DTT was supplied to stabilise T7RNAP. NTPs were added as energy source and substrate for transcription. RNAse inhibitor was added to protect transcribed mRNA from degradation and protease inhibitors to prevent proteosomal degradation. A dual energy regeneration system was used based on phosphoenolpyruvate (PEP), acetyl phosphate (AcP) and respective kinases as energy sources to rebuild ATP and GTP for prolonged reactions. Folinic acid was added for the formation of the initiator formyl-methionine and tRNAs and amino acids in large excess to provide substrate for translation. PEG in molecular masses of ~8 kDa was added to mimic the viscosity of the cytoplasm. The system was buffered with HEPES to a pH of 7.0 and concentration of crucial ions K^+ and Mg^{2+} were tightly controlled.

Hardware set-up in the CECF-mode was prepared with analytical scale self-made containers with a volume of 40 – 100 µl for reaction mixture (RM) and commercial 24-well plates with a volume of 500 – 1000 µl for FM. Preparative scale reaction were set-up with commercial Slide-A-Lyzers (Thermo Scientific) with a volume of 1 – 3 ml and self-made FM container with a volume of 15 – 50 ml (Fig. 1.3). Detailed descriptions on component concentrations, stock solutions and reaction set-ups are given in the methods section (3.2).

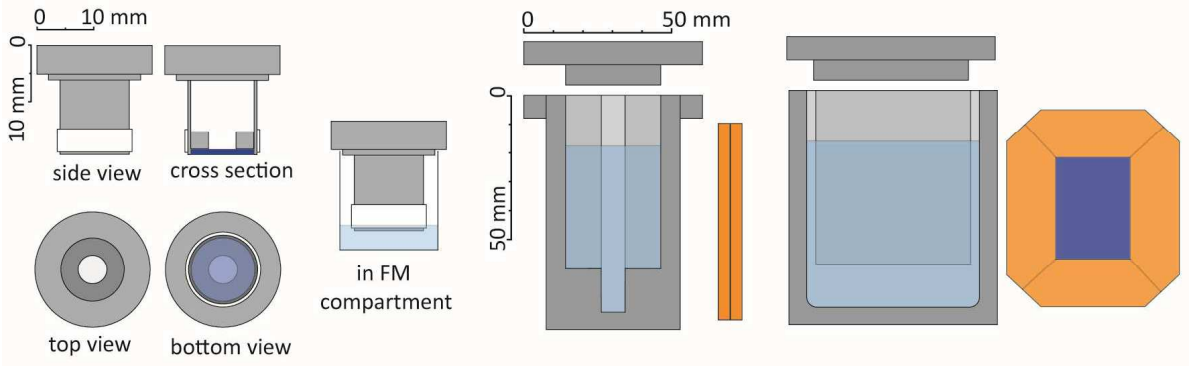

Fig. 1.3 CECF-reaction set-up.

Left: Analytical scale CECF set-up with self-made reaction containers for volumes of 40 – 100 µl. Right: Preparative scale set-up with commercial Slide-A-Lyzers (Thermo Scientific) with a volume of 1 – 3 ml and self-made FM containers with a volume of 15 – 50 ml. Dark blue = RM, light blue = FM.

1.3.2 Protocol for optimisation

Protocols for optimisation of CFPS reactions are routinely performed in a 3-level protocol, exemplified in Fig. 1.4.

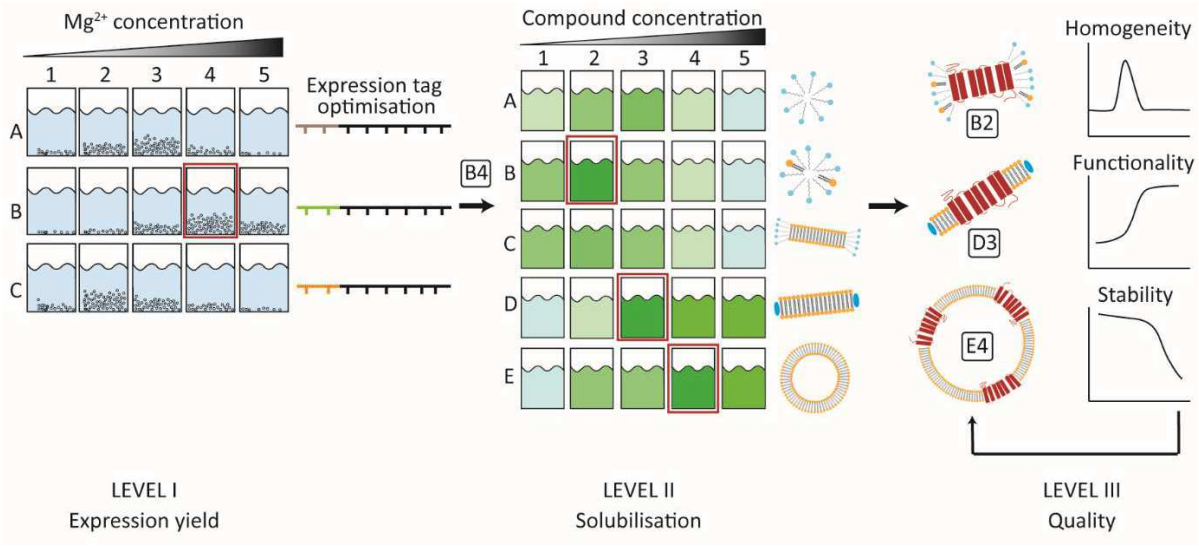

Fig. 1.4 Optimisation protocol for cell-free production of GPCRs.

Level I: Optimisation of basic production and yield by Mg^{2+} and expression tag screen. The Mg^{2+} concentration of 4 units in combination with expression tag B gave highest yields, as judged by pellet size of the precipitated GPCR. Level II: Solubilisation agents are tested for the efficiency to solubilise the GFP-tagged receptor. Lipomicelles, nanodiscs and liposomes were found to be most suitable, judged on the GFP-fluorescence of the supernatant. Level III: Receptor in proteolipomicelles, nanodiscs and liposomes are analysed for homogeneity, functionality and stability. The outcome of the analysis is used for further optimisation of the respective solubilisation tool. Adapted from Rues et al. 2014.

In the first level, overall production efficiency is enhanced by optimisation of basic reaction conditions like Mg^{2+} ion concentration and optimisation in DNA template design by expression tag variation (Haberstock et al. 2012). This step is usually done in done in P-CF mode, as potential interferences with hydrophobic compounds are excluded. In the second level, a toolbox for co-translational solubilisation is applied. A wide and continuously increasing toolbox of detergents, amphipathic compounds or membrane mimetics can be used in this step. Important parameters are the type and the concentration of the added compound. The receptor is tagged with GFP and yields of soluble GPCR are analysed by fluorescence read-out of the supernatant after centrifugation. Best hits are then further optimised in the third level, which focus on the quality of the GPCR. Therefore, proper read-out assays need to be applied to analyse the functionality as well as stability and homogeneity, if necessary. Based on the outcome of this analysis, further optimisation steps are applied and the solubilisation agents are modulated e.g. by addition of lipids to D-CF expressions or altered lipid compositions of supplied nanodiscs (ND) or liposomes (LP).

Basic reaction protocols have previously been optimised (Klammt et al. 2007, Haberstock et al. 2012) and ND were previously found to be highly suitable as membrane mimetics for the soluble

synthesis of ETB receptor (Proverbio et al. 2013). The present work was therefore mainly focused on the quality optimisation of CF-synthesised GPCRs in membrane mimetics using ND.

1.3.3 Lipid supplemented cell-free synthesis using nanodiscs

The NDs used in this study are reconstituted high density lipoprotein (rHDL) particles with discoidal shape and a lipid content of approx. 50 – 200 molecules, depending on the disc size and lipid characteristics (Bayburt and Sligar 2010). When brought together in correct ratios, structures self-assemble where the lipids are forming a bilayer that is circumvented in a belt like form by two α-helical membrane scaffold proteins (MSP) in antiparallel orientation (Fig. 1.5). The hydrophobic residues of each helix are oriented towards and shielding the hydrophobic areas of the lipid bilayer, making the structure highly water-soluble. The MSPs are stabilised by up to 28 simultaneous salt bridges and intermolecular cation-PI-stacking in an arginine zipper like arrangement (Bibow et al. 2017), making the structure highly stable.

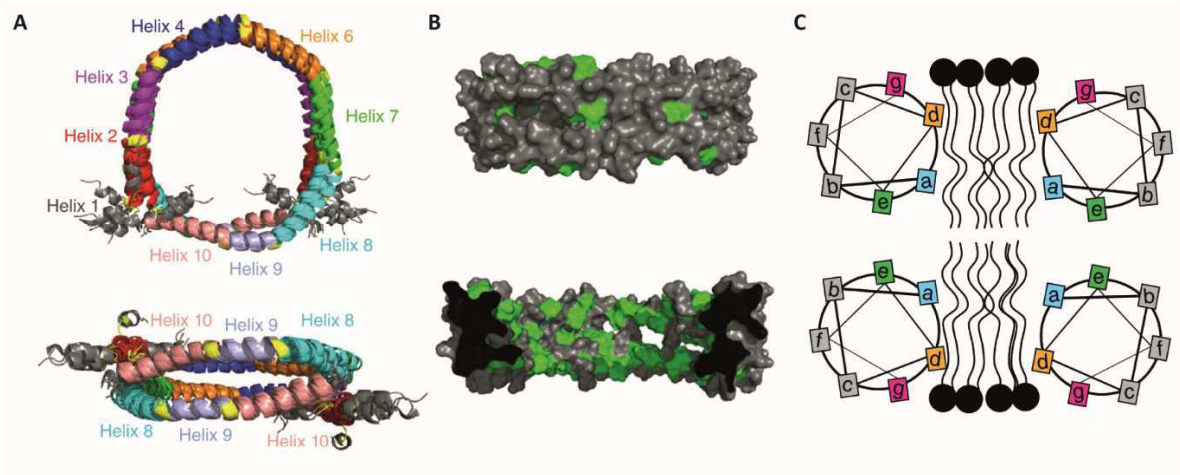

Fig. 1.5 Structure of a MSP-nanodisc.

Solution-state NMR structure of MSPΔH5-DMPC nanodiscs. A: Two MSP molecules are oriented in an antiparallel belt circumventing the lipid bilayer content (lipids are not shown). B: Hydrophobic residues (green) are oriented towards the inner side and interacting with the fatty acid side chains. The outer side is largely hydrophilic (grey), making the structure water-soluble. C: Orientation of the MSP-helices. Residues a and d are interacting with the fatty acid side chains, residues g are interacting with the polar headgroups. Residues b, c, and f are responsible for water-solubility and residues e of both MSPs are interacting in intermolecular salt-bridges and cation-Pi-stackings to stabilise the structure. Adapted from Bibow et al. 2017.

The MSP is an apolipoprotein A1 derivate from the mammalian HDL metabolism (Zannis et al. 2015). In its original size, MSP has 10 amphipathic helices and forms NDs with a hydrodynamic stokes diameter of 9.7 nm (Fig. 1.6). MSPs with insertion of up to three 22-mer amphipathic helices have been designed, called MSP1E1 – E3. ND formation with these MSP derivatives results in structures with a larger stokes diameters (Fig. 1.6). The first 11 amino acids of the MSP sequence are not involved in ND formation and can be deleted. The respective constructs are called MS1PD1 (Denisov et al. 2004). Further developments include deletion of helix 5 of the MSP, called MSPΔH5, with forms ND with a

smaller stokes diameter and was specifically designed for solution NMR analysis (Hagn et al. 2013). In this thesis, ND were made with MSP1E3D1 constructs with a stokes diameter of ca. 11 nm.

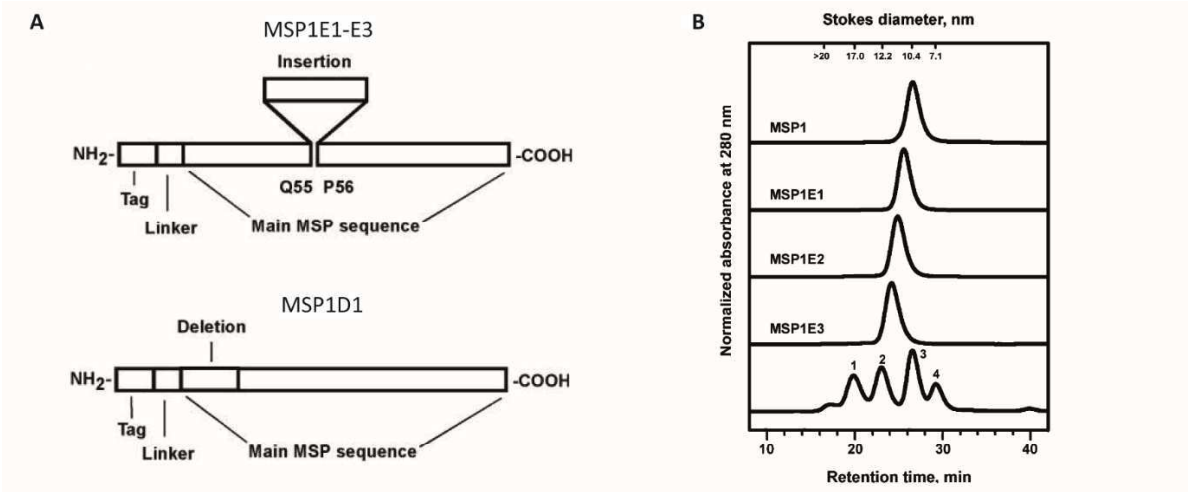

Fig. 1.6 MSP variants for formation of nanodiscs with different diameter.

Several modifications have been applied to the original MSP. A: MSP1E1-E3 were designed by insertion of one to three 22-mer amphipathic helices and MSP1D1 was designed by deletion of 11 N-terminal amino acids. B: Insertion leads to NDs with a larger stokes diameter in SEC. The lower chromatogram shows elution profiles of calibration proteins with a defined stokes diameter of 17 nm (1), 12.2 nm (2), 10.4 nm (3) and 7.1 nm (4). Adapted from Denisov et al. 2004.

NDs can be used for co-translational solubilisation of MPs during CFPS (Roos et al. 2013). The process of association and insertion of the nascent peptide chain in this process is only partly understood and highly dependent on the MP. For several MPs, stepwise insertion of multiple proteins in one ND and complex formation has been demonstrated at stoichiometric ND to MP ratios (Henrich et al. 2017). In these cases, insertion seems to be correlated with a partial removal of the lipid content of the NDs (Peetz et al. 2017). On the other hand, for ETB receptor, overtitration of ND (DMPC) was necessary for complete solubilisation of the receptor. Additionally, only minor fractions of the receptor were found to be ligand binding competent. Taken together, these results might indicate limitations in the insertion mechanism of ETB receptor in ND (DMPC) (Proverbio et al. 2013).

1.3.4 The GPCRs analysed in this study

β1-adrenergic receptors

The β-adrenergic receptors (βAR) are key players in the mediation of sympathetic nervous system regulated cardiovascular functions. Three receptor subtypes called (β1 - 3AR) were identified in human and pharmacologically characterised (Post et al. 1999). Cardiovascular functions are mainly regulated through β1- and β2AR, while β3AR is involved in the metabolism of adipose tissues. Through binding of catecholamine hormones in the cardiovascular tissues, βAR activate cAMP coupled downstream signalling events that are responsible for increased heart beating rates (chronotropism), force of cardiac contraction (inotropism), the rate of cardiac relaxation (lusitropism) and automaticity (Post et al. 1999).

Disturbances in βAR signalling pathways are associated with severe diseases like congestive heart failure and a large group of drugs called β-blockers are directly addressing βARs in the cardiovascular system (Post et al. 1999, Fisker et al. 2015).

In relation to its high pharmacological importance, βARs are in the main focus of structural analysis and, after photo-rhodopsin, β2- and β1AR were the second and third distinct GPCRs from which high-resolution structures could be obtained. Human β2AR could be crystallised in lipidic cubic phase with an inverse agonist bound after insertion of T4-lysozyme in the ICL 3 (Cherezov et al. 2007). Human β1AR is highly sensitive to detergents and high temperatures (Serrano-Vega and Tate 2009) and crystallisation trials were therefore focused on the more robust turkey β1AR, which could be crystallised in octylthioglucoside with a ligand after N- and C-terminal and ICL 3 truncation and introduction of eight thermostabilising mutations (Warne et al. 2008) (Fig. 1.7).

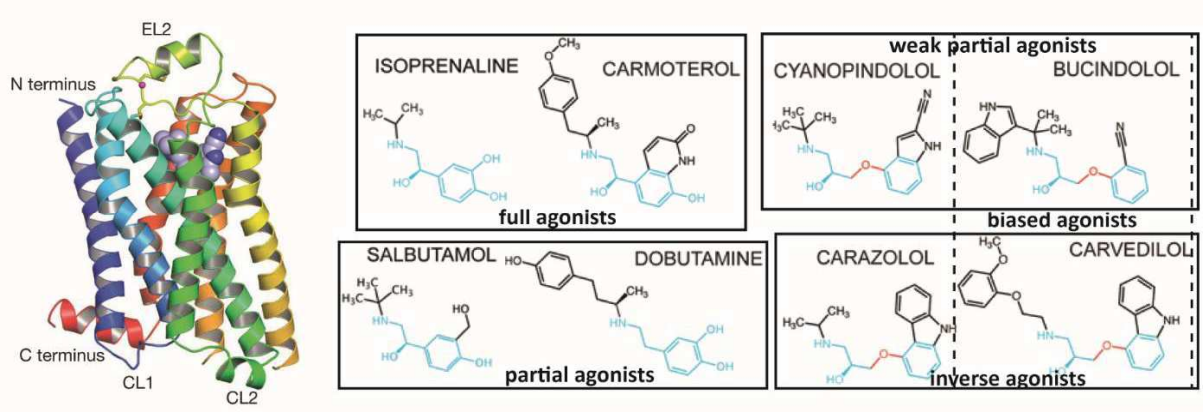

Fig. 1.7 Structures of a β1-adrenergic receptor and its ligands.

Left: Thermostabilised turkey β1AR bound to cyanopindolol was the third GPCR that could be crystallised in high resolution. Right: The pronounced pharmacological profile of β1AR includes full and partial agonists as well as inverse and biased agonists. Figures adapted from Warne et al. 2008 and Warne and Tate 2013.

β1AR has a pronounced pharmacological profile and a set of both full and partial agonists exist as well as inverse and biased agonists (Fig. 1.7). Up to date, 18 distinct structures of turkey β1AR are openly available, with bound inverse agonists, (neutral) antagonists and partial agonists as well as a structure crystallised without any ligand (Isberg et al. 2016). This profound data set helped in identification of critical determinants of ligand efficacy and biased signalling, which are based on differences in the contraction of the ligand binding pocket and a change in rotameric conformation of Ser 5.46 upon formation of a hydrogen bond with the ligand (Warne and Tate 2013).

The extensive structural information as well as high stability through thermostabilising mutations were the main reasons for the CFPS trials performed in the present study. A schematical overview on the constructs is given in Fig. 1.8. Mainly, a turkey β1AR construct was analysed containing deletions in the N- and C-terminus and in the ICL 3, with and without 11 point mutations, making the receptor highly thermostable. The thermostabilised construct was highly similar to a previously published design, where three additional mutations resulted in an increased stability compared to the β1AR construct used for initial crystallisation (Miller and Tate 2011). DNA templates for stabilised and non-stabilised turkey

β1AR were kindly provided by Ali Jazayeri (Heptares Therapeutics, Welwyn Garden City, UK). Furthermore, human β1AR was analysed in this study with thermostabilising mutations and truncations adapted from the turkey receptor and as full-length construct. Human β1AR has a sequence similarity of 76% with turkey β1AR, excluding the N- and C-terminal regions (Serrano-Vega and Tate 2009).

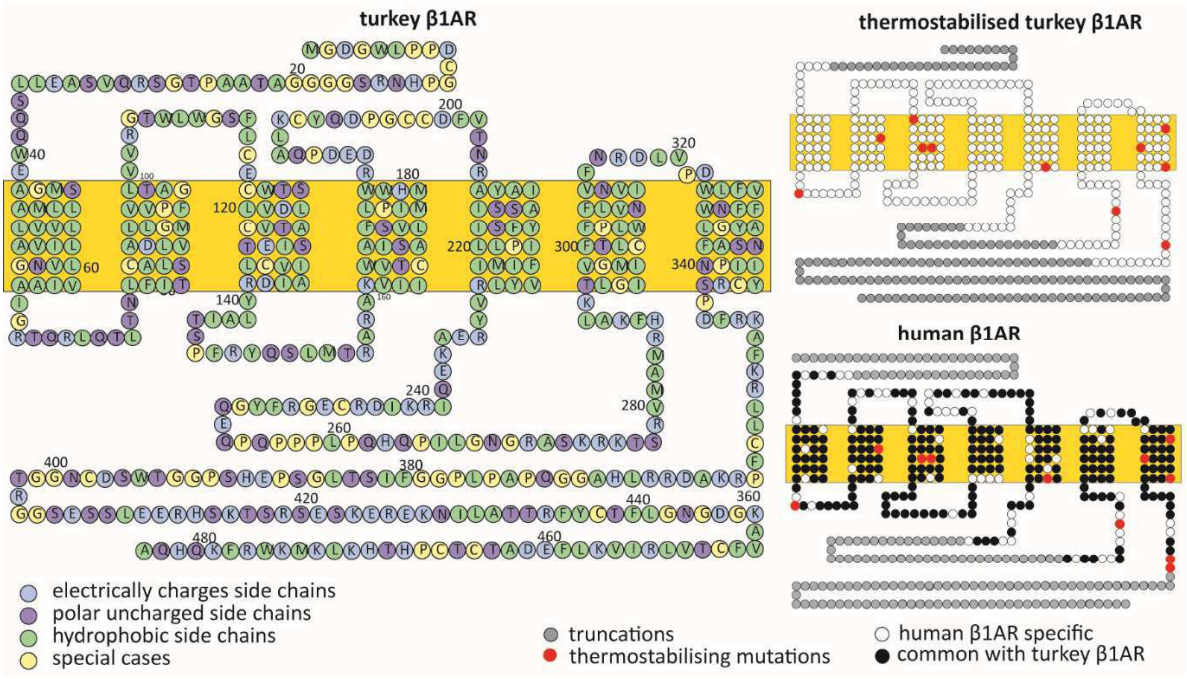

Fig. 1.8 β1-adrenergic receptor constructs analysed in this thesis.

The full-length turkey β1AR depicted on the left side was modified by truncations of the N- and C-terminus and in the ICL 3 and by introduction of 11 point mutations, making the receptor highly thermostable (top right). Human β1AR has a high sequence identity to the turkey variant and was analysed as a full-length thermostabilised truncated thermostabilised and truncated non-stabilised construct in this thesis (bottom right).

Receptors of the Endothelin system

The Endothelin system mediates the strongest vasoconstriction effects found so far in humans and other mammals (Alexander et al. 2015). It is pharmacologically addressed for the treatment of pulmonary arterial hypertension, chronic kidney disease, chronic heart failure and others. In humans, physiological effects are primarily mediated by three 21-amino acid long peptides called Endothelin 1 - 3 (ET-1 - 3), acting on the two Endothelin receptors type A and B (ETA and ETB). While ETA receptor shows and order of magnitude higher specificity to ET-1 and ET-2 than for ET-3, binding of all three Endothelins to ETB receptor is equally potent (Alexander et al. 2015). ET-1 is the most abundant Endothelin isoform in the human cardiovascular system. After its release from the endothelium, ET-1 mediates vasoconstriction mainly in a paracrine manner via ETA receptors in the adjacent smooth muscle cells, where phospholipase C mediated downstream signalling events cause Ca^{2+} influx and subsequent constriction (Vignon-Zellweger et al. 2012). Autocrine effects of ET-1 on ETB receptor the endothelium cells cause vasodilatation in the vascular system by nitric oxide release.

Additionally, ETB acts as a clearing receptor that binds, internalizes and removes ET-1 from circulation in the intercellular space (Vignon-Zellweger et al. 2012). Additional tissue distributions and functions have been reported for both receptors, with highest mRNA expression levels of ETB found in brain tissues that might be associated with high ET-3 levels in this body part (Alexander et al. 2015). High ETB receptor concentrations were also found in the kidney, where the Endothelin system contributes to renal hemodynamics and regulation of glomerular pressure (Vignon-Zellweger et al. 2012). ET-2 shows high pharmacological similarities to ET-1 and might have compensatory effects. Key roles in ovarian physiology and ovulation as well as chemokine roles in the inflammatory system are further debated (Alexander et al. 2015).

From a molecular and structural perspective, all three Endothelins are 21-amino acid long peptides that share sequence homology in the seven C-terminal amino acids. Two intramolecular disulphide bonds are further common characteristics, while the N-terminal part, which adapts α-helical shape in all three Endothelins, shows sequence alterations, in particular for the ET-3 peptide (Fig. 1.9).

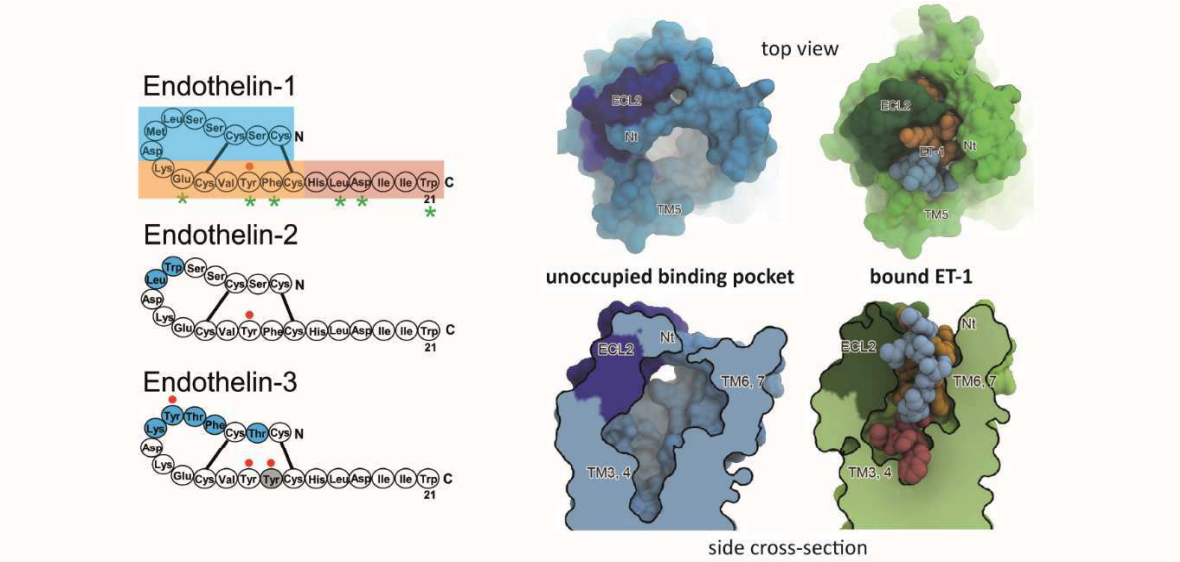

Fig. 1.9 Structural details of Endothelins and Endothelin receptors.

Left: Endothelin 1 - 3 show high sequence homology in the C-terminal region and common disulphide bridge formation, while the N-terminal region is altered, in particular in ET-3 (blue). Green stars indicate residues that are thought to form a stripe due secondary helical structure arrangements and red dots indicate potential sites for radiolabelling with ^{125}I. Right: The crystal structures of ETB with and without bound ET-1 offer structural insights in the binding affinity and specificity of the Endothelin system. Figures adapted from Davenport et al. 2016 and Shihoya et al. 2016.

Ligand specificity towards the two Endothelin receptors is mediated by the N-terminal part of the peptide, with Endothelin-3 having an order of magnitude lower affinity to ETA receptor, as mentioned earlier. The disulphide bridges have further effects on the ligand specificity and affinity of all three Endothelins to ETA is drastically reduced when they are abolished, while binding to ETB receptor is unimpaired (Tam et al. 1994, Lättig et al. 2009).

Two recently published crystal structures reveal structural insights in the binding mechanism of ET-1 to ETB receptor (Shihoya et al. 2016). The ligand is forming a question mark structure with the C-

terminus deeply inserted in the ligand binding cavity formed by the TMS of the ETB receptor (Fig. 1.9). An exceptional role for high affinity binding is mediated by the C-terminal Trp in ET-1 and mutations of this amino acid completely abolish ligand binding (Lättig et al. 2009). The curved region in the ET-1 question mark structure is pointing towards and interacting with the ECL 2 and N-term region of ETB and, although no high resolution structure of ETA is available to date, this interaction is thought to mediate ligand specificity, in accordance with the sequence alteration in ET-3 in this region (Lättig et al. 2009, Shihoya et al. 2016).

Not least because of their interesting ligand specificity and high physiological relevance, both ETA and ETB receptor were previously analysed by CFPS techniques (Klammt et al. 2007, Junge et al. 2010, Proverbio et al. 2013). So far, best production conditions of ETA receptor in a *E. coli* based CFPS system were found by P-CF-synthesis, solubilisation in LPPG and subsequent detergent exchange to either Brij-35 or Fos-16. Receptor samples were found to be homogeneous on SEC and ligand binding competent, although with significantly lower affinity than previously published data (Junge et al. 2010). For ETB receptor, so far best results were obtained by supplementation of ND (DMPC) in the CF-synthesis reaction. A distinct ligand binding behaviour could be observed by SPR-techniques, with affinities in the nanomolar range. However, upon radioligand binding assays, only minor fractions of the receptor were found to be ligand binding competent (Proverbio et al. 2013). Further ETB receptor synthesis in a an insect cell based CFPS system with ER-derived microsomes showed similar low folding efficiencies, which were accounted mainly for shortcomings of the membrane insertion machineries of the microsomes (Merk et al. 2015).

In this thesis, CFPS of both ETA and ETB receptor was studied (Fig. 1.10). The focus was on the ETB receptor, which was synthesised with a N-terminal deletion of the first 26 amino acids, which form a putative signal sequence and are truncated *in vivo* during receptor maturation and localisation at the plasma membrane (Saito et al. 1991). Furthermore, thermostabilised ETB receptor construct ranging from amino acid position 27 to 401 was analysed, as well as the full-length ETA receptor, which shows 63% sequence similarity with ETB receptor (Davenport et al. 2016).

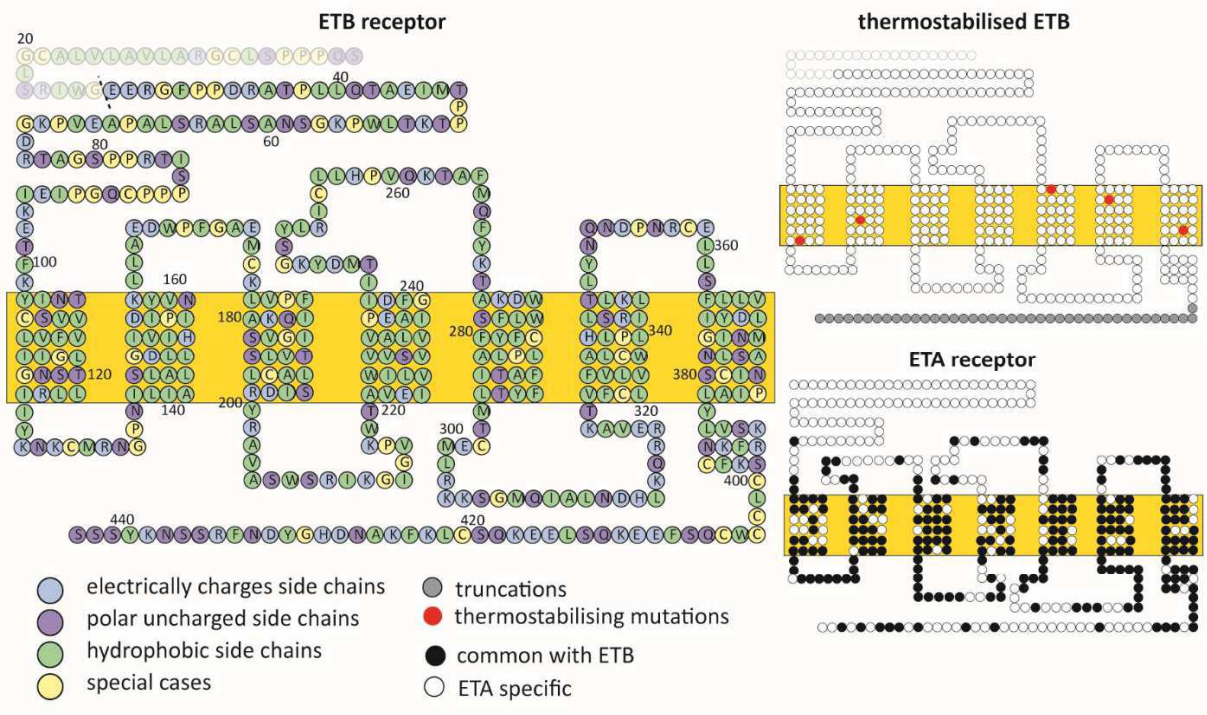

Fig. 1.10 Endothelin receptors analysed in this thesis.

ETB receptor was analysed as a construct without the 26 amino acid long N-terminal putative signal sequence and as a thermostabilised truncation construct. ETA receptor was analysed as a full-length construct, which shows 63% sequence similarity to ETB.

2 Materials

2.1 Equipment

2.1.1 Common equipment

Equipment	Type and manufacturer
Centrifuge	Mikro 22 R; Hettich (Tuttlingen, Germany) 5810 R; Eppendorf (Wesseling-Berzdorf, Germany) Megafuge 16R; Thermo Scientific (Langenselbold, Germany) Sorvall RC-5B; Thermo Scientific (Langenselbold, Germany) Sorvall RC-5C; Thermo Scientific (Langenselbold, Germany) Sorvall RC 3C +; Thermo Scientific (Langenselbold, Germany) Sorvall RC12BP+; Thermo Scientific (Langenselbold, Germany)
Extruder	Mini-Extruder; Avanti Polar Lipids (Alabaster, USA)
Glass equipment	Schott Duran (Mainz, Germany)
Heating block	Digital dry bath; Labnet International (Edison, USA) Standard Heatblock; VWR (Darmstadt, Germany)
Heating stirrer	Combimag RCT; IKA (Staufen, Germany)
Incubation chamber	Thermostatic cabinet; Lovibond (Amesbury, UK) Type BE 400; Memmert (Schwabach, Germany)
Microvave oven	Type A;817ASW; Bosch (Stuttgart, Germany)
pH-meter	PHM210; Radiometer (Copenhagen, Denmark)
Pipettes	Eppendorf Research; Eppendorf (Wesseling-Berzdorf, Germany)
Rotary evaporator	Rotavapor RE12; Buechi (Essen, Germany)
Rotary table	Promax 2020; Heidolph (Schwabach, Germany)
Spectrophotometer	Nanodrop 1000; Peqlab (Erlangen, Germany) U-1100; Hitachi (Duesseldorf, Germany) Spectrostar Nano; BMG Labtech (Ortenberg, Germany) SmartSpec Plus; Bio-Rad (Muenchen, Germany)
UV-light imager	Chroma 42; Vetter (Wiesloch, Germany)
Ultrapure water suspenser	Milli-Q academic; Merck-Millipore (Darmstadt, Germany)
Water bath	Type 002-2987; Haake (Hohenems, Austria)

2.1.2 Cloning and DNA preparation

Equipment	Type and manufacturer
Agarose gel electrophoresis chamber	Type 40-0911; Peqlab (Erlangen, Germany) Type 40-0708; Peqlab (Erlangen, Germany)
Agarose gel electrophoresis power supply	Pharmacia Biotech EPS 300; GE Life Sciences (Muenchen, Germany)
DNA purification kit	Miniprep Nucleospin Plasmid Kit; Macherey-Nagel (Dueren, Germany) Midiprep NucleoSpin Plasmid Kit; Macherey-Nagel (Dueren, Germany) QIAquik Gel Extraction Kit; Qiagen (Hilden, Germany) QIAquik PCR Purification Kit; Qiagen (Hilden, Germany)
PCR cycler	Peqstar 96 universal gradient; Peqlab (Erlangen, Germany)

2.1.3 *E. coli* handling

Equipment	Type and manufacturer
Autoclave	Type FNR 9252E; Integra (Gießen, Germany) Type GE 446EC-1; Gettinge (Rastatt, Germany)
Culture flasks	500 ml baffled flasks; Schott Duran (Mainz, Germany) 2 l baffled flasks; Schott Duran (Mainz, Germany)
Fermenter	Type 884 124/1; B. Braun (Melsungen, Germany)
French pressure cell disrupter	SLM; Amico Instruments (USA)
Incubation shaker	Multitron II; Infors (Bottmingen, Switzerland) innova 4330; Eppendorf (Wesseling-Berzdorf, Germany)
Ultra-sonificator	Labsonic U; B. Braun (Melsungen, Germany)

2.1.4 Protein purification

Equipment	Type and manufacturer
Anion exchange chromatography column	Q-Sepharose; GE Life Sciences (Muenchen, Germany)
Dialysis membrane	Spectra/Por 2 Dialysis Membrane MWCO 12-14 kDa; Carl Roth (Karlsruhe, Germany) Slide-A-Lyzer 1-3 ml, MWCO 10 kDa; Thermo Scientific (Langenselbold, Germany)
FPLC system	Aekta Prime plus; GE Life Sciences (Muenchen, Germany) Aekta Pure; GE Life Sciences (Muenchen, Germany) Aekta Purifier; GE Life Sciences (Muenchen, Germany)
Immobilised metal affinity chromatography column	HiTrap IMAC HP 5 ml; GE Life Sciences (Muenchen, Germany) Sepharose 6 Fast Flow; GE Life Sciences (Muenchen, Germany)
Peristaltic pump	ip-12; Ismatec (Wertheim, Germany)
Sepharose beads for ligand affinity chromatography column	Sepharose 4B; Sigma-Aldrich (Taufkirchen, Germany)
Size exclusion chromatography column	Superdex 200 3.2/300; GE Life Sciences (Muenchen, Germany) Superdex 200 3.2/300 increase; GE Life Sciences (Muenchen, Germany) Superdex 200 10/300 GL; GE Life Sciences (Muenchen, Germany)
Ultrafiltrator	Amicon Ultra-4, 10 kDa MWCO; Merck Millipore (Darmstadt, Germany) Amicon Ultra-15, 10 kDa MWCO; Merck Millipore (Darmstadt, Germany) Centriprep YM-10; Merck Millipore (Darmstadt, Germany)

2.1.5 Protein analysis

Equipment	Type and manufacturer
PAGE gel casting system	Mini-Protean Handcast systems; Bio-Rad (Muenchen, Germany)
PAGE gel power supply	Power Pac 3000; Bio-Rad (Muenchen, Germany)
PAGE chamber	Mini-Protean Tetra Cell; Bio-Rad (Muenchen, Germany)
Fluorescence reader	Genius Pro; Tecan (Meannedorf, Switzerland)
Luminescence imager	Lumi Imager F1; Roche (Penzberg, Germany)
Scintilication counter	300 SL; Hidex (Turku, Finland)
Semi-dry western blot device	Trans-Blot Turbo; Bio-Rad (Muenchen, Germany)
System for radioligand filter binding assay	Multiscreen HTS; Merck-Millipore (Darmstadt, Germany)

2.2 DNA and bacterial strains

2.2.1 Vectors and plasmids

Purpose	Vector
Vector for cell-free expression	pET-21a
Expression vector for MSPE3D1	pET-28a
Expression vector for roGFP1-iE	pQE-30
Expression vector for DsbA	pET-39b
Expression vector for DsbC	pET-40b

2.2.2 DNA templates

DNA templates for the turkey β1AR were kindly provided by Ali Jazayeri (Heptares Therapeutics, Welwyn Garden City, UK. Synthesised DNA for other receptors was obtained from Geneart (Germany). DNA template for roGFP1-iE was obtained from Addgene and kindly provided by S. James Remington (Department of Physics and Institute of Molecular Biology, University of Oregon, USA). Vector templates were obtained from Merck-Millipore (Darmstadt Germany). Coding DNA sequences for the receptor constructs analysed in this thesis are given in the appendix.

2.2.3 *E. coli* strains

Purpose	Strain
Production of cell-extract for CFPS	A19
DNA plasmid amplification	DH5α
Protein production in *E. coli*	BL21 (DE3) Star
Expression vector for DsbA	T7-express

2.3 Reagents and Chemicals

2.3.1 Common reagents and chemicals

1,4-Dithiotreitol (DTT)	Carl Roth (Karlsruhe, Germany)
2-Mercaptoethanol/β-Mercaptoethanol	Carl Roth (Karlsruhe, Germany)
Acetyl phosphate lithium potassium salt (ACP)	Sigma-Aldrich (Taufkirchen, Germany)
Adenosine 5'-triphosphate (ATP)	Roche (Penzberg, Germany)
Amino acids for CF expression	Sigma-Aldrich (Taufkirchen, Germany)
Ampicillin	Carl Roth (Karlsruhe, Germany)
Antifoam Y-30 emulsion	Sigma-Aldrich (Taufkirchen, Germany)
Bactotryptone	Carl Roth (Karlsruhe, Germany)
Bovine serum albumin Fraction V	Sigma-Aldrich (Taufkirchen, Germany)
Complete protease inhibitor cocktail	Roche (Penzberg, Germany)
Cytidine 5'-triphosphate di-sodium salt (CTP)	Sigma-Aldrich (Taufkirchen, Germany)
Dimethylsulfoxide (DMSO)	Carl Roth (Karlsruhe, Germany)
Dipotassium hydrogenphosphate (K_2HPO_4)	Carl Roth (Karlsruhe, Germany)
Ethidiumbromide (EtBr)	Carl Roth (Karlsruhe, Germany)
Ethylenediaminetetraacetic acid (EDTA)	Carl Roth (Karlsruhe, Germany)
Folinic acid calcium salt	Sigma-Aldrich (Taufkirchen, Germany)
Gene ruler 100bp, 1kb DNA ladder	ThermoScientific (Langenselbold, Germany)
Glucose monohydrate	Carl Roth (Karlsruhe, Germany)
γ-L-Glutamyl-L-cysteinyl-glycin (glutathione)	Carl Roth (Karlsruhe, Germany)
Glycerol	Carl Roth (Karlsruhe, Germany)
Guanosine 5'-triphosphate di-sodium salt (GTP)	Sigma-Aldrich (Taufkirchen, Germany)
HEPES	Carl Roth (Karlsruhe, Germany)
hydrochloric acid (32% HCl)	Carl Roth (Karlsruhe, Germany)
Imidazole	Carl Roth (Karlsruhe, Germany)
Isopropyl-β-D-thiogalactopyranosid (IPTG)	Carl Roth (Karlsruhe, Germany)
kanamycin	Carl Roth (Karlsruhe, Germany)

Lithiumchloride ($LiCl_2$)	Carl Roth (Karlsruhe, Germany)
Magnesium acetate tetrahydrate ($Mg(oAc)_2$)	Sigma-Aldrich (Taufkirchen, Germany)
Magnesium chloride hexahydrate ($MgCl_2$)	Sigma-Aldrich (Taufkirchen, Germany)
Natriumazid (NaN_3)	Sigma-Aldrich (Taufkirchen, Germany)
PEG 8,000	Sigma-Aldrich (Taufkirchen, Germany)
Peptone, tryptic digest	Carl Roth (Karlsruhe, Germany)
Phenylmethylsufonylfluoride (PMSF)	Sigma-Aldrich (Taufkirchen, Germany)
Phosphoenol pyruvic acid monopotassium salt (PEP)	Sigma-Aldrich (Taufkirchen, Germany)
Potassium chloride (KCl)	Carl Roth (Karlsruhe, Germany)
Potassium acetate (KoAc)	Sigma-Aldrich (Taufkirchen, Germany)
Potassium dihydrogenphosphate (KH_2PO_4)	Carl Roth (Karlsruhe, Germany)
Pyruvate kinase (PK)	Roche (Penzberg, Germany)
Restriction enzymes	NEB (Frankfurt, Germany)
RiboLock RNase inhibitor	ThermoScientific (Langenselbold, Germany)
Sodium chloride (NaCl)	Carl Roth (Karlsruhe, Germany)
T4 DNA-ligase	NEB (Frankfurt, Germany)
TCEP	Thermo Scientific (Langenselbold,Germany)
Tris-(hydroxymethyl)-aminomethan (TRIS)	Carl Roth (Karlsruhe, Germany)
tRNA E.coli MRE 600	Roche (Penzberg, Germany)
Turbo-Pfu DNA polymerase	Stratagene (Waldbronn, Germany)
Uridine 5'-triphosphate tri-sodium salt (UTP)	Sigma-Aldrich (Taufkirchen, Germany)
Sodium chloride	Carl Roth (Karlsruhe, Germany)
Yeast extract	Carl Roth (Karlsruhe, Germany)

2.3.2 Antibodies and horse-radish-peroxidase conjugates

Anti-penta His IgG from mouse	Qiagen (Hilden, Germany)
Anti-mouse IgG HRP conjugate from goat	Sigma-Aldrich (Taufkirchen, Germany)
Precision Protein StrepTactin-HRP conjugate	Bio-Rad (München, Germany)

2.3.3 Detergents and Lipids

Brij-35, polyoxyethylene-(23)-lauryl-ether	Sigma-Aldrich (Taufkirchen, Germany)
Brij-58, polyoxyethylene-(20)-cetyl-ether	Sigma-Aldrich (Taufkirchen, Germany)
Brij-78, polyoxyethylene-(20)-stearyl-ether	Sigma-Aldrich (Taufkirchen, Germany)
TritonX-100, polyethylene-glycol-P-1,1,3,3-tetramethylbutylphenyl-ether	Sigma-Aldrich (Taufkirchen, Germany)
Digitonin	Sigma-Aldrich (Taufkirchen, Germany)
SDS, sodium-dodecyl-sulfate	Carl Roth (Karlsruhe, Germany)
Sodium cholate	Carl Roth (Karlsruhe, Germany)
Tween-20, polyoxy-ethylene-sorbitan-mono-laurate 20	Carl Roth (Karlsruhe, Germany)
DDM, n-dodecyl-β-D-maltoside	Anatrace (Affymetrix, USA)
DPC, Fos-12, n-dodecylphosphocholine	Anatrace (Affymetrix, USA)
LMPG, 1-myristoyl-2-hydroxy-sn-glycero-3-[phospho-rac-(1-glycerol)]	Anatrace (Affymetrix, USA)
DH_7PC, 1,2-diheptanoyl-sn-glycero-3-phos-phocholine	Anatrace (Affymetrix, USA)
Fos-16, n-hexadecylphosphocholine	Anatrace (Affymetrix, USA)
DMPC, 1,2-dimyristoyl-sn-glycero-3-phos-phocholine	Avanti Polar Lipids (Alabaster, USA)
DMPG, 1,2-dimyristoyl-sn-glycero-3-phospho-(1'-rac-glycerol)	Avanti Polar Lipids (Alabaster, USA)
DPPG ,1,2-dipalmitoyl-sn-glycero-3-phos-pho-(1'-rac-glycerol)	Avanti Polar Lipids (Alabaster, USA)
POPC, -palmitoyl-2-oleoyl-sn-glycero-3-phosphocholine	Avanti Polar Lipids (Alabaster, USA)
POPG, 1-palmitoyl-2-oleoyl-sn-glycero-3-phospho-(1'-rac-glycerol)	Avanti Polar Lipids (Alabaster, USA)
POPS, 1-palmitoyl-2-oleoyl-sn-glycero-3-phospho-L-serine	Avanti Polar Lipids (Alabaster, USA)
DOPA, 1,2-dioleoyl-sn-glycero-3-phosphate	Avanti Polar Lipids (Alabaster, USA)
DOPE, 1,2-dioleoyl-sn-glycero-3-phosphoethanolamine	Avanti Polar Lipids (Alabaster, USA)
DOPC, 1,2-dioleoyl-sn-glycero-3-phosphocholine	Avanti Polar Lipids (Alabaster, USA)
DOPG, 1,2-dioleoyl-sn-glycero-3-phospho-(1'-rac-glycerol)	Avanti Polar Lipids (Alabaster, USA)
DOPS, 1,2-dioleoyl-sn-glycero-3-phospho-L-serine	Avanti Polar Lipids (Alabaster, USA)
DEPG, 1,2-dielaidoyl-sn-glycero-3-phospho-(1'-rac-glycerol)	Avanti Polar Lipids (Alabaster, USA)
SOPG, 1-stearoyl-2-oleoyl-sn-glycero-3-phospho-(1'-rac-glycerol)	Avanti Polar Lipids (Alabaster, USA)
Cholesterol	Sigma Aldrich (Taufkirchen, Germany
Cholesteryl hemisuccinate	Sigma Aldrich (Taufkirchen, Germany)

2.3.4 Ligands

[^{3}H]-dihydroaprenolol	Biotrend (Cologne, Germany)
[^{125}I]-Endothelin-1	PerkinElmer (Rodgau, Germany)
Endothelin1	Dr. Michael Beyermann, FMP Berlin (Germany)
Dihydroalprenolol	Tocris Bioscience (Bristol, UK)
Carvedilol	Tocris Bioscience (Bristol, UK)
Labetalol	Sigma Aldrich (Taufkirchen, Germany)
Metoprolol	Sigma Aldrich (Taufkirchen, Germany)
Nebivolol	Sigma Aldrich (Taufkirchen, Germany)

2.4 Buffers and Solutions

2.4.1 *E.coli* handling

1000 x ampicillin stock	100 mg/ml ampicillin in 50% ethanol
1000 x kanamycin stock	30 mg/ml kanamycin in water
LB agar plates	5 g/l yeast extract 10 g/l peptone 10 g/l NaCl 15 g/l agar agar
LB medium	5 g/l yeast extract 10 g/l peptone 10 g/l NaCl
SOC medium	5 g/l yeast extract 20 g/l peptone 0.5 g/l NaCl 1 M KCl
YPTG medium	10 g/l yeast extract 16 g/l peptone 5 g/l NaCl 100 mM glucose 22 mM KH_2PO_4 40 mM K_2HPO_4
DB salt buffer	5.22 mM $(NH_4)H_2PO_4$ 0.05 mM $mgSO_4$ 0.2 mM KCl 44% glycerol

2.4.2 S-30 extract preparation

LY buffer	10 mM Tris-acetate pH 8.2 14 mM magnesium acetate 250 mM KCl
LY-A	LY buffer + 6 mM β-mercaptoethanol
LY-B	LY buffer + 1 mM DTT + 1 mM PMSF
LY-C	LY buffer

2.4.3 T7-RNA polymerase preparation

buffer A	30 mM Tris-Cl pH 8.0 50 mM NaCl 10 mM EDTA 10 mM β-mercaptoethanol 5% glycerol
Buffer B	buffer A but 1 mM EDTA
Buffer C	10 mM K_2HPO_4/ KH_2PO_4 pH 8.0 10 mM NaCl 0.5 mM EDTA 1 mM DTT 5% glycerol

2.4.4 Cell-free protein synthesis

HE buffer stock	2.5 M HEPES-KOH pH 8.0 500 mM EDTA
S30 buffer	10 mM Tris-acetate pH 8.2 14 mM magnesium acetate 250 mM KCl

2.4.5 MSP1E3D1 purification

MSP-buffer	40 mM Tris-Cl pH 8.0 300 mM NaCl
MSP-A	MSP-buffer + 1% (v/v) Triton X-100
MSP-B	MSP-buffer + 50 mM sodium cholate pH 8.9
MSP-C	MSP-buffer pH 8.9
MSP-D	MSP-buffer
MSP-E	MSP-buffer + 50 mM imidazole
MSP-F	MSP-buffer + 300 mM imidazole
MSP-G	MSP-buffer + 10% glycerol

2.4.6 RoGFP purification

Buffer A	40 mM Tris-Cl pH 8.0 300 mM NaC
Buffer B	buffer A + 300 mM imidazole
Buffer C	20 mM Tris-Cl pH 7.5 150 mM NaCl

2.4.7 DsbA and DsbC purification

Buffer A	40 mM Tris-Cl pH 8.0 300 mM NaCl 10 mM imidazole
Buffer B	40 mM Tris-Cl pH 8.0 300 mM NaCl 300 mM imidazole
Buffer C	20 mM Tris-Cl pH 8.0 150 mM NaCl 1 mM DTT 5% glycerol

2.4.8 Nanodisc and liposome preparation

DF-buffer	10 mM Tris-Cl pH 7.5 100 mM NaCl

2.4.9 Purification of Endothelin receptor type B in nanodiscs by IMAC

Buffer A	40 mM Tris-Cl pH 8.0 300 mM NaCl
Buffer B	40 mM Tris-Cl pH 8.0 300 mM NaCl 25 mM imidazole
Buffer C	40 mM Tris-Cl pH 8.0 300 mM NaCl 300 mM imidazole
Buffer D	20 mM Tris-Cl pH 7.5 200 mM NaCl

2.4.10 Purification of β1-adrenergic receptor in nanodiscs by IMAC

Buffer A	20 mM Tris-Cl pH 8.0 350 mM NaCl 10 mM imidazole
Buffer B	20 mM Tris-Cl pH 8.0 350 mM NaCl 30 mM imidazole
Buffer C	20 mM Tris-Cl pH 8.0 350 mM NaCl 300 mM imidazole

2.4.11 Purification of β1-adrenergic receptor in nanodiscs by LAC

Buffer A	20 mM Tris-Cl pH 8.0 350 mM NaCl 1 mM EDTA
Buffer B	20 mM Tris-Cl pH 8.0 1 M NaCl 1 mM EDTA
Buffer C	20 mM Tris-Cl pH 8.0 350 mM NaCl 1 mM EDTA 500 µM dihydro-alprenolol
Buffer D	10 mM Tris-Cl pH 7.5 100 mM NaCl

2.4.12 SDS-PAGE and western blot

4% stacking gel	130 mM Tris-Cl pH 6.8 17% (v/v) Rotiphorese Gel 30 (Carl Roth) 0.1% (w/v) SDS 0.1% (w/v) APS 0.1% (v/v) TEMED in water
15% (12%) separating gel	375 mM Tris-Cl pH 8.0 50 (40)% (v/v) Rotiphorese Gel 30 (Carl Roth) 0.1% (w/v) SDS 0.1% (w/v) APS 0.1% (v/v) TEMED in water
5-fold sample buffer	125 mM Tris-Cl pH 6.8 2 mM EDTA 0.04% (w/v) bromphenolblue 4% (w/v) SDS 10% (v/v) β-mercaptoethanol 20% (v/v) glycerol in water
SDS-electrophoresis buffer	25 mM Tris 190 mM glycine 0.1% (w/v) SDS in water
Coomassie staining solution	2.5 mg/ml Coomassie Brilliant Blue R-250 50% (v/v) methanol 10% (v/v) glacial acetic acid in water
Destaining solution	50% (v/v) methanol 10% (v/v) glacial acetic acid in water
PBS	8 mM Na_2HPO_4 0.15 mM NaH_2PO_4 0.3 mM KCl 137 mM NaCl
PBS-T	PBS + 0.05% (v/v) Tween-20
Blocking buffer	PBS-T + 4% (w/v) skim milk powder
ECL-solution	1:1 mixture of ECL Prime solution 1 + 2 (GE Life Sciences)

2.4.13 Radioligand filter binding assay

Binding buffer	50 mM HEPES/NaOH pH 7.5 1 mM $CaCl_2$ 5 mM $mgCl_2$ 0.2% (w/v) BSA
Pre-wash buffer	50 mM HEPES/NaOH pH 7.5 0.5% (w/v) BSA
Wash buffer	50 mM HEPES/NaOH pH 7.5 500 mM NaCl 0.1% (w/v) BSA

2.4.14 Protein analysis and quantification

SEC-buffer	20 mM Tris-Cl pH 7.5 200 mM NaCl
Bradford solution	0.01% (w/v) Coomassie Brilliant Blue G250 5% (v/v) ethanol 8.5% (v/v) phosphoric acid
GFP-buffer	20 mM Tris-Cl pH 7.5 150 mM NaCl

3 Methods

All buffer compositions are listed in detail in 2.4.

3.1 Molecular- and microbiology

3.1.1 Cloning and DNA preparation

Concentration of DNA in aqueous solutions was routinely determined by absorbance at 260 nm on a spectrophotometer (Nanodrop 1000, Peqlab) using Lambert-Beer's law and an extinction coefficient of 50 µg/ml.

DNA templates for CF-expression were generally inserted in pET-21a by standard restriction cloning procedures. First, respective restriction sites were introduced in the DNA template by polymerase chain reaction (PCR) produce using specifically designed primers. PCR reaction was performed in a PCR cycler (Peqstar 96 universal gradient, Peqlab) in 50 µl volumes according the protocol given in Tab. 3.1.

Tab. 3.1 Polymerase chain reaction (PCR) in 50 µl scale.

Compound	Stock conccentration	Final concentration.	PCR cycle
DNA template	variable	1-6 µg/ml	7 min, 95°C
5'-primer	10 µM	10 pM	
3'-primer	10 µM	10 pM	35 x repeat:
DNTP mixture	10 mM (2.5 mM each)	200 µM	1 min, 95°C
Polymerase buffer	10 x	1 x	30s, 42-65°C
PfuUltra HF DNA polymerase	2.5 U/µl	0.02 U/µl	1.5 min, 72°C
			7 min, 72°C

Amplified DNA was purified with standard purification procedures (QIAquik PCR Purification Kit, Qiagen) and DNA template as well as target vector DNA were cut with the respective restriction enzymes according to manufacturer instructions (New England Biolabs). DNA template and target vector were then purified by separation in a 1% agarose gel and extracted by applying standard DNA gel extraction procedures (QIAquik Gel Extraction Kit, Qiagen). Both purified DNA preparation were then used for 30 µl ligation reaction with a stoichiometric ratio of insert to vector of 7:1. Ligation was performed at 16°C for over night subsequently transformed in *E. coli* strain DH5α for amplification. Correct insertion of the DNA template was analysed by sequencing.

DNA purification was performed from cultures with transformed *E. coli* strain DH5α in LB medium grown for over night at 37°C. Analytical scale preparations for sequencing and other DNA analyses were performed from 5 ml cultures using the Miniprep NucleoSpin Plasmid Kit (Macherey-Nagel) and preparative purification for CF-expression was performed from 200 ml cultures using the Midiprep NucleoSpin Plasmid Kit (Macherey-Nagel).

3.1.2 *E. coli* handling

Handling of genetically modified *E. coli* was performed by selection through implanted resistance for antibiotics. Routinely, either ampicillin in a final concentration of 100 µg/ml or kanamycin in a final concentration of 30 µg/ml was used.

For DNA transformation in chemical competent *E. coli* cell strain DH5α, ca. 50 µl of a glycerol cell stock were thawed on ice and approx. 50 - 500 ng DNA were added as a aqueous solution, thoroughly mixed and incubated on ice for 20 min. A heat shock of 42°C was applied for 45 s, followed by a rest period of approx. 5 min on ice. 300 µl of SOC-medium was added and incubated at 37°C for 45 min before platting 10 - 20 µl of the culture on a agar plate. If transformation was subsequent to ligase reaction, cells were pelleted and resuspended in a smaller volume before plating to increase the likelihood of positive clones.

For preparation of glycerol stocks, DNA was transformed in *E. coli* strain DH5α and plated on a agar plate. A clone was picked and used for inoculation of a 5 ml culture of sterile LB medium, which was grown over night at 37°C. Cells were pelleted by centrifugation at 6,000 x g for 10 min and resuspended in 500 µl of DB salt buffer. Glycerol stocks were stored at -80°C.

3.2 Cell-free-protein synthesis

E. coli based CF-protein synthesis was performed with strain A19 derived S30-extract under control of T7 regulatory elements with supplied T7-RNA polymerase at 30°C for approx. 17 h, if not stated elsewhere. Synthesis was performed in continuous exchange CF mode (CECF) with a feeding mixture (FM) that was connected to the reaction mixture (RM) with a semi-permeable membrane (MWCO 12-14 kDa) and acting as a supply for small molecular mass compounds. Ratios of RM to FM were routinely 1:15 to 1:20.

3.2.1 S30-extract preparation

E. coli strain A19 was used for preparation of the CF-extract. Cells from a glycerol stock were plated on an agar-plate and colonies were grown over night. Several colonies were picked for inoculation of a pre-culture with 120 ml of sterile LB medium in a baffled 500 ml flask. Pre-culture was incubated over night at 37°C while shaking at 180 rpm. The next day, 100 ml of the pre-culture were transferred 10 l of YPTG medium in a fermenter. Cells were grown in the fermenter at 37°C, stirring at 500 rpm and continuous air supply to an $OD_{600\,nm}$ of approx. 3.5 to 4.5. Culture was cooled down to approx. 20°C within 20 – 40 min in the fermenter and cells were harvested by centrifugation at 6,800 x g for 15 min. The pellet was sequentially resuspended in 300 ml LY-A buffer and pelleted again by centrifugation at 8,000 x g for 10 min for a total of three cycles. After removal of the supernatant from the last washing step, the pellet was weighted and resuspended in 110% (w/v) LY-B buffer. Cells were disrupted by using a french pressure cell disrupter (SLM, Amico Instruments) and cell debris was removed by sequential centrifugation at 30,000 x g for 30 min for two cycles. Supernatant was then transferred to a fresh tube and a final concentration of 400 mM NaCl was supplemented. The lysate was incubated for 45 min in a water bath at 42°C for removal of stalled ribosomes. The solution became turbid and was dialysed against a 100-fold excess of LY-C buffer in a 12 - 14 kDa cut-off membrane. The buffer was changed after 2 - 3 hours and dialysis was continued for over night. The next day, precipitated proteins were removed by repeated centrifugation at 30,000 x g for 30 min (2 cycles). The final S30-extract was aliquoted, shock-frozen in liquid nitrogen and stored at -80°C. All centrifugation and handling steps were performed on ice or at 4°C, if not indicated elsewhere.

3.2.2 Preparation of T7-RNA polymerase

DNA template for T7-RNA polymerase (T7RNAP) in pAR1219 vector was freshly transformed in *E. coli* strain BL21 (DE3) Star and plated on an agar-plate. A 100 ml pre-culture of sterile LB medium in a 500 ml baffled flask was inoculated and grown over night at 37°C. The next day, 10 ml pre-culture was transferred in 1 l of sterile LB medium in a baffled 2 l flask and grown to $OD_{600\,nm}$ = 0.6 – 0.8 at 37°C under continuous shaking at 180 rpm before T7RNAP expression was induced by addition of 1 mM IPTG and performed for 3 h without temperature change. Cells were harvested by centrifugation at 6,800 x g for 15 min and resuspended in 30 ml of buffer A before cell disruption using a french pressure cell disrupter. The cell debris was removed by centrifugation at 20,000 x g for 30 min and 3% streptomycin sulfate was added dropwise under gentle stirring in order to precipitate nucleic acids. After 5 min incubation on ice, precipitate was removed by centrifugation at 20,000 x g for 30 min. All steps

were performed either on ice or at 4°C to this point. The supernatant was next loaded on a 40 ml Q-Sepharose column (GE Life Sciences) pre-equilibrated with two CV of buffer B and unbound protein was removed by rinsing with buffer B until $A_{280\,nm}$ in the elution became stable. Protein was eluted by applying a gradient from 50 to 500 mM of NaCl and fractions of 1 ml were collected. All purification steps were performed at 16°C on a FPLC system (Aekta Purifier, GE Life Sciences) with a flow rate of 3 ml/min. Elution fractions were analysed by SDS-PAGE and Coomassie staining for a prominent T7RNAP band at 90 kDa. T7RNAP containing fractions were pooled and dialysed against a 100-fold excess of buffer C. Buffer was changed after 2 - 3 h and dialysis continued for over night. T7RNAP was then concentrated by ultrafiltration (Amicon Ultra-4, 10 kDa MWCO, Merck-Millipore) to a final concentration of 4 – 8 mg/ml. Glycerol was added in a final concentration of 50% (v/v) and aliquots were stored at -80°C.

3.2.3 Preparation of reaction mixture and feeding mixture

CF-reaction was routinely performed in analytical scale with a reaction mixture (RM) volume of 55 µl and a feeding mixture (FM) volume of 950 µl or in preparative scale with a RM volume of 1 – 3 ml and a FM volume of 17 – 45 ml. Both mixtures were freshly prepared from stock solutions stored at -20°C, if not stated elsewhere. Components were thoroughly mixed before addition and volumes were calculated with a 15% excess to compensate for pipetting losses. Component concentrations and volumes are given in Tab. 3.2 for a 1 ml RM/17 ml FM setup.

Tab. 3.2 CF-reaction setup for 1 ml RM and 17 ml FM.

Master mixture (MM)

Compound	Stock conc.	Final conc.	Volume
20 amino acid mixture~	25 mM	1 mM	726 µl
Acetyl phosphate (Li^+, K^+) (AcP), pH 7.0	1 M	20 mM	363 µl
Phospho(enol)pyruvic acid (K+) (PEP), pH 7.0	1 M	20 mM	363 µl
NTP mixture, pH 7.0+	75 x	1 x	242 µl
DTT#	500 mM	2 mM	72.6 µl
Folinic acid	10 mg/ml	100 µg/ml	181.5 µl
Complete protease inhibitor (Roche)	50 x	1 x	363 µl
HE buffer, pH 8.0*	24 x	1 x	756 µl
Magnesium acetate	2 M	12.4 (18) mM$	112.5 µl
Potassium acetate	4 M	130 (290) mM&	590 µl
PEG 8000	40%	2%	908 µl
Sodium azide	10%	0.05%	90.8 µl
Total volume			4.8 ml

Feeding mixture (FM)

compound	Stock conc.	Final conc.	Volume
MM			4.5 ml
20 amino acid mixture	25 mM	1 mM	680 µl
S30 buffer	1 x	0.4 x§	6.8 ml
Water°			5,6 ml
Total volume			17 ml

Reaction mixture (RM)

compound	Stock conc.	Final conc.	Volume
MM			302 µl
S30-extract	1 x	0.4 x	460 µl
DNA template	500 µg/ml	30 µg/ml	69 µl
RNAse inhibitor (RiboLock, Thermo Fischer)	40,000 U/ml	300 U/ml	8.63 µl
T7RNAP	3200 U/ml	40 U/ml	14.38 µl
E. coli tRNA	40 mg/ml	0.5 mg/ml	14.38 µl
Pyruvate kinase (Sigma Aldrich)	10 mg/ml	0.04 mg/ml	4.6 µl
Water‘			277 µl
Total volume			1.15 ml

~ Amino acid mixture was prepared as a suspension with 25 mM of each amino acid in water

+ NTP mixture stock contained 360 mM ATP and each 240 mM CTP, GTP, UTP

DTT was substituted with TCEP from a 500 mM stock or GSH/GSSG mixtures from a 100 mM stock in some assays. All redox reagent stocks were freshly prepared before usage.

* HE buffer stock was prepared with 2.5 M HEPES/KOH (pH 8.0) and 500 mM EDTA

$ Optimal concentration of Mg^{2+} ions in the CF-reaction was extract-dependent and usually in a range from 16 – 22 mM. A concentration of 5.6 mM Mg^{2+} ions was generally assumed to be contributed by the S30-extract, resulting in a final concentration of 18 mM in this example.

& A concentration of 160 mM K^+ ions was contributed by the S30-extract (21 mM), AcP (22 mM), PEP (67 mM) and HE buffer (50 mM), resulting in a final concentration of 290 mM in this example.

§ S30 buffer was added in the FM corresponding to the S30-extract in the RM.

, Variable volumes of water were added to fill up to the total volume of RM and FM.

In a first step, a master mix was prepared containing small molecular mass compounds for both RM and FM. The respective volume fraction for the FM was removed and supplemented with additional amino acids and S30-buffer corresponding to the S30-extract in the RM. The FM was then filled up to the final volume with water. RM was next supplemented with high molecular weight compounds including DNA

and the S30-extract. Both RM and FM were thoroughly mixed before transfer into the continuous exchange cell free (CECF) setup (see 1.3.1).

3.2.4 Reaction container assembly and cell free-synthesis reaction

Continuous exchange cell free (CECF) reactions were performed using custom made analytical scale reaction containers for RM and 24-well plates for FM. Dialysis membranes were prepared as patches from standard dialysis tubes (MWCO 12-14 kDa) which were previously prepared. Therefore, ca. 20 – 30 cm of dialysis tubes were submerged in a beaker with 300 ml water and a spatula-tip of sodium dihydrogenphosphate and heated in a microwave oven for 3 min at 800 W. Tubes were rinsed with water, submerged in an aqueous solution of 2 mM EDTA and heated again in a microwave oven. Tubes were subsequently rinsed extensively with water to remove EDTA and submerged in water, followed by another cycle of heating and rinsing. Prepared tubes were stored in 0.02% sodium azide at 4°C. For preparative scale reactions, commercial dialyser cartridges (Slide-A-Lyzer 1-3 ml, MWCO 10 kDa, Thermo Fischer) were used for RM with custom made FM containers.

CF-synthesis was usually performed at 30°C for approx. 17 h under continuous shaking at ca. 120 rpm, if not stated elsewhere. After synthesis reaction, RM was thoroughly mixed in order to suspend potential precipitates and removed from the reaction container. Potential precipitates were subsequently separated by centrifugation at 18,000 x g and 4°C for 10 min. If precipitates were further processed, a rinsing procedure was applied to remove contaminations from the RM. Therefore, precipitates from one analytical scale reaction (55 µl) were usually resuspended in 100µl of S30-buffer and centrifuged at 18,000 x g and 4°C for 10 min. The process was repeated once before further processing of the precipitate.

3.3 Protein expression in *E. coli*

3.3.1 Expression of MSP1E3D1

MSP1E3D1 DNA template with an N-terminal Hi_6-tag in a pET-28a vector was freshly transformed in *E. coli* strain Bl21 (DE3) Star. Several colonies were picked and used for inoculation of pre-cultures of autoclaved LB medium (4 x 200 ml) supplemented with 30 µg/ml kanamycin. Pre-cultures were grown for over night at 37°C and continuous shaking at 180 rpm in baffled 500 ml flasks. The next day, pre-cultures were pooled and each 50 ml were added to 12 baffled 2 l flasks containing 600 ml of sterile LB medium supplemented with 0.5% (w/v) sterile glucose and 30 µg/ml kanamycin. Cells were grown at 37°C and continuous shaking at 180 rpm until $OD_{600\ nm}$ = 1.0 before induction of MSPE3D1 expression with 1 mM of freshly prepared IPTG. Expression was performed with shaking at 180 rpm at 37°C for 1 h and another 3 – 4 h at 28°C. Cells were pelleted by centrifugation at 6,000 x g for 20 min at 4°C and resuspended in 100 ml of the supernatant. Suspension was transferred to 50 ml tubes and centrifuged again at 6,000 x g at 4°C for 20 min. Supernatant was removed and cell pellets (usually 4 x 5 to 10 g) were stored at – 80°C.

3.3.2 Expression of roGFP1-iE

DNA template for roGFP1-iE with an N-terminal His_6-tag in a pQE30 vector was freshly transformed in an *E. coli* BL21 strain (T7 express, New England Biolabs). Several colonies were picked and used for inoculation of 1 l sterile LB medium supplemented with 100 µg/ml ampicillin in a 2 l baffled flask. Cells were grown at 37°C for over night while shaking with 180 rpm and roGFP expression was induced with 1 mM IPTG. Expression was performed at 18°C for 24 h at continuous shaking. Cells were harvested by centrifugation at 30,000 x g for 30 min and stored at -80°C. Approx. 3 g of wet cell pellet could be harvested from 1 l of expression.

3.3.3 Expression of DsbA and DsbC

DNA templates for DsbA or DsbC with a C-terminal His_6-tag in pET-39b or pET-40b vector were freshly transformed in an *E. coli* BL21 strain (T7 express, New England Biolabs). Several colonies were picked used for inoculation of 100 ml of pre-culture of sterile LB medium supplemented with 30 µg/ml kanamycin in 500 ml baffled flasks. Cells were grown over night at 37°C while continuous shaking at 180 rpm. The next day, 50 ml of pre-culture was added to 1 l sterile LB medium supplemented with 30 µg/ml kanamycin in 2 l flasks. Cells were grown to $OD_{600\ nm}$ = 1.0 at 37°C and shaking at 180 rpm. Expression was induced by addition of 1 mM IPTG and sustained for 3 h at 37°C. Cells were harvested by centrifugation at 30,000 x g for 30 min at 4°C and stored at -80°C. Approx. 5 g of wet cell pellet could be obtained from 1 l of expression for both constructs.

3.4 Protein purification

3.4.1 MSP1E3D1 purification

Frozen cell pellets (5 – 10 g) from MSPE3D1 expression (see 3.3.1) were thawed on ice and resuspended in 100 ml freshly prepared ice-cold MSP-buffer containing Complete protease inhibitor (Roche) and 1 mM PMSF from a 100 mM stock in ethanol. Triton X-100 was added in a final concentration of 1% (v/v) from a 10% (v/v) stock in water. Cells were disrupted by pulsed ultra-sonification for 3 x 60 s and 3 x 45 s and 60 s rest period after each cycle. Suspension was kept on ice during cell disrupting procedure and gently stirred during rest periods on ice. Cell debris was removed by centrifugation at 30,000 x g at 4°C for 30 min. Supernatant was briefly applied to ultra-sonification (1 x 30 s) to ensure breakage of remaining DNA strands before it was filtered trough a 0.45 µm filter. The filtered lysate was loaded on a Ni^{2+}-immobilized IMAC column with a bed volume of ca. 15 ml that was pre-equilibrated with MSP-A buffer. The loading procedure was performed at room temperature with a flow rate of 2 ml/min. IMAC column was subsequently washed with 80 ml of MSP-A, 80 ml of MSP-B, 40 ml of MSP-C, 80 ml of MSP-D and 80 ml of MSP-E buffer at a flow rate of 3 ml/min at room temperature. Purified MSPE3D1 was eluted with MSP-F buffer at a flow rate of 3 ml/min in fractions of 2 ml. All washing steps were performed at room temperature on a FPLC system (Aekta Prime plus, GE Healthcare). Protein containing fractions were pooled and glycerol was added in a final concentration of 10% (v/v), followed by dialysis against 5 l of MSP-G buffer at 4°C for 2 – 3 h and another dialysis step with 5 l MSP-G buffer at 4°C for over night. Aliquots of ca. 5 – 10 ml containing ca. 80 – 100 µM of MSPE3D1 were shock-frozen in liquid nitrogen and stored at -80°C.

3.4.2 RoGFP1-iE purification

Frozen cell pellets from 1l of roGFP1-iE expression (ca. 3 g, see 3.3.2) were thawed on ice and resuspended in 50 ml of buffer A supplemented with Complete protease inhibitor (GE Life Sciences). Cells were disrupted by ultra-sonification for 3 x 60 s with a rest period of 60 s between each cycle. Cells were kept on ice during ultra-sonification procedure and gently stirred on ice during the rest period. Cell debris was removed by centrifugation for 30 min at 30,000 x g at 4°C and supernatant was loaded at a flow rate of 2 mL/min on a 5 ml HiTrap IMAC HP column (GE Life Sciences) pre-equilibrated with buffer A. After rinsing with five CV of buffer A, protein was eluted by applying a gradient of 0 to 100% buffer B for 40 CV at a flow rate of 2 ml/min and collected in 1 ml fractions. Purification was performed on a FPLC system (Aekta Pure, GE Life Sciences) at 4°C. The GFP protein was traced during elution by its specific absorbance at 485 nm. Fractions containing roGFP were pooled and concentrated by ultrafiltration (Amicon Ultra-15, 10 kDa MWCO, Merck Millipore) to a final volume of 3 ml and a protein concentration of 200 µM, as checked by absorbance at 280 nm. Protein was dialysed against buffer C, aliquoted in 200 µl fraction, shock frozen in liquid nitrogen and stored at -80°C. All purification and dialysis steps were performed at 4°C.

3.4.3 DsbA and DsbC purification

Frozen cell pellets from 1 l of DsbA or DsbC expression (ca. 5 g, see 3.3.3) were thawed on ice and resuspended in 50 ml of buffer A supplemented with Complete protease inhibitor (Roche). Cells were disrupted by ultra-sonification for 3 x 60 s with a rest period of 60 s between each cycle. Cells were kept on ice during ultra-sonification and gently stirred during rest periods. Removal of cell debris was performed by centrifugation (30 min, 30,000 x g, 4°C) and supernatant was loaded on a 5 ml HiTrap IMAC HP column (GE Life Sciences) pre-equilibrated with buffer A. Column was washed with 40 CV of buffer A and protein was eluted in buffer B in 1 ml fractions. All purification steps were performed at 16°C on a FPLC system (Aekta Purifier, GE Life Sciences) with a flow rate of 1.5 ml/min. Protein containing fractions were pooled and dialysed against buffer C. Protein samples were centrifuged at 30,000 x g for 30 min at 4°C to remove potential aggregates. Approx. 5.5 ml containing 250 µM of DsbA or 100 µM DsbC could be obtained from 1 l expression culture. Aliquots of 100-500 µl aliquots were stored at -80°C after shock freezing in liquid nitrogen.

3.4.4 Purification of Endothelin receptor type B in nanodiscs

After CF synthesis of ETB derivatives in presence of ND in a RM volume of 1 ml, potential precipitates were removed by centrifugation at 18,000 x g for 10 min at 4°C. Supernatant was diluted five fold in buffer A and loaded on a 1 ml Ni^{2+} immobilised IMAC column (Sepharose 6 Fast Flow, GE Life Sciences) that was pre-equilibrated with 5 CV of buffer A. Column was rinsed with 5 CV of buffer A and 10 CV of buffer B and ND-receptor complexes were eluted by applying buffer C in 500 µl fractions. All purification steps were performed at 4°C in a gravity flow setup and receptor was traced by its sfGFP fluorescence. Receptor containing fractions were pooled and dialysed against buffer D for over night at 4°C.

3.4.5 Purification of β1-adrenergic receptor in nanodiscs by IMAC

IMAC purification of β1AR was performed according the protocol described for ETB receptor purification (see 3.4.4) but with slightly different buffer compositions (see 2.4.10). Purification was performed at 16°C for thermostabilised turkey β1AR and at 4°C for the non-stabilised variant.

3.4.6 Purification of β1-adrenergic receptor in nanodiscs by LAC

Covalent coupling of alprenolol to agarose beads

Synthesis of alprenolol sepharose was performed according the protocol previously described (Caron et al. 1979). In this protocol, sepharose is first activated by addition of butanediol-diglycidylether in alkali conditions. Next, sodium thiosulfate is coupled to the activated sepharose. Coupling of alprenolol is then achieved by addition of the sulfhydryl group to the propylene side chain of alprenolol by a free radical chain addition reaction under reducing conditions.

For synthesis of activated sepharose, 25 ml of Sepharose 4B (Sigma-Aldrich) were first washed extensively with water to remove ethanol containing storage solution. The moist sepharose gel was then

resuspended in 60 ml of 0.3 M NaOH. Under gentle stirring, 1,4-butanediol-diglycidylether (Sigma-Aldrich) was added dropwise and continuously stirred at room temperature for over night. The gel was then washed extensively with water until neutral pH.

For synthesis of sodium thiosulfate derivatised sepharose, each 40 ml of 0.5 M sodium phosphate buffer at pH 6.3 and 2 M sodium thiosulfate were added to the activated sepharose and the mixture was stirred for 8 h. Afterwards, the sepharose gel was washed extensively with water to remove free sodium thiosulfate, which was analysed by addition of silver nitrate in the flow through fractions.

For coupling of alprenolol, sodium thiosulfate sepharose was next equilibrated and resuspended in 12.5 ml sodium bicarbonate pH eight containing 5 mg of EDTA. 500 mg of DTT was added and the mixture was gently stirred for 3 h at room temperature. The gel was rapidly washed with > 125 ml of water that was freshly bubbled with nitrogen. Afterwards, 5 ml sepharose gel was resuspended in 10 ml aqueous solution containing 50 mg of alprenolol hydrochloride (Tocris) and gently stirred for 10 min at room temperature before transfer to a 100 ml round-bottom synthesis flask. The flask was immersed in a 90°C water bath and 0.5 ml of aqueous potassium persulfate (46 mg/ml) were added every 12 min for 2 h under gentle stirring while carefully keeping the synthesis temperature at 90°C. Afterwards, the alprenolol derivatised gel was washed with > 2 litres of water at 4°C, > 200 ml of 0.1 M sodium bicarbonate and finally treated with ca. 20 ml of a 1% solution of sodium borohydride in 0.1 M sodium carbonate-bicarbonate buffer at pH 9 for 3 h at 4°C under continuous stirring. Afterwards, the gel was again washed extensively with water (> 4 l) and stored at 4°C in 0.02% sodium azide.

Performance of ligand affinity chromatography

Purified receptor-ND complexes were diluted five-fold in buffer A and loaded on a 1 ml LAC column at a flow rate of 0.1 ml/min. The flow rate was increased to 2.5 ml/min and the column was alternatingly washed with two CV of buffer B and two CV of buffer A for two cycles. For elution, the flow rate was reduced to 0.1 ml/min and a gradient was applied from zero to 10% buffer C for eight CV. Elution fractions of 0.5 CV were collected. Purification steps were performed at 16°C on a FPLC system (Aekta Purifier, GE Life Sciences). Receptor concentration in the elution fraction was analysed by the fluorescence of the sfGFP moiety and protein-containing fractions were pooled and concentrated by ultrafiltration (Amicon Ultra-4, 10 kDa MWCO, Merck Millipore). To remove the alprenolol for subsequent ligand binding analysis, the purified receptor sample was dialysed against a 1000-fold excess of buffer D with buffer exchange after 3 h and 24 h.

3.5 Nanodisc and liposome preparation

3.5.1 Nanodisc assembly by dialysis

An aliquot of purified MSPE3D1 (usually 5-10 ml with a protein concentration of 80-100 µM) (see3.4.1) was thawed at room temperature and potential precipitates were removed by centrifugation at 30,000 x g for 30 min at 4°C. DPC was added in a final concentration of 0.1% (w/v) and lipids were added in a defined final stoichiometric ratio with MSP from a stock usually containing 50 mM lipid in 300 mM sodium cholate. Mixture was filled up with DF-buffer to a final volume of approx. 10 ml.

Apparently optimal ratios for the lipids used in this thesis are given in Tab. 3.3. For screening of optimal lipid to MSP ratios, see 3.5.2.

Tab. 3.3 Lipid ratios for ND formation.

Lipid	Molar ratio per MSPE3D1
DMPC	115
DMPG	110
DPPG	85
POPC	85
POPG	90
POPS	90
DOPA	90
DOPE	80
DOPC	80
DOPG	80
DOPS	90
DEPG	80
SOPG	80

ND assembly mixtures were incubated for 60 – 90 min under gentle stirring and subsequently dialysed against a 3 x 5 l of DF-buffer, with buffer exchange after approx. 6 h, 24 h and 48 h. Afterwards, potential precipitates were removed by centrifugation at 30,000 x g for 30 min at 4°C. Supernatants were concentrated in molecular centrifugal filters (Centriprep YM-10, Merck Millipore) by centrifugation at 2000 x g at 4°C to a final volume of ca. 100 – 300 µl containing approx. 1000 – 2000 µM of MSPE3D1, corresponding to 500 – 1000 µM of ND. ND assembly and dialysis was performed at temperatures above the phase transition temperature of the respective lipid (at 50°C for DPPG and at RT for all other lipids).

3.5.2 Screen for optimal MSP – lipid ratios

Screening procedures were performed with the same protocol as described in 3.5.1 in smaller volumes (usually 100 µl) and excluding concentration steps. Lipid ratios were titrated in a suitable range during ND preparation (usually 60:1 to 130:1 in steps of 10) and homogeneity was analysed on an analytical scale SEC column (Superdex 200 increase 3.2/300, GE Life Sciences). SEC performance is described in 3.6.3.

3.5.3 Additional nanodisc purification by size exclusion chromatography

ND with apparently inhomogeneous characteristics even with optimised lipid: MSP ratios were further purified with an additional semi-preparative size exclusion chromatography (SEC) step. Therefore, ND were concentrated to a final volume of 500 µl and loaded on a semi-preparative SEC column (Superdex 200 10/300 GL, GE Life Sciences) as described in 3.6.3.

3.5.4 Liposome preparation

40 mg of lipids were solubilised in 2 ml chloroform and transferred to a round-bottom flask. The flask was connected to a rotary evaporator (Rotavapor RE12, Buechi) and vacuum was applied. Chloroform was evaporated during flask rotation over night to produce a thin lipidic film. For liposome formation,

the dried film was resuspended in 2 ml DF-buffer with the help of ultra-sonification, if necessary. Liposomes were extruded in a Mini-Extruder (Avanti Polar Lipids) in two subsequent steps to a size of 0.2 µm diameter and used directly.

3.6 Protein analysis

3.6.1 Polyacrylamide gel electrophoresis and staining

For sample preparation, one to four volume fractions of sample were incubated with one fraction of 5-fold sample buffer and filled up with water. Samples were subsequently incubated at 42°C for 30 min or 95°C for 10 min. Separation of 1-10 µl of the prepared sample was performed in 12 or 15% Tris-glycine-SDS gels for 15 min at 120 V, followed by 45-60 min at 200 V. Protein bands were visualised after incubation for 5-10 min under UV light, if trichloroethanol was supplemented during gel cast. Otherwise, gels were stained by incubation for 4 to 6 h in Coomassie staining solution followed by over night incubation in destaining solution and 30 min incubation in water.

3.6.2 Western blot and immunostaining

Subsequent to sample separation by SDS-PAGE, proteins were transferred to a PVDF-membrane by semi-dry western blot (Trans-Blot Turbo, Bio-Rad). Transfer was done for 7 min at 1.3 A and 25 V. Afterwards, membranes were incubated for 1 h with blocking buffer and subsequently incubated over night with the primary antibody in antibody buffer at 4°C. Membranes were washed three times by incubation in PBS-T for 5 min, 10 min and 15 min at room temperature. Membranes were incubated with secondary antibody in antibody buffer for 60 min at room temperature and washed again three times with PBS-T for 5 min, 10 min and 15 min. Membranes were finally rinsed in PBS for 10 min and incubated in freshly prepared ECL solution for 1 min, followed by luminescence read-out (Lumi Imager F1, Roche).
For STREP-tag staining, a horseradish peroxidase coupled strep-tactin conjugate was used like a primary antibody. After incubation over night at 4°C, membrane was rinsed in PBS-T for 5 min, 10 min and 15 min and treated for luminescence read-out like previously described.

3.6.3 Size exclusion chromatography

For analytical scale size exclusion chromatography (SEC), approx. 10 – 30 µg of protein in 50 µl SEC buffer were loaded on a analytical scale SEC column (Superdex 200, 3.2/30 increase or Superdex 200, 3.2/30, GE Life Sciences) pre-equilibrated with 2-3 CV of SEC-buffer at a flow rate of 50 – 75 µl/min. Sample elution was performed at the same flow rate and protein content during elution was traced by absorbance at 280 nm. For semi-preparative SEC, 1 – 9 mg in 500 µl SEC-buffer were loaded on a semi-preparative SEC column (Superdex 200, 10/300, GE Life Sciences) pre-equilibrated with SEC-buffer at a flow rate of 500 µl/min. Sample elution was performed at a flow rate of 500 µl/min and protein content during elution was traced by absorbance at 280 nm. All samples were centrifuged for 10 min at 18,000 x g to ensure removal of potential precipitates. SEC analysis was performed on a semi-automated FPLC system (Äkta purifier, GE Life Sciences) at 16°C.

3.6.4 Protein quantification

Quantification of total protein concentration by Bradford assay

Protein concentration in the *E. coli* extract was determined by Bradford assay. Therefore, 10 µl of the sample were incubated with 990 µl of Bradford solution for 3 min at room temperature and absorbance at 595 nm was measured and blank subtracted and compared to a reference curve previously determined with BSA standard solutions.

Quantification of protein and peptide concentration by UV absorbance

The concentration of purified proteins and Endothelin-1 peptide was routinely determined by measuring the light absorbance of the sample at 280 nm and applying the Lambert-Beer law. Extinction coefficients and molecular masses of the respective proteins were calculated from the amino acid sequence, assuming complete oxidation of all cysteine residues (Tab. 3.4).

Tab. 3.4 Molar extinction coefficients for protein and peptide quantification.

Construct	Molar extinction coefficient $\varepsilon_{280\ nm}$ ($M^{-1}\ cm^{-1}$)	Molecular mass (g mol^{-1})
Human Δ-β1AR-sfGFP-His_{10}	84,060	63,314
Human ts-Δ-β1AR-sfGFP-His_{10}	86,580	63,260
Human ts-fl-β1AR-sfGFP-His_{10}	92,330	80,428
Turkey Δ-β1AR-sfGFP-His_6	90,590	62,987
Turkey ts-Δ-β1AR-sfGFP-His_6	95,310	70,342
Turkey ts-Δ-β1AR-His_{10}	71,555	36,442
Cyclic ET-1	7,240	2,491
ETA-sfGFP-His_6	85,145	78,396
ETB-sfGFP-His_6	90,520	72,887
Ts-ETBΔC-sfGFP-His_6	84,645	70,313
MSP1E3D1	28,420	31,962
roGFP1-iE	23,380	30,632
DsbA	28,420	24,461
DsbC	17,420	26,978

Quantification of GFP-concentration by fluorescence

Receptor concentration in protein mixtures was routinely determined by the fluorescence intensity of the c-terminal sfGFP-tag. 6 µl of the sample were diluted in a total of 300 µl GFP-buffer in a black 96-well plate and incubated at room temperature for 1 h. Fluorescence emission intensity at 510 nm was measured during excitation at 495 nm on a fluorescence reader (Genius Pro, Tecan) and compared with reference curve previously determined with purified GFP.

3.6.5 Radioligand filter binding assay

Determination of ligand binding sites

1 - 1000 nM of non-purified receptor (according to its GFP fluorescence) were incubated with 50 - 200 nM ^{3}H-dihydroalprenolol (^{3}H-alprenolol) (Biotrend) or 0.5 nM ^{125}I-Tyr$_{13}$-Endothelin-1 (^{125}I-ET-1) for 30 - 60 min at room temperature in binding buffer. GF/B glass fibre filters (Merck-Millipore) were prepared by incubation with 150 µl of 0.3% (w/v) polyethyleneimine for 30 min and subsequent 4-times washing with 150 µl of pre-wash buffer. Incubated samples were applied on the prepared glass fibre filters and soaked through to bind receptor-ligand complexes on the filter membrane. To remove unbound ligand, filters were washed 8 times with ice-cold wash buffer. Filters were collected and retained radioactivity was counted on a liquid scintillation counter (Hidex, Finland) after addition of liquid scintillation cocktail. Unspecific binding was determined by incubation of the receptor with a large excess of cold ligand (4 µM Endothelin-1 or 40 µM alprenolol) for 30-60 min in binding buffer prior to radioligand filter binding assay. Filter assay was performed in a 96-well format on a vacuum manifold (MultiScreen HTS, Merck-Millipore).

To ensure complete determination of ligand binding sites, the receptor concentration was chosen in way that the concentration of ligand binding competent receptor was lower than the concentration of radiolabelled ligand to prevent ligand saturation. If the fraction of ligand binding competent receptor could not be estimated prior to assay performance, suitable conditions had to be determined by titration of the receptor in the radioligand filter-binding assay.

The receptor-bound ligand was determined from the retained radioactivity in the glass fibre filters using the specific activity of the radiolabelled ligand as given from the specifications from the supplier. Ligand binding sites in the initial sample were then calculated from the sample dilution factor applied in the assay. For analysis of statistical significance, a student t-test (t-test, unpaired, two-tailed) was applied using GraphPad Prism 5.

Determination of ligand affinities

For K_D determinations, low concentrations of the non-purified receptors (usually 5 nM for ETB and 50 nM for β1AR) were incubated with increasing concentrations of ^{3}H-alprenolol or ^{125}I-ET-1 for 30 - 60 min at room temperature. Unspecific binding was again determined by pre-incubation of the receptor with a large excess of unlabelled ligand and filter-binding assay was performed as described above. A one-site binding model (one-site – total and non-specific binding) was fitted on the obtained data set using GraphPad Prism 5 (GraphPad Software)

For K_i determinations, 100 nM of the non-purified receptor was first incubated with a mixture of 10 nM of ^{3}H-alprenolol and 50 nM of non-labelled alprenolol for 1 h in RA binding buffer at room temperature. Afterwards, samples were mixed in a one to one ratio with binding buffer with various concentrations of the competitors and incubated for another 60 min at room temperature before ligand separation on a glass fibre filter as described above. A one-site binding model (one site – fit K_i) was fitted on the obtained data set using GraphPad Prism 5. For analysis of statistical significance, a student t-test (t-test, unpaired, two-tailed) was applied using GraphPad Prism 5.

Thermostability assays

IMAC purified receptors were incubated for 30 - 45 min at various temperatures using a gradient on a PCR cycler. Samples were centrifuged at 18,000 x g for 10 min at 4°C to remove potential precipitates and remaining ligand binding activity was determined by radioligand filter binding assay as described above. For T_M calculation, a dose response model (log (inhibitor) vs. normalized response – variable slope) was fitted on the obtained data set using GraphPad Prism 5.

3.6.6 Redox analysis with roGFP

Spectroscopic read-out of roGFP1-iE oxidation state was performed in freshly degassed and N_2 bubbled buffer F on a fluorescence reader (Genius Pro, Tecan). For calibration assays, 3 µM of purified protein were incubated for 24 h in GFP buffer with 2 mM DTT or 4 mM GSSG. Oxidation state was determined by recording the fluorescence emission intensities (I_{ex}) at 510 nm during excitation at 390 and 485 nm and calculating the ratio $R = I_{ex\ 485\ nm} / I_{ex\ 390\ nm}$. Ratios for samples incubated with DTT or GSSG were then used to calculate the fraction of oxidised protein $F_{ox} = (R - R_{GSSG}) / (R_{DTT} - R_{GSSG})$. For analyses of roGFP1-iE oxidation state in the CF-reactions, the supernatant of the RM containing 7.5 µM roGFP1-iE was 3-fold diluted in freshly degassed and N_2 bubbled GFP buffer and fluorescence intensities were recorded without delay. Intensity ratios were calculated and oxidation state was calculated from the calibration data.

4 Results

4.1 Cell-free synthesis and characterisation of chatecholamine receptors

4.1.1 Cell-free synthesis of the turkey β1-adrenergic receptor as a precipitate

Cell-free synthesis as a precipitate (P-CF) is usually the fastest and most economic way for CF-production of membrane proteins, as synthesis yields are frequently high and interferences of hydrophobic supplements are excluded. Synthesised membrane proteins quantitatively precipitate during reaction and synthesis efficiencies can thus easily be compared by the size of the formed pellet after centrifugation. Therefore, optimisation of basic reaction parameters is usually performed in the P-CF mode.

The turkey β1-adrenergic receptor constructs ts-Δ-β1AR-His_{10}, ts-Δ-β1AR-sfGFP-His_6 and Δ-β1AR-sfGFP-His_6 were first synthesised in P-CF mode to verify the expression of the DNA templates and to determine the optimum Mg^{2+} concentration for CECF-synthesis. Therefore, CF-synthesis was performed without addition of any solubilising agent at Mg^{2+} concentrations ranging from 16 to 22 mM. The synthesised proteins precipitated quantitatively in the reactions. Precipitates were harvested by centrifugation and rinsed in S30-buffer. Mg^{2+} concentration optima were determined by the pellet size and found to be 20 mM for Δ-β1AR-sfGFP-His_6 and ts-Δ-β1AR-His_{10} and 22 mM for ts-Δ-β1AR-sfGFP-His_6. Pellets at the Mg^{2+}-optimum were analysed by SDS-PAGE and subsequent Coomassie-staining and by western-blot and immunostaining of the His-tag (Fig. 4.1).

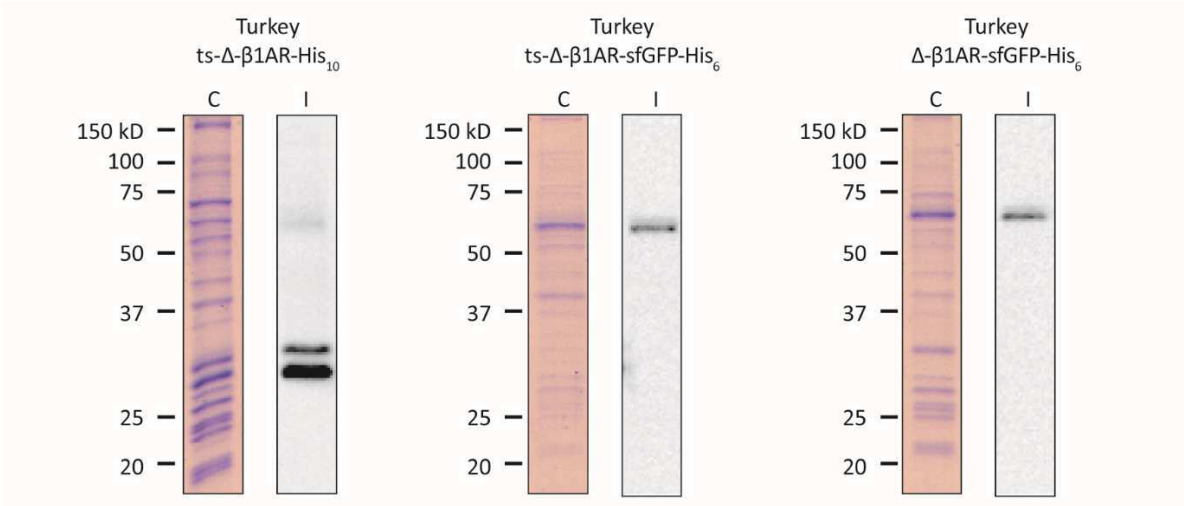

Fig. 4.1 P-CF production of turkey β1AR constructs.

Rinsed pellets from P-CF expression of ts-Δ-β1AR-His10, ts-Δ-β1AR-sfGFP-His6 and Δ-β1AR-sfGFP-His6 were resuspended in 100 µl S30 buffer and 1-2 µl were loaded on a 15% SDS-PAGE. Gels were stained with Coomassie (C) or with immunostaining of the His-tag (I) after western blot.

Ts-Δ-β1AR-His_{10} shows two prominent bands in the immunostaining at approximately 28 and 30 kDa, as compared to the molecular mass marker. The existence of two bands might be caused by N-terminal

cleavage of the receptor or by two distinct unfolding states of the receptor, as unusual SDS binding and subsequent differences in the running behaviour upon SDS-PAGE are frequently observed for membrane proteins (Rath et al. 2009). A faint third band could be detected at ca. 60 kDa and might be accounted for dimer formation. Δ-β1AR-sfGFP-His_6 was found at ca. 60 and ts- Δ-β1AR-sfGFP-His_6 at ca. 65 kDa. Co-precipitation of proteins from the CF-extract were visible in the Coomassie-stained gels and particularly high for ts-Δ-β1AR-His_{10}.

Precipitation upon P-CF synthesis does not necessarily mean complete unfolding of the membrane protein and for some proteins resolubilisation in mild detergents resulted in high quality protein samples even without the need of extensive refolding steps (Maslennikov and Choe 2013, Boland et al. 2014). To test the feasibility of this approach, solubilisation efficiency of various detergents was tested for the ts-Δ-β1AR-His_{10} precipitate (Fig. 4.2).

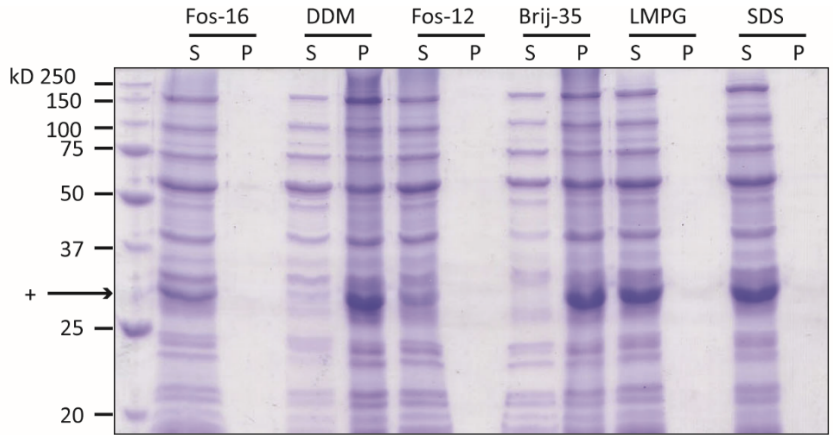

Fig. 4.2 Detergent solubilisation screen of P-CF produced thermostabilised β1AR.

Rinsed precipitate from a P-CF synthesis of ts-Δ-β1AR-His_{10} was incubated with indicated detergents in a final concentration of 1% for 1 h at room temperature. Remaining pellet was separated by centrifugation and resuspended in 50 µl S30-buffer. 2 µl of each supernatant (S) and pellet (P) were analysed on a 15% SDS-PAGE. Solubilisation efficiencies were judged by eye from band intensities of ts-Δ-β1AR-His_{10} (+).

Sufficient solubilisation was achieved with Fos-16, Fos-12, LMPG and SDS, while DDM and Brij-35 failed to solubilise the receptor, as indicated by the dominant band at the height of ts-Δ-β1AR-His_{10} in the SDS-PAGE analysis of the remaining pellet after solubilisation. Radioligand binding analyses to the inverse agonist alprenolol were performed with the solubilised receptor samples (assays were performed by Dr. Giselle Wiggin, Heptares Therapeutics, Welwyn Garden City, UK), but non of the samples were found to be ligand binding competent. As this approach did not give promising results for the thermostabilised receptor, detergent solubilisation trials were not performed with the non-stabilised receptor variant.

4.1.2 Soluble cell-free synthesis modes for turkey β1-adrenergic receptor

Solubilisation of thermostabilised β1AR derived from P-CF synthesis was not found to result in ligand binding competent receptor, concluding that the receptor either did not fold in this mode or folded structures were lost during detergent solubilisation. To avoid extensive refolding screens, co-

translational solubilisation was assumed a more promising strategy. As folding was expected to be enhanced by thermostabilising mutations in the receptor, soluble synthesis and folding screens were performed with ts-Δ-β1AR.

Assays were performed in detergent-supplemented (D-CF) and lipid-supplemented (L-CF) modes using detergent-lipid mixtures, liposomes (LP) and nanodiscs (ND). For D-CF modes, the two Brij-detergents Brij-58 and -78 as well as digitonin in concentrations known to be tolerated by the CF-system were chosen because of the previously promising results for Endothelin binding receptors (Junge et al. 2010, Proverbio et al. 2013). As allosteric lipid binding can have stabilising effects on detergent solubilised GPCRs (Grisshammer 2009), cholesteryl-hemisuccinate (CHS), dimyristoyl-phosphocholine (DMPC) and diheptanoyl-phosphocholine (DH_7PC) were added to the D-CF expressions. For L-CF synthesis mode, LP (DMPC) and LP (L-α–phosphatidylcholine, AsoPC) were tested in a final concentration of 4 mg/ml as well as ND (DMPC) in a final concentration of 80 µM. Solubilisation efficiency was monitored by the fluorescence of the sfGFP moiety of the ts-Δ-β1AR-sfGFP-His_6 construct, while ligand binding competence to the inverse agonist alprenolol was analysed by radioligand binding assays (partly performed by Dr. Giselle Wiggin, Heptares Therapeutics, Welwyn Garden City, UK). The fraction of ligand binding active receptor was calculated from both values assuming a one to one binding mode (Fig. 4.3).

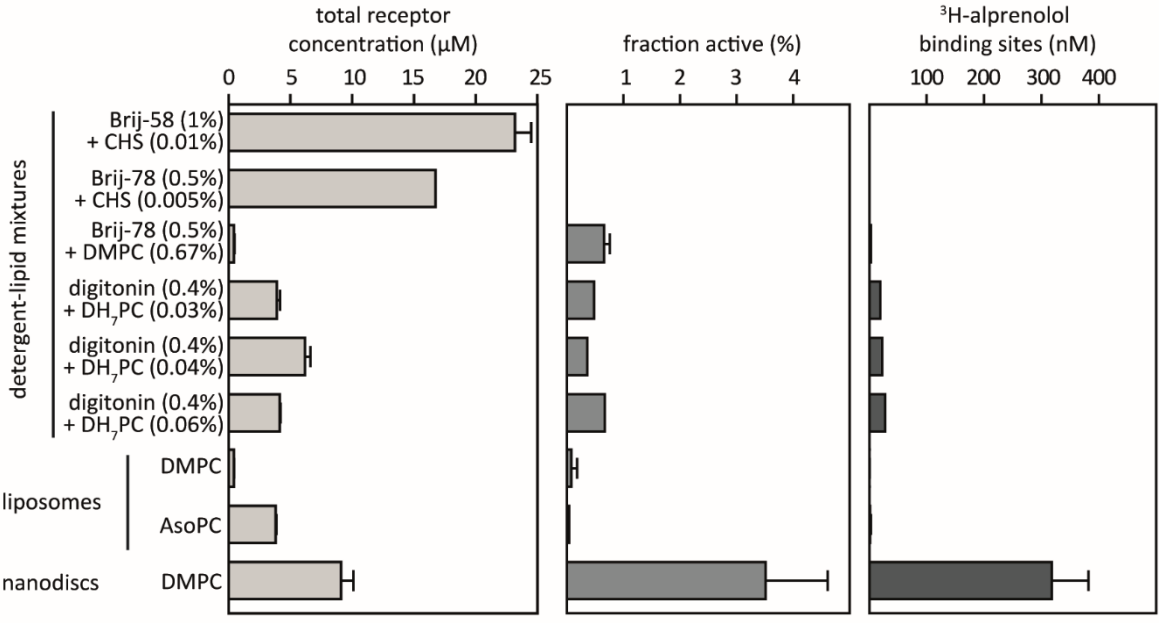

Fig. 4.3 Quantity and quality of CF-synthesised β1AR in hydrophobic environments.

CF-synthesis of ts-Δ-β1AR-sfGFP-His_6 was performed after addition of detergent-lipid mixtures at the indicated concentrations, 4 mg/ml liposomes (DMPC or AsoPC) or 80 µM preformed nanodiscs (DMPC). Total receptor concentration in the supernatant (for synthesis in detergent or ND) or precipitate (for synthesis in liposomes) was determined by the fluorescence of the sfGFP-moiety and alprenolol binding sites by radioligand binding assays. The fraction of active receptor was calculated assuming one ligand binding site per receptor. For ligand binding site determination in detergent-lipid mixtures, samples from two CF-reactions were pooled and values are given from single determinations. In the case of Brij-78 + CHS sample, values are given from a single CF-reaction. Values are given as mean and deviation from two CF reactions for total receptor determinations of all other detergent-lipid mixture samples. Values are also given as mean and deviation from two CF-reactions for liposome samples and as mean and SD of three CF-reactions for the nanodisc sample.

Overall yield of solubilised receptor was highest with the Brij-CHS mixtures, with a total receptor concentration of roughly 23 µM for Brij-58 and 16 µM for Brij-78, corresponding to 1500 and 1000 µg of soluble ts-Δ-β1AR-sfGFP-His_6 per ml of reaction mixture. However, these samples did not show any specific binding to the inverse agonist alprenolol. Interestingly, exchange of CHS with DMPC seems to enhance folding efficiency and a fraction of roughly 0.5% of the receptor was found to be ligand binding competent in this case. Unfortunately, the overall yield of soluble receptor was very low in this condition and therefore less than 10 nM of ligand binding sites could be detected in this sample. For the D-CF expression screens, digitonin gives the most promising results in terms of ligand binding sites, which were found in a range of 25 to 50 nM while overall yield was in between 4 to 8 µM. Thus, less than 1% of the soluble receptor was found to be ligand binding active also for samples produced with supplementation of digitonin.

Synthesis yield was very low in LP (DMPC) and ca. 5 µM in LP (AsoPC). Almost no ligand binding could be detected in both cases. Besides that, LPs precipitated in the reaction, which might be a disadvantage for subsequent assays. Supplementation of ND (DMPC) in a final concentration of 80 µM resulted in a soluble yield of some 9 µM, corresponding to 550 µg soluble ts-Δ-β1AR-sfGFP-His_6 per ml of reaction mixture. Ligand binding activity was much higher than for the other tested conditions. Roughly 3% of the receptor was found to be ligand binding competent, corresponding to ca. 300 nM ligand binding sites or 19 µg/ml active receptor in the RM.

To analyse the quality of the receptor in the ND, binding affinity of thermostabilised turkey β1AR in ND (DMPC) to alprenolol was next tested in radioligand filter binding assay and the dissociation constant (K_D) was found to be 11 nM (Fig. 4.4). This is in good agreement with the previously published K_D of 10.6 nM found for a highly similar thermostabilised turkey β1AR variant that was *in vivo* synthesised and solubilised in DDM (Miller and Tate 2011). The finding indicates a high quality of the folded fraction of the CF-synthesised receptor in ND. Nevertheless, the major fraction of ca. 95 - 97% of ts-Δ-β1AR-sfGFP-His_6 showed no ligand binding competence and appeared to be incorrectly folded. Additionally, no ligand binding was observed with the non-stabilised receptor variant, despite similar yields of soluble receptor were achieved. The thermostabilised β1AR construct was therefore chosen for further optimisation of L-CF synthesis in presence of NDs.

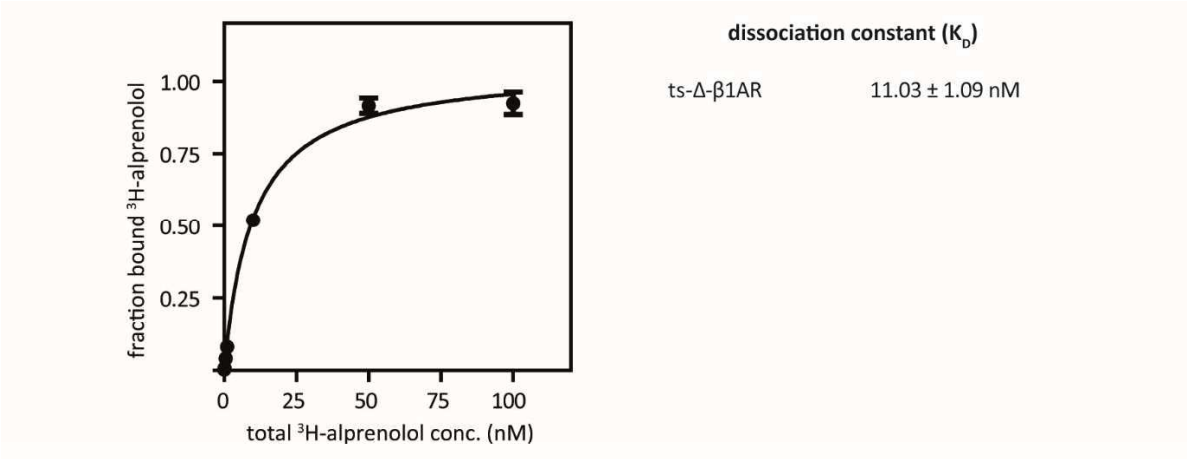

Fig. 4.4 Binding affinity of thermostabilised turkey β1AR in ND (DMPC) to alprenolol.

Ts-Δ-β1AR-sfGFP-His_6) was CF-synthesised in presence of ND (DMPC). Dissociation constant (K_D) to alprenolol was determined by radioligand filter binding assay using increasing concentrations of ^{3}H-labeled alprenolol and constant receptor concentrations. Values are given as mean and SD of three measurements.

4.1.3 Impact of nanodisc concentration and homogeneity on turkey β1-adrenergic receptor

From the various tested co-translational solubilisation strategies, the lipoprotein environment of ND appeared to be most suitable for correct folding of the β1-adrenergic receptor. In a first approach, ca. 550 µg soluble ts-Δ-β1AR-sfGFP-His_6 could be synthesised per ml reaction mixture. From that, ca. 3 - 5% or 15 - 30 µg were ligand binding competent. ND (DMPC) were initially added in a final concentration of 80 µM, as high ND (DMPC) concentrations are necessary for complete solubilisation of Endothelin receptor type B (Proverbio et al. 2013). For economical and sample handling reasons, the minimum necessary ND concentration for complete solubilisation of turkey β1AR was determined in a next step. Therefore, ND (DMPC) were titrated in the CF-reaction of ts-Δ-β1AR-sfGFP-His_6 and the concentrations of soluble and precipitated receptor were determined by the fluorescence of the sfGFP moiety in both the supernatant and the pellet after centrifugation of the RM.

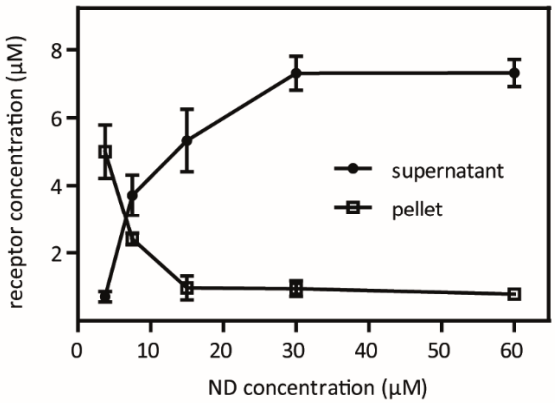

Fig. 4.5 Co-translational formation of β1AR-nanodisc complexes in CF-reactions.

Ts-Δ-β1AR-sfGFP-His_6 was CF-synthesised in presence of increasing concentrations of preformed ND (DMPC). Precipitates were separated from soluble protein by centrifugation and resuspended in S30 buffer. Receptor concentration in the supernatant and resuspension was determined by the fluorescence of the sfGFP moiety. Values are given as mean and SD of three CF-reactions (adapted from Rues et al. 2016).

The receptor was found in the supernatant only when sufficient concentrations of ND were present, indicating a co-translational formation of receptor-ND complexes (Fig. 4.5). With higher ND concentration, the concentration of soluble receptor increased and less receptor was found in the precipitate. With 15 µM ND in the CF reaction, precipitated protein was already below 1 µM while further increase in soluble receptor concentration was obtained up to a final concentration of 30 µM. Maximum yields of ca. 7 µM soluble ts- Δ-β1AR-sfGFP-His_6 could be obtained, corresponding to a total of ca. 440 µg per ml RM. A fraction of ca. 10% or 0.8 µM of the receptor was insoluble and remained in the precipitate despite high ND concentrations in the CF-reaction.

The ND concentration screen revealed that a 4.2-fold excess of ND over synthesised ts-Δ-β1AR-sfGFP-His_6 was necessary to ensure high solubilisation of the receptor, indicating that only a fraction of the supplied ND might be competent for insertion of the receptor. A critical parameter for receptor solubilisation might thus be the homogeneity of the supplied ND. To test the effect of ND inhomogeneities on receptor solubilisation and folding, ND (DMPC) were assembled with low (1:75), high (1:195) and optimal (1:115) MSP1E3D1 to lipid ratios, resulting in ND with altered size and homogeneity (Fig. 4.6A). Furthermore, ND formed at apparently optimal ratio were purified by preparative SEC to further enhance homogeneity. All four ND samples were used as supplements in the CF-synthesis of ts-Δ-β1AR-sfGFP-His_6 in a final concentration of 30 µM (Fig. 4.6B). Solubilisation efficiency was apparently unimpaired and only slight variations in the competence to bind alprenolol could be observed. Within the analysed range, it therefore appears that the homogeneity of ND (DMPC) is not a critical parameter for the L-CF synthesis of ts-Δ-β1AR-sfGFP-His_6.

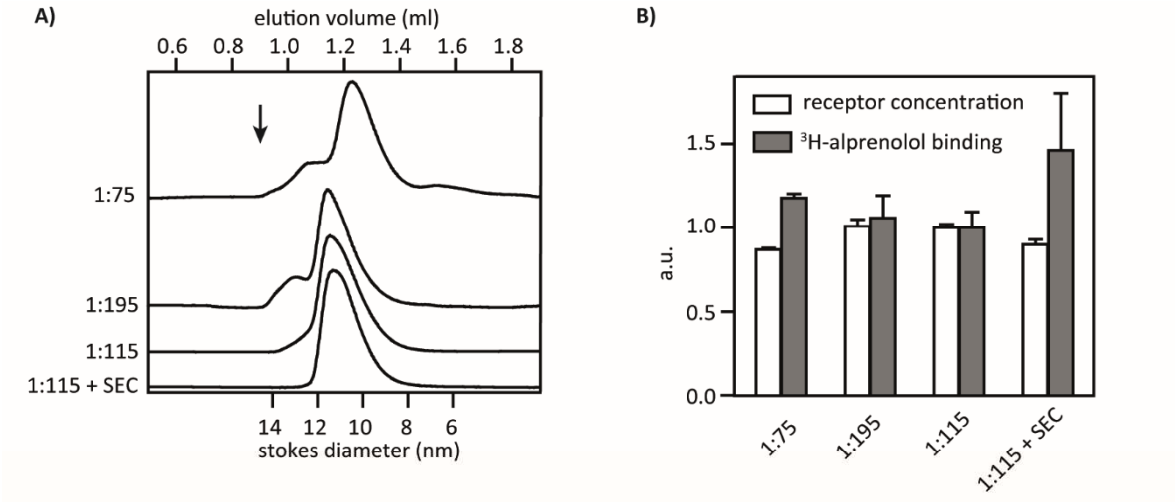

Fig. 4.6 Altered ND (DMPC) homogeneity for CF-synthesis of β1AR.

ND (DMPC) were assembled with low (1:75), high (1:195) and apparently optimal (1:115) MSP1E3D1:lipid ratios. ND (DMPC) formed with apparently optimal ratios were additionally further purified by preparative SEC. A: Homogeneity of the preformed ND was analysed by SEC on a Superdex 200 3.2/300 column. B: The preformed ND were supplemented to CF-synthesis reactions of ts-Δ–β1AR-sfGFP-His_6. After removal of potential precipitates, total receptor concentration was determined by the fluorescence of the sfGFP moiety while alprenolol binding activity was analysed by radioligand filter binding assays. Values are given as mean and SD of three CF-reactions (adapted from Rues et al. 2016).

4.1.4 Optimisation of nanodisc lipid composition for turkey β1-adrenergic receptor

Despite the high solubility and ligand binding activity compared to other soluble CF-synthesis modes, the fast majority of thermostabilised β1AR co-translationally solubilised with ND (DMPC) still appeared to be un- or incorrectly folded. A major bottleneck might be insufficient stability of the receptor, leading to a denaturation of the freshly synthesised protein during the CF-reaction, which is usually performed for 14 - 18 h at 30°C. This is supported by the finding that non-stabilised β1AR did not show any ligand binding activity after CF-synthesis with ND (DMPC). Cholesterol is known to be an allosteric modulator for many GPCRs and cholesterol-derivatives are frequently used for the stabilisation of β-adrenergic receptors and other GPCRs during purification in detergents (Hanson et al. 2008, Grisshammer 2009, Oates and Watts 2011). It was therefore tested if addition of cholesterol in the ND might have a positive effect on the ligand binding activity of thermostabilised β1AR. ND were assembled with mixtures of DMPC and cholesterol in various ratios and supplemented to the CF-synthesis of ts-Δ-β1AR-sfGFP-His_6 (Fig. 4.7). Solubilisation efficiency appeared to be unimpaired by addition of cholesterol in the ND but a major drop in alprenolol binding activity was observed with high cholesterol concentrations. While the reason for this negative impact remains unclear, it implies that addition of cholesterol in the ND (DMPC) is not beneficial but rather harmful for the receptor.

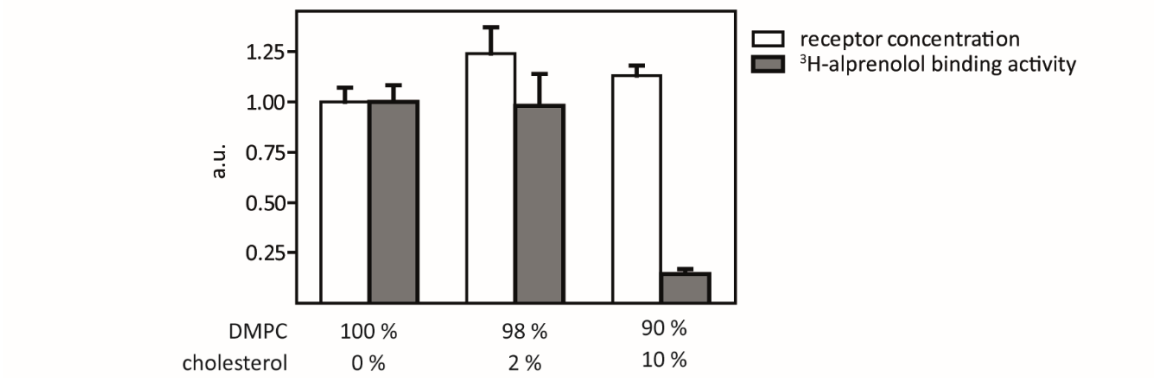

Fig. 4.7 ND formed with cholesterol mixtures for the CF-synthesis thermostabilised β1AR.

Ts-Δ-β1AR-sfGFP-His_6 was CF-synthesised in presence of 30 µM ND formed with DMPC and increasing concentrations of cholesterol. After removal of potential precipitates, receptor concentration was measured by the fluorescence of the sfGFP moiety and alprenolol binding activity by radioligand filter binding assay. Values are given as mean and deviation from two CF-reactions.

In a next step, the impact of the lipid headgroup and fatty acid chain composition on the solubilisation and folding of thermostabilised β1AR was tested. Therefore, ND were formed with a variety of lipids and supplied to the CF-synthesis of ts-Δ-β1AR-sfGFP-His_6 (Fig. 4.8).

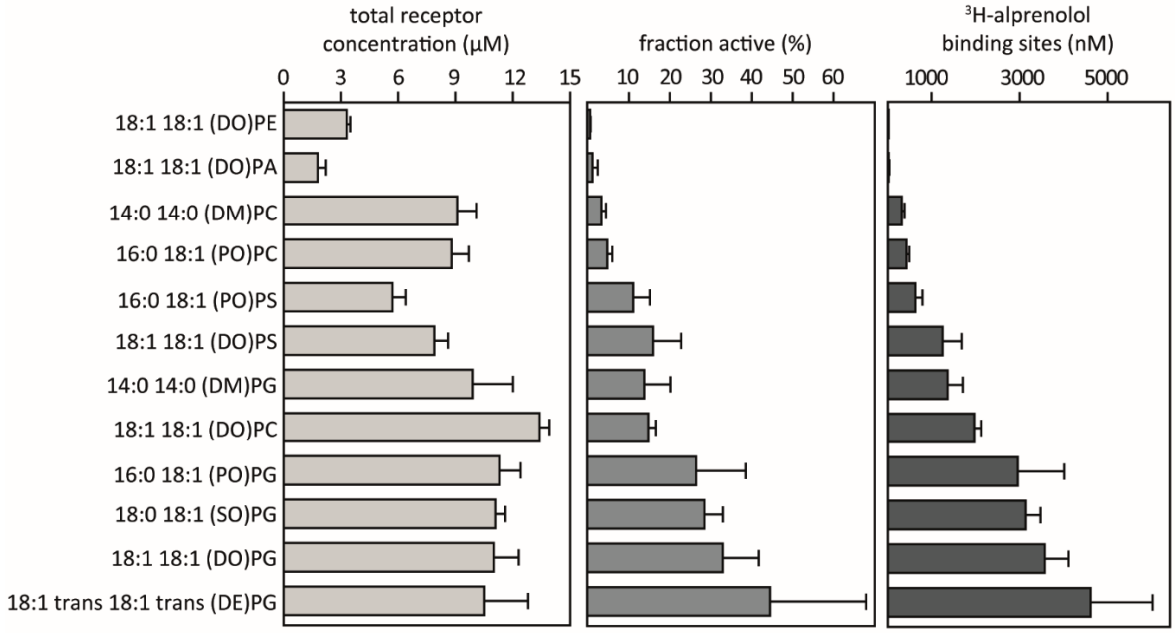

Fig. 4.8 ND lipid screen for the CF-synthesis of thermostabilised β1AR.

Ts-Δ-β1AR-sfGFP-His_6 was CF synthesised in presence of 30 µM ND with different lipid compositions. After removal of potential precipitates, the total receptor concentration in the reaction mixture was determined by the fluorescence of the sfGFP-moiety and the concentration of alprenolol binding sites by radioligand filter binding assay. The fraction of active receptor was calculated assuming one ligand binding site per receptor. Values are given as mean and SD from six (POPG and DMPG) or three (all others) CF-reactions (adapted from Rues et al. 2016).

The yield of ligand binding competent receptor depends on two basic parameters: The overall yield of soluble receptor and the fraction of this that is correctly folded and ligand binding active. For the L-CF synthesis of thermostabilised β1AR, both parameters seem to be affected by the lipid composition. Regarding their positive impact on soluble yield, one could rank the lipids in the following order (from low to high): DOPA, DOPE, POPS, DOPS, DMPC, POPC, DMPG, DEPG, DOPG, SOPG, POPG and DOPC. It seems that the overall yield of soluble β1AR rather depends on the lipid headgroup than on the fatty acid chain length or saturation state. There seems to be a preference for phosphoglycerol (PG) headgroups, as all of the four tested lipids with PG-headgroups rank in the five best working lipids in regard to the soluble yield of β1AR. Lipids with phosphocholine (PC) headgroups also seem to be very efficient and ND formed with DOPC lipids were the best working supplement in regard of soluble overall yield of β1AR. Phosphoserine (PS) headgroups were slightly less effective than PG- or PC-headgroups for both DO- and PO-lipids ($P < 0.05$ for DOPG vs. DOPS and POPC vs. POPS and $P < 0.01$ for DOPC vs. DOPS and POPG vs. POPS). Differences in the soluble yield are not very pronounced except for DO-phosphatidic acid (PA) and DO-phosphoethanolamine (-PE) lipids, where the yields of soluble receptor were significantly lowered ($P < 0.01$ for DOPC/PG/PS vs. DOPA/PE). Additionally, large precipitates containing non-solubilised receptor were formed in CF-reactions with these lipids. It thus seems that these ND were not very effective in solubilising the receptor. It is noteworthy that ND formation with PA-, PE- and to some extend also with PS-lipids was not effective using the standard approach and an additional SEC purification step had to be performed to ensure ND homogeneity. Both PA- and PE-headgroup lipids tend to form non-bilayer phases and induce membrane curvature stress (Booth 2005, Dickey and Faller 2008), a characteristic that is detrimental for the flat lipid bilayer of the ND.

While the yield of soluble receptor was only minor affected for most tested cases, the ability of the receptor to fold in a ligand binding competent state was highly influenced by the ND lipid composition. The fraction of ligand binding active receptor ranged from almost zero in DOPE to 40 - 50% in DEPG (Fig. 4.8). The findings clearly indicate that the ability of thermostabilised turkey β1AR to fold in a ligand binding competent state depends on both lipid headgroup as well as lipid chain length of the supplied ND. Long chain lengths seem to be preferred over short ones, as the folding efficiency was significantly lower in both DMPC and DMPG compared to their long-chain analogs DOPC and DOPG ($P < 0.001$ for DMPC vs DOPC and $P < 0.05$ for DMPG vs. DOPG). PG-headgroups seem to have a high positive impact on the folding of the receptor. It was significantly enhanced in DMPG over DMPC ($P < 0.05$) and more than 20% of ts-Δ-β1AR were folded to a ligand binding competent state in all other tested PG-headgroup lipids. PS-headgroup lipids apparently also support receptor folding and more than 10% active ts-Δ-β1AR were found with both ND (DOPS) and ND (POPS). PC-headgroups seem to be somewhat less favourable for receptor folding, as the fraction of active receptor is significantly lower in all DM-, PO- and DOPC lipids compared to their PG-analogs ($P < 0.05$ for all). PE- and PA-headgroups apparently do not support receptor folding.

Interestingly, the data set indicates that the effects of lipid headgroup and fatty acid chain length can be reciprocal. For example, DMPG is supposed to be rather inefficient in support of receptor folding with regard to its short fatty acid chain length but very efficient with regard to its headgroup. Both parameters seem to counteract and result in ca. 14% of correctly folded receptor. DOPC on the other

hand has a supposedly very efficient fatty acid chain length but a rather inefficient lipid headgroup. The fraction of active receptor in ND (DOPC) is similar to ND (DMPG) and can be interpreted accordingly.

High ligand binding activities could only be achieved with long chain lipids with a PG-headgroup and resulted in more than 3000 nM of ligand binding sites in the reaction mixture for SOPG, DOPG and DEPG. Highest activities could be measured with DEPG samples, with an average of ca. 4500 nM ligand binding sites in the RM. However, variations were very high with this lipid. More reliable results with almost similar yields of correctly folded receptor could be achieved with ND (DOPG). An average of 3600 nM ligand binding sites could be found in the RM, which corresponds to 33% correctly folded receptor or or 220 µg of ligand binding competent ts-Δ-β1AR-sfGFP-His_6 per ml of CF-reaction.

While already 3 - 5% of the thermostabilised turkey β1AR was correctly folded after CF-synthesis in presence of ND (DMPC), the non-stabilised receptor construct did not show any specific ligand binding activity with this approach, despite similar yields of soluble total receptor. Folding of thermostabilised β1AR was found to be 9 to 12 fold more efficient in ND (DOPG) or ND (DEPG) than in ND (DMPC). It was therefore tested, if these NDs could enhance binding of the non-stabilised receptor, too (Fig. 4.9).

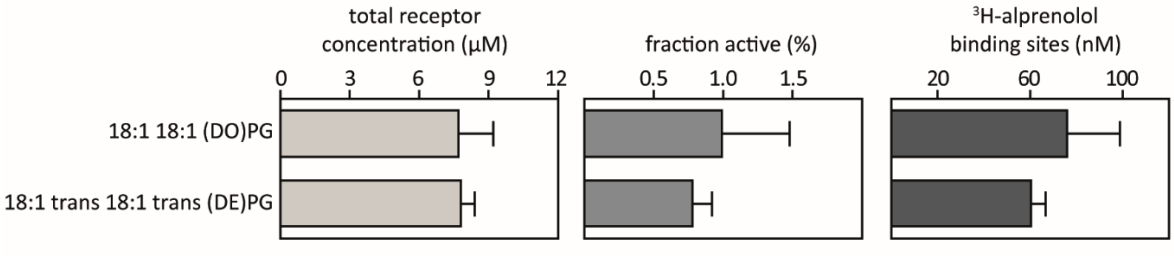

Fig. 4.9 Quantity and quality of CF-synthesised non-stabilised β1AR with selected NDs.

Non-stabilised Δ-β1AR-sfGFP-His_6 was CF-synthesised in presence of 60 µM ND with optimised lipid compositions. After removal of potential precipitates, the total receptor concentration in the reaction mixture was determined by the fluorescence of the sfGFP-moiety and the concentration of alprenolol binding sites by radioligand filter binding assay. The fraction of active receptor was calculated assuming one ligand binding site per receptor. Values are given as mean and SD of three CF-reactions (adapted from Rues et al. 2016).

Specific binding was indeed observable for Δ-β1AR-sfGFP-His_6 synthesised in presence of ND (DOPG) or ND (DEPG), although to a much lesser extend if compared with corresponding samples of the ts-Δ-β1AR-sfGFP-His_6. With both samples, ca. 60 nM of alprenolol binding sites could be detected in the reaction mixture, roughly 25% of the binding sites found for ts-Δ-β1AR-sfGFP-His_6 in ND (DMPC). Given the overall soluble yield of 7.8 µM, this corresponds to ca. 1% of ligand binding active receptor (Fig. 4.9).

Based on the recorded data, one can thus synthesise up to ca. 3.5 nmol or 220 µg of functionally folded ts-Δ-β1AR-sfGFP-His_6 and approximately 60 pmol or 4 µg of functionally folded Δ-β1AR-sfGFP-His_6 in 1 ml CF-reaction mixture with this approach.

4.1.5 Stability of turkey β1-adrenergic receptors in nanodiscs

A major challenge for the handling of purified GPCRs in detergents is their frequent sensitivity to high temperatures. ND offer a more native lipid environment that might be advantageous fir the stability of GPCRs. To analyse the thermostability of the CF-produced turkey β1AR in ND (DOPG), both thermostabilised and non-stabilised turkey β1AR were purified by IMAC and incubated for 30 min at increasing temperatures before performing radioligand filter binding assays (Fig. 4.10).

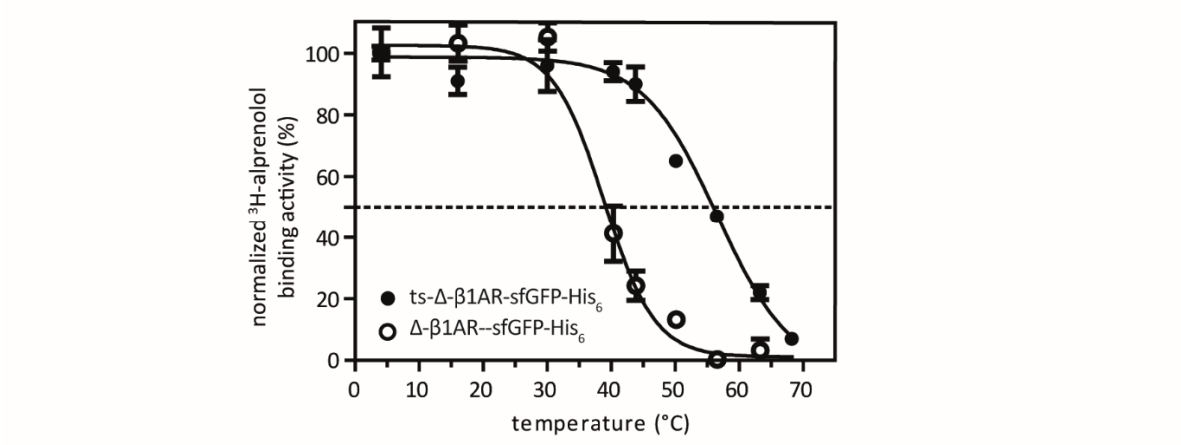

Fig. 4.10 Thermostability of IMAC purified turkey β1AR in ND (DOPG).

Thermostabilised (ts-Δ-β1AR-sfGFP-His$_6$) and non-stabilized (Δ-β1AR-sfGFP-His$_6$) receptors were CF-synthesised in presence of 30 µM ND (DOPG) and purified by IMAC. Thermostability was analysed by incubation of the purified receptors in ND for 30 min at indicated temperatures and subsequent radioligand filter binding assay with ^{3}H-alprenolol. Thermostability is given as the temperature retaining 50% of the ligand binding activity of samples stored at 4°C. Values are given as mean and SD of three measurements (adapted from Rues et al. 2016).

Ts- Δ-β1AR was found to be fully stable for temperatures up to 40°C and 50% of initial ligand binding activity could still be detected after incubation at 55°C. No drop in ligand binding activity was found for non-stabilised β1AR incubated at temperatures up to 30°C and half of its initial activity should still be detectable for temperatures between 35 and 40°C based on the present data set (Fig. 4.10). Purified receptors in ND (DOPG) were stored at -80°C, 4°C and 16°C and ligand binding activity was unimpaired in all tested conditions for at least three weeks.

4.1.6 Cell-free synthesis of human β1-adrenergic receptor variants

So far, the majority of *in vitro* studies with the β1AR have been performed with the turkey receptor, primarily for reasons of instability upon detergent treatment for the human β1AR (Serrano-Vega and Tate 2009). The L-CF-synthesis in presence of NDs avoids any detergent contact and the receptor can be synthesised in a soluble form directly into a relatively defined and homogeneous lipid environment. The feasibility of the L-CF-synthesis to produce ligand binding competent human β1AR was therefore evaluated.

The results with the turkey β1AR showed the importance of thermostabilisation for the correct folding of the receptor. Furthermore, both thermostabilised and non-stabilised turkey β1AR have been truncated at the N- and C-terminus as well as in the intracellular loop 3 (ICL 3). Therefore, three variants of the human β1AR were designed. The thermostabilising mutations of the turkey β1AR were transferred to a full-length and a truncated version of human β1AR (ts-fl-β1AR and ts-Δ-β1AR, respectively). Additionally, a truncated receptor variant without potentially thermostabilising mutations was designed (Δ-β1AR) (see 1.3.4). Like the turkey β1AR, all three variants were designed with a C-terminal sfGFP-tag to simplify the quantification of total receptor yields.

To assure the expression of the DNA-construct in the CECF-system, all three constructs were first synthesised in P-CF mode and analysed by SDS-PAGE and subsequent Coomassie-staining and western-blot and immunostaining of the His-tag (Fig. 4.11).

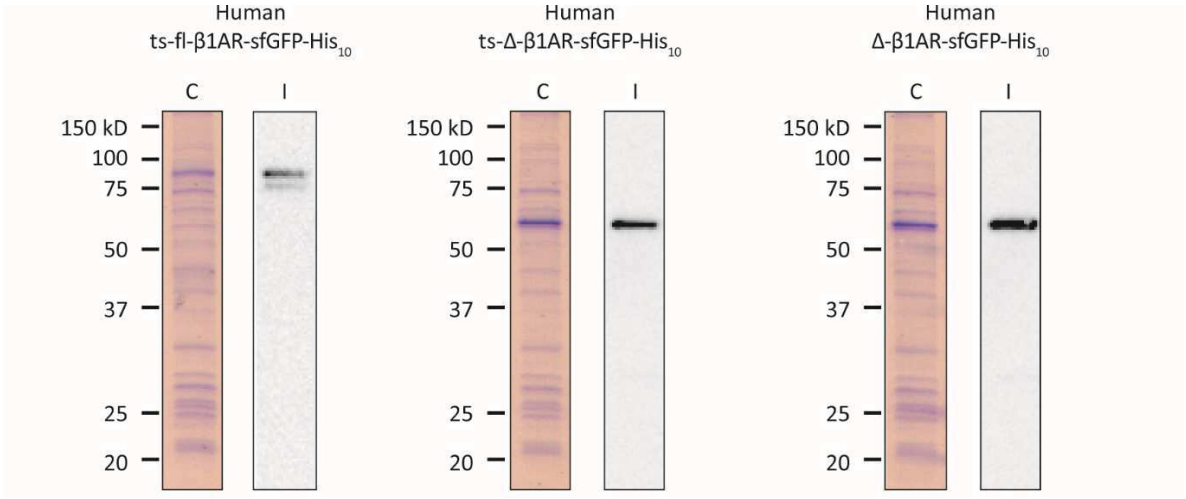

Fig. 4.11 P-CF production of human β1AR constructs.

Rinsed pellets from P-CF expression of human ts-fl-β1AR-sfGFP-His_{10}, ts-Δ-β1AR-sfGFP-His_{10} and Δ-β1AR-sfGFP-His10 were resuspended in 100 µl S30 buffer and 1-2 µl were loaded on a 15% SDS-PAGE. Gels were stained with Coomassie (C) or with immunostaining of the His-tag (I) after western blot.

In comparison with the molecular mass marker, ts-fl-β1AR-sfGFP-His_{10} was found at ca. 85 kDa and both ts-Δ-β1AR-sfGFP-His_6 and Δ-β1AR-sfGFP-His_6 at ca. 60 kDa in the western-blot. A faint slightly lower protein band was detected in the western-blot for ts-fl-β1AR that might be caused by N-terminal cleavage or unusual running behaviour in SDS-PAGE (Rath et al. 2009). The Coomassie-stained SDS-PAGE revealed the co-precipitation of proteins from the RM with the receptors. Distinct receptor bands were found in the Coomassie-stained gel for both deletion constructs, while the according band was relatively faint for ts-fl-β1AR. Expression efficiency might thus be somewhat reduced for the full-length construct.

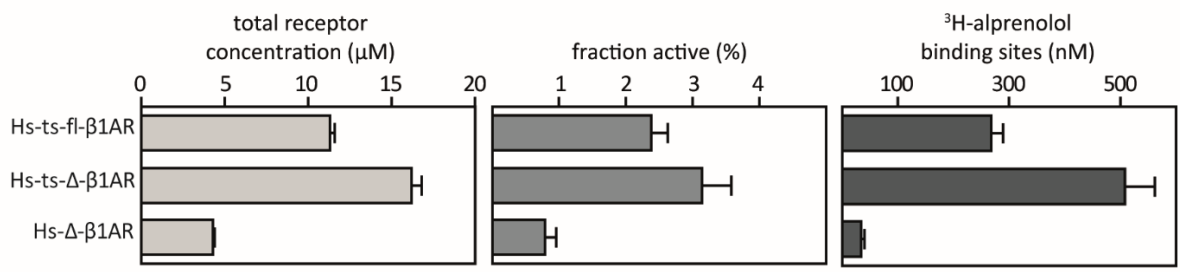

Fig. 4.12 Quantity and quality of CF-synthesised human β1AR in ND (DOPG).

Thermostabilised full-length (ts-fl-β1AR), thermostabilised truncated (ts-Δ-β1AR) and non-stabilised truncated (Δ-β1AR) human Adrenergic receptors were CF-synthesised as C-terminal sfGFP-His_6 fusion constructs in presence of 60 µM ND (DOPG). After removal of potential precipitates, the total receptor concentrations in the reaction mixtures were determined by the fluorescence of the sfGFP-moieties and the concentration of alprenolol binding sites by radioligand filter binding assay. The fraction of active receptor was calculated assuming one ligand binding site per receptor. Values are given as mean and SD of three independent CF-reactions.

In a next step, soluble yields and ligand binding competence of the constructs were tested after CF-synthesis in presence of 60 µM ND (DOPG) (Fig. 4.12). In accordance to the findings for P-CF synthesis, soluble yield of ts-fl-β1AR was ca. 30% lower than for the truncated thermostabilised receptor variant (11 µM and 16 µM, respectively). The fraction of ligand binding competent receptor was almost similar for both stabilised receptor variants and in a range between 2 and 3%. This corresponds to approximately 270 nM of ligand binding sites (ca. 15 µg/ml) for ts-fl-β1AR-sfGFP-His_6 and approximately 510 nM of ligand binding sites (ca. 30 µg/ml) for ts-Δ-β1AR.

L-CF-synthesis of the non-stabilised human β1AR variant appeared to be less efficient than for the thermostabilised constructs, with total soluble yields of only 4.3 µM. Additionally, only 0.8% of this were found to be ligand binding competent, corresponding to ca. 30 nM ligand binding sites in the reaction mixture or roughly 2 µg/ml of ligand binding competent Δ-β1AR-sfGFP-His_6.

In a next step, the affinities of the human β1AR constructs towards alprenolol were evaluated. Therefore, radioligand filter binding assays were performed with the thermostabilised human β1AR variants with constant receptor concentrations and increasing concentrations of ^{3}H-labeled alprenolol (Fig. 4.13). As the concentration of ligand binding sites was insufficiently low for the non-stabilised human β1AR variant, affinity measurements were not performed with this construct.

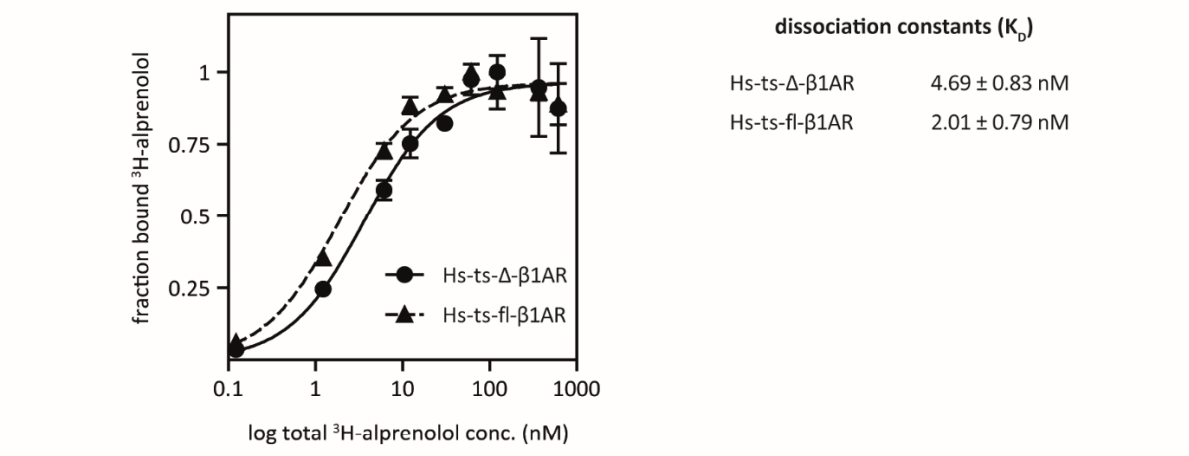

Fig. 4.13 Binding affinities of human β1AR constructs in ND (DOPG) to alprenolol.

Truncated (ts-Δ-β1AR) and full-length (ts-fl-β1AR) thermostabilised human β1-adrenergic receptor variants were CF-synthesised as C-terminal sfGFP-His_6 fusions in presence of 30 µM ND (DOPG). Dissociation constants (K_D) to alprenolol were determined by radioligand filter binding assay using increasing concentrations of ^{3}H-labeled alprenolol and constant receptor concentrations. Values are given as mean and SD of three measurements.

Both truncated and full-length thermostabilised human β1AR show high affinity to alprenolol with K_D of 4.7 nM and 2.0 nM, respectively. This indicates a high quality of the folded fraction of the respective receptor.

Taken together, the findings show that the effect of the thermostabilising mutations could be partly transferred to the human β1AR. Yields of ligand binding competent receptor appear to be some 7 to 10-fold lower than for the turkey thermostabilised β1AR but should be still sufficient to perform lipid dependent ligand binding studies like the one described earlier in this thesis (see 4.3.1). For the non-stabilised human β1AR, fractions of ligand binding competent receptor appear to be similar to the non-stabilised turkey β1AR and in the range of ca. 1%. Additionally, soluble yields in L-CF synthesis were found to be relatively low. Thus, further optimisation might be necessary to enhance both quantity and quality of the CF-synthesis of non-stabilised human β1AR.

4.2 Cell-free synthesis and characterisation of Endothelin receptors.

4.2.1 Optimisation of nanodisc lipid composition for Endothelin receptor type B

Synthesis of the human Endothelin receptor type B (ETB) in an *E. coli* based CECF-system has been previously established and profound screens have been performed for enhancement of both quantity and quality in P-CF, D-CF and L-CF mode (Klammt et al. 2007, Junge et al. 2010, Proverbio et al. 2013). For ETB receptor, L-CF synthesis in presence of ND (DMPC) has been found to produce ligand binding competent receptor in scales suitable for ligand binding studies and differential ligand binding patterns could be demonstrated for ETB in ND (DMPC) (Proverbio et al. 2013). However, only 650 ng of the overall 150 µg of synthesised ETB-sfGFP-His_6 were found to be ligand binding competent in radioligand filter binding assays, corresponding to a fraction of correctly folded receptor of less than 0.5%.

The lipid composition of the supplied ND was found to have a large impact on the folding efficiency of CF-synthesised β1AR receptor constructs (see 4.1.4) and the fraction of correctly folded receptor could be increased by a factor of 9 to 12. It was therefore tested if the modulation of the ND lipid composition could also have an impact on the solubilisation and folding of the human ETB receptor. A set of ND was prepared with lipids varying in headgroup, fatty acid chain length and saturation state. The preformed NDs were added to CF-synthesis reactions of ETB-sfGFP-His_6 in a final concentration of 60 µM. After removal of potential precipitates by centrifugation, the total soluble receptor concentration in the reaction mixture was determined by the fluorescence of the sfGFP moiety and the concentration of ligand binding sites by radioligand filter binding assays with the ^{125}I-labeled agonist ET-1.

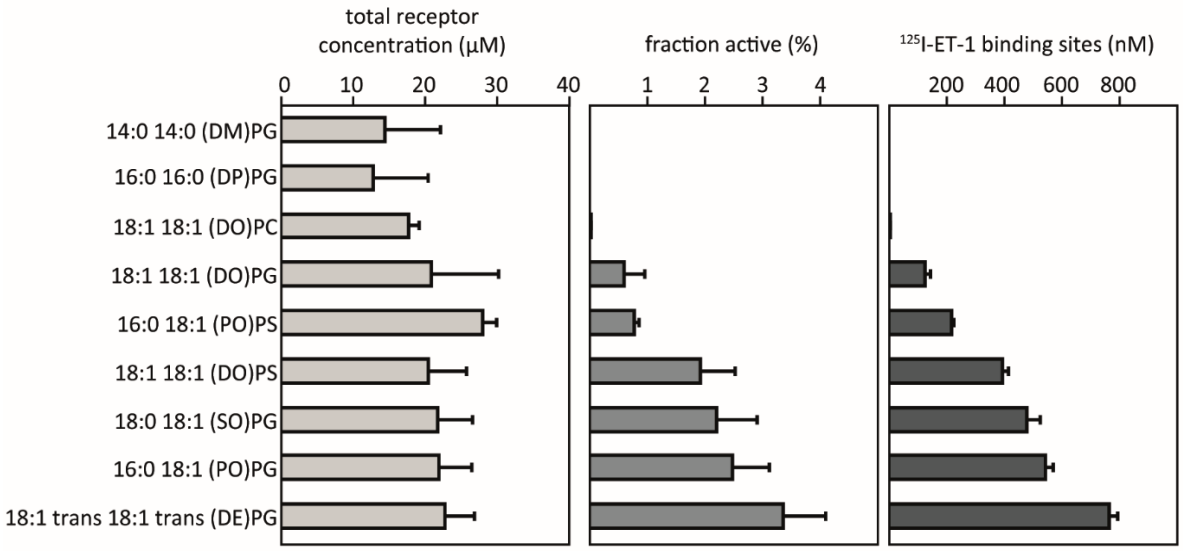

Fig. 4.14 ND lipid screen for the L-CF synthesis of human ETB receptor.

ETB-sfGFP-His_6 was CF synthesised in presence of 60 µM ND with different lipid compositions. After removal of potential precipitates, the total receptor concentration in the reaction mixture was determined by the fluorescence of the sfGFP-moiety and the concentration of ET-1 binding sites by radioligand filter binding assay. The fraction of active receptor was calculated assuming one ligand binding site per receptor. Values are given as mean and SD from four (DOPG + POPG) or three (all others) CF-reactions.

The overall yield of solubilised ETB was in a range of 14 to 28 µM, without any visible tendency towards a specific lipid type (Fig. 4.14). However, binding competence of ETB to the natural agonist ET-1 was highly depended on both lipid headgroup and fatty acid chain composition and the fractions of ligand binding active receptor altered in a range from zero to ca. 3.5%. Based on their efficiency to support ETB folding, the lipids can be categorised in three groups. Lipids in the first group were apparently not efficient and the solubilised receptor was almost completely inactive. DMPG, DPPG and DOPC belong to this group ($P < 0.001$). They have either a relatively short chain length or a PC headgroup. The second group showed some ability to support ETB folding and the fraction of active receptor was in the range of ca. 1% with this group. It is composed of a long chain lipid with a PG-headgroup (DOPG) and a lipid with a PS-headgroup and a medium long chain length (POPS) ($P < 0.05$). High ligand binding activity above 2% was found with DOPS, SOPG, POPG and DEPG, being primarily lipids with a PG-headgroup and a medium to long fatty acid chain length. Based on this categorisation, medium to long fatty acid chain lengths seem to be important for the folding of the receptor as well as PG- or PS-headgroups. With the exception of DOPG, it seems that either long fatty chain lengths with a PG- or PS-headgroup or medium chain lengths with a PG- headgroup are necessary to achieve high receptor folding. Therefore, is might indicate a trend towards PG-headgroups being more efficient than PS-headgroups and long fatty acid chain lengths being more efficient than medium chain lengths. However, it remains unclear with the current data set, if the relatively low folding efficiency measured with DOPG is only an artefact caused by discrepancies e.g. in the ND preparation, or if a synergetic effect of the headgroup and fatty acid chain composition applies.

Another parameter affecting the receptor folding might be the rigidity of the formed lipid bilayer in the NDs. While the actual rigidity in the NDs can only be determined by additional assays, the transition temperature of the respective lipid can be used as an indicator. Published phase transition temperatures for DOPG and POPG are -18°C and -2°C (Caffrey and Hogan 1992), making POPG lipid bilayers supposedly more rigid at ambient temperatures. To the knowledge of the author, no phase transition temperatures are published for SOPG and DEPG, but the published values for the respective PC-lipids are 6°C for SOPC (Caffrey and Hogan 1992) and 12°C for DEPC (Smith et al. 2014a) and phase transition temperatures are not drastically altered for PG- and PC-headgroup lipids (Caffrey and Hogan 1992). Interestingly, for PG-lipids, the supposed increase in rigidity appears to be reflected in the efficiency to support ETB folding and higher rigidity seems to be beneficial for the ligand binding activity of the receptor (Fig. 4.14). However, synergetic effects can again not be excluded at this point, as e.g. POPS was apparently inefficient in support of ETB folding despites its high phase transition temperature of 14°C, while DOPS with a much lower transition temperature of -11°C seems to support ETB folding more efficiently.

Exceptionally high concentrations of ET-1 binding sites were found in samples prepared with ND (DEPG) and a total of ca. 760 nM ligand binding sites could be determined in the reaction mixture. In assumption of a one to one binding mode, this corresponds to some 60 µg of ligand binding competent ETB-sfGFP-His_6 or ca. 3.5% correctly folded receptor.

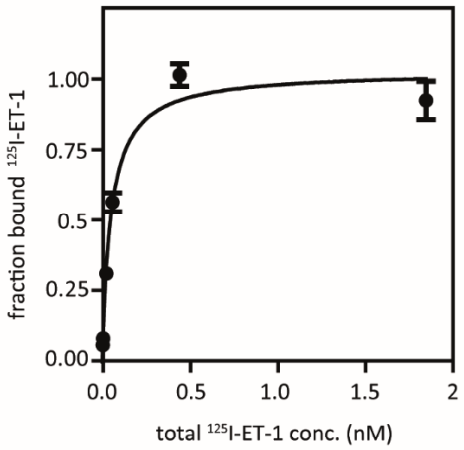

dissociation constant (K_D)	
ETB	76.3 ± 13 pM

Fig. 4.15 Binding affinity of human ETB receptor in ND (DEPG) to ET-1.

Human ETB-sfGFP-His_6 was CF-synthesised in presence of 60 µM ND (DEPG). Dissociation constant (K_D) to ET-1 was determined by radioligand filter binding assay using increasing concentrations of ^{125}I-labeled ET-1and constant receptor concentrations. Values are given as mean and SD from three measurements.

In a next step, the affinity of the CF-synthesised ETB receptor towards its natural agonist was analysed by radioligand filter binding assay. Human ETB-sfGFP-His_6 was therefore CF-synthesised in presence of 60 µM ND (DEPG) and radioligand filter binding assay was performed with constant receptor concentrations and increasing concentrations of radiolabelled ET-1 (Fig. 4.15). The K_D of the binding was found to be ca. 75 pM and is thus in high similarity with previously published results (35 pM, Lättig et al. 2009). This indicates a high quality of the folded fraction of the CF-synthesised receptor.

4.2.2 Impact of nanodisc concentration on the cell-free synthesis of ETB receptor

The initial screens for the ND supplemented CF-synthesis of ETB have been performed with relatively high ND concentrations of 60 µM, as ND (DMPC) have been previously found to be inefficient in solubilising the receptor when supplied in lower concentrations (Proverbio et al. 2013). For reasons of ND consumption and sample handling, it was analysed whether low ND concentrations might be sufficient for receptor solubilisation with the optimised lipid composition. Therefore, ND (DEPG) were titrated to CF-synthesis reactions of ETB-sfGFP-His_6 in a range of 30 to 110 µM. Potential precipitates were removed by centrifugation and the concentrations of soluble receptor as well as ligand binding sites in the RM were determined by the fluorescence of the sfGFP moiety or radioligand filter binding assays, respectively.

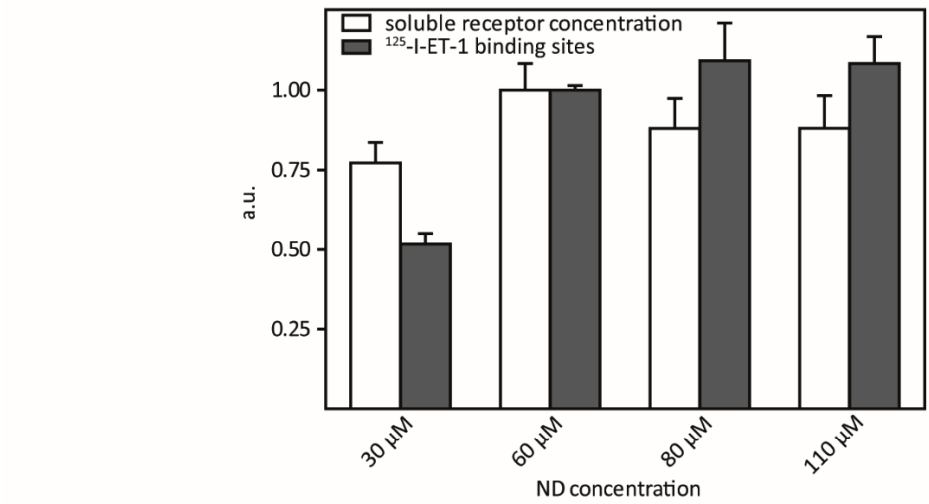

Fig. 4.16 Quality and quantity of ETB receptor with altered ND (DEPG) concentration.

ETB-sfGFP-His_6 was CF-synthesised in presence of increasing concentrations of ND (DEPG). Potential precipitates were separated by centrifugation and receptor concentration in the supernatant was determined by the fluorescence of the sfGFP-moiety and ligand binding sites by radioligand filter binding assay. Values are given as mean and SD from three determinations.

Yields of soluble receptor appeared to be relatively independent from the ND (DEPG) concentration in the analysed range (Fig. 4.16) and were in between 18 and 24 µM. A fluorescent pellet was visible also for high ND (DEPG) concentrations, indicating that some receptor still precipitated during reaction and solubilisation with ND (DEPG) was thus not fully efficient.

Interestingly, higher ND (DEPG) concentrations apparently correlated with an increase in ligand binding activity in a range between 30 and 80 µM ND concentration and maximum fractions of folded receptor could only be achieved in presence of 80 µM or 110 µM ND (DEPG). This might indicate the existence of a relative complex folding mechanism, where the high availability of ND is important not only for solubilisation but also for folding of the ETB receptor.

4.2.3 Folding behaviour of cell-free synthesised ETB receptor.

Despite large progress that could be made for the folding of CF-produced ETB receptor by alteration of the lipid composition of supplied ND, a majority of the synthesised receptor remained incompetent to bind ET-1. This might have been caused by denaturation of the freshly synthesised receptor during the CF-reaction that is usually performed for 14 - 18 h at 30°C. It was therefore tested, if a reduction in CF-reaction temperature might lead to an increase in ligand binding competent receptor. Therefore, CF-synthesis of ETB-sfGFP-His_6 was performed in presence of ND (DEPG) at various temperatures in between 18 and 30°C for 17 h (Fig. 4.17).

Overall yield of soluble ETB was highly affected by a decrease in reaction temperature with only ca. 50% soluble yields at 25°C and only some 15% at 18°C reaction temperature as compared to CF-synthesis at 30°C. The measured fraction of active receptor was only slightly increased for synthesis at 25°C and no significant change in ligand binding activity was observed for synthesis at 18°C. Due to lower synthesis yield, the concentration of ligand binding sites were reduced in both 25 and 18°C reactions. Hence, it was concluded that a reduction in reaction temperature would not lead to an increase in concentration of ligand binding sites.

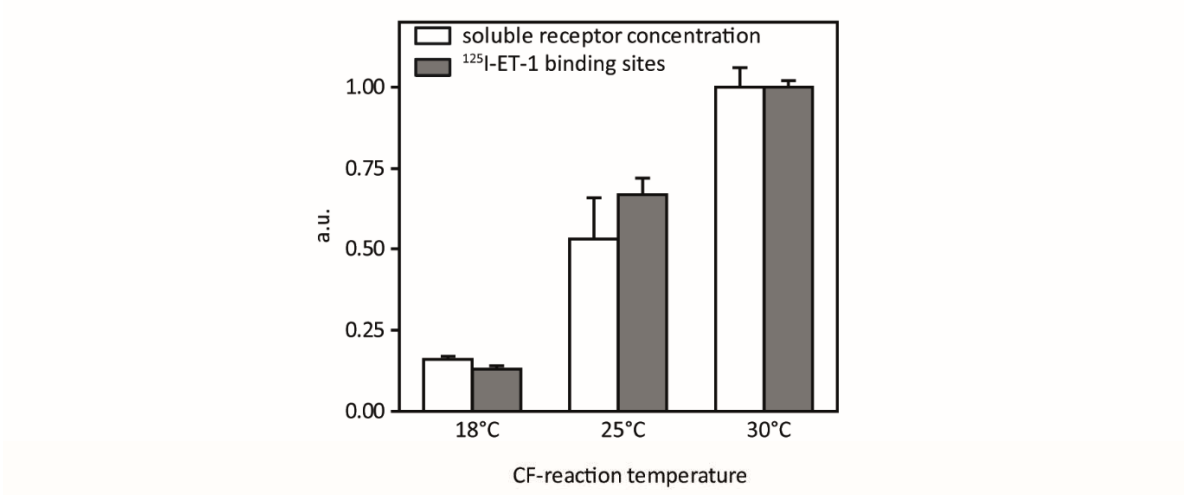

Fig. 4.17 CF-synthesis of ETB receptor in ND (DEPG) at altered temperatures.

ETB-sfGFP-His_6 was CF-synthesised in presence of 60 µM ND (DEPG) at indicated reaction temperatures for 17 h. Synthesis yields were determined by the fluorescence of the GFP moiety and ligand binding sites by radioligand filter binding assay with ET-1. Values are given as mean and SD of three CF-reactions.

In a next approach, the impact of shorter reaction times on the CF-production of ligand binding competent ETB was analysed. Therefore, ETB-sfGFP-His_6 was again CF-synthesised in presence of 60 µM ND (DEPG), harvested after 4, 8, 23, 28 and 46 h and analysed for total receptor yield and receptor ligand binding activity (Fig. 4.18 A)

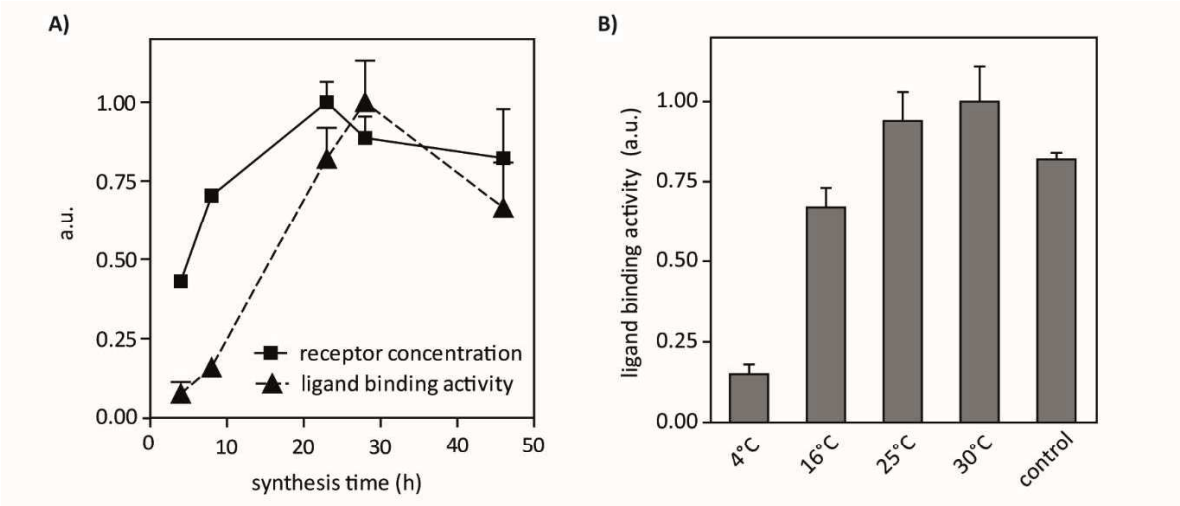

Fig. 4.18 Time-dependent CF-synthesis and post-translational folding of ETB receptor.

ETB-sfGFP-His_6 was CF-synthesised in presence of 60 µM ND (DEPG). Synthesis yields were determined by the fluorescence of the GFP moiety and folding by radioligand filter binding assays with ET-1 at constant receptor concentrations. A: Synthesis and folding of ETB-sfGFP during CF-reactions at 30°C. Values are given as mean and SD from three CF-reactions. B: Post-translational folding of ETB-sfGFP in ND (DEPG) at different temperatures. The receptor was synthesised for 4 h, translation was stopped with kanamycin and then further incubated without feeding mixture for additional 19 h at the indicated temperatures before performing radioligand filter binding assays. The control represents the ligand binding activity from a standard CF synthesis of ETB in ND (DEPG) for 23 h without translation stop. Values are given as mean and SD from three measurements.

As expected, the concentration of soluble receptor increased due to expression of ETB-sfGFP-His_6 and reached a plateau after 23 h. According to the sfGFP-fluorescence, almost 50% of the receptor was synthesised in the first 5 h and 75% in the first 10 h of CF-reaction. Interestingly, the receptor was found to be almost complete inactive in the first few hours after synthesis and the vast majority of ligand binding sites could only be detected after prolonged incubation for 23 h. This indicates a relatively slow post-translational folding process of the freshly synthesised ETB receptor.

In order to further analyse this folding process, the CF-synthesis of ETB was stopped after 4 h by addition of kanamycin to the RM and removal of the FM. The RM was then further incubated for 19 h at different temperatures ranging from 4°C to 30°C. For comparison, a standard CF-reaction was simultaneously performed for the total 23 h of the experiment. The fraction of folded receptor was then determined by radioligand binding assays with ^{125}I-labeled ET-1 (Fig. 4.18 B). Ligand binding activity comparable to the control reaction was only achieved after incubation at temperatures above 25°C, indicating a temperature dependence of the post-translational folding.

4.2.4 Importance of disulphide bridge formation on the folding of ETB receptor

Findings from the CF-reaction temperature and time screens clearly indicated the existence of a relatively slow and temperature dependent folding mechanism for ETB receptor. In previous studies with an insect cell lysate based CF-expression system, ETB receptor maturation was found to be dependent on the application of redox active compounds (Merk et al. 2015). This was accounted to the formation of a conserved disulphide bridge connecting extracellular loop (ECL) 1 and ECL 2, a common feature found for many GPCRs (Venkatakrishnan et al. 2013).

To verify the existence of this disulphide bridge in ETB receptor samples derived from the *E. coli* lysate based CECF-expression system, the corresponding cysteines C174 and C225 were pairwise or singly mutated to alanine in the DNA template of a C-terminal truncated ETB variant. The resulting constructs ETB-ΔC-C174A-sfGFP-His_6, ETB-ΔC-C225A-sfGFP-His_6 and ETB-ΔC-C174-C225A-sfGFP-His_6 as well as the control ETB- ΔC-sfGFP-His_6 were CF-synthesised in presence of ND (DEPG) for 23 h and analysed for soluble yield and ligand binding activity (Fig. 4.19 A) (data was kindly provided by Fang Dong, Institute of Biophysical Chemistry, Goethe-University Frankfurt, Germany).

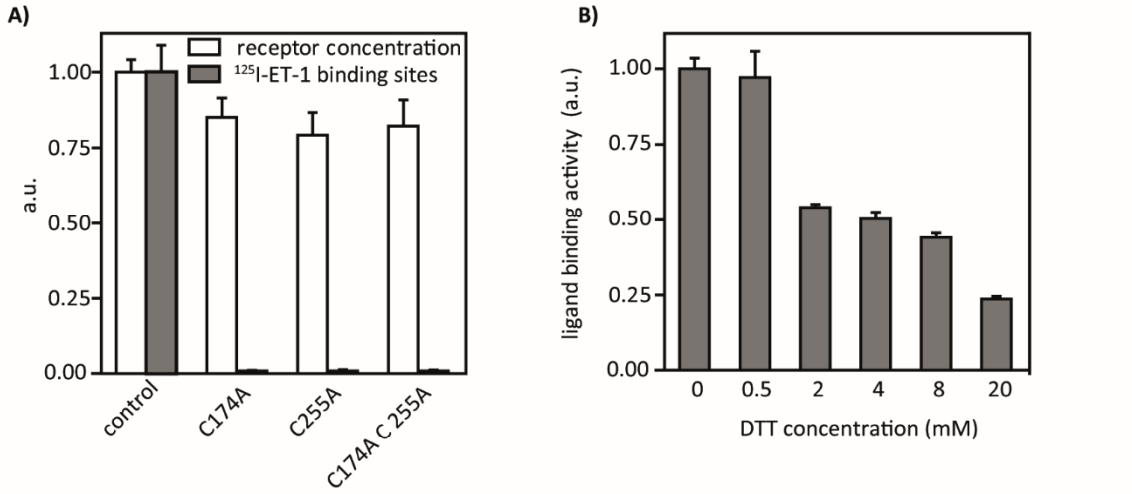

Fig. 4.19 Impact of disulphide bridge formation on ETB ligand binding activity.

A: ETB-sfGFP-His_6 and cysteine mutants were CF-synthesised for 24 h in presence of ND (DEPG). Receptor concentration was determined by sfGFP fluorescence and ET-1 binding competence by radioligand filter binding assay. Values are given as mean and SD from three CF-reactions. B: ETB-sfGFP-His_6 in ND (DEPG) was purified by IMAC and incubated over night at room temperature with increasing concentrations of the reducing agent DTT before determining ET-1 binding competence by radioligand filter binding assay. Values are given as mean and SD from three measurements.

Despite similar yields of soluble protein, the mutants were found to be complete incompetent to bind the natural agonist ET-1, indicating an impaired disulphide bridge formation in the mutants. To further verify the existence of the disulphide bridge in the non-mutated ETB receptor, ETB-sfGFP-His_6 was CF-synthesised in presence of ND (DEPG) and purified by IMAC before incubation with increasing concentrations of the reducing agent DTT at room temperature for ca. 18 h (Fig. 4.19 B). As expected, the binding competence of the purified receptor to ET-1 was impaired after incubation with 2 mM or higher concentrations of DTT. Interestingly, some 25% of remaining ligand binding activity could be found also after incubation with DTT concentrations as high as 20 mM, indicating that the formed disulphide bridge is either relatively stable or the receptor remains parts of its ligand binding capacity if it is once folded.

Taken together, these data verify the importance of the conserved disulphide bridge in ETB for ET-1 binding and strongly indicate its formation at least in a fraction of the CF-produced receptor.

4.2.5 Optimisation of redox conditions in cell-free synthesis of ETB receptor

The maturation of the ETB receptor to a ligand binding competent state was shown to be dependent on the formation of a conserved disulphide bridge connecting ECL 1 and 2 and maturation was somehow delayed and temperature dependent for CF-synthesised ETB in ND (DEPG). The standard CECF-reaction is supplemented with 2 mM of the reducing agent DTT, which has been demonstrated to impair the ligand binding competence of the receptor. DTT is known to be relatively sensitive to high temperatures (Han and Han 1994). It was therefore assumed that the maturation of ETB was impeded by the presence of DTT in the CF-reaction and only takes place after DTT degradation due to prolonged incubation of the CF-reaction at high temperatures. Simple omission of the reducing agent was not applicable, since this would result in a drastic drop in expression efficiency, probably caused by undesired oxidation of the ribosomes (Traut and Haenni 1967, Schwarz et al. 2007). It was therefore tried to improve the redox conditions in the CF-reaction in order to find a balanced condition that enables disulphide bond formation of the ETB receptor and simultaneously allows protein production.

Several redox active compounds were tested in various concentrations and oxidation potentials during CF reaction were monitored by the addition of the redox sensitive GFP variant roGFP1-iE (Lohman and Remington 2008). RoGFP is redox sensitive due to the introduction of a cysteine pair that forms a labile disulphide bridge, which leads to a shift of the GFP fluorescence excitation maximum (Pouvreau 2014). The oxidation state of roGFP can be monitored by calculating the ratio R of the fluorescence intensities at 510 nm after excitation at 485 and 390 nm ($R = I_{ex\ 485\ nm}/I_{ex\ 390\ nm}$). Knowing the ratios for fully reduced (R_{red}) and oxidised (R_{ox}) roGFP, the fraction of oxidised protein (F_{ox}) can then be calculated as $F_{ox} = (R - R_{ox}) / (R_{red} - R_{ox})$. R_{red} and R_{ox} was determined after incubation of roGFP with 2 mM DTT and 4 mM GSSG for 24 h and found to be 3.76 and 0.84, respectively (Tab. 4.1).

Tab. 4.1 Fluorescence intensity ratios and fraction of oxidised roGFP.

Redox active compound	R[a]	F_{ox}[b]
2 mM DTT	3.76 ± 0.09	0%
2 mM TCEP	3.16 ± 0.03	21%
4 mM GSH	1.91 ± 0.13	64%
4 mM GSSG	0.84 ± 0.01	100%

[a] Fluorescence intensity ratios were calculated from the fluorescence intensities at 510 nm after excitation at 485 and 390 nm. Values are averages from three independent measurements.

[b] Fraction of oxidised roGFP were determined from the fluorescence intensity ratios after incubation with 2 mM DTT (full reduced) and 4 mM GSSG (full oxidised)

The ratio of the maximum and minimum intensity ratios ($\delta = R_{red} / R_{ox}$) is a measure of the maximum attainable signal/noise ratio (Hanson et al. 2004) and was found to be 4.5, which is similar to the value found by Lohman et al. (Lohman and Remington 2008). The protein is thus suitable as a monitor for oxidation potentials in the reducing environment of CFPS.

The redox active compounds DTT and TCEP were next tested for their stability during CF-synthesis reactions. Therefore, CF-synthesis of ETB-strep was performed in presence of ND (DEPG), 7.5 µM roGFPiE and either 2 mM DTT or 2 mM TCEP and oxidation potential as well as ligand binding sites were monitored by roGFP-fluorescence and radioligand filter binding assay, respectively (Fig. 4.20).

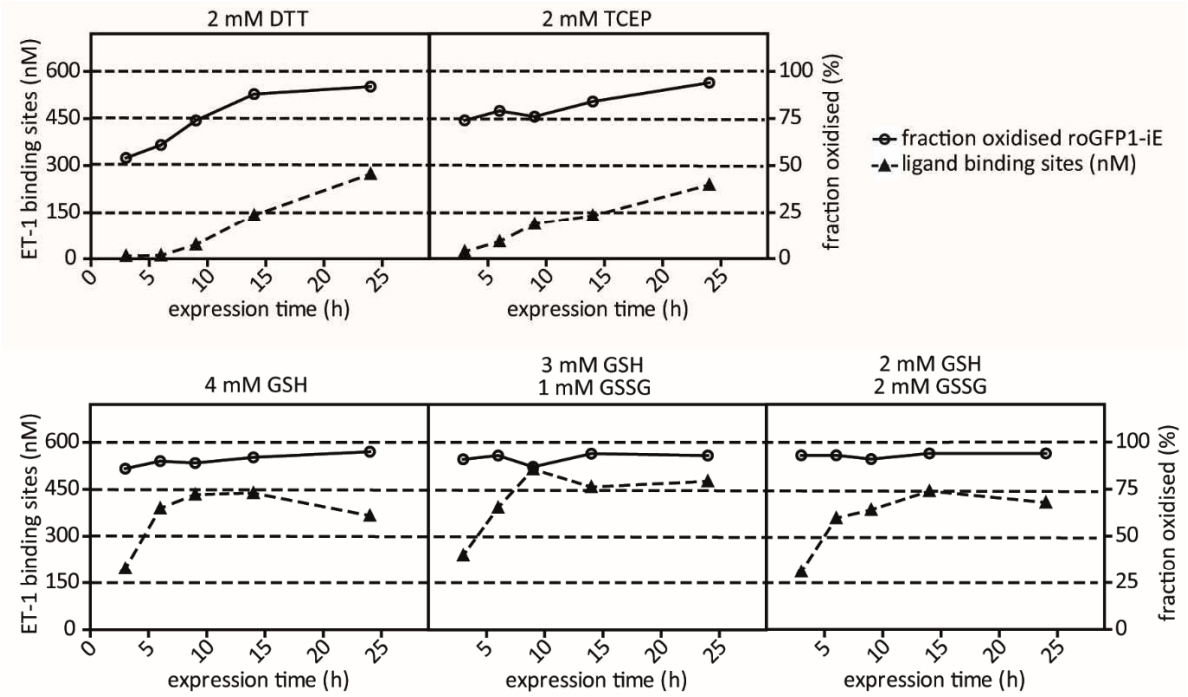

Fig. 4.20 Changes in the redox environment and ETB folding during CF-reactions.

ETB-strep was CF-synthesised in presence of ND (DEPG), 7.5 µM roGFP1-iE and different redox active compounds. Reactions were collected after 3, 6, 9, 14 and 24 h and potential precipitates were removed by centrifugation. A part of the supernatant was shock-frozen in liquid nitrogen and stored at -80°C before determining the ET-1 ligand binding sites by radioligand filter binding assays. Oxidation state of roGFP1-iE was determined by its fluorescence intensity ratio R. Therefore, a part of the supernatant was 3-fold diluted in freshly degassed and N_2 bubbled buffer (20 mM TRIS-Cl pH 7.5, 150 mM NaCl) and fluorescence emission at 510 nm after excitation at 390 and 485 nm was measured without delay.

For both compounds, the roGFP probe was partially reduced in the beginning and was gradually oxidised over the time of incubation. TCEP is reported to be more thermostable than DTT (Han and Han 1994) and one would except that redox-changes are less pronounced in a TCEP supplemented system. This seemed to be the case for the first 10 h of incubation. However, after prolonged incubation for 24 h, the roGFP probe is almost completely oxidised also in the TCEP supplemented reactions. TCEP is also known to be less reducing than DTT. Commonly accepted midpoint potentials are $E'^{\circ}_{DTT} = -330$ mV (Cleland 1964) and $E'^{\circ}_{TCEP} = -290$ mV (Pullela et al. 2006). This seems to be reflected in the initially higher oxidation state of roGFP in the TCEP supplemented reaction.

Surprisingly, the oxidation state of the redox probe in both DTT and TCEP supplemented CF-reactions appeared to be higher than what would be expected from the calibration measurements. Here, roGFP oxidation state was determined to 0% or 20% after incubation with 2 mM DTT or 2 mM TCEP, respectively (Tab. 4.1), while it was found to be 50% or 75% oxidised in the CF-reactions at the first point of measurement (Fig. 4.20). Nevertheless, the initial oxidation potential in the DTT supplemented CF-system was still too low for disulphide bond formation in the ETB receptor and receptor maturation only started after prolonged incubation and potential degradation of DTT. The initial oxidation potential in the TCEP supplemented system was apparently high enough for partial disulphide bond formation but the majority of the receptor appeared to maturate post-translationally also in this system.

In a next step, the redox compounds were substituted with a total of 4 mM reduced (GSH) and oxidised (GSSG) glutathione in various ratios (Fig. 4.20). GSH is known to be less reducing than DTT and TCEP. A commonly accepted midpoint potential is $E'^{\circ}_{GSH} = -240$ mV (Schafer and Buettner 2001). In accordance to this, the initial oxidation state of roGFP was found to be higher than that for DTT or TCEP and the oxidation potential indeed appeared to be high enough to enable disulphide bond formation in the ETB receptor, as high ligand binding competence was already found after 4 h of CF synthesis. After partial substitution with 1 mM GSSG, a further increase in the concentration of ligand binding competent receptor was found, with a maximum of ca. 500 nM ET-1 binding sites after 9 h of CF reaction. Longer incubation times or higher ratios of GSSG had no further positive effect. Therefore, the optimum of all tested redox conditions seems to be supplementation of 3 mM GSH and 1 mM GSSG in the CF-reaction and synthesis for ca. 8 - 10 h.

Like for the DTT and TCEP supplemented CF-reactions, the roGFP oxidation state in the GSH and GSH/GSSG supplemented CF-reactions appeared to be higher than what would be expected from the calibration data. The redox probe appeared to be almost completely oxidised in these conditions, indicating a high oxidation potential. This might be accounted to the presence of oxidases and disulphide isomerases like DsbA and DsbC derived from the *E. coli* lysate (Foshag et al. 2017) or simply to oxidation by molecular oxygen (Mamathambika and Bardwell 2008), as the reactions did not take place under inert atmosphere.

It is principally possible to quantify the redox potentials in the CF-reaction. The theoretical ambient redox potentials E'_{theo} at a certain concentration of a redox active compound are defined by the Nernst equation (Eq. 4.1).

$$E'_{theo} = E'^{\circ}_{redoxcompound} - \frac{RT}{nF} \times ln \frac{c_{red}}{c_{ox}} \qquad \text{Eq. 4.1}$$

R is the gas constant (8.315 J K^{-1} mol^{-1}), T is the absolute temperature in Kelvin, n is the number of transferred electrons (2), F is the Faraday constant (9.649 x 10^4 C mol^{-1}) and c_{red} and c_{ox} are the molar concentrations of reduced and oxidised redox compound. Ambient redox potentials can also by calculated from the based on the oxidation state of roGFP by applying Eq. 4.2

$$E'_{CF-reaction} = E'^{\circ}_{roGFP1iE} - \frac{RT}{nF} \times ln \frac{F_{red}}{F_{ox}} \qquad \text{Eq. 4.2}$$

$E'^{\circ}_{roGFP1iE}$ is the midpoint potential of roGFP1-iE (-236 mV, Lohman and Remington 2008) and F is the fraction of reduced or oxidised roGFP, respectively. Using Eq. 4.1 and Eq. 4.2, one can calculate the theoretical redox potentials and apparently measured redox potentials in the calibration assay and in the CF-reactions, while later values can only be calculated in a range of ca. -275 mV to -200 mV, due to the maximum and minimum oxidation state of roGFP-iE (Tab. 4.2).

Tab. 4.2 Theoretical and measured values for ambient redox potentials.

redox active compound	E'_{theo}	$E'_{calibration}$	$E'_{CF\text{-}reaction,\ 3h}$	$E'_{CF\text{-}reaction,\ 24h}$
2 mM DTT	- 309 mV	<-275 mV	- 234 mV	>-200 mV
2 mM TCEP	- 269 mV	- 254 mV	- 223 mV	>-200 mV
4 mM GSH	- 228 mV	- 229 mV	- 212 mV	>-200 mV

While the measured redox potentials in the calibration assay apparently fit to the theoretical values, it seems that the redox potentials in the CF-reactions are notably higher. Redox potentials for GSSG supplemented reactions and for reactions after 24 h incubation could not be reliably calculated due to the high oxidation state of roGFP, but should be at least -200 mV or higher and thus close to the redox potentials found in the ER and secretory pathway of mammalian hybridoma cells (E'_{ER} = -180 to-175 mV, Hwang et al. 1992). It needs to be mentioned that care must be taken in comparison of ambient redox potentials, as total values are pH and temperature dependent (Schafer and Buettner 2001, Mamathambika and Bardwell 2008). Nevertheless, the present data set strongly indicates surprisingly high redox potentials in the CF-reactions, especially after prolonged incubation or supplementation of GSH/GSSG mixtures.

Using an assay based on radiolabelled cysteine peptides and HPLC techniques, Hwang et al. found the ratio between GSH and GSSG in the ER and secretory pathway of mammalian hybridoma cells to be 3:1 to 1:1, with an overall glutathione concentration in a range between 1 and 10 mM (Hwang et al. 1992). With regard to these values, the optimised redox conditions in CF-system (3 mM GSH, 1 mM GSSG) seem to mimic the conditions found in the natural folding environment of the ETB receptor. However, the total amount of ligand binding active receptor was only increased for some 100% as compared to 2 mM DTT, indicating the presence of further bottlenecks in receptor folding.

To find out whether disulphide bridge formation in ETB could be further enhanced by even more oxidising conditions, CF-synthesis of ETB-sfGFP-His_6 was performed in presence of GSSG concentrations up to 3 mM (Fig. 4.21).

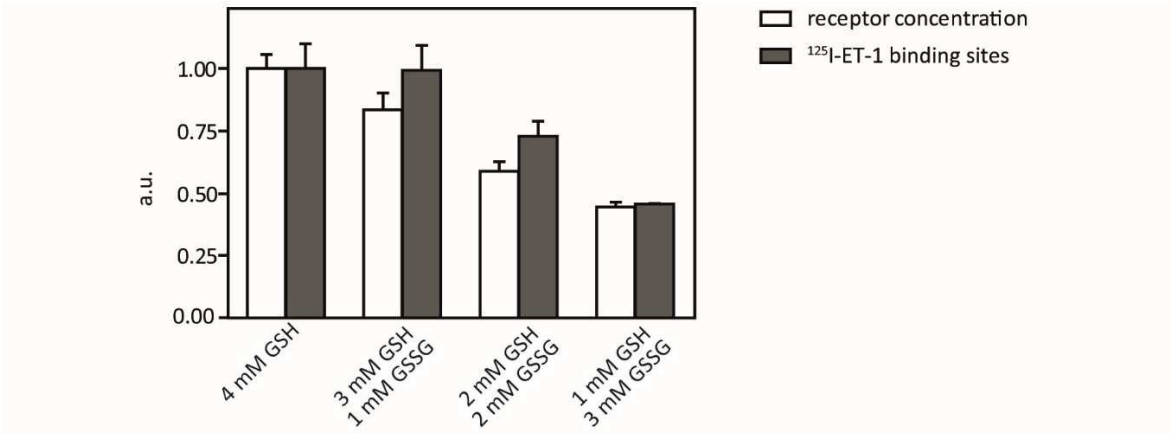

Fig. 4.21 Quantity and quality of CF-synthesised ETB at high GSSG ratios.

ETB-sfGFP-His_6 was CF-synthesised in presence of ND (DEPG) and various ratios of oxidised (GSSG) and reduced (GSH) glutathione. After removal of potential precipitates, receptor concentration was determined by the fluorescence of the sfGFP-moiety and ET-1 binding competence by radioligand filter binding assay. Values are given as mean and SD of three CF-reactions.

As expected, total yields of soluble receptor decreased with increasing concentrations of GSSG, as measured by the fluorescence of the sfGFP moiety. However, folding efficiency was not further enhanced with high GSSG concentrations, resulting in an overall decrease in ligand binding sites.

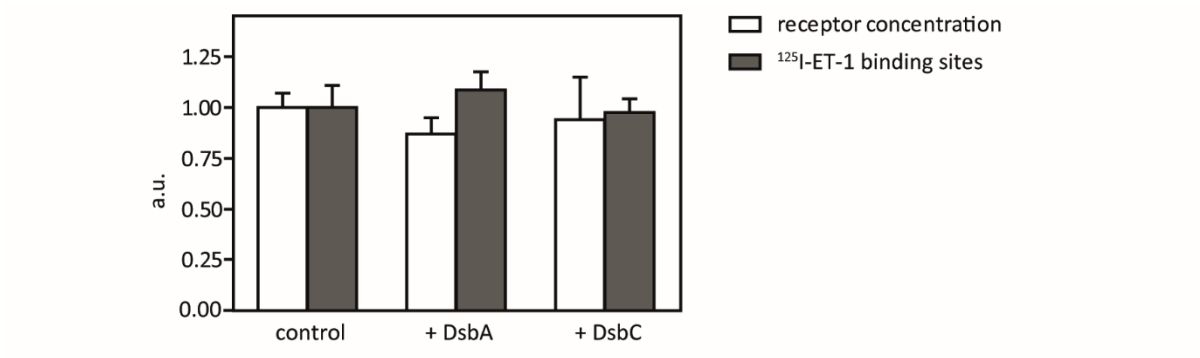

Fig. 4.22 Impact of DsbA and -C on the CF synthesis and folding of ETB receptor.

ETB-sfGFP-His_6 was CF-synthesised in presence of 60 µM ND (DEPG), 4 mM GSH and with or without 30 µM DsbA or 5 µM DsbC. After removal of potential precipitates, receptor concentration was determined by the fluorescence of the sfGFP-moiety and ET-1 binding competence by radioligand filter binding assay. Values are given as mean and SD of three CF-reactions.

Correct disulphide bridge formation in ETB might be further enhanced by the addition of oxidases or disulphide isomerases to the reaction mixture. The first is known to enhance disulphide bridge formation while the later is known to act as a chaperone, removing incorrectly formed and therefore instable disulphide bonds, thus resolving misfolded states (Ito and Inaba 2008). The *E. coli* derived oxidases and disulphide isomerases DsbA and DsbC were purified and supplemented to CF-expressions of ETB-sfGFP-His_6. However, no impact on both total yield and ligand binding activity could be detected (Fig. 4.22), indicating that supplemented DsbA and DsbC were either inactive in the tested conditions or could not further enhance correct disulphide bond formation.

It has been previously reported that incubation of the *E. coli* cell lysate with iodacetamide (IAM) prior to CF-reaction synthesis can have a positive impact on disulphide bond formation, especially in combination with the application of disulphide bond isomerase DsbC (Kim and Swartz 2004, Knapp et al. 2007, Bundy and Swartz 2011). IAM has been used to block reactive cysteine groups in the *E. coli* lysate and thus apparently prevented undesired disulphide shuffling while DsbC has apparently enhanced correct disulphide bond formation due to its chaperone activity. It was therefore tested whether treatment with IAM alone or in combination with the addition of DsbA to the RM could further enhance ETB folding in the CF-reaction. However, the fraction of folded receptor was found to be apparently unaffected, while total receptor yields were reduced by some 25 to 50%. The resulting drop in ligand binding site concentration renders this approach insufficient for the present CECF-reaction system (Fig. 4.23).

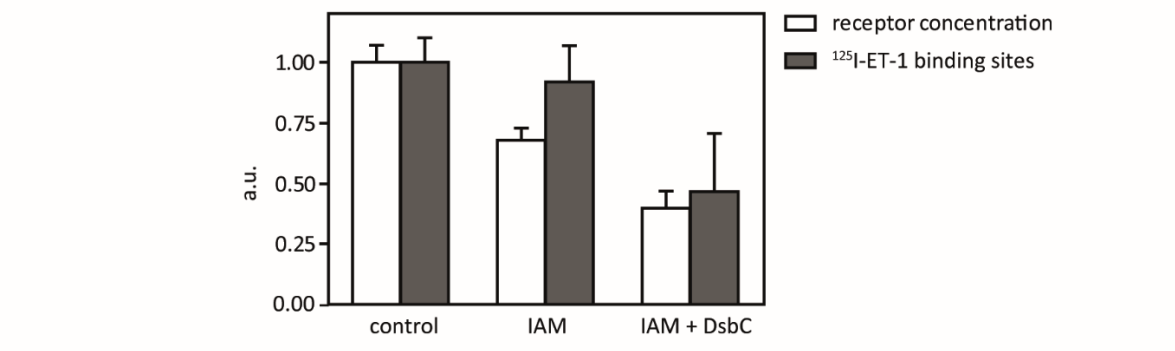

Fig. 4.23 Impact of iodacetamide treatment on CF-synthesis and folding of ETB receptor.

ETB-sfGFP-His_6 was CF-synthesised in presence of 60 µM ND (DEPG), 4 mM GSH and 100 µM DsbC using *E. coli* extract pre-treated with 500 µM IAM for 30 min at room temperature. After removal of potential precipitates, receptor concentration was determined by the fluorescence of the sfGFP-moiety and ET-1 binding competence by radioligand filter binding assay. Values are given as mean and SD of three CF-reactions.

4.2.6 Further optimisation of cell-free synthesis and folding of ETB receptor

The folding process of CF-synthesised ETB in ND could be enhanced by the modulation of the lipid environment of the supplied ND and by optimisation of the redox conditions during CF-reaction. However, a substantial fraction of the synthesised ETB was still found to be incompetent to bind its natural agonist ETB. Therefore, further optimisation steps were considered.

Chaperones are frequent folding helpers *in vivo* and act by prevention and removal of misfolded protein states. Heat shock (HS) chaperone enriched *E. coli* lysate as well as lysates which were specifically enriched with the *E. coli* derived chaperone pair GroEL/ES by overexpression were added to the CF-reaction synthesis of ETB-sfGFP-His_6 in a 3:7 mixture with standard lysate (Lysates were kindly provided by Dr. Frank Bernhard, Institute of Biophysical Chemistry, Goethe-University Frankfurt, Germany. For a protocol on preparation of the HS extract, see Foshag et al. 2017). This ratio was found to be most suitable, as higher concentrations of modified lysates substantially reduced overall synthesis yield.

For both tested conditions, overall yield of soluble receptor was decreased by ca. 25% compared to the control. No enhancement in the fraction of ligand binding receptor competent was found after supplementation of GroEL/ES enriched extract but the fraction of ligand binding active ETB was found to be almost doubled by supplementation of 30% HS extract and resulted in an increase in ligand binding site by roughly 60% (Fig. 4.24).

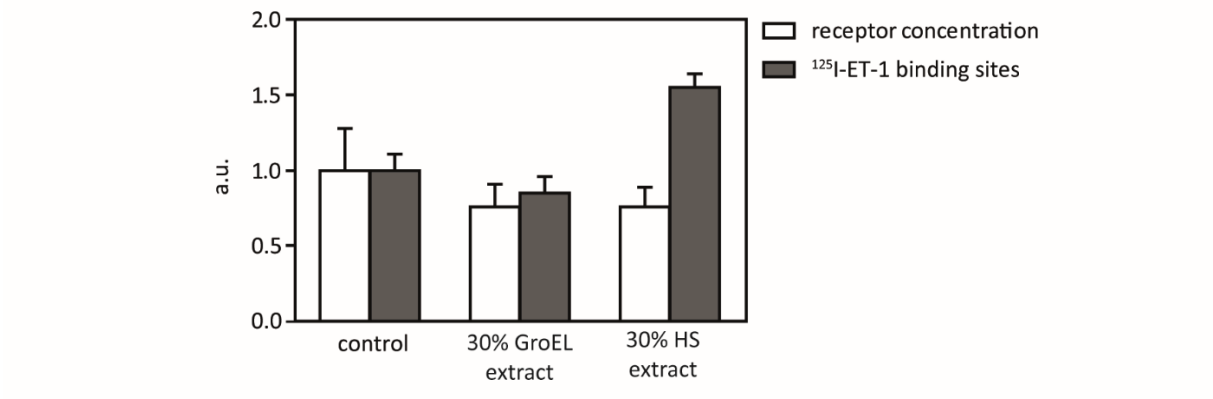

Fig. 4.24 Impact of chaperone enriched extracts on CF-synthesis of ETB receptor.

ETB-sfGFP-His_6 was CF-synthesised in presence of 60 µM ND (DEPG), 3mM GSH, 1 mM GSSG and using extract blends with 30% *E. coli* extract enriched with GroEL or heat shock chaperones (HS). After removal of potential precipitates, receptor concentration was determined by the fluorescence of the sfGFP-moiety and ET-1 binding competence by radioligand filter binding assay. Values are given as mean and SD of three CF-reactions.

An effective way for stabilisation of GPCRs is the insertion of point mutations at critical positions found by thermostabilisation screens (Vaidehi et al. 2016, Magnani et al. 2016). The high impact on the folding efficiency of β1-adrenergic receptors was shown earlier in this thesis (see 4.1). A recent report demonstrated the thermostabilisation of a human ETB receptor construct, which was a breakthrough step for crystallisation and structure determination at high resolution (Okuta et al. 2016, Shihoya et al. 2016). A DNA template of a C-terminal truncated ETB receptor carrying the five corresponding point mutations and a sfGFP reporter tag (ts-ETB-ΔC-sfGFP-His_6) was designed. Furthermore, the codons in the DNA template were optimised for expression in the *E. coli* based CECF-system (DNA template was kindly provided by Fang Dong, Institute of Biophysical Chemistry, Goethe-University Frankfurt, Germany). CF-synthesis reactions of the ts-ETB-ΔC-sfGFP-His_6, a non-stabilised truncated ETB construct (ETB-ΔC-sfGFP-His_6) and of full-length ETB-sfGFP-His_6 were then performed in the so far optimised CECF-system.

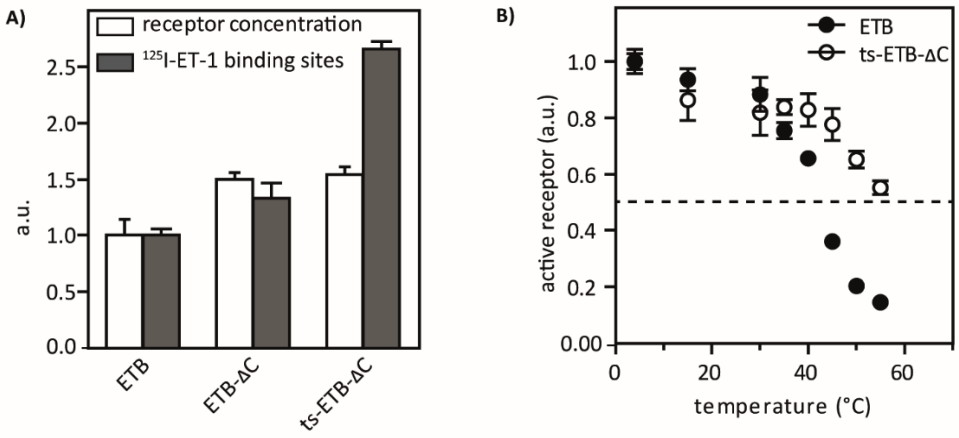

Fig. 4.25 DNA template optimisation for ETB receptor.

ETB-sfGFP-His_6 or ts-ETB-ΔC-sfGFP-His_6 were CF-synthesised in presence of 60 µM ND (DEPG), 3mM GSH and 1 mM GSSG and 30% HS extract. A: After removal of potential precipitates, receptor concentration was determined by the fluorescence of the sfGFP-moiety and ET-1 binding competence by radioligand filter binding assay. Values are given as mean and SD of three CF-reactions. Data for ETB-Δ-C were kindly provided by Fang Dong, Institute of Biophysical Chemistry, Goethe-University Frankfurt, Germany). B: Both constructs in ND (DEPG) were IMAC purified and incubated for 45 min at indicated temperatures before analysing binding to ET-1 in radioligand filter binding assays. Thermostability is given as the temperature retaining 50% of the ligand binding activity of samples stored at 4°C. Values are given as mean and SD of three measurements.

Both soluble yield and fraction of ligand binding competent receptor were increased with the ts-ETB-ΔC-sfGFP-His_6 construct, while non-stabilised ETB-ΔC-sfGFP-His_6 showed a ca. 50% increase in soluble yield but no altered folding efficiency. The total ligand binding site concentration depends on both parameters and was therefore ca. 200% higher in the thermostabilised construct and ca. 40% higher in the non-stabilised truncated construct compared to wild type ETB receptor (Fig. 4.25 A). In total, roughly 1.6 µM or 9% of the thermostabilised receptor were found to be ligand binding competent, corresponding to ca. 100 µg of correctly folded the ts-ETB-ΔC-sfGFP-His_6 per ml of reaction mixture.

To verify the effect of template optimisation on the stability of ETB, both ETB-sfGFP-His_6 and ts-ETB-ΔC-sfGFP-His_6 in ND (DEPG) were purified by IMAC and incubated for 45 min at increasing temperatures before performing a radioligand filter binding assay. Thermostability was found to be enhanced by ca. 15°C with 50% activity remaining at ca. 55°C compared to 40°C with the wild type ETB receptor (Fig. 4.25 B). Both purified receptor samples in ND (DEPG) were stored at -80°C and 4°C and did not show a decrease in ligand binding activity in both conditions for at least three weeks.

4.2.7 Summary of the optimisation steps for cell-free synthesis of ETB receptor

Tab. 4.3 summarises the consecutive optimisation steps for the CF-synthesis and folding of ETB receptor. In a first step (I), asolectin liposomes (LP) were used for the L-CF-synthesis of ETB receptor, resulting in some 0.3 nM concentration of ligand binding sites. Substitution with ND (DMPC) resulted in higher solubilisation efficiencies for ETB receptor (II). These experiments were initially performed by Proverbio et al. and could be verified in this thesis (Proverbio et al. 2013). Optimisation of the lipid composition of the supplied ND could drastically improve folding efficiency (III). Folding was further optimised by the application of a redox system (IV) and addition of a heat shock chaperone enriched

extract (V). CF-expression efficiency was further enhanced by DNA codon optimisation and in assumption that the fraction of active receptor would not increase without codon optimisation, one might probably find some 1 µM of ligand binding competent receptor after DNA template optimisation (VI). Thermostabilisation likely accounts for a further increase in folding efficiency and a total of approximately 1.6 µM ligand binding sites could be found with thermostabilised, truncated ETB receptor with optimised DNA codon usage (VII).

Tab. 4.3 Optimisation steps for L-CF synthesis of ETB receptor.

Optimisation step	Synthesis condition	Total soluble receptor yield (µM)	Ligand binding activity (nM)	Fraction active (%)
I	2 mg/ml LP (asolectin)	3.6 ± 0.7	0.26 ± 0.03	0.007 ± 0.001
II	60 µM ND (DMPC)	8.1 ± 2.2	0.96 ± 0.37	0.012 ± 0.005
III	60 µM ND (DEPG)	16.9 ± 0.3	344 ± 81	2.04 ± 0.48
IV (+III)	3 mM GSH 1 mM GSSG	15.9 ± 1.8	517 ± 101	3.22 ± 0.35
V (+IV)	30% HS extract	12.3 ±1.2	802 ± 48	6.55 ± 0.63
VIa (+V)	DNA codon optimisation and truncation	17.5	1103	6.55
VIIb (+V)	Thermostabilisation	17.5 ± 2.8	1565 ± 158	9.01 ± 0.65

[a] Calculated values for a hypothetical engineered DNA template without thermostabilisation based on the 1.42-fold higher expression efficiency of ts-ETBΔC.

[b] Measured values for the engineered DNA template of ts-ETBΔC.

4.2.8 Cell-free synthesis and ligand binding activity of Endothelin receptor type A

Unlike for the ETB receptor, L-CF-synthesis of the Endothelin receptor type A (ETA) in presence of ND (DMPC) was not found to be very efficient in previous studies (Proverbio et al. 2013). A main reason was the low solubilisation efficiency of the supplied ND (DMPC) for this receptor. Modulation of the lipid composition of the supplied ND was found to have a large impact on the quality of L-CF produced ETB receptor. It was therefore tested whether NDs with optimised lipid composition could have a positive impact also on the total soluble yield and folding of the ETA receptor, too (Fig. 4.26). Indeed, solubilisation appeared to be more effective with DOPG than with the corresponding lipid carrying a PC-headgroup (DOPC) ($P < 0.05$). No further significant increase in the solubilisation efficiency could be found with DEPG. Furthermore, folding efficiency was not significantly enhanced with DOPG and DEPG and thus only 5 to 10 nM of ET-1 binding sites could be detected.

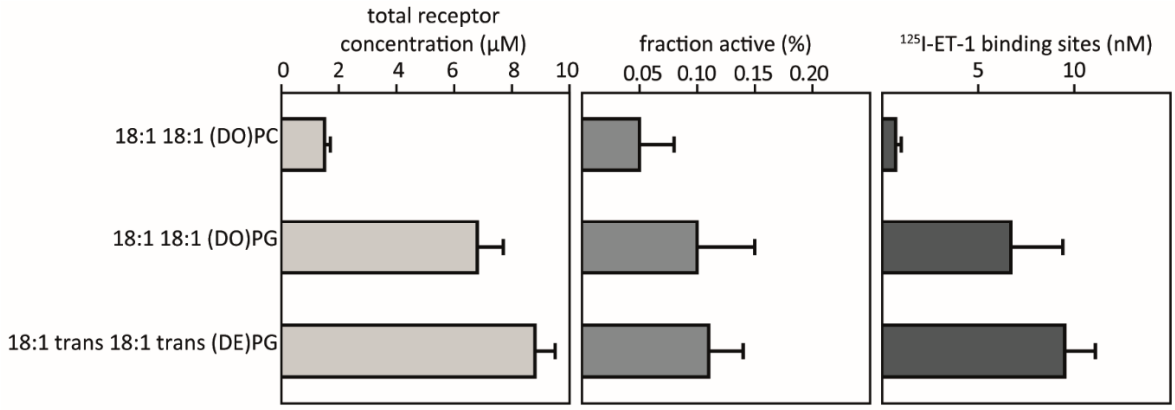

Fig. 4.26 Quantity and quality of ETA receptor in ND with selected lipid compositions.

ETA-sfGFP-His_6 was CF-synthesised in presence of 60 µM ND with various lipid compositions. After removal of potential precipitates, the total receptor concentration in the reaction mixture was determined by the fluorescence of the sfGFP-moiety and the concentration of ET-1 binding sites by radioligand filter binding assay. The fraction of active receptor was calculated assuming one ligand binding site per receptor. Values are given as mean and SD from three CF-reactions.

For CF-synthesis of the ETB receptor, the formation of a disulphide bridge between ECL 1 and 2 has been found to be crucial for receptor maturation and was enhanced after optimisation of the redox conditions during CF-synthesis. The disulphide bridge is a conserved feature for GPCRs. It was therefore tested, if changes of the redox conditions in the CF-synthesis would have an impact on the folding of ETA receptor. Furthermore, the HS-extract was applied in a ratio of 30% with normal S30-extract.

Concentration of ligand binding sites was significantly increased after supplementation of DTT with GSH/GSSG ($P < 0.001$), indicating the importance of disulphide bridge formation also in this receptor. On the other hand, application of the heat shock enriched extract had no further positive effect on ETA receptor folding (Fig. 4.27).

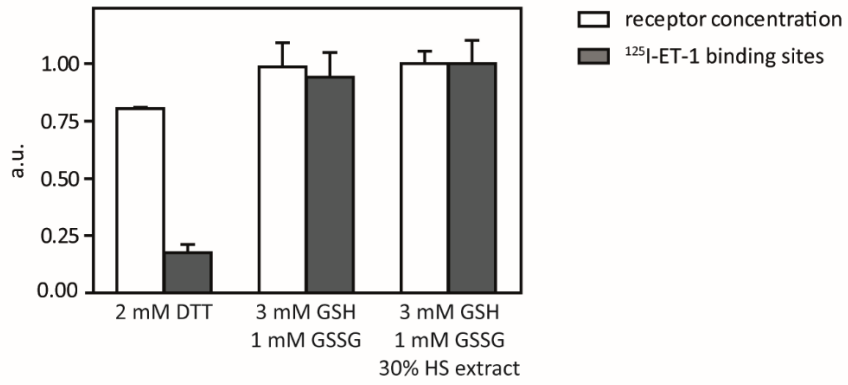

Fig. 4.27 Quantity and quality of ETA receptor using optimised CFPS conditions.

ETA-sfGFP-His_6 was CF-synthesised in presence of 60 µM ND (DEPG), indicated redox active compounds and with or without addition of 30% HS extract. After removal of potential precipitates, the total receptor concentration in the reaction mixture was determined by the fluorescence of the sfGFP-moiety and the concentration of ET-1 binding sites by radioligand filter binding assay. Values are given as mean and SD of three CF-reactions.

Earlier in this thesis, thermostability was demonstrated to be an important factor for the ligand binding activity of CF-produced ETB and β1AR constructs (see 4.1 and 4.2.6). As ETA receptor might be thermodynamically instable and degrade over the course of CF-reaction, it was analysed whether a reduction in reaction time might have a positive impact on the receptor. Indeed, a larger fraction of the receptor was found to be ligand binding competent when synthesis was performed for only 2 h as compared to 24 h (Fig. 4.28). The results are preliminary and need to be verified by additional experiments, but they might give a first indication that the stability of the CF-produced ETA receptor could be insufficiently low.

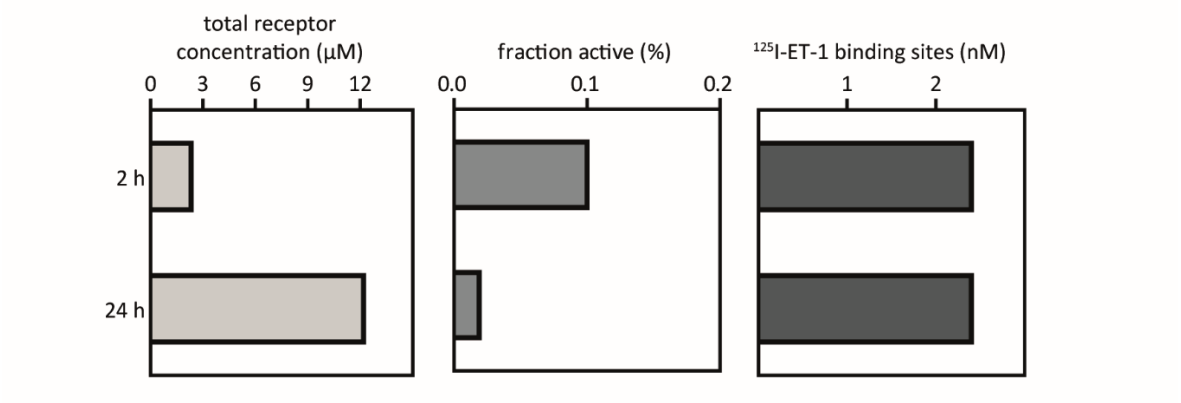

Fig. 4.28 Impact of short synthesis times on ETA receptor quality.

ETA-sfGFP-His_6 was CF-synthesised in presence of 60 µM ND (DEPG) and 4 mM GSH for 2 h or 24 h. After removal of potential precipitates, the total receptor concentration in the reaction mixture was determined by the fluorescence of the sfGFP-moiety and the concentration of ET-1 binding sites by radioligand filter binding assay. The fraction of active receptor was calculated assuming one ligand binding site per receptor. Values are given from single measurements.

Also with drastically decreased synthesis time, only ca. 0.1% of the receptor was found to be ligand binding competent, resulting in ca. 2 nM of ligand binding sites in this assay. A promising optimisation step might thus be the enhancement of the stability of ETA receptor, e.g. by screening for thermostabilising mutations. However, this approach would exceed the scope of this thesis.

4.3 Applications for CF-synthesised GPCR samples

In all tested cases, only parts of the cell-free synthesised GPCRs were found to be ligand binding competent. Nevertheless, the strategy of CFPS offers various advantages, as it is fast, reliable and highly adaptable to specific purposes. It allows the synthesis of GPCRs in a defined lipid environment and the receptors samples are directly accessible without the need of detergents and cell disruption techniques. Some possible applications were therefore explored with the turkey β1AR in ND.

4.3.1 Pharamacological analysis of β1-adrenergic receptor in defined lipid environments

NDs can be assembled with a variety of lipids or lipid mixtures and the combination with CF-expression systems offers the possibility to study lipid dependent effects on membrane proteins without the need of laborious reconstitution screens. In particular, β1AR could be synthesised in presence of ND with selected lipid compositions and the impact of different lipid environments on specific ligand binding characteristics could be analysed without prior purification of the receptor-nanodisc complex in a timescale of less than 24 h. Therefore, thermostabilised and non-stabilised turkey β1AR in ND with different lipid compositions were analysed for their binding affinities to a set of ligands using a radioligand filter binding assay. The previously mentioned inverse antagonist alprenolol as well as the second-generation β-blocker metoprolol and the third generation β-blockers nebivolol, labetalol and carvedilol were analysed, which differ in their selectivity towards β-adrenergic receptors. While nebivolol is a highly hydrophobic compound and selective for β1AR, both labetalol and carvedilol are non-selective antagonists with different hydrophobicity and labetalol being the least lipophilic compound (Fisker et al. 2015). Affinity of wild-type β1AR is high for alprenolol, carvedilol and nebivolol and in the range of 1 nM (Pauwels et al. 1988, Pönicke et al. 2002; Miller and Tate 2011) and somewhat lower for metoprolol and labetalol, being 10 and 50 nM, respectively (Hoffmann et al. 2004). Binding of those ligands was first analysed to thermostabilised turkey β1AR in ND with DMPC, POPG, DOPC, DOPG or DEPG lipid compositions (Fig. 4.29).

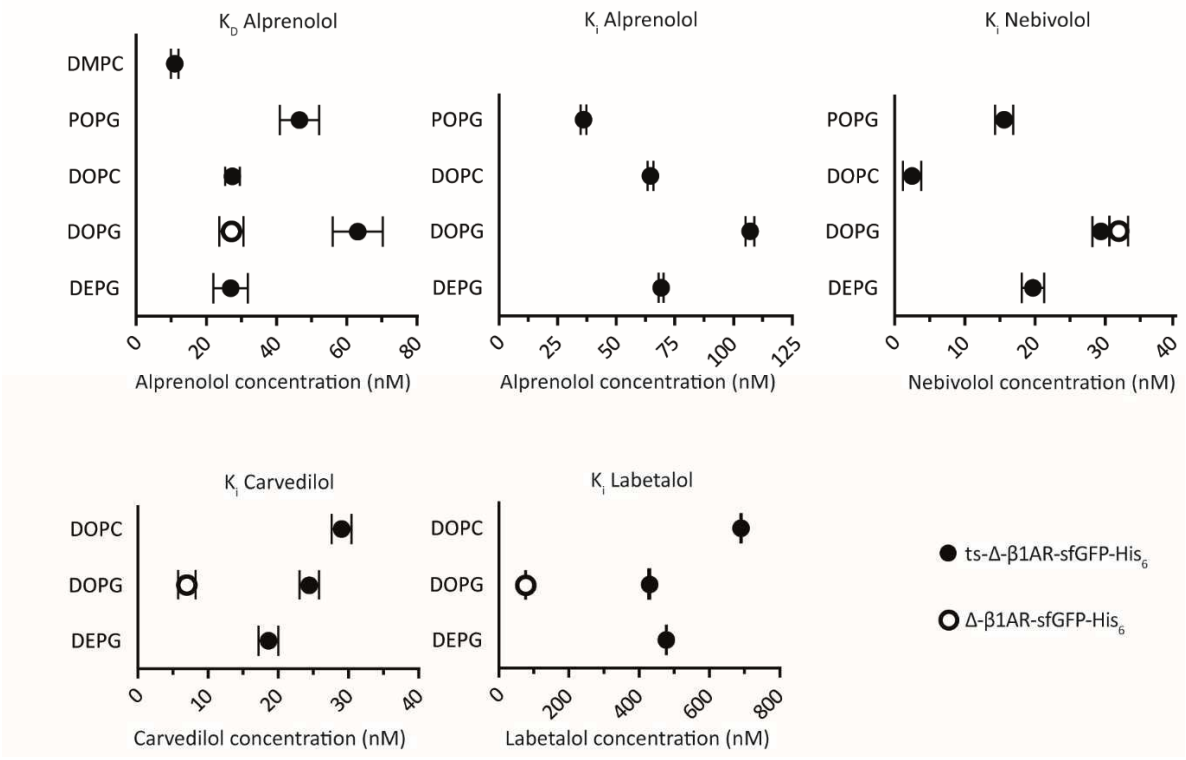

Fig. 4.29 Lipid dependent ligand screen of turkey β1AR derivatives.

Thermostabilised (ts-Δ-β1AR-sfGFP-His_6) and non-stabilised (Δ-β1AR-sfGFP-His_6) receptors were co-translationally inserted in nanodiscs with different lipid composition and binding affinities to various inverse agonists were analysed by radioligand filter binding assays. Dissociation constant (K_D) values were determined with increasing concentrations of ^{3}H-alprenolol. Inhibition constant (K_i) values were determined with constant ^{3}H concentrations and titration of the indicated non-labelled ligands. Concentration of unpurified receptor was constant in all analyses. Values are given as mean and SD of three measurements (adapted from Rues et al. 2016).

Clear variations in ligand affinity of ts-Δ-β1AR-sfGFP-His_6 in the different lipid environments could be detected, although changes were relatively moderate. Binding to alprenolol shows an apparent K_D variation of ca. 5-fold between DMPC (11 nM) and DOPG (63 nM) ($P < 0.001$). Those values are in agreement with previous determinations using a highly similar β1AR construct derived from *in vivo* synthesis (Miller and Tate 2011). Inhibition constants (K_i) for alprenolol were accordingly similar and showed an approximate 3-fold variation, which is also in the range of previously published results (Miller and Tate 2011). Relatively high K_i variations could be detected for nebivolol binding with a ca. 7-fold change between DOPC and DOPG (4 nM and 29 nM, respectively, $P < 0.001$). In contrast, carvedilol and labetalol binding to thermostabilised β1AR seems to be only moderately affected by the tested lipid alterations. Lipid dependent changes in ligand affinities thus do not follow an overall trend but seem to be rather ligand specific. Affinities of the selected ligands were also analysed for the non-stabilised turkey β1AR variant in ND (DOPG). Affinity to nebivolol was similar to that of the thermostabilised construct and slightly lower than for the thermostabilised construct for both alprenolol and carvedilol binding ($P < 0.001$). Remarkably, differences in labetalol binding were more pronounced

than for the other ligands and the apparent K_i value was ca. 10-fold lower in the non-stabilised construct than in the thermostabilised variant ($P < 0.001$).

While lipid dependent effects on the ligand binding characteristics of β1AR are thus clearly visible, more data sets and complementary assays would be necessary to draw conclusions for the observed effects. However, the results indicate the feasibility of the approach and indicate the suitability for future studies, in particular in regard to the possibility to observe ligand binding effects for non-stabilised turkey β1AR variants.

4.3.2 Function-related purification of β1-adrenergic receptor in ND

While ligand binding studies can mostly be done in crude cell extracts, well-purified and homogeneous protein samples are a basic prerequisite for a broad range of biophysical and biochemical assays, especially for structural approaches. The results in quality and production efficiency of thermostabilised β1AR with optimised ND composition appeared to be promising enough for purification in mg scales. Therefore, a pilot study for the purification of ts-Δ-β1AR-sfGFP-His_6 in ND (DOPG) was performed. The two-step purification strategy was adapted from (Warne et al. 2003): CF-synthesised receptor in ND (DOPG) was first purified by ion-metal-affinity-chromatography (IMAC) with utilisation of the His-tag on both the receptor and the scaffold protein of the ND. This would result in a mixture of empty ND and ND filled with both ligand binding competent and incompetent receptor. To separate correctly folded receptor from misfolded ones and empty ND, a second purification step was performed were the receptor-ND complexes were specifically bound to the ligand alprenolol, which was covalently coupled to an agarose-matrix (ligand affinity chromatography, LAC). After elution with an excess of free alprenolol, one would ideally receive only ligand binding competent receptor in ND (DOPG). Purification was performed at 16°C and sample purity as well as homogeneity was checked by SDS-PAGE and SEC after each purification step (Fig. 4.30). Receptor concentration and recovery efficiency was analysed by fluorescence of the sfGFP moiety.

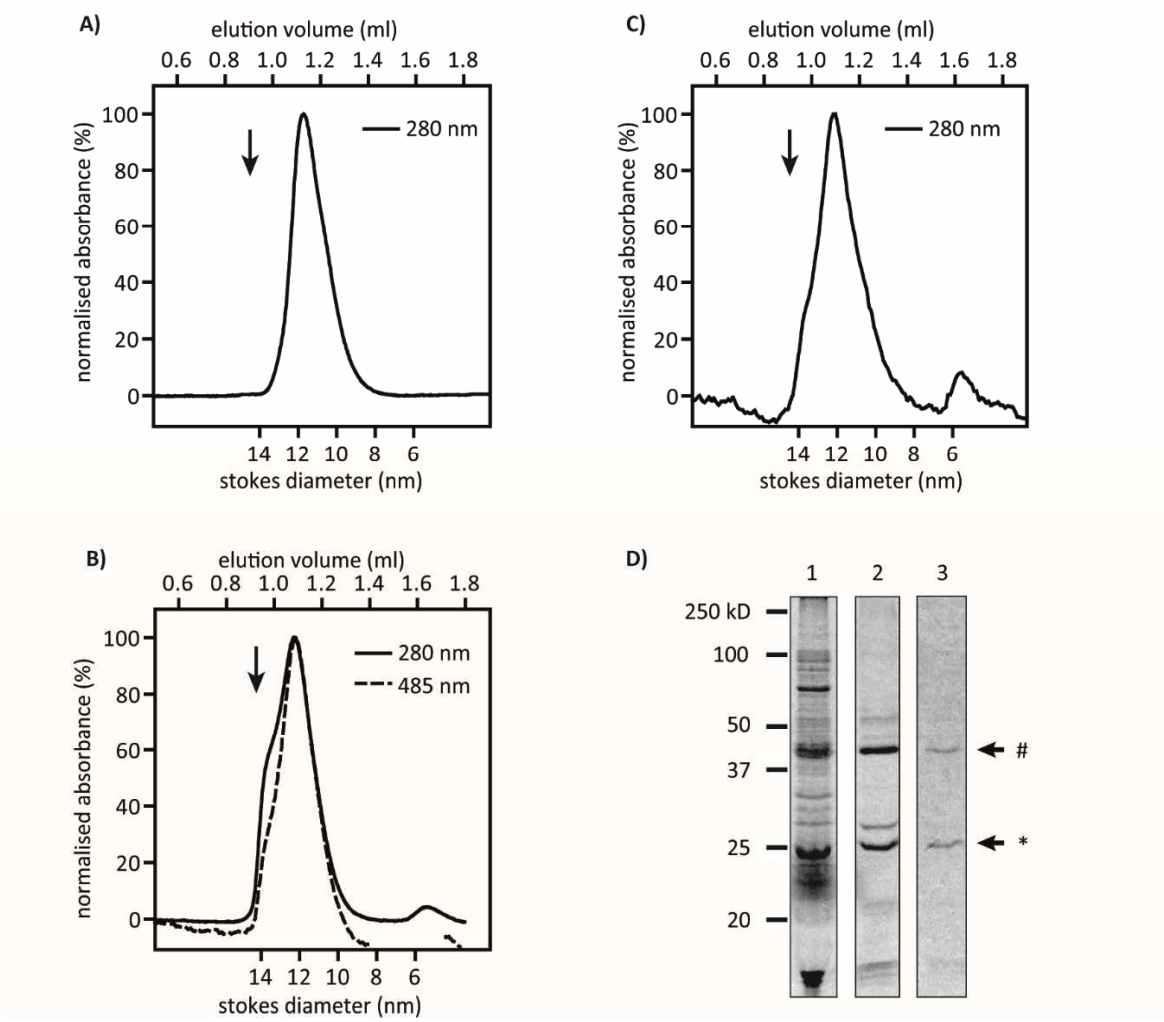

Fig. 4.30 Two-step purification of thermostabilised β1AR-ND (DOPG) complexes.

Ts-Δ-β1AR-sfGFP-His_6 was CF-synthesised in presence of ND (DOPG) and purified by IMAC and subsequent ligand affinity chromatography (LAC) using alprenolol coupled to an agarose matrix. A: SEC elution profile of empty ND (DOPG). B: SEC elution profile of β1AR-ND complexes after IMAC purification. Receptor was traced by the specific absorbance of the sfGFP-tag at 485 nm. C: SEC elution profile of β1AR-ND complexes after subsequent LAC purification. SEC runs were performed on a Superdex 200 3.2/300 column and total protein concentration in the elution was measured by absorbance at 280 nm. The arrow indicates the void volume of the column. D: Trichloroethanol stained SDS-PAGE of the CF-reaction mixture (1), IMAC elution (2) and LAC elution (3). Ts-Δ-β1AR-sfGFP-His_6 runs at ca. 40 kDa (#) and MSPE3D1 of the ND at ca. 28 kDa (*)(adapted from Rues et al. 2016).

Cell-free synthesis of ts-Δ-β1AR-sfGFP-His_6 was performed in presence of 30 µM ND (DOPG) for 17 h. IMAC purified receptor-ND complex appeared to be slightly larger than empty ND (DOPG) with a main elution peak at 1.08 ml as compared to 1.13 ml found for empty ND (Fig. 4.30 A and B). This corresponds to a stokes diameter of 11.7 nm for empty ND (DOPG) and 12.2 nm for ts-Δ-β1AR-sfGFP-His_6-ND (DOPG) complexes and a gain of molecular mass of roughly 100 kDa. Based on the amino acid sequence, the receptor construct has a molecular mass of 63 kDa. The gain in molecular mass seems thus to be somewhat larger than what would be expected for simple insertion of a single receptor protein per ND but to small to indicate insertion of receptor dimers, at least if dimer insertion would happen

without lipid loss in the ND. However, molecular mass prediction by SEC is relatively imprecise and meaningful statements on receptor dimerisation in ND (DOPG) could only be made with the use of additional assays. Nevertheless, the elution peak shift clearly indicates the formation of receptor-ND complexes that are stable during IMAC purification and SEC. This is strongly supported by the elution peak overlay for absorbance at 485 nm, which traces the sfGFP-tagged receptor specifically (Fig. 4.30 B).

Aggregated protein complexes are found in the void volume of the SEC of the IMAC purified sample. However, the aggregation peak is much smaller for the specific receptor absorbance at 485 nm, which indicates that most of the receptor is not found in these aggregates. Indeed, most of the aggregates could be removed by second step LAC and the resulting sample appeared to be relatively homogeneous in SEC (Fig. 4.30 B and C). While impurities were found in the IMAC purified sample also in SDS-PAGE analysis, the LAC purified appeared to be pure and only bands for the receptor and ND could be found (Fig. 4.30 D).

Total soluble receptor yield in the RM was ca. 400 µg per ml, as measured by the fluorescence of the sfGFP moiety. After IMAC purification, 68.8 +/- 11.3% of the receptor could be recovered, corresponding to 275 µg per ml of initial reaction mixture. With subsequent LAC, 55.6 +/- 8.2% of the IMAC purified receptor could be recovered. Taken together, ca. 150 µg of ts-Δ-β1AR-sfGFP-His_6 could be purified from 1 ml of reaction mixture with the two-step purification protocol, corresponding to a total recovery rate of 37.5%.

5 Discussion

5.1 Parameters for quality improvements of cell-free synthesised GPCRs

The open nature of CF-expression technologies offers new possibilities and a completely different set of strategies for quality improvement of membrane protein samples. Pronounced quality improvement of CF-produced β1AR and ETB receptor was presented in this thesis and was achieved by systematic improvement of the following CF-expression parameters: i) the CF-expression mode, ii) hydrophobic environment and lipid bilayer composition, iii) conformational thermostabilisation, iv) disulphide bridge formation and v) folding improvement by chaperones. In this paragraph, the optimised parameters will be discussed and further ideas for improvements will be outlined. Furthermore, suggestions will be made based on the recent findings that might lead to a quality enhancement also for other CF-produced GPCRs.

5.1.1 The CF-expression modes

CF-expression is a generally open system that allows the addition of a high variety of agents to solubilise the newly synthesised membrane proteins. In the P-CF mode, no hydrophobic supplements are added to the reaction, causing the quantitative precipitation of the freshly synthesised membrane protein. Synthesis yields are usually high in this mode and precipitation can already be seen as a first purification step, even when some co-precipitation of proteins from the CF-extract frequently happens (Schwarz et al. 2007). In addition to that, interference of hydrophobic substances is excluded, resulting in a highly robust expression system. It is thus the most economic way to produce membrane proteins in CF-expression systems but requires post-translational solubilisation of the target protein. For some cases, solubilisation in mild detergents and subsequent protein purification was sufficient to yield high quality membrane protein samples (Maslennikov et al. 2010, Boland et al. 2014). P-CF synthesis with post-translational reconstitution in liposomal vesicles has been reported for the Histamine H_1 and the Dopamine D2 receptor showing some ligand binding activity (Sansuk et al. 2008, Basu et al. 2013). Both ETA and ETB receptor derived from P-CF synthesis have previously been solubilised in a variety of detergents and reconstituted into proteoliposomes and analysed for homogeneity and ligand binding, but ligand affinities were found to be only moderate (Klammt et al. 2007, Junge et al. 2010, Proverbio et al. 2013). In the present study, the P-CF reconstitution approach was not successful to produce ligand binding competent receptor even in the case of thermostabilised turkey β1AR (see 4.1.1), which has been demonstrated to have an enhanced folding behaviour (see 4.1.4). On the other hand, refolding of a thermostabilised receptor derived from recombinant expression in *Sf9*-cells has been reported (Di Bartolo et al. 2016). A key parameter of the successful refolding was the complete unfolding with high concentrations of urea in this case. Pronounced un- and refolding steps might therefore be necessary for P-CF derived thermostabilised β1AR.

Soluble synthesis in the presence of detergents has been reported for several GPCRs, including the Endothelin receptors type A and B (ETA/ETB) and a β2AR fusion with $G_{\alpha,s}$ (Ishihara et al. 2005, Klammt et al. 2007, Kaiser et al. 2008, Junge et al. 2010, Corin et al. 2011a, Proverbio et al. 2013, Chi et al. 2015, Chi et al. 2016, Shilling et al. 2017). A prerequisite for this approach is the insensitivity of

the respective membrane protein towards the supplemented detergent and most of these studies have been done in either digitonin or Brij-derivates. High synthesis yields in Brij-derivates could be observed for turkey thermostabilised β1AR in the present study but the receptor appeared to be not ligand binding active. Some ligand binding activity could only be achieved in digitonin supplemented with lipids or when DMPC was added to the CF-synthesis in Brij-78. In the later case, bicelle like structure may have formed, based on the relatively high ratio of DMPC to Brij-78 detergent. It appears that this expression mode was inefficient to produce soluble receptor. However, based on this initial data set and on the finding that receptor folding is lipid dependent, CF-synthesis in presence of optimised bicelles might be a promising alternative to the relatively labor intense ND approach.

Even when membrane proteins show structural folding in detergents, the frequently lack activity and show altered structural dynamics, indicating that insertion into a lipid environment might be generally more suitable option (Ding et al. 2015, Frey et al. 2017). L-CF synthesis of GPCRs has been reported with liposomes (Ritz et al. 2013), nanodiscs (Yang et al. 2011, Shilling et al. 2017) or even tethered lipid membrane systems (Robelek et al. 2007, Leutenegger et al. 2008). In preceding studies with the ETB receptor (Proverbio et al. 2013) and in the present study with the turkey β1AR, nanodiscs were found to be superior for the L-CF synthesis of functionally folded receptors. ND (DMPC) with a larger diameter appeared to be more efficient in solubilisation of the ETA and ETB receptor and a stoichiometric overtitration of ND was necessary to achieve full solubilisation of the ETB receptor (Proverbio et al. 2013). This was also the case for the turkey β1AR in the present study. It appears that solubilisation of the receptors with the ND is partly impaired. This is not the case for some other membrane proteins including the 7 transmembrane segment containing proteins bacteriorhodopsin and proteorhodopsin, which show multiple insertion and oligomerisation when ND are supplied in an undertitrated stoichiometric ratio (Roos et al. 2012, Zocher et al. 2012, Henrich et al. 2017). The reason for the inefficient solubilisation with the tested GPCRs is so far unknown, but might be related to the lipid composition of the ND and the stability of the GPCRs (see respective subsection 5.1.2 and 5.1.3 for further discussion).

ND are dense and stable membrane patches (Bibow et al. 2017) and insertion into preformed ND might be energetically difficult. An interesting approach to circumvent this issue was reported by Gao et al. 2012. Here, membrane scaffold proteins were co-expressed with several GPCRs in presence of DMPC unilamellar vesicles. This lead to the co-translational formation of ND-like particles and solubilisation of the respective GPCRs. Among the CF-synthesised GPCRs, neurokinin 1 receptor was further analysed for ligand binding and affinities in the nanomolar range were observed (Gao et al. 2012). Alternative solubilisation strategies involving lipid environments might therefore be promising also for the GPCRs tested in the present study.

5.1.2 Lipid environment

Overall solubilisation efficiency and correct folding are the basic parameters that affect the yield of ligand binding competent receptor in the L-CF expression mode using ND. Both parameters were found to be dependent on the ND lipid composition. Solubilisation of the thermostabilised turkey β1AR was highest with phosphoglycerol (PG) and phosphocholine (PC) headgroup lipids but very inefficient with tested lipids carrying a phosphoethanolamine (PE) or phosphatidic acid (PA) headgroup. Lipids with

these headgroup tend to form non-bilayer phases and induce membrane curvature stress and might therefore be detrimental for the flat bilayer of the ND (Booth 2005, Dickey and Faller 2008). Indeed, homogeneity of ND (DOPE) and ND (DOPA) comparable with the other tested lipids was only achievable after additional SEC purification. Insufficient ND formation might thus have been the reason for the low solubilisation and folding efficiency with DOPE and DOPA lipids.

Similar solubilisation yields with all tested PC-, PG- and phosphatidylserine (PS) lipids were found for the ETB receptor but solubilisation of the ETA receptor was clearly enhanced with DOPG relative to DOPC. Positive effects of PG-headgroup lipids on the solubilisation efficiency of both Endothelin receptors have also been reported in preceding studies for ND (DMPC) and ND (DMPG) (Proverbio et al. 2013) and might be accounted to electrostatic interactions of positively charged residues of the nascent peptide chain with the negatively charged lipid headgroups, triggering the association of the membrane protein with the ND, as previously reported, e.g. for the association and integration of antimicrobial peptides in lipid membranes (Lakey et al. 1994).

As only parts of the solubilised receptors were found to be ligand binding competent even in the best cases, it appears obvious that solubilisation of the receptor with the ND is no direct indicator for the insertion or folding of the membrane protein but might be solely accounted to its association with the ND. However, it seems likely that correct folding requires insertion of the receptor in the lipid bilayer. Folding efficiency of both thermostabilised turkey β1AR and ETB receptor was generally higher in anionic PG- and PS-headgroup lipids than in neutral charged PC-headgroup lipids. Lipid headgroup charge and resulting membrane surface potential might thus have an impact not only on the association of the nascent peptide chain with the ND but also on the insertion in the lipid bilayer.

Insertion process might happen co- or post-translationally. In the later case, preliminary folding steps may be required at the membrane surface prior to insertion. Using time-resolved Surface-Enhanced InfraRed Absorption Spectroscopy (SEIRAS) measurements, Harris et al. have recently analysed the folding of two *E. coli* membrane proteins that were CF-synthesised in presence of ND. While insertion and folding of the rhomboid protease GlpG was apparently co-translational, the oxidoreductase DsbB showed a post-translational folding behaviour. The authors postulated different folding pathways for both proteins, with the nascent polypeptide chain of DsbB being post-translationally associated to the membrane surface prior to insertion (Harris et al. 2017). In another example, co-translational insertion of the CF-produced mitochondrial inner membrane transporter ADP/ATP Carrier (AAC) into liposomes has been demonstrated based on the identification of ribosome-AAC-liposome complexes (Long et al. 2012). Co- and post-translational insertion mechanisms are thus both conceivable for CF-synthesised membrane proteins. The co-translational insertion mechanism of CF-produced membrane proteins in ND was recently analysed for the monomeric signal peptidase LspA, the tetrameric pottasium channel KcsA and the hexameric proton pump proteorhodopsin in more detail using laser-induced liquid bead ion desorption (LILBID) mass spectrometry. Here, the insertion for the oligomeric proteins was found to be cooperative, indicating the existence of a multi-ribosomal complex or polysome acting on one ND. Addtionally, 1D-NMR analysis revealed that the insertion goes in hand with a removal of lipids from the ND bilayer (Peetz et al. 2017). For CF-synthesised GPCRs, exact mechanism for insertion into preformed ND is unknown so far but might be further analysed with the recent techniques.

For both turkey thermostabilised β1AR and ETB receptor, long chain lipids with a PG-headgroup were most efficient in support of receptor folding and high ligand binding activity. Fatty acid chain length has a direct impact on the thickness of the formed lipid bilayer. DOPE, a main component of the disc membranes in the rod outer segments of photoreceptor cells, forms bilayers with thickness of approx. 27 Å that perfectly match with the transmembrane segments of rhodopsin. Hydrophobic mismatch caused by lipids below and above the optimal fatty acid chain length results in conformational deformations in rhodopsin (Soubias et al. 2008, Soubias and Gawrisch 2012). Similar effects are likely for other GPCRs and reduced lipid bilayer thickness in e.g. ND (DMPC) and ND (DMPG) might thus cause hydrophobic mismatches with the GPCR transmembrane segments having a negative impact on the functional folding of the receptors.

Folding efficiency might further be modulated by the bilayer flexibility and lateral pressure on the transmembrane segments. Based on findings for the insertion and folding of bacteriorhodopsin in liposomes, the authors proposed that low membrane curvature stress and chain pressure favours insertion of transmembrane domains, while a moderate increase in stress and chain pressure can assist the folding, respectively helix packing and high chain pressure stabilises the folded state of a membrane protein (Booth 2005). The lateral pressure of the lipid bilayer of the ND is unknown in the given conditions, but is generally affected by the lipid headgroup and its tendency to induce membrane curvature stress as well as by the number of unsaturated bonds in the fatty acid chains and their orientation (Booth 2005) and should be comparable if only one parameters is changed. For ETB receptor in PG-headgroup lipids, folding efficiency is enhanced with lipids having more unsaturated fatty acid chains and a higher phase transition temperature, causing higher rigidity and lateral pressure in the ND bilayer. This finding might reflect the model proposed by Booth with folding and receptor stabilisation being most efficiently enhanced by the lateral pressure giving by the ND (DEPG). However, the effect appears to be opposed for PS-headgroup lipids, with DOPS supporting the folding of ETB more efficiently than POPS despites its lower phase transition temperature. Additionally, both thermostabilised and non-stabilised turkey β1AR do not show a pronounced folding enhancement towards DEPG compared with DOPG. Further assays are therefore necessary to analyse the effective lateral pressure in the ND and their impact on receptor folding in more detail.

Further synergetic effects on receptor stabilisation and folding may occur through direct allosteric binding of a specific lipid to the respective receptor (Laganowsky et al. 2014). From the tested lipids, DOPG offered one of the best folding environments for β1AR. A binding preference for PG-lipids and especially DOPG was found recently for β2AR. After *in vivo* expression in *Sf*9 cells, receptor was purified in mild detergents and associated lipids were quantitatively analysed by mass spectrometry. In relation to its abundance in the cell membrane, DOPG was 70-fold enriched in the purified β2AR sample (Dawaliby et al. 2016), indicating the *in vivo* preference of the receptor towards this lipid. Even if the slightly different human β2AR was analysed by Dawaliby et al., turkey β1AR has a 59% sequence identity with human β2AR in the transmembrane region (Serrano-Vega and Tate 2009) and the high folding efficiency found with ND (DOPG) might thus be reflected by the degree of mimicking the natural lipid environment of β1AR.

Interestingly, addition of cholesterol to ND (DMPC) was not found to be supportive for folding of thermostabilised turkey β1AR. Effects of cholesterol on stability, signalling activity and receptor

dimerisation have widely been reported for GPCRs (Oates and Watts 2011, Gahbauer and Böckmann 2016) and a putatively conserved cholesterol binding motif has been found in crystal structures of several GPCRs (Cherezov et al. 2007, Hanson et al. 2008, Genheden et al. 2017). Furthermore, cholesterol or the cholesterol derivative cholesteryl-hemisuccinate (CHS) are abundantly used as stabilisers in the detergent based purification of GPCRs and frequently added in lipidic cubic phase crystallisation trials (Yao and Kobilka 2005, Rosenbaum et al. 2011, Warne et al. 2011, Oates et al. 2012). On the other hand, several GPCRs, including thermostabilised β1AR, show ligand binding activity also when synthesised in cholesterol-free *E. coli* membranes (Miller and Tate 2011, Oates and Watts 2011) and thermostabilised turkey β1AR has been demonstrated to have high folding efficiency, ligand binding activity and stability in ND without supplemented cholesterol. Cholesterol was even found to be detrimental for the folding of β1AR in ND (DMPC). Stabilising effects of cholesterol on this specific receptor might therefore predominantly appear after solubilisation in detergents. However, addition of cholesterol was only tested for ND (DMPC) and effects may vary for other lipids, lipid mixtures or receptors. Addition of CHS in the ND was tested for both β1AR and ETB receptor in the course of the present study, but high variations in ligand binding were observed, excluding reliable statements. The dataset was therefore omitted in this thesis. Further strategies might need to be implemented to analyse the potential effects of cholesterol on CF-synthesised GPCRs.

In summary, the first association of the nascent peptide chain with the ND could be affected by the lipid headgroup composition and resulting membrane potential and might be enhanced with negatively charged PG-headgroups, at least for ETA receptor. In a next step, co- or post-translational insertion is a likely prerequisite for receptor activity and might be triggered by anionic charged PG- and PS-headgroups for both ETB and β1AR. Compact helix packing and stabilisation might occur in a third step and could be supported by the lateral pressure given by the lipid headgroup and fatty acid chain composition of the ND. Optimal membrane thickness resulting in hydrophobic matching with the transmembrane segments might further be important for receptor folding and stabilisation and appears to be optimal with fatty acid chain lengths of 18 carbon atoms and a resulting membrane thickness of apparently 27 Å for both ETB and β1AR. Additionally, specific lipid preferences of the respective GPCRs and direct allosteric interaction could modulate the folding and stability of the receptor further. Therefore, some general requirements can be outlined but screening of lipids and lipid mixtures might still be unavoidable for the L-CF synthesis of new GPCR targets with ND to find the most suitable lipid composition for the respective receptor.

5.1.3 Conformational thermostabilisation

While only approx. 1% of non-stabilised turkey β1AR was found to be ligand binding competent in ND (DOPG) or ND (DEPG), 35 - 50% of the thermostabilised turkey β1AR showed ligand binding activity in those lipids. For ETB receptor, thermostabilisation resulted in an increase of roughly 35% in ligand binding activity. Human β1AR folding could be improved by ca 4-fold after transfer of the thermostabilising mutations from turkey to the human receptor construct. Approx. 3% of the thermostabilised human β1AR were found to be ligand competent and folding efficiency was thus notably lower than for the thermostabilised turkey β1AR construct. The approach of transfering

thermostabilising mutations found in the turkey β1AR to human β-adrenergic receptor variants has previously been reported by Serrano-Vega and Tate. The authors transferred 6 point mutations that were found to increase the thermostability of a turkey β1AR construct in 0.1% DDM by 22°C to truncated forms of human β1- and β2AR construct and found an increase in thermostability by 17°C for β1AR and 12°C for β2AR derived from HEK293 cells and solubilised in DDM (Serrano-Vega and Tate 2009). However, as the initial human β1AR was relatively unstable, the thermostabilisation resulted in a T_M of apparently 27°C, which is relatively low compared to 45°C found for the turkey thermostabilised β1AR construct. The β1AR receptor analysed in the present study contained some additional thermostabilising mutations that cause a further stabilising effect on turkey β1AR of additionally 10°C (Miller and Tate 2011). Thus, the thermostabilised human β1AR construct analysed in the present study might have a higher thermostability than the modified human β1AR described by Serrano-Vega and Tate. However, while not tested, it is likely that the thermostability is still lower than for the turkey variant and that might be a reason for the apparently lower folding efficiency of thermostabilised human β1AR.

As folding of all receptors tested in this study was significantly enhanced after thermostabilisation, it appears likely that this approach can open a general path to increase the quality of CF-produced GPCRs. Thermostabilisation has been accomplished for various GPCRs, including the β-adrenergic receptor β1AR (Miller and Tate 2011), Neurotensin receptor NTS1 (Shibata et al. 2013), Adenosine receptor A_{2A} (Lebon et al. 2011) and the Endothelin receptor type B (Okuta et al. 2016). However, transfer of thermostabilising mutations is only possible for closely related receptors sharing high sequence identity (Serrano-Vega and Tate 2009) and the design of thermostabilising variants for a new GPCR target is relatively time- and labour intense. In brief, a thermostabilisation approach is usually done by mutating all residues in the TMS region to alanine or leucine, if the respective amino acid is an alanine in the beginning, yielding a total of 300-400 mutants (Magnani et al. 2016). These constructs are usually expressed in *E. coli*, e.g. with a MBP-fusion tag, and prepared for ligand binding analysis, e.g. by solubilisation in DDM. Samples are heated, analysed by radioligand binding assay and compared to a non-heated control. Positive hits are then further analysed and combined to eventually receive a thermostabilised construct. This technique usually requires some basic soluble expression and activity of the non-stabilised receptor in *E. coli* as well as detergent tolerance (Lebon et al. 2011, Shibata et al. 2013, Magnani et al. 2016). It might therefore be hampered for relatively unstable receptors like the human β1AR (Serrano-Vega and Tate 2009). On the other hand, recent progress has been made e.g. by expression in yeast and detergent free solubilisation using Styrene Maleic Acid (SMA) co-polymers that might reduce these limitations to some extent (Jamshad et al. 2015).

Compared to classical *in vivo* systems, CF-expression is fast, scalable and relatively target independent. It therefore appears to be suitable to combine the directed mutagenesis approach with the CF-expression system for simultaneous synthesis and testing of multiple constructs in a relatively short time scale. In the best case, each construct would have to be tested only once for its folding efficiency in a first round (Shibata et al. 2013, Magnani et al. 2016), making both ND and radioligand consumption manageable.

On the other hand, the thermostabilising approach stabilises a specific state of the GPCRs (Robertson et al. 2011, Niesen, Michiel J M et al. 2013, Vaidehi et al. 2016). This ultimately causes

variations in the ligand binding behaviour. It would therefore be preferable to circumvent the need of introducing extensive thermostabilising mutations in the CF-produced GPCRs when pharmaceutical analysis should be performed on the receptor target. In the present study, approx. 1% of both turkey and human non-stabilised β1AR were found to be ligand binding competent when CF-synthesised in presence of ND (DOPG) and ca. 6.5% of non-stabilised human ETB receptor under optimised expression conditions. As radioligand binding studies usually require only minor amounts of receptor, the findings indicate the feasibility of pharmaceutical tests with non-modified CF-synthesised receptors at least for some GPCRs.

5.1.4 Formation of disulphide bridges

The optimisation of redox conditions in CF-synthesis reactions presented in this study apparently lowered the folding kinetics of ETB receptor and increased the folding efficiency by approx. 60%. The effects are probably related to the enhanced ability to form a disulphide bridge between the first and second extracellular loop (ECL) under this conditions. The respective disulphide bond is a highly conserved motif GPCRs and is related to stability and activity in most of the tested receptors. It acts on the extracellular part of helix 3 of the GPCR and brings transmembrane segment (TMS) 3 close to the binding pocket (Venkatakrishnan et al. 2013). The optimised redox conditions might likely support folding also for other CF-synthesised GPCRs and, as there was no obvious drawback on CF-production yields, it might be a general advantage to supply these conditions in CF-production of membrane proteins that require disulphide bridge formation.

Optimal redox conditions were found in the present study with 4 mM glutathione in a 1 to 3 stoichiometric ratio of reduced (GSH) to oxidised glutathione (GSSG). Glutathione is the major redox buffer in the secretory pathway of eukaryotic cells and was found in total concentration of ca. 10 mM in the endoplasmatic reticulum (ER) and secretory pathway of mammalian cell lines, with apparent GSH to GSSG ratios of 1:1 to 3:1 (Hwang et al. 1992). The proposed optimised GSH and GSSG concentrations therefore apparently reflect the conditions found in the natural folding environment of the GPCRs.

Nevertheless, only a fraction of the synthesised and solubilised ETB receptor was found to be ligand binding competent even in this conditions. Additionally, in previous studies, higher concentrations of GSSG, addition of redox chaperones like DsbA and DsbC and saturation of reactive cysteines in the *E. coli* lysate by IAM treatment were found to be necessary to ensure complete disulphide bond formation (Kim and Swartz 2004, Knapp et al. 2007, Bundy and Swartz 2011, Michel and Wüthrich 2012). All these conditions were tested in the present study and were not found to further enhance ETB receptor folding. Furthermore, redox potentials during CF-synthesis were measured using the redox sensitive GFP probe roGFP1-iE and potentials were calculated to be above -200 mV with optimised redox conditions, thus more close to the redox potential found in the ER (-175 to -180 mV, Hwang et al. 1992) than to the potentials found in the cytosol of mammalian cell lines (-325 to -315 mV, Dooley et al. 2004). While the comparison of total values for redox potentials is delicate due to the high impact of pH and temperature conditions (Schafer and Buettner 2001, Mamathambika and Bardwell 2008), the finding of roGFP1-iE being almost completely oxidised in the optimised CF-reaction strongly indicates a high

oxidation potential, as the redox probe was specifically designed to measure the redox conditions in the ER and secretory pathway (Lohman and Remington 2008).

The reasons for the differences in GSH and GSSG concentrations found here to the previously published results are unknown but might be related to the specific CF-expression system. Matsuda et al. found similar glutathione concentrations with the ones proposed in this thesis, with 4 mM GSH, 1 mM GSSG and addition of 400 µg/mL DsbC to be most suitable condition for disulphide bond formation of soluble proteins synthesised in an *E. coli* lysate based CECF-expression system. They accounted the differences to previously published glutathione concentrations to differences in the supplied energy source, as they used creatine phosphate and creatine kinase instead of PEP or glucose, the later two causing the production of NADH during consumption. NADH was supposed to reduce GSSG and therefore higher GSSG concentration would be necessary in a PEP or glucose supplied CF-expression system, according to the authors (Matsuda et al. 2013). While PEP was also used as energy source in the current CF-expression system no NADH or NADH precursors where added, making this hypothesis at least conceivable.

Variations might also arise from differences in the hardware setup. The CECF-expression system used in the present study is a relatively open system and not operated under inert gas and reaction times are 4 - 24 h in the CECF-mode, much longer than batch reactions which were primarily performed by other research groups and lasted for ca. 2 h (Kim and Swartz 2004, Knapp et al. 2007, Michel and Wüthrich 2012). This leaves rooms for the possibility of oxidation by air contact (Mamathambika and Bardwell 2008).

In contrast to Matsuda et al. 2013 and other studies (Kim and Swartz 2004, Michel and Wüthrich 2012), addition of the redox chaperones DsbA and DsbC was not found to enhance disulphide bond formation and ETB receptor maturation. However, both proteins have recently been found by mass spectrometric analysis in *E. coli* S30 lysates prepared in a highly similar manner to the ones used in the present study (Foshag et al. 2017). Further addition of these redox chaperones might therefore be redundant in the current CF-expression system.

The Dsb system is the major disulphide bond formation system in the periplasm of *E. coli* (Ito and Inaba 2008). DsbA is an oxidoreductase and catalyses disulphide bridge formation. Activity of the intrinsic DsbA might account for the relatively high oxidation potentials that were found in the CF reaction mixture already when the reducing substances DTT or TCEP were supplemented. DsbC acts as a disulphide bridge isomerase and removes incorrectly formed disulphide bridges, thus preventing missfolding of the respective protein. The prevention and removal of incorrectly formed disulphide bridges might be necessary also for the functional folding of CF-produced GPCRs. For example, abnormal disulphide bridge formation in mutated Rhodopsin caused missfolding of the receptor (Hwa et al. 2001).

With the present data set, it is not possible to state whether the intrinsic DsbA and DsbC in the S30-extract are functionally active. Both proteins require specific and opposed redox states to work properly. While DsbA needs to be oxidised to introduce disulphide bonds, DsbC requires a reduced state that gets oxidised upon elimination of incorrectly formed disulphide bridges in the target protein. *In vivo*, activity of both proteins is tightly regulated and requires the precursor proteins DsbB and DsbD. DsbB acts as a electron drain and oxidises DsbA while DsbD provides electrons for reduction of the catalytically active

disulphide bridges in DsbC (Ito and Inaba 2008). Both DsbB and DsbD are membrane proteins and are probably removed during S30-extract preparation and were not found in S30-extracts by mass spectrometry (Foshag et al. 2017). The finding that both DsbA and DsbC supported disulphide bridge formation in CF-expression systems published by various research groups implies that the enzymes show functional activity also in absence of their precursor proteins.

In addition to DsbC, GSH also acts as a disulphide isomerase and reduces incorrectly formed and therefore instable disulphide bridges (Mamathambika and Bardwell 2008). Therefore, a certain concentration of GSH in the CF-reaction might be beneficial for correct disulphide bond formation in the synthesised protein and prevention of incorrect folding stages.

Disulphide bridge formation requires the close proximity of the reactive thiolate anions of the respective cysteine residues (Mamathambika and Bardwell 2008). Insertion and correct orientation of the TMS helices in the lipid bilayer of the supplied ND is therefore most likely a prerequisite for correct disulphide bridge formation. Simultaneously, disulphide bridge formation stabilises the correct folding stage and enables receptor maturation (Creighton 1986, Mamathambika and Bardwell 2008). At least for ETB receptor, the folded stage appears then to be relatively stable, as even high concentrations of DTT could not fully unfold the once matured receptor in a ligand binding incompetent state.

5.1.5 Stabilisation by chaperones

Molecular chaperones and folding enzymes may compromise up to 25% of all proteins in the eukaryotic ER and are effective *in vivo* tools to prevent protein aggregation and promote proper folding in both eukaryotic and prokaryotic cells (van Anken and Braakman 2005, Mamipour et al. 2017). Application of chaperones on CF-produced GPCRs might therefore be beneficial for the proper folding of the receptors.

Besides addition of DsbA and DsbC, two strategies for chaperone treatment have been applied in the present study. In one approach, enhancement of the concentrations of GroEL and GroES by recombinant overexpression has been tested. The chaperonin pair GroEL/ES acts as ATP driven folding chaperone mainly by incorporation of the misfolded protein in a cage formed by GroEL as a double-ring structure and GroES acting as lid. The closed folding compartment and exclusion of interaction partners are then thought to provide a beneficial microenvironment for protein folding (Koldewey et al. 2017).

Intrinsic GroEL/ES was found in a lysate preparation similar to the ones used in the recent study (Foshag et al. 2017). Overproduction by recombinant expression yielded in further enrichment of both proteins in the extract. However, the enrichment of the chaperonin pair in the *E. coli* extract was not found to enhance ETB receptor folding. A similar approach was recently found to be successful and enhance both folding kinetics and folded yield of the GPCRs human CC chemokine receptor 5 (CCR5) and human C-X-C chemokine receptor type 4 (CXCR4) (Chi et al. 2015, Chi et al. 2016). Both receptors were produced in an *E. coli* lysate based CF-system supplemented with 0.2% Brij-35. The folding of the receptors was measured by their lowered sensitivity to proteolysis and a post-translational folding behaviour of the receptors was observed. Addition of GroEL/ES in the CF-reaction could reduce the post-translational folding effect and furthermore the soluble yield and ligand binding affinity were enhanced, as studied by quartz microbalance techniques. In contrast to the present study, D-CF mode

was used for solubilisation of the GPCRs, resulting in Brij-35 derived proteomicelles. Compared to ND-GPCR complexes, these proteomicelles are relatively small and might have been more suitable for incorporation in the GroEL/ES chaperonin complex, although potentially open folding mechanisms were also described for this chaperone (Koldewey et al. 2017).

In a second approach, chaperone enrichment in the CF-extract was achieved by applying a heatshock in the process of cell cultivation, inducing the production of heatshock chaperones (Foshag et al. 2017). This strategy was more successful and resulted in roughly 100% increased folding efficiency for ETB receptor. 27 significantly upregulated proteins were found in the S30-extract after heatshock induction, among them several chaperones like GroEL/ES (HSP60), dnaK (HSP70) and spy (Foshag et al. 2017, Koldewey et al. 2017).

The mechanism by which ETB folding was enhanced remains unknown at the moment. It is conceivable that upregulated heat shock chaperones stabilise the extracellular domains of the receptor and thus provide higher efficiency for disulphide bridge formation and receptor maturation. It is also possible that chaperones act on the nascent peptide chain of the freshly synthesised receptor and stabilise its association with the ND prior to insertion of the transmembrane segments. Specific enhancement of the S30-extract with distinct the chaperones found to be upregulated by Foshag et al., e.g. by recombinant overexpression, might shed light on the folding partners and eventually on the folding mechanism of CF-produced ETB and other GPCRs in presence of ND.

5.1.6 Reasons for inactive receptor fractions and outline for further improvements

High differences were found for the ligand binding competence of the GPCRs analysed in the present study and plenty of reasons are plausible for this. If no refolding approaches are applied, the once folded receptor needs to keep its state during the CF-reaction process, usually for 6 - 17 h at 30°C. Sensitivity to high temperatures might therefore be a main reason for the high rates of inactive receptor found for ETA and human β1AR. Numerous approaches are conceivable to circumvent problems with the instability for some GPCR including: i) reduction of CF-reaction temperature or time, ii) stabilisation by chaperones, inverse agonists or allosteric binders like G-proteins, Arrestins or nanobodies iii) design of a thermostable receptor variant or iv) P-CF production and refolding approaches based on the requirements found in this thesis. Some of them were already tested and previously discussed in this thesis and should be briefly summarised here.

Reduction of CF-reaction temperature or time could lead to higher rates of folded receptor. Preliminary results with the ETA receptor indicate that this approach might be promising. It will however lower the overall yield of synthesised protein and a balance is needed between yield and folding efficiency. This probably depends on both the receptor and the subsequent assays to be performed.

Enrichment of heatshock chaperones in the CF-extract was found to be beneficial for folding of the ETB receptor and might have positive effects also for other GPCRs. The mechanism of folding enhancement of ETB receptor is unknown so far but interaction of heat shock chaperones with the GPCR might stabilise the protein during CF-reaction (Koldewey et al. 2017). An interesting approach was presented by Welsh et al. 2011. Here, assisted folding during CF-expression of soluble, secreted proteins was achieved directly at the ribosomes by tethering eukaryotic Hsp70 to the ribosomes via trigger factor to mimic the chaperone assisted folding in the ER (Welsh et al. 2011).

GPCRs naturally show high flexibility and exist in an equilibrium of states that are competent or incompetent for G-protein activation (Kobilka and Deupi 2007). Stabilisation of a specific, presumingly inactive state might increase thermostability and could be done by addition of inverse agonists in the CF-reaction (Vukoti et al. 2012). If the ligand is labelled, it might be even possible to perform receptor-ligand interaction studies during CF-reaction or to purify the receptor by ligand affinity chromatography in a pulldown-like assay. At least the first strategy has previously been demonstrated (Yang et al. 2011).

Stabilisation of a specific state might further be achieved by addition of allosteric modulators in the CF-reaction (Gentry et al. 2015). Those includes Arrestins and G-proteins and receptor specific nanobodies that bind to the receptor in a defined state and might preferentially stabilise it (Kobilka and Deupi 2007, Manglik et al. 2017). They might thus have a stabilising effect on the receptor also during CF-reaction. Cholesterol and specific lipids can also be seen as allosteric modulators and are frequently reported to enhance receptor stability, as previously discussed (5.1.2).

An alternative approach might be the conformational thermostabilisation by mutagenesis, which was found to be very effective for the folding of CF-produced turkey β1AR. This approach however preferentially stabilises the inactive conformation and might thus be of limited use for pharmaceutical analysis (Robertson et al. 2011, Niesen, Michiel J M et al. 2013).

The GPCRs analysed in the present study are naturally stable and active *in vivo* at notably higher temperatures. A main reason for this might be the perfect embedding in the lipid bilayer of the cell membrane. Enhancement of insertion efficiency of the CF-produced receptor in the lipid bilayer of the ND might thus be another key parameter to further optimise the expression conditions. Co-translational insertion of proteorhodopsin has extensively been studied and seems to go in hand with a partly release of the lipids in the ND (Peetz et al. 2017). Alternative scenarios might be the reorganisation of the membrane lipids around the inserted proteins or expansion of the nanodisc, as the structure of the membrane scaffold proteins was reported to be highly dynamic (Kynde et al. 2014; Morgan et al. 2011).

All the plausible alternatives require some changes in the thermodynamical state and might therefore be energetically difficult. Co-translational ND formation during CF-synthesis might be an promising approach to circumvent insertion limitations, as discussed earlier (5.1.1). Insertion efficiency might also be enhanced by embedding translocon machineries in the supplied lipid membranes. For example, Ohta et al. found a significant increase of co-translational insertion efficiency of CF-produced *E. coli* multidrug transporter EmrE when using liposomes preloaded with the *E. coli* derived Sec YEG complex (Ohta et al. 2016). It was previously shown that ND can be pre-loaded with the Sec translocon complex (Alami et al. 2007). However, it needs to be evaluated whether size restrictions due to the relatively small ND diameter might have an impact on insertion or folding efficiencies.

A rather different approach is a CF-system based on insect cell endoplasmatic reticulum derived microsomes that can take advantage of the natural eukaryotic translocation machinery (Merk et al. 2015, Zemella et al. 2017). This CF-system was tested for production of ETB and ETA receptor and folded receptor appeared to have a proper folding with high affinity towards its ligand ET-1. Insertion appeared to be unidirectional, as ligand binding activity could only be measured after detergent treatment of the microsomal vesicles. On the other hand, rather low yields of active receptors and folding efficiencies below 0.1% were reported. While overall yields of synthesised receptor could be enhanced by the use of a CECF system, the yields of ligand binding competent receptor were not drastically improved,

indicating that the insertion machinery of the microsomal vesicles might have been saturated (Merk et al. 2015).

Besides bilayer insertion limitations and receptor instability, it might be possible that the correct environment for the receptors is not found so far and co-factors are missing. For several GPCRs, glycosylation and palmitoylation were reported to have an impact on receptor maturation and ligand binding activity (McCusker et al. 2007). Receptor activity and ligand binding profile might further depend on homo- and heterooligomerisation (Harding et al. 2009, Gahbauer and Böckmann 2016, Prasanna et al. 2016). The state of oligomerisation of the tested GPCRs in ND is unknown but the principal ability for oligomerisation of co-translationally inserted membrane proteins has been demonstrated with other seven transmembrane segment containing proteins such as bacteriorhodopsin or proteorhodopsin as well as other membrane proteins (Roos et al. 2012, Zocher et al. 2012, Henrich et al. 2017).

Cooperative insertion was observed for the potassium channel KcsA and the proton pump proteorhodopsin, which both are known to form oligomers *in vivo*. Insertion of these were preferred in pre-inserted ND over empty ones, causing the formation of oligomers even when ND are supplied in a overtitrated stoichiometric ratio to the CF-reaction (Peetz et al. 2017). Triggering cooperative insertion of GPCRs in ND might be challenging, as a stoichiometric overtitration of ND was necessary to achieve complete receptor solubilisation but might be approached by resupply of previously produced ND-GPCR complexes to another round of CF-expression.

Furthermore, difficulties in the detection of ligand binding sites may not solely accounted on the insufficient folding of the receptor but might also be caused by the setup of the readout-assay. For example, the K_D of purified ETA to its natural agonist ET-1 was previously reported to be ca. 17 nM, being significantly lower than affinities found for unpurified receptors in crude membrane preparations (Lee et al. 2012). Additionally, only ca. 40% of thermostabilised β1AR derived from *Sf9*-cell expression were previously reported to be ligand binding competent in radioligand binding assays even after purification of the receptor via ligand affinity chromatography (Warne et al. 2003, Di Bartolo et al. 2016).

For the later reason, care must be taken in the setup of the read-out assay used for optimisation purposes and complimentary assays might be considered. Additionally, several parameters discussed here might work not only additively but also comparatively, meaning that the optimum of parameter A might be influenced by parameter B. Combinatory screening schemes might therefore be most suitable and straightforward.

5.2 Cell-free synthesised GPCRs in defined lipid bilayers – scopes of application

CF-expression offers direct and fast access to the synthesised protein with usually high expression success rates (Haberstock et al. 2012) while ND technology offers manifold possibilities for the *in vitro* analyses of membrane proteins in defined lipid environments (Schuler et al. 2013). The combinatorial approach presented in this study thus opens new avenues for *the in vitro* characterisation of lipid dependent effects on GPCRs. In the next paragraph, several conceivable and promising applications will be discussed.

5.2.1 Ligand binding analysis in defined lipid environments

To exemplify the use of CF-derived GPCRs for pharmaceutical studies a lipid dependent ligand binding screen has been performed for β1AR. Significant alterations in the binding behaviour for a set of inverse agonists were found for thermostabilised turkey β1AR in this assay after insertion in ND with different lipid compositions (see 4.3.1).

Similar studies of lipid dependent ligand binding affinities have recently been studied for human β2AR post-translationally inserted in ND (Dawaliby et al. 2016). It was found that negatively charged lipids, i.e. DOPG, DOPS and DOPI favour receptor activation as they act as allosteric modulators that enhance the timescale of receptor activation and stabilise the active conformation of the cytoplasmic side of β2AR (Dawaliby et al. 2016).

In the present study, the affinities of thermostabilised turkey β1AR towards its inverse agonists alprenolol and nebivolol was significantly lower in DOPG than in DOPC. This might reflect the finding of Dawaliby et al., where negatively charged lipids were found to preferentially bind and stabilise the inactive and not the active receptor state. On the other hand, no significant binding differences were found for alprenolol binding between DOPC and DOPG by Dawaliby et al. and IC_{50} values were only lower with DOPS and DOPE, which were not tested in the present study. Additionally, they found that DOPG stabilises the active state of the receptor and binding affinities towards the agonist isoproterenol were highest with this lipid. The β1AR analysed in the present study was conformationally thermostabilised in its inactive state, preventing analysis of agonist binding. Comparability of both studies is thus limited, however, the further findings in this study of non-stabilised turkey and human β1AR being partly ligand binding competent opens the possibility to analyse the ligand binding behaviour in more detail. While not tested so far, shortcomes in the folding efficiency of the receptors in e.g. ND (DOPE) might be reduced by the use lipid mixtures rather than pure DOPE lipid.

A pronounced binding preference of β2AR towards DOPG *in vivo* was additionally found by Dawaliby et al., which might be reflected by the high folding efficiency of β1AR in DOPG found in the present study, as discussed earlier in this thesis (5.1.2). Strikingly, similar positive effects of anionic lipids on G-protein activation or Arrestin binding have been observed for other receptors, including Cannabinoid type 2 receptor CB2 (Kimura et al. 2012), Neurotensin receptor NTS1 (Inagaki et al. 2012) and Rhodopsin (Tsukamoto et al. 2010), (Soubias and Gawrisch 2012). Lipid dependent ligand binding screens might therefore be interesting also with other CF-produced GPCRs.

5.2.2 Outlook – the relevance of this study for synthetic biology and structural analysis of GPCRs

Compared to classical solubilisation strategies involving detergents, ND are advantageously stable and easy in handling. Labelling of the MSP enables studies even without the need to modify the membrane protein in any way. For example, Klebe labelled MSP with a fluorescent dye and could thereby study lipid dependent interactions of ND embedded NTS1 receptor with its G-protein (Klebe 2015).

CF-synthetic biology provides a new set of possibilities to improve membrane protein analysis and pharmaceutical research (Casteleijn et al. 2013, Hodgman and Jewett 2012). Protein *in situ* arrays and membrane biochips have been developed and are conceivable also with GPCR-CF-expression techniques (Stoevesandt et al. 2011, Cook and He 2014, Chadli et al. 2017), as co-translational, unidirectional insertion of CF-produced GPCRs into surface coupled planar lipid bilayers for biophysical studies has already been demonstrated (Robelek et al. 2007, Leutenegger et al. 2008).

Tremendous progress has been made in the past decade towards the structural understanding of GPCR signalling. More than 200 high resolution crystal structures from 46 different GPCRs are presently available (Isberg et al. 2016). Progress has also been made in the solution-state NMR analysis of GPCRs (Kofuku et al. 2014, Isogai et al. 2016, Ye et al. 2016). Besides those achievements, expression and purification of a new GPCR target is still no easy task and usually requires extensive optimisation and screening procedures ((Milić and Veprintsev 2015). CF-protein synthesis offers new optimisation strategies and a completely different toolbox for the production of GPCRs. The fast and reliable synthesis might be useful to optimise new GPCR targets e.g. by the simplification of screens for thermostabilised receptor mutants, which so far largely depends on the feasibility of soluble GPCR expression in *E. coli* (Magnani et al. 2016)(see 5.1.3 for further discussion). Cost-effective labeling with high success rates for NMR- and DEER-spectroscopy and new strategies for the incorporation of non-natural amino acids are further reasons for the merge of CFPS and structural analysis of GPCRs (Harris and Jewett 2012, Laguerre et al. 2015).

Yields of functionally folded thermostabilised turkey β1AR were found to be in a range of some 100 µg per ml of CF-reaction mixture in this study. Furthermore, the feasibility to synthesise and purify the GPCR in a time period of less than 24 h has been demonstrated. The obtained receptor sample was pure and stable inserted in homogeneous ND, as shown by SEC and radioligand binding assays (see 4.3.2). These results are promising for the possibility of structural analysis of CF-derived GPCRs. In particular, the circumvention of detergent contact at any time point might be highly useful, as detergents can have a tremendous impact on membrane protein activity and structural dynamics (Kofuku et al. 2014, Zhang et al. 2015, Frey et al. 2017).

The suitability of MSP nanodisc system with solution-state NMR has previously been demonstrated (Raschle et al. 2009, Etzkorn et al. 2013, Hagn et al. 2013) and new strategies for solution-state NMR analysis of membrane proteins in lipid bilayers have recently been developed. In one approach, CF-synthesised membrane proteins in ND were titrated with detergent, leading to the formation of small isotropic bicelles and vast improvements in signal intensity in solution-state NMR analysis (Laguerre et al. 2016). In another study, size-adaptable Salipro nanoparticles, which were made from lysosome derived sphingolipid activator proteins (SapA) surrounding a small lipid bilayer and embedded

membrane proteins, have been demonstrated for their suitability in solution-state NMR analysis. The authors could even observe structural changes in thermostabilised β1AR upon agonist and nanobody binding (Chien et al. 2017).

The combination of the presented and other strategies with the optimised CF-expression system developed in the present study might eventually lead to new breakthroughs in the toolbox of GPCR analysis and hopefully contributes to a deeper understanding of these fascinating molecular signal processing machines.

6 References

Alami, M., Dalal, K., Lelj-Garolla, B., Sligar, S. G., Duong, F. 2007 **Nanodiscs unravel the interaction between the SecYEG channel and its cytosolic partner SecA**. *EMBO J.* 26, 1995–2004.

Alexander, S. P., Davenport, A. P., Kelly, E., Marrion, N., Peters, J. A., Benson, H. E., Faccenda, E., Pawson, A. J., Sharman, J. L., Southan, C., Davies, J. A. 2015 **The Concise Guide to PHARMACOLOGY 2015/16: G protein-coupled receptors**. *Br J Pharmacol* 172, 5744–5869.

Ballesteros, J. A. and Weinstein, H. **1998 Integrated methods for the construction of three-dimensional models and computational probing of structure-function relations in G protein-coupled receptors**. *Methods in Neurosciences* 25, 366–428.

Basu, D., Castellano, J. M., Thomas, N., Mishra, R. K. 2013 **Cell-free protein synthesis and purification of human dopamine D2 receptor long isoform**. *Biotechnol Prog* 29, 601–608.

Bayburt, T. H. and Sligar, S. G. 2010 **Membrane protein assembly into Nanodiscs**. *FEBS Lett* 584, 1721–1727.

Bernhard, F. and Tozawa, Y. 2013 **Cell-free expression—making a mark**. *Curr Opin Struct Biol* 23, 374–380.

Bibow, S., Polyhach, Y., Eichmann, C., Chi, C. N., Kowal, J., Albiez, S., McLeod, R. A., Stahlberg, H., Jeschke, G., Güntert, P., Riek, R. 2017 **Solution structure of discoidal high-density lipoprotein particles with a shortened apolipoprotein A-I**. *Nat Struct Mol Biol* 24, 187–193.

Boland, C., Li, D., Shah, Syed Tasadaque Ali, Haberstock, S., Dötsch, V., Bernhard, F., Caffrey, M. 2014 **Cell-free expression and in meso crystallisation of an integral membrane kinase for structure determination**. *Cell Mol Life Sci* 71, 4895–4910.

Booth, P. J. 2005 **Sane in the membrane: designing systems to modulate membrane proteins**. *Curr Opin Struct Biol* 15, 435–440.

Borch, J. and Hamann, T. 2009 **The nanodisc: a novel tool for membrane protein studies**. *Biol Chem* 390.

Bundy, B. C. and Swartz, J. R. 2011 **Efficient disulfide bond formation in virus-like particles**. *J Biotechnol* 154, 230–239.

Caffrey, M. and Hogan, J. 1992 **LIPIDAT: a database of lipid phase transition temperatures and enthalpy changes. DMPC data subset analysis**. *Chem Phys Lipids* 61, 1–109.

Carlson, E. D., Gan, R., Hodgman, C. E., Jewett, M. C. 2012 **Cell-free protein synthesis: applications come of age**. *Biotechnol Adv* 30, 1185–1194.

Caron, M. G., Srinivasan, Y., Pitha, J., Kociolek, K., Lefkowitz, R. J. 1979 **Affinity chromatography of the beta-adrenergic receptor**. *J Biol Chem* 254, 2923–2927.

Carpenter, B. and Tate, C. G. 2017 **Active state structures of G protein-coupled receptors highlight the similarities and differences in the G protein and arrestin coupling interfaces**. *Curr Opin Struct Biol* 45, 124–132.

Casteleijn, M. G., Urtti, A., Sarkhel, S. 2013 **Expression without boundaries: cell-free protein synthesis in pharmaceutical research**. *Int J Pharm* 440, 39–47.

Chadli, M., Rebaud, S., Maniti, O., Tillier, B., Cortès, S., Girard-Egrot, A. 2017 **New Tethered Phospholipid Bilayers Integrating Functional G-Protein-Coupled Receptor Membrane Proteins**. *Langmuir* 33, 10385–10401.

Cherezov, V., Rosenbaum, D. M., Hanson, M. A., Rasmussen, S. G. F., Thian, F. S., Kobilka, T. S., Choi, H.-J., Kuhn, P., Weis, W. I., Kobilka, B. K., Stevens, R. C. 2007 **High-Resolution Crystal Structure of an Engineered Human 2-Adrenergic G Protein-Coupled Receptor**. *Science* 318, 1258–1265.

Chi, H., Wang, X., Li, J., Ren, H., Huang, F. 2015 **Folding of newly translated membrane protein CCR5 is assisted by the chaperonin GroEL-GroES**. *Sci Rep* 5, 17037.

Chi, H., Wang, X., Li, J., Ren, H., Huang, F. 2016 **Chaperonin-enhanced Escherichia coli cell-free expression of functional CXCR4**. *J Biotechnol* 231, 193–200.

Chien, C.-T. H., Helfinger, L. R., Bostock, M. J., Solt, A., Tan, Y. L., Nietlispach, D. 2017 **An Adaptable Phospholipid Membrane Mimetic System for Solution NMR Studies of Membrane Proteins**. *J Am Chem Soc* 139, 14829–14832.

Cleland, W. W. 1964 **DITHIOTHREITOL, A NEW PROTECTIVE REAGENT FOR SH GROUPS**. *Biochemistry* 3, 480–482.

Cook, E. A. and He, M. 2014 **Preparation of protein arrays using cell-free protein expression**. *Methods Mol Biol* 1118, 245–255.

Corin, K., Baaske, P., Ravel, D. B., Song, J., Brown, E., Wang, X., Geissler, S., Wienken, C. J., Jerabek-Willemsen, M., Duhr, S., Braun, D., Zhang, S., Lu, J. R. 2011a **A Robust and Rapid Method of Producing Soluble, Stable, and Functional G-Protein Coupled Receptors**. *PLoS ONE* 6, e23036.

Corin, K., Baaske, P., Ravel, D. B., Song, J., Brown, E., Wang, X., Wienken, C. J., Jerabek-Willemsen, M., Duhr, S., Luo, Y., Braun, D., Zhang, S., Gelain, F. 2011b **Designer Lipid-Like Peptides: A Class of Detergents for Studying Functional Olfactory Receptors Using Commercial Cell-Free Systems**. *PLoS ONE* 6, e25067.

Creighton, T. E. 1986 **Disulfide bonds as probes of protein folding pathways**. *Methods Enzymol* 131, 83–106.

Davenport, A. P., Hyndman, K. A., Dhaun, N., Southan, C., Kohan, D. E., Pollock, J. S., Pollock, D. M., Webb, D. J., Maguire, J. J. 2016 **Endothelin**. *Pharmacol Rev* 68, 357–418.

Dawaliby, R., Trubbia, C., Delporte, C., Masureel, M., van Antwerpen, P., Kobilka, B. K., Govaerts, C. 2016 **Allosteric regulation of G protein-coupled receptor activity by phospholipids**. *Nat Chem Biol* 12, 35–39.

Denisov, I. G., Grinkova, Y. V., Lazarides, A. A., Sligar, S. G. 2004 **Directed Self-Assembly of Monodisperse Phospholipid Bilayer Nanodiscs with Controlled Size**. *J Am Chem Soc* 126, 3477–3487.

Di Bartolo, N., Compton, Emma L R, Warne, T., Edwards, P. C., Tate, C. G., Schertler, G. F. X., Booth, P. J. 2016 **Complete Reversible Refolding of a G-Protein Coupled Receptor on a Solid Support**. *PLoS ONE* 11, e0151582.

Dickey, A. and Faller, R. **2008 Examining the contributions of lipid shape and headgroup charge on bilayer behavior**. *Biophys J* 95, 2636–2646.

Ding, Y., Fujimoto, L. M., Yao, Y., Plano, G. V., Marassi, F. M. 2015 **Influence of the lipid membrane environment on structure and activity of the outer membrane protein Ail from Yersinia pestis.** *Biochim Biophys Acta* 1848, 712–720.

Dooley, C. T., Dore, T. M., Hanson, G. T., Jackson, W. C., Remington, S. J., Tsien, R. Y. 2004 **Imaging dynamic redox changes in mammalian cells with green fluorescent protein indicators**. *J Biol Chem* 279, 22284–22293.

Dürr, Ulrich H N, Soong, R., Ramamoorthy, A. 2013 **When detergent meets bilayer: birth and coming of age of lipid bicelles**. *Prog Nucl Magn Reson Spectrosc* 69, 1–22.

Egloff, P., Hillenbrand, M., Klenk, C., Batyuk, A., Heine, P., Balada, S., Schlinkmann, K. M., Scott, D. J., Schütz, M., Plückthun, A. 2014 **Structure of signaling-competent neurotensin receptor 1 obtained by directed evolution in Escherichia coli**. *Proc Natl Acad Sci U S A* 111, E655-62.

Endo, Y. and Sawasaki, T. 2006 **Cell-free expression systems for eukaryotic protein production**. *Curr Opin Biotechnol* 17, 373–380.

Esmaili, M. and Overduin, M. 2017 **Membrane biology visualized in nanometer-sized discs formed by styrene maleic acid polymers.** *Biochim Biophys Acta* 1860, 257–263.

Etzkorn, M., Raschle, T., Hagn, F., Gelev, V., Rice, A. J., Walz, T., Wagner, G. 2013 **Cell-free expressed bacteriorhodopsin in different soluble membrane mimetics: biophysical properties and NMR accessibility**. *Structure* 21, 394–401.

Fenz, S. F., Sachse, R., Schmidt, T., Kubick, S. 2014 **Cell-free synthesis of membrane proteins: tailored cell models out of microsomes**. *Biochim Biophys Acta* 1838, 1382–1388.

Fisker, F. Y., Grimm, D., Wehland, M. 2015 **Third-Generation Beta-Adrenoceptor Antagonists in the Treatment of Hypertension and Heart Failure**. *Basic Clin Pharmacol Toxicol* 117, 5–14.

Foshag, D., Henrich, E., Hiller, E., Schäfer, M., Kerger, C., Burger-Kentischer, A., Diaz-Moreno, I., García-Mauriño, S. M., Dötsch, V., Rupp, S., Bernhard, F. 2018 **The *E. coli* S30 lysate proteome: A prototype for cell-free protein production**. *N Biotechnol*. 40, 245-260 [epub ahead of print]

Frauenfeld, J., Löving, R., Armache, J.-P., Sonnen, A. F.-P., Guettou, F., Moberg, P., Zhu, L., Jegerschöld, C., Flayhan, A., Briggs, John A G, Garoff, H., Löw, C., Cheng, Y., Nordlund, P. 2016 **A saposin-lipoprotein nanoparticle system for membrane proteins**. *Nat Methods* 13, 345–351.

Fredriksson, R., Lagerström, M. C., Lundin, L.-G., Schiöth, H. B. 2003 **The G-protein-coupled receptors in the human genome form five main families. Phylogenetic analysis, paralogon groups, and fingerprints**. *Mol Pharmacol* 63, 1256–1272.

Frey, L., Lakomek, N.-A., Riek, R., Bibow, S. 2017 **Micelles, Bicelles, and Nanodiscs: Comparing the Impact of Membrane Mimetics on Membrane Protein Backbone Dynamics**. *Angewandte Chemie (International ed. in English)* 56, 380–383.

Gahbauer, S. and Böckmann, R. A. 2016 **Membrane-Mediated Oligomerization of G Protein Coupled Receptors and Its Implications for GPCR Function**. *Front Physiol* 7, 494.

Gao, T., Petrlova, J., He, W., Huser, T., Kudlick, W., Voss, J., Coleman, M. A. 2012 **Characterization of De Novo Synthesized GPCRs Supported in Nanolipoprotein Discs**. *PLoS ONE* 7, e44911.

Genheden, S., Essex, J. W., Lee, A. G. 2017 **G protein coupled receptor interactions with cholesterol deep in the membrane**. *Biochim Biophys Acta* 1859, 268–281.

Gentry, P. R., Sexton, P. M., Christopoulos, A. 2015 **Novel Allosteric Modulators of G Protein-coupled Receptors**. *J Biol Chem* 290, 19478–19488.

Grisshammer, R. 2009 **Purification of recombinant G-protein-coupled receptors**. *Methods Enzymol* 463, 631–645.

Haberstock, S., Roos, C., Hoevels, Y., Dötsch, V., Schnapp, G., Pautsch, A., Bernhard, F. 2012 **A systematic approach to increase the efficiency of membrane protein production in cell-free expression systems**. *Protein Expr Purif* 82, 308–316.

Hagn, F., Etzkorn, M., Raschle, T., Wagner, G. 2013 **Optimized phospholipid bilayer nanodiscs facilitate high-resolution structure determination of membrane proteins**. *J Am Chem Soc* 135, 1919–1925.

Han, J. C. and Han, G. Y. 1994 **A procedure for quantitative determination of tris(2-carboxyethyl)phosphine, an odorless reducing agent more stable and effective than dithiothreitol**. *Anal Biochem* 220, 5–10.

Hanson, G. T., Aggeler, R., Oglesbee, D., Cannon, M., Capaldi, R. A., Tsien, R. Y., Remington, S. J. 2004 **Investigating mitochondrial redox potential with redox-sensitive green fluorescent protein indicators**. *J Biol Chem* 279, 13044–13053.

Hanson, M. A., Cherezov, V., Griffith, M. T., Roth, C. B., Jaakola, V.-P., Chien, Ellen Y T, Velasquez, J., Kuhn, P., Stevens, R. C. 2008 **A specific cholesterol binding site is established by the 2.8 A structure of the human beta2-adrenergic receptor**. *Structure* 16, 897–905.

Harding, P. J., Attrill, H., Boehringer, J., Ross, S., Wadhams, G. H., Smith, E., Armitage, J. P., Watts, A. 2009 **Constitutive dimerization of the G-protein coupled receptor, neurotensin receptor 1, reconstituted into phospholipid bilayers**. *Biophys J* 96, 964–973.

Harris, D. C. and Jewett, M. C. 2012 **Cell-free biology: exploiting the interface between synthetic biology and synthetic chemistry**. *Curr Opin Biotechnol* 23, 672–678.

Harris, N. J., Reading, E., Ataka, K., Grzegorzewski, L., Charalambous, K., Liu, X., Schlesinger, R., Heberle, J., Booth, P. J. 2017 **Structure formation during translocon-unassisted co-translational membrane protein folding**. *Sci Rep* 7, 8021.

Hauser, A. S., Attwood, M. M., Rask-Andersen, M., Schiöth, H. B., Gloriam, D. E. 2017 **Trends in GPCR drug discovery: new agents, targets and indications**. *Nat Rev Drug Discov*.

Henrich, E., Peetz, O., Hein, C., Laguerre, A., Hoffmann, B., Hoffmann, J., Dötsch, V., Bernhard, F., Morgner, N. 2017 **Analyzing native membrane protein assembly in nanodiscs by combined non-covalent mass spectrometry and synthetic biology**. *eLife* 6.

Hodgman, C. E. and Jewett, M. C. 2012 **Cell-free synthetic biology: thinking outside the cell**. *Metab Eng* 14, 261–269.

Hoffmann, C., Leitz, M. R., Oberdorf-Maass, S., Lohse, M. J., Klotz, K.-N. 2004 **Comparative pharmacology of human beta-adrenergic receptor subtypes--characterization of stably transfected receptors in CHO cells**. *Naunyn Schmiedebergs Arch Pharmacol* 369, 151–159.

Hwa, J., Klein-Seetharaman, J., Khorana, H. G. 2001 **Structure and function in rhodopsin: Mass spectrometric identification of the abnormal intradiscal disulfide bond in misfolded retinitis pigmentosa mutants**. *Proc Natl Acad Sci U S A* 98, 4872–4876.

Hwang, C., Sinskey, A. J., Lodish, H. F. 1992 **Oxidized redox state of glutathione in the endoplasmic reticulum**. *Science* 257, 1496–1502.

Inagaki, S., Ghirlando, R., White, J. F., Gvozdenovic-Jeremic, J., Northup, J. K., Grisshammer, R. 2012 **Modulation of the interaction between neurotensin receptor NTS1 and Gq protein by lipid**. *J Mol Biol* 417, 95–111.

Isberg, V., Mordalski, S., Munk, C., Rataj, K., Harpsøe, K., Hauser, A. S., Vroling, B., Bojarski, A. J., Vriend, G., Gloriam, D. E. 2016 **GPCRdb: an information system for G protein-coupled receptors**. *Nucleic Acids Res* 44, D356-64.

Ishihara, G., Goto, M., Saeki, M., Ito, K., Hori, T., Kigawa, T., Shirouzu, M., Yokoyama, S. 2005 **Expression of G protein coupled receptors in a cell-free translational system using detergents and thioredoxin-fusion vectors**. *Protein Expr Purif* 41, 27–37.

Isogai, S., Deupi, X., Opitz, C., Heydenreich, F. M., Tsai, C.-J., Brueckner, F., Schertler, G. F. X., Veprintsev, D. B., Grzesiek, S. 2016 **Backbone NMR reveals allosteric signal transduction networks in the β1-adrenergic receptor**. *Nature* 530, 237–241.

Ito, K. and Inaba, K. 2008 **The disulfide bond formation (Dsb) system**. *Curr Opin Struct Biol* 18, 450–458.

Jamshad, M., Charlton, J., Lin, Y.-P., Routledge, S. J., Bawa, Z., Knowles, T. J., Overduin, M., Dekker, N., Dafforn, T. R., Bill, R. M., Poyner, D. R., Wheatley, M. 2015 **G-protein coupled receptor solubilization and purification for biophysical analysis and functional studies, in the total absence of detergent**. *Biosci Rep* 35.

Junge, F., Luh, L. M., Proverbio, D., Schäfer, B., Abele, R., Beyermann, M., Dötsch, V., Bernhard, F. 2010 **Modulation of G-protein coupled receptor sample quality by modified cell-free expression protocols: A case study of the human endothelin A receptor**. *J Struct Biol* 172, 94–106.

Kaiser, L., Graveland-Bikker, J., Steuerwald, D., Vanberghem, M., Herlihy, K., Zhang, S. 2008 **Efficient cell-free production of olfactory receptors: detergent optimization, structure, and ligand binding analyses**. *Proc Natl Acad Sci U S A* 105, 15726–15731.

Katritch, V., Cherezov, V., Stevens, R. C. 2013 **Structure-function of the G protein-coupled receptor superfamily**. *Annu Rev Pharmacol Toxicol* 53, 531–556.

Kim, D.-M. and Swartz, J. R. 2004 **Efficient production of a bioactive, multiple disulfide-bonded protein using modified extracts of Escherichia coli**. *Biotechnol Bioeng* 85, 122–129.

Kimura, T., Yeliseev, A. A., Vukoti, K., Rhodes, S. D., Cheng, K., Rice, K. C., Gawrisch, K. 2012 **Recombinant cannabinoid type 2 receptor in liposome model activates g protein in response to anionic lipid constituents**. *J Biol Chem* 287, 4076–4087.

Klammt, C., Perrin, M. H., Maslennikov, I., Renault, L., Krupa, M., Kwiatkowski, W., Stahlberg, H., Vale, W., Choe, S. 2011 **Polymer-based cell-free expression of ligand-binding family B G-protein coupled receptors without detergents**. *Protein Sci* 20, 1030–1041.

Klammt, C., Schwarz, D., Eifler, N., Engel, A., Piehler, J., Haase, W., Hahn, S., Dötsch, V., Bernhard, F. 2007 **Cell-free production of G protein-coupled receptors for functional and structural studies**. *J Struct Biol* 158, 482–493.

Klammt, C., Schwarz, D., Fendler, K., Haase, W., Dötsch, V., Bernhard, F. 2005 **Evaluation of detergents for the soluble expression of α-helical and β-barrel-type integral membrane proteins by a preparative scale individual cell-free expression system**. *FEBS Journal* 272, 6024–6038.

Klebe, G. 2015 **Applying thermodynamic profiling in lead finding and optimization**. *Nat Rev Drug Discov* 14, 95–110.

Knapp, K. G., Goerke, A. R., Swartz, J. R. 2007 **Cell-free synthesis of proteins that require disulfide bonds using glucose as an energy source**. *Biotechnol Bioeng* 97, 901–908.

Kobilka, B. K. and Deupi, X. 2007 **Conformational complexity of G-protein-coupled receptors**. *Trends Pharmacol Sci* 28, 397–406.

Kofuku, Y., Ueda, T., Okude, J., Shiraishi, Y., Kondo, K., Mizumura, T., Suzuki, S., Shimada, I. 2014 **Functional dynamics of deuterated β2-adrenergic receptor in lipid bilayers revealed by NMR spectroscopy**. *Angew Chem Int Ed Engl* 53, 13376–13379.

Kolakowski, L. F. 1994 **GCRDb: a G-protein-coupled receptor database**. *Receptors channels* 2, 1–7.

Koldewey, P., Horowitz, S., Bardwell, J. 2017 **Chaperone-client interactions: Non-specificity engenders multifunctionality**. *J Biol Chem* 292, 12010–12017.

Kynde, S. A., Skar-Gislinge, N., Pedersen, M. C., Midtgaard, S. R., Simonsen, J. B., Schweins, R., Mortensen, K., Arleth, L. 2014 **Small-angle scattering gives direct structural information about a membrane protein inside a lipid environment**. *Acta Crystallogr D Biol Crystallogr* 70, 371–383.

Laganowsky, A., Reading, E., Allison, T. M., Ulmschneider, M. B., Degiacomi, M. T., Baldwin, A. J., Robinson, C. V. 2014 **Membrane proteins bind lipids selectively to modulate their structure and function**. *Nature* 510, 172–175.

Laguerre, A., Löhr, F., Bernhard, F., Dötsch, V. 2015 **Labeling of membrane proteins by cell-free expression**. *Methods Enzymol* 565, 367–388.

Laguerre, A., Löhr, F., Henrich, E., Hoffmann, B., Abdul-Manan, N., Connolly, P. J., Perozo, E., Moore, J. M., Bernhard, F., Dötsch, V. 2016 **From Nanodiscs to Isotropic Bicelles: A Procedure for Solution Nuclear Magnetic Resonance Studies of Detergent-Sensitive Integral Membrane Proteins**. *Structure*.

Lakey, J. H., Parker, M. W., González-Mañas, J. M., Duché, D., Vriend, G., Baty, D., Pattus, F. 1994 **The role of electrostatic charge in the membrane insertion of colicin A. Calculation and mutation**. *Eur J Biochem* 220, 155–163.

Lättig, J., Oksche, A., Beyermann, M., Rosenthal, W., Krause, G. 2009 **Structural determinants for selective recognition of peptide ligands for endothelin receptor subtypes ET A and ET B**. *J Pept Sci* 15, 479–491.

Lebon, G., Bennett, K., Jazayeri, A., Tate, C. G. 2011 **Thermostabilisation of an agonist-bound conformation of the human adenosine A(2A) receptor**. *J Mol Biol* 409, 298–310.

Lee, K., Jung, Y., Lee, J. Y., Lee, W.-K., Lim, D., Yu, Y. G. 2012 **Purification and characterization of recombinant human endothelin receptor type A**. *Protein Expr Purif* 84, 14–18.

Lee, K.-H. and Kim, D.-M. 2013 **Applications of cell-free protein synthesis in synthetic biology: Interfacing bio-machinery with synthetic environments**. *Biotechnol J* 8, 1292–1300.

Leutenegger, M., Lasser, T., Sinner, E.-K., Robelek, R. 2008 **Imaging of G protein-coupled receptors in solid-supported planar lipid membranes**. *Biointerphases* 3, FA136-FA145.

Lohman, J. R. and Remington, S. J. 2008 **Development of a family of redox-sensitive green fluorescent protein indicators for use in relatively oxidizing subcellular environments**. *Biochemistry* 47, 8678–8688.

Long, A. R., O'Brien, C. C., Alder, N. N. **2012 The cell-free integration of a polytopic mitochondrial membrane protein into liposomes occurs cotranslationally and in a lipid-dependent manner.** *PLoS ONE* 7, e46332.

Lundstrom, K., Wagner, R., Reinhart, C., Desmyter, A., Cherouati, N., Magnin, T., Zeder-Lutz, G., Courtot, M., Prual, C., André, N., Hassaine, G., Michel, H., Cambillau, C., Pattus, F. 2006 **Structural genomics on membrane proteins: comparison of more than 100 GPCRs in 3 expression systems**. *J Struct Funct Genomics* 7, 77–91.

Luttrell, L. M. 2008 **Reviews in molecular biology and biotechnology: transmembrane signaling by G protein-coupled receptors.** *Mol Biotechnol* 39, 239–264.

Lyukmanova, E. N., Shenkarev, Z. O., Khabibullina, N. F., Kulbatskiy, D. S., Shulepko, M. A., Petrovskaya, L. E., Arseniev, A. S., Dolgikh, D. A., Kirpichnikov, M. P. 2012 **N-terminal fusion tags for effective production of g-protein-coupled receptors in bacterial cell-free systems**. *Acta Naturae* 4, 58–64.

Maeda, S. and Schertler, G. F. X. 2013 **Production of GPCR and GPCR complexes for structure determination**. *Curr Opin Struct Biol* 23, 381–392.

Magalhaes, A. C., Dunn, H., Ferguson, S. S. G. 2012 **Regulation of GPCR activity, trafficking and localization by GPCR-interacting proteins**. *Br J Pharmacol* 165, 1717–1736.

Magnani, F., Serrano-Vega, M. J., Shibata, Y., Abdul-Hussein, S., Lebon, G., Miller-Gallacher, J., Singhal, A., Strege, A., Thomas, J. A., Tate, C. G. 2016 **A mutagenesis and screening strategy to generate optimally thermostabilized membrane proteins for structural studies**. *Nat Protoc* 11, 1554–1571.

Mamathambika, B. S. and Bardwell, J. C. 2008 **Disulfide-linked protein folding pathways**. *Annu Rev Pharmacol Toxicol* 24, 211–235.

Mamipour, M., Yousefi, M., Hasanzadeh, M. 2017 **An overview on molecular chaperones enhancing solubility of expressed recombinant proteins with correct folding.** *Int J Biol Macromol* 102, 367–375.

Manglik, A., Kim, T. H., Masureel, M., Altenbach, C., Yang, Z., Hilger, D., Lerch, M. T., Kobilka, T. S., Thian, F. S., Hubbell, W. L., Prosser, R. S., Kobilka, B. K. 2015 **Structural Insights into the Dynamic Process of β2-Adrenergic Receptor Signaling**. *Cell* 161, 1101–1111.

Manglik, A., Kobilka, B. K., Steyaert, J. 2017 **Nanobodies to Study G Protein-Coupled Receptor Structure and Function**. *Annu Rev Pharmacol Toxicol* 57, 19–37.

Martí-Solano, M., Sanz, F., Pastor, M., Selent, J. 2014 **A dynamic view of molecular switch behavior at serotonin receptors: implications for functional selectivity**. *PLoS ONE* 9, e109312.

Martí-Solano, M., Schmidt, D., Kolb, P., Selent, J. 2016 **Drugging specific conformational states of GPCRs: challenges and opportunities for computational chemistry.** *Drug Discov Today* 21, 625–631.

Maslennikov, I. and Choe, S. 2013 **Advances in NMR structures of integral membrane proteins**. *Curr Opin Struct Biol* 23, 555–562.

Maslennikov, I., Klammt, C., Hwang, E., Kefala, G., Okamura, M., Esquivies, L., Mörs, K., Glaubitz, C., Kwiatkowski, W., Jeon, Y. H., Choe, S. 2010 **Membrane domain structures of three classes of histidine kinase receptors by cell-free expression and rapid NMR analysis**. *Proc Natl Acad Sci U S A* 107, 10902–10907.

Matsuda, T., Watanabe, S., Kigawa, T. 2013 **Cell-free synthesis system suitable for disulfide-containing proteins**. *Biochem Biophys Res Commun* 431, 296–301.

May, S., Andreasson-Ochsner, M., Fu, Z., Low , Ying Xiu, Tan, D., de Hoog, Hans-Peter M., Ritz, S., Nallani, M., Sinner, E.-K. 2013 **In Vitro Expressed GPCR Inserted in Polymersome Membranes for Ligand-Binding Studies**. *Angew Chem Int Ed Engl* 52, 749–753.

McCusker, E. C., Bane, S. E., O'Malley, M. A., Robinson, A. S. 2007 **Heterologous GPCR Expression: A Bottleneck to Obtaining Crystal Structures**. *Biotechnol Prog* 23, 540–547.

Merk, H., Rues, R.-B., Gless, C., Beyer, K., Dong, F., Dötsch, V., Gerrits, M., Bernhard, F. 2015 **Biosynthesis of membrane dependent proteins in insect cell lysates: identification of limiting parameters for folding and processing**. *Biol Chem* 396, 1097–1107.

Michalke, K., Gravière, M.-E., Huyghe, C., Vincentelli, R., Wagner, R., Pattus, F., Schroeder, K., Oschmann, J., Rudolph, R., Cambillau, C., Desmyter, A. 2009 **Mammalian G-protein-coupled receptor expression in Escherichia coli: I. High-throughput large-scale production as inclusion bodies**. *Anal Biochem* 386, 147–155.

Michel, E. and Wüthrich, K. 2012 **Cell-free expression of disulfide-containing eukaryotic proteins for structural biology**. *FEBS J* 279, 3176–3184.

Milić, D. and Veprintsev, D. B. **2015 Large-scale production and protein engineering of G protein-coupled receptors for structural studies**. *Front Pharmacol* 6, 66.

Miller, J. L. and Tate, C. G. 2011 **Engineering an ultra-thermostable β(1)-adrenoceptor**. *J Mol Biol* 413, 628–638.

Morgan, C. R., Hebling, C. M., Rand, K. D., Stafford, D. W., Jorgenson, J. W., Engen, J. R. 2011 **Conformational transitions in the membrane scaffold protein of phospholipid bilayer nanodiscs**. *Mol Cell Proteomics* 10, M111.010876.

Niesen, Michiel J M, Bhattacharya, S., Grisshammer, R., Tate, C. G., Vaidehi, N. 2013 **Thermostabilization of the β1-adrenergic receptor correlates with increased entropy of the inactive state**. *J Phys Chem B* 117, 7283–7291.

Oates, J., Faust, B., Attrill, H., Harding, P., Orwick, M., Watts, A. 2012 **The role of cholesterol on the activity and stability of neurotensin receptor 1**. *Biochim. Biophys. Acta* 1818, 2228–2233.

Oates, J. and Watts, A. **2011 Uncovering the intimate relationship between lipids, cholesterol and GPCR activation.** *Curr Opin Struct Biol* 21, 802–807.

Ohta, N., Kato, Y., Watanabe, H., Mori, H., Matsuura, T. 2016 **In vitro membrane protein synthesis inside Sec translocon-reconstituted cell-sized liposomes**. *Sci Rep* 6, 36466.

Okuta, A., Tani, K., Nishimura, S., Fujiyoshi, Y., Doi, T. 2016 **Thermostabilization of the Human Endothelin Type B Receptor**. *J Mol Biol* 428, 2265–2274.

Pauwels, P. J., Gommeren, W., van Lommen, G., Janssen, P. A., Leysen, J. E. 1988 **The receptor binding profile of the new antihypertensive agent nebivolol and its stereoisomers compared with various beta-adrenergic blockers**. *Mol Pharmacol* 34, 843–851.

Peetz, O., Henrich, E., Laguerre, A., Löhr, F., Hein, C., Dötsch, V., Bernhard, F., Morgner, N. 2017 **Insights into Cotranslational Membrane Protein Insertion by Combined LILBID-Mass Spectrometry and NMR Spectroscopy**. *Anal Chem*. 89, 12314-12318

Pönicke, K., Heinroth-Hoffmann, I., Brodde, O.-E. 2002 **Differential effects of bucindolol and carvedilol on noradenaline-induced hypertrophic response in ventricular cardiomyocytes of adult rats**. *J Pharmacol Exp Ther* 301, 71–76.

Popot, J.-L. 2010 **Amphipols, Nanodiscs, and Fluorinated Surfactants: Three Nonconventional Approaches to Studying Membrane Proteins in Aqueous Solutions.** *Annu Rev Biochem* 79, 737–775.

Post, S. R., Hammond, H. K., Insel, P. A. 1999 **Beta-adrenergic receptors and receptor signaling in heart failure**. *Annu Rev Pharmacol Toxicol* 39, 343–360.

Pouvreau, S. 2014 **Genetically encoded reactive oxygen species (ROS) and redox indicators**. *Biotechnol J* 9, 282–293.

Prasanna, X., Sengupta, D., Chattopadhyay, A. 2016 **Cholesterol-dependent Conformational Plasticity in GPCR Dimers**. *Sci Rep* 6, 31858.

Proverbio, D., Roos, C., Beyermann, M., Orbán, E., Dötsch, V., Bernhard, F. 2013 **Functional properties of cell-free expressed human endothelin A and endothelin B receptors in artificial membrane environments**. *Biochim Biophys Acta* 1828, 2182–2192.

Pullela, P. K., Chiku, T., Carvan, M. J., Sem, D. S. 2006 **Fluorescence-based detection of thiols in vitro and in vivo using dithiol probes**. *Anal Biochem* 352, 265–273.

Rajagopal, K., Lefkowitz, R. J., Rockman, H. A. 2005 **When 7 transmembrane receptors are not G protein-coupled receptors**. *J Clin Invest* 115, 2971–2974.

Ranjan, R., Dwivedi, H., Baidya, M., Kumar, M., Shukla, A. K. 2017 **Novel Structural Insights into GPCR-β-Arrestin Interaction and Signaling**. *Trends Cell Biol* 27, 851-862

Raschle, T., Hiller, S., Yu, T.-Y., Rice, A. J., Walz, T., Wagner, G. 2009 **Structural and functional characterization of the integral membrane protein VDAC-1 in lipid bilayer nanodiscs**. *J Am Chem Soc* 131, 17777–17779.

Rath, A., Glibowicka, M., Nadeau, V. G., Chen, G., Deber, C. M. 2009 **Detergent binding explains anomalous SDS-PAGE migration of membrane proteins**. *Proc Natl Acad Sci U S A* 106, 1760–1765.

Ritz, S., Hulko, M., Zerfaß, C., May, S., Hospach, I., Krasteva, N., Nelles, G., Sinner, E. K. 2013 **Cell-free expression of a mammalian olfactory receptor and unidirectional insertion into small unilamellar vesicles (SUVs)**. *Biochimie* 95, 1909–1916.

Robelek, R., Lemker, E. S., Wiltschi, B., Kirste, V., Naumann, R., Oesterhelt, D., Sinner, E.-K. 2007 **Incorporation of In Vitro Synthesized GPCR into a Tethered Artificial Lipid Membrane System**. *Angew Chem Int Ed Engl* 46, 605–608.

Robertson, N., Jazayeri, A., Errey, J., Baig, A., Hurrell, E., Zhukov, A., Langmead, C. J., Weir, M., Marshall, F. H. 2011 **The properties of thermostabilised G protein-coupled receptors (StaRs) and their use in drug discovery**. *Neuropharmacology* 60, 36–44.

Roos, C., Kai, L., Proverbio, D., Ghoshdastider, U., Filipek, S., Dötsch, V., Bernhard, F. 2013 **Co-translational association of cell-free expressed membrane proteins with supplied lipid bilayers**. *Mol Membr Biol* 30, 75–89.

Roos, C., Zocher, M., Müller, D., Münch, D., Schneider, T., Sahl, H.-G., Scholz, F., Wachtveitl, J., Ma, Y., Proverbio, D., Henrich, E., Dötsch, V., Bernhard, F. 2012 **Characterization of co-translationally formed nanodisc complexes with small multidrug transporters, proteorhodopsin and with the *E. coli* MraY translocase**. *Biochim Biophys Acta* 1818, 3098–3106.

Rosenbaum, D. M., Rasmussen, S. G. F., Kobilka, B. K. 2009 **The structure and function of G-protein-coupled receptors**. *Nature* 459, 356–363.

Rosenbaum, D. M., Zhang, C., Lyons, J. A., Holl, R., Aragao, D., Arlow, D. H., Rasmussen, Søren G F, Choi, H.-J., DeVree, B. T., Sunahara, R. K., Chae, P. S., Gellman, S. H., Dror, R. O., Shaw, D. E., Weis, W. I., Caffrey, M., Gmeiner, P., Kobilka, B. K. 2011 **Structure and function of an irreversible agonist-β(2) adrenoceptor complex**. *Nature* 469, 236–240.

Rues, R.-B., Dötsch, V., Bernhard, F. 2016 **Co-translational formation and pharmacological characterization of beta1-adrenergic receptor/nanodisc complexes with different lipid environments.** *Biochim Biophys Acta* 1858, 1306–1316.

Rues, R.-B., Orbán, E., Dötsch, V., Bernhard, F. 2014 **Cell-free expression of G-protein coupled receptors: new pipelines for challenging targets**. *Biol Chem* 395, 1425–1434.

Saito, Y., Mizuno, T., Itakura, M., Suzuki, Y., Ito, T., Hagiwara, H., Hirose, S. 1991 **Primary structure of bovine endothelin ETB receptor and identification of signal peptidase and metal proteinase cleavage sites**. *J Biol Chem* 266, 23433–23437.

Sansuk, K., Balog, C. I. A., van der Does, A. M., Booth, R., de Grip, W. J., Deelder, A. M., Bakker, R. A., Leurs, R., Hensbergen, P. J. 2008 **GPCR Proteomics: Mass Spectrometric and Functional Analysis of Histamine H 1 Receptor after Baculovirus-Driven and in Vitro Cell Free Expression**. *J Proteome Res* 7, 621–629.

Schafer, F. Q. and Buettner, G. R. 2001 **Redox environment of the cell as viewed through the redox state of the glutathione disulfide/glutathione couple**. *Free Redic Biol Med* 30, 1191–1212.

Scheerer, P. and Sommer, M. E. 2017 **Structural mechanism of arrestin activation**. *Curr Opin Struct Biol* 45, 160–169.

Schlinkmann, K. M., Honegger, A., Türeci, E., Robison, K. E., Lipovšek, D., Plückthun, A. 2012 **Critical features for biosynthesis, stability, and functionality of a G protein-coupled receptor uncovered by all-versus-all mutations**. *Proc Natl Acad Sci U S A* 109, 9810–9815.

Schmidt, P., Berger, C., Scheidt, H. A., Berndt, S., Bunge, A., Beck-Sickinger, A. G., Huster, D. 2010 **A reconstitution protocol for the in vitro folded human G protein-coupled Y2 receptor into lipid environment**. *Biophys Chem* 150, 29–36.

Schneider, B., Junge, F., Shirokov, V. A., Durst, F., Schwarz, D., Dötsch, V., Bernhard, F. 2010 **Membrane protein expression in cell-free systems**. *Methods Mol Biol* 601, 165–186.

Schuler, M. A., Denisov, I. G., Sligar, S. G. 2013 **Nanodiscs as a new tool to examine lipid-protein interactions**. *Methods Mol Biol* 974, 415–433.

Schwarz, D., Junge, F., Durst, F., Frölich, N., Schneider, B., Reckel, S., Sobhanifar, S., Dötsch, V., Bernhard, F. 2007 **Preparative scale expression of membrane proteins in Escherichia coli-based continuous exchange cell-free systems**. *Nat Protoc* 2, 2945–2957.

Seddon, A. M., Curnow, P., Booth, P. J. 2004 **Membrane proteins, lipids and detergents: not just a soap opera**. *Biochim Biophys Acta* 1666, 105–117.

Serrano-Vega, M. J. and Tate, C. G. 2009 **Transferability of thermostabilizing mutations between β-adrenergic receptors**. *Mol Membr Biol* 26, 385–396.

Shenoy, S. K. and Lefkowitz, R. J. 2011 **β-Arrestin-mediated receptor trafficking and signal transduction**. *Trends Pharmacol Sci* 32, 521–533.

Shibata, Y., Gvozdenovic-Jeremic, J., Love, J., Kloss, B., White, J. F., Grisshammer, R., Tate, C. G. 2013 **Optimising the combination of thermostabilising mutations in the neurotensin receptor for structure determination**. *Biochim Biophys Acta* 1828, 1293–1301.

Shihoya, W., Nishizawa, T., Okuta, A., Tani, K., Dohmae, N., Fujiyoshi, Y., Nureki, O., Doi, T. 2016 **Activation mechanism of endothelin ETB receptor by endothelin-1**. *Nature* 537, 363–368.

Shilling, P. J., Bathgate, Ross A D, Gooley, P. R. 2013 **Cell-free protein synthesis as a tool to study RXFP3-relaxin-3 protein interactions**. *Ital J Anat Embryol* 118, 7–9.

Shilling, P. J., Bumbak, F., Scott, D. J., Bathgate, Ross A D, Gooley, P. R. 2017 **Characterisation of a cell-free synthesised G-protein coupled receptor**. *Sci Rep* 7, 1094.

Shimizu, Y. and Ueda, T. 2010 **PURE technology**. *Methods Mol. Biol.* 607, 11–21.

Smith, E. A., Smith, C., Tanksley, B., Dea, P. K. 2014a **Effects of cis- and trans-unsaturated lipids on an interdigitated membrane**. *Biophys Chem* 190-191, 1–7.

Smith, M. T., Wilding, K. M., Hunt, J. M., Bennett, A. M., Bundy, B. C. 2014b **The emerging age of cell-free synthetic biology**. *FEBS Lett* 588, 2755–2761.

Sonnabend, A., Spahn, V., Stech, M., Zemella, A., Stein, C., Kubick, S. 2017 **Production of G protein-coupled receptors in an insect-based cell-free system**. *Biotechnol Bioeng*.

Soubias, O. and Gawrisch, K. 2012 **The role of the lipid matrix for structure and function of the GPCR rhodopsin**. *Biochim Biophys Acta* 1818, 234–240.

Soubias, O., Niu, S.-L., Mitchell, D. C., Gawrisch, K. 2008 **Lipid-rhodopsin hydrophobic mismatch alters rhodopsin helical content**. *J Am Chem Soc* 130, 12465–12471.

Stoevesandt, O., Vetter, M., Kastelic, D., Palmer, E. A., He, M., Taussig, M. J. 2011 **Cell free expression put on the spot: advances in repeatable protein arraying from DNA (DAPA)**. *N Biotechnol* 28, 282–290.

Tam, J. P., Liu, W., Zhang, J. W., Galantino, M., Bertolero, F., Cristiani, C., Vaghi, F., Castiglione, R. de 1994 **Alanine scan of endothelin: importance of aromatic residues**. *Peptides* 15, 703–708.

Thomas, J. and Tate, C. G. 2014 **Quality control in eukaryotic membrane protein overproduction**. *J Mol Biol* 426, 4139–4154.

Thoring, L., Wüstenhagen, D. A., Borowiak, M., Stech, M., Sonnabend, A., Kubick, S. 2016 **Cell-Free Systems Based on CHO Cell Lysates: Optimization Strategies, Synthesis of "Difficult-to-Express" Proteins and Future Perspectives**. *PLoS ONE* 11, e0163670.

Traut, R. R. and Haenni, A. L. 1967 **The effect of sulfhydryl reagents on ribosome activity**. *Eur J Biochem* 2, 4–73.

Tsukamoto, H., Sinha, A., DeWitt, M., Farrens, D. L. 2010 **Monomeric rhodopsin is the minimal functional unit required for arrestin binding**. *J Mol Biol* 399, 501–511.

Vaidehi, N., Grisshammer, R., Tate, C. G. 2016 **How Can Mutations Thermostabilize G-Protein-Coupled Receptors?** *Trends Pharmacol Sci* 37, 37–46.

van Anken, E. and Braakman, I. 2005 **Versatility of the endoplasmic reticulum protein folding factory**. *Crit Rev Biochem Mol Biol* 40, 191–228.

Venkatakrishnan, A. J., Deupi, X., Lebon, G., Tate, C. G., Schertler, G. F., Babu, M. M. 2013 **Molecular signatures of G-protein-coupled receptors**. *Nature* 494, 185–194.

Vignon-Zellweger, N., Heiden, S., Miyauchi, T., Emoto, N. 2012 **Endothelin and endothelin receptors in the renal and cardiovascular systems**. *Life Sci* 91, 490–500.

Villar, Van Anthony M, Cuevas, S., Zheng, X., Jose, P. A. 2016 **Localization and signaling of GPCRs in lipid rafts**. *Methods Cell Biol* 132, 3–23.

Vukoti, K., Kimura, T., Macke, L., Gawrisch, K., Yeliseev, A. 2012 **Stabilization of functional recombinant cannabinoid receptor CB(2) in detergent micelles and lipid bilayers**. *PLoS ONE* 7, e46290.

Wang, X., Corin, K., Baaske, P., Wienken, C. J., Jerabek-Willemsen, M., Duhr, S., Braun, D., Zhang, S. 2011 **Peptide surfactants for cell-free production of functional G protein-coupled receptors**. *Proc Natl Acad Sci U S A* 108, 9049–9054.

Wang, X., Cui, Y., Wang, J. 2013a **Efficient expression and immunoaffinity purification of human trace amine-associated receptor 5 from *E. coli* cell-free system**. *Protein Pept. Lett.* 20, 473–480.

Wang, X., Wang, J., Ge, B. 2013b **Evaluation of cell-free expression system for the production of soluble and functional human GPCR N-formyl peptide receptors.** *Protein Pept Lett* 20, 1272–1279.

Warne, T., Chirnside, J., Schertler, G. F. 2003 **Expression and purification of truncated, non-glycosylated turkey beta-adrenergic receptors for crystallization.** *Biochim Biophys Acta* 1610, 133–140.

Warne, T., Moukhametzianov, R., Baker, J. G., Nehmé, R., Edwards, P. C., Leslie, Andrew G W, Schertler, G. F. X., Tate, C. G. 2011 **The structural basis for agonist and partial agonist action on a β(1)-adrenergic receptor**. *Nature* 469, 241–244.

Warne, T., Serrano-Vega, M. J., Baker, J. G., Moukhametzianov, R., Edwards, P. C., Henderson, R., Leslie, Andrew G W, Tate, C. G., Schertler, G. F. X. 2008 **Structure of a beta1-adrenergic G-protein-coupled receptor**. *Nature* 454, 486–491.

Warne, T. and Tate, C. G. 2013 **The importance of interactions with helix 5 in determining the efficacy of β-adrenoceptor ligands**. *Biochem Soc Trans* 41, 159–165.

Welsh, J. P., Bonomo, J., Swartz, J. R. 2011 **Localization of BiP to translating ribosomes increases soluble accumulation of secreted eukaryotic proteins in an Escherichia coli cell-free system**. *Biotechnol Bioeng* 108, 1739–1748.

Yang, J.-P., Cirico, T., Katzen, F., Peterson, T. C., Kudlicki, W. 2011 **Cell-free synthesis of a functional G protein-coupled receptor complexed with nanometer scale bilayer discs**. *BMC Biotechnol* 11, 57.

Yao, Z. and Kobilka, B. 2005 **Using synthetic lipids to stabilize purified β2 adrenoceptor in detergent micelles**. *Analytical Biochemistry* 343, 344–346.

Ye, L., van Eps, N., Zimmer, M., Ernst, O. P., Prosser, R. S. 2016 **Activation of the A2A adenosine G-protein-coupled receptor by conformational selection**. *Nature* 533, 265–268.

Zannis, V. I., Fotakis, P., Koukos, G., Kardassis, D., Ehnholm, C., Jauhiainen, M., Chroni, A. 2015 **HDL biogenesis, remodeling, and catabolism**. *Handb Exp Pharmacol* 224, 53–111.

Zawada, J. F., Yin, G., Steiner, A. R., Yang, J., Naresh, A., Roy, S. M., Gold, D. S., Heinsohn, H. G., Murray, C. J. 2011 **Microscale to manufacturing scale-up of cell-free cytokine production--a new approach for shortening protein production development timelines**. *Biotechnol Bioeng* 108, 1570–1578.

Zemella, A., Grossmann, S., Sachse, R., Sonnabend, A., Schaefer, M., Kubick, S. 2017 **Qualifying a eukaryotic cell-free system for fluorescence based GPCR analyses**. *Sci Rep* 7, 3740.

Zhang, M., Huang, R., Im, S.-C., Waskell, L., Ramamoorthy, A. **2015 Effects of membrane mimetics on cytochrome P450-cytochrome b5 interactions characterized by NMR spectroscopy**. *J Biol Chem* 290, 12705–12718.

Zhang, S. 2012 **Lipid-like self-assembling peptides**. *Acc Chem Res* 45, 2142–2150.

Zhou, L. and Bohn, L. M. 2014 **Functional selectivity of GPCR signaling in animals**. *Curr Opin Cell Biol* 27, 102–108.

Zocher, M., Roos, C., Wegmann, S., Bosshart, P. D., Dötsch, V., Bernhard, F., Müller, D. J. 2012 **Single-molecule force spectroscopy from nanodiscs: an assay to quantify folding, stability, and interactions of native membrane proteins**. *ACS nano* 6, 961–971.

Appendix

Calibration data of SEC columns

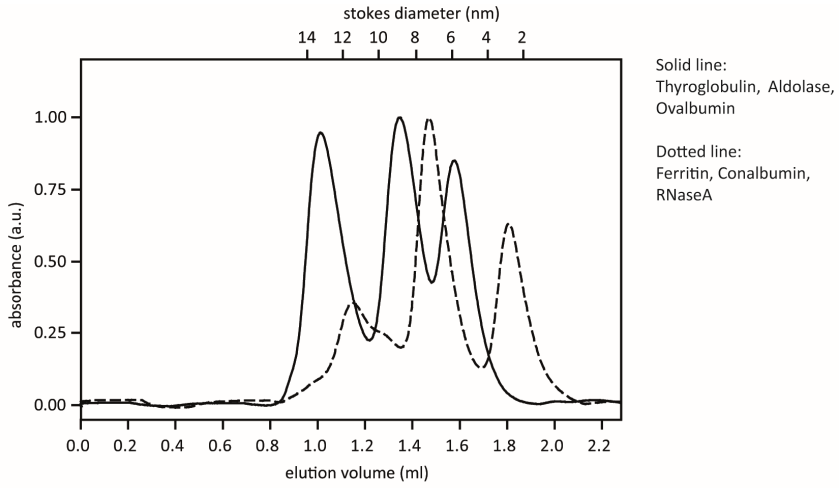

protein	Molecular mass	Stokes diameter	Elution volume
Thyroglobulin	669 kDa		1.012 ml
Ferritin	440 kDa	12.2 nm	1.148 ml
Aldolase	158 kDa	9.62 nm	1.348 ml
Conalbumin	75 kDa		1.469 ml
Ovalbumin	44 kDa	6.10 nm	1.576 ml
RNaseA	14 kDa	3.28 nm	1.810 ml

Column name: Superdex 200 3.2/30

Column vol. (CV): 2.4 ml

Void vol. (V_0): 0.89 ml

Elution vol. (V_e)

partition coefficient (K_{AV})

$$K_{AV} = (V_e - V_0) / (CV - V_0)$$

Molecular mass (M_R)

$$K_{AV} = a + b * \ln M_R$$

a = 1.8625
b = -0.1314

Stokes diameter (ø)

$$K_{AV} = b + a * ø$$

a = 28.689
b = -14.28

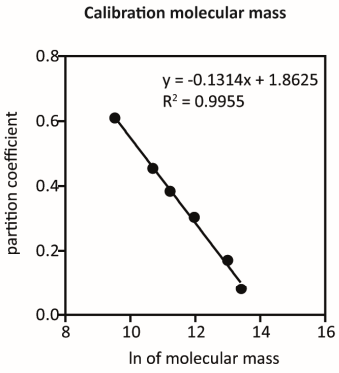

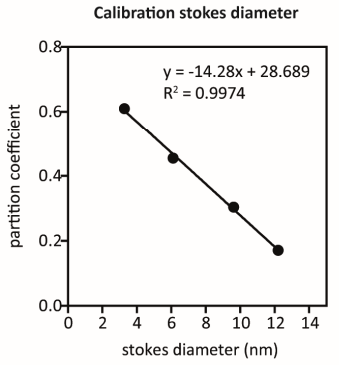

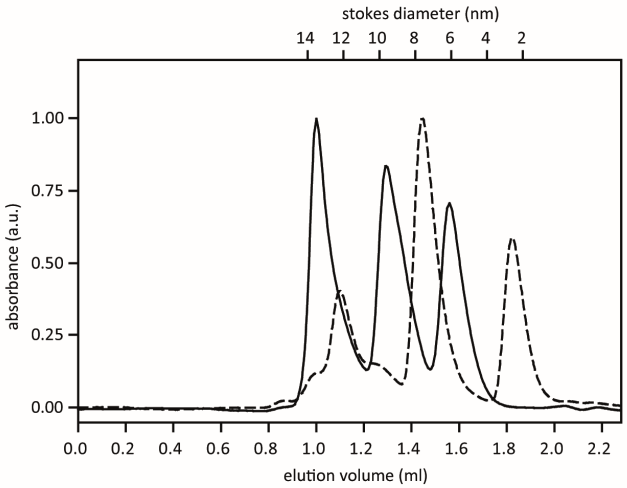

Solid line:
Thyroglobulin, Aldolase, Ovalbumin

Dotted line:
Ferritin, Conalbumin, RNaseA

protein	Molecular mass	Stokes diameter	Elution volume
Thyroglobulin	669 kDa		1.000 ml
Ferritin	440 kDa	12.2 nm	1.100 ml
Aldolase	158 kDa	9.62 nm	1.290 ml
Conalbumin	75 kDa		1.448 ml
Ovalbumin	44 kDa	6.10 nm	1.559 ml
RNaseA	14 kDa	3.28 nm	1.821 ml

Column name: Superdex 200 3.2/30 increase

Column vol. (CV): 2.4 ml

Void vol. (V_0): 0.89 ml

Elution vol. (V_e)

partition coefficient (K_{AV})

$$K_{AV} = (V_e - V_0) / (CV - V_0)$$

Molecular mass (M_R)

$$K_{AV} = a + b * \ln M_R$$

a = 1.9221
b = -0.1379

Stokes diameter (ø)

$$K_{AV} = b + a * ø$$

a = 26.783

Calibration molecular mass

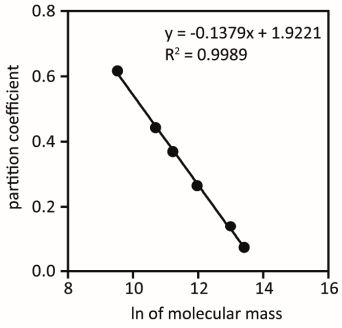

Calibration stokes diameter

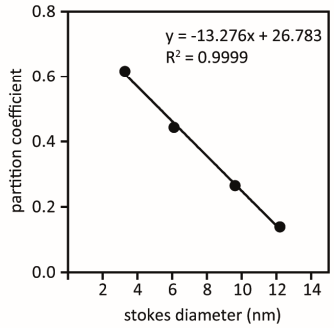

Characteristica of lipids and ND

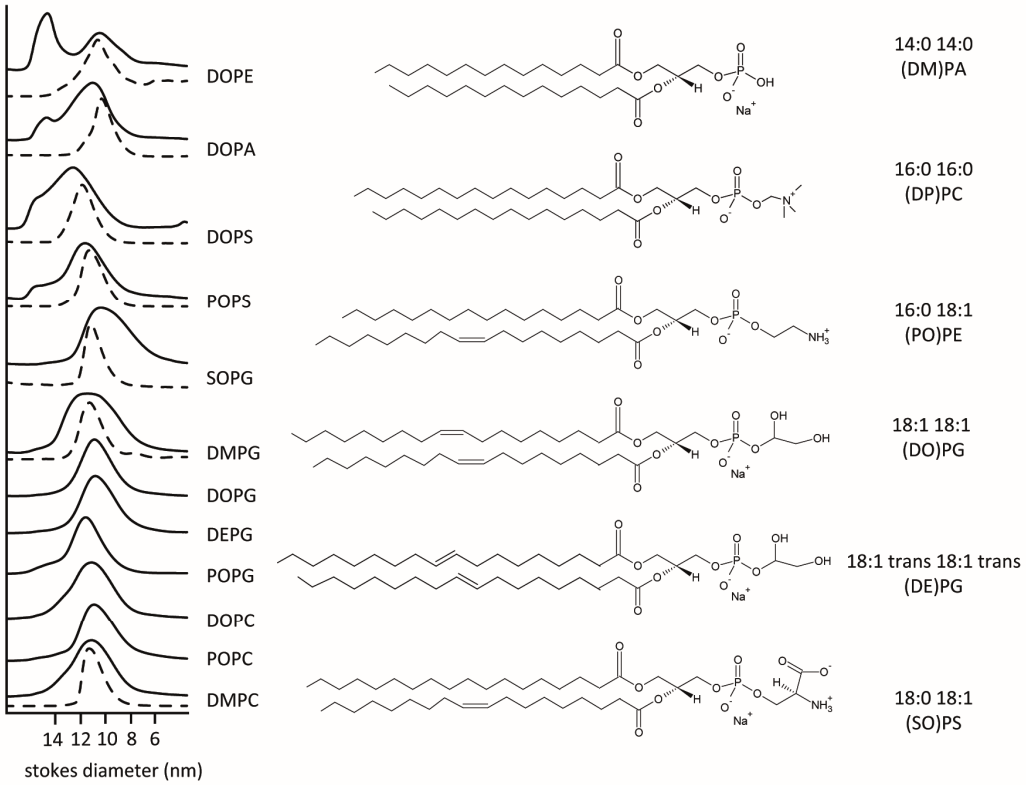

Left: SEC profiles of preformed ND with different lipid composition. Formed ND were analysed on a Superdex 200 3.2/30 column. For some ND, an additional purification step using preparative SEC on a Superdex 200 3.2/300 column was performed to increase homogeneity (dotted lines). Adapted from Rues et al. 2016.

Right: Structural chemical formula of lipids with fatty acid chains and headgroups used in this thesis.

Bottom: Overview on lipids used in this thesis

short name	long name	headgroup	chain 1 length	chain 1 double bonds	chain 2 length	chain 2 double bonds	transition temperature (°C)	mol. mass (g/mol)
DMPC	1,2-dimyristoyl-*sn*-glycero-3-phosphocholine	phosphocholine	14	0	14	0	24	677.933
DMPG	1,2-dimyristoyl-*sn*-glycero-3-phospho-(1'-rac-glycerol)	phosphoglycerol	14	0	14	0	23	688.845
DPPC	1,2-dipalmitoyl-*sn*-glycero-3-phosphocholine	phosphocholine	16	0	16	0	41	734.039
POPC	1-palmitoyl-2-oleoyl-*sn*-glycero-3-phosphocholine	phosphocholine	16	0	18	1	-2	760.076
POPG	1-palmitoyl-2-oleoyl-*sn*-glycero-3-phospho-(1'-*rac*-glycerol)	phosphoglycerol	16	0	18	1	-2	770.989
POPS	1-palmitoyl-2-oleoyl-*sn*-glycero-3-phospho-L-serin	phosphoserine	16	0	18	1	14	783.988
DOPC	1,2-dioleoyl-*sn*-glycero-3-phosphocholine	phosphocholine	18	1	18	1	-17	786.113
DOPG	1,2-dioleoyl-*sn*-glycero-3-phospho-(1'-*rac*-glycerol)	phosphoglycerol	18	1	18	1	-18	797.026
DOPA	1,2-dioleoyl-*sn*-glycero-3-phosphate	phosphate	18	1	18	1	-8	722.948
DOPE	1,2-dioleoyl-*sn*-glycero-3-phosphoethanolamine	ethanolamine	18	1	18	1	-18	744.034
DOPS	1,2-dioleoyl-*sn*-glycero-3-phospho-L-serine	phosphoserine	18	1	18	1	-11	810.025
DEPG	1,2-dielaidoyl-*sn*-glycero-3-phospho-(1'-*rac*-glycerol)	phosphoglycerol	18	1 (trans)	18	1 (trans)	n.a.	797.026
SOPG	1-stearoyl-2-oleoyl-*sn*-glycero-3-phospho-(1'-*rac*-glycerol)	phosphoglycerol	18	0	18	1	n.a.	799.042
DLPG	1,2-dilinoleoyl-*sn*-glycero-3-phospho-(1'-*rac*-glycerol)	phosphoglycerol	18	2	18	2	n.a.	792.994

DNA sequences

Coding DNA sequences for the receptor-constructs analysed in this study are given with the following marks:
Expression-tag, Receptor, sfGFP, His-tag, STOP-codon

Thermostabilised truncated turkey Beta1AR with His_{10}-tag (Mg Ts-Delta-Beta1AR-His_{10})
Vector: pET21a(+)
Restriction sites: non (restriction free cloning)

```
atgggagcagaattattatcacagcagtgggaggcgggcatgagcctgctgatggccctggtggtgctgctcatcgtggccgg
caacgtgctggtgatcgcggccatcgggagcacgcagcggctgcagacgctcaccaacctcttcatcacctcgctggcctgcg
ccgacctggtggtggggctgctggtggtgcctttcggggccacgctggtggtgcggggcacctggctgtggggctccttcctc
tgcgagctctggacatcgctggacgtgctttgcgtgacggcaagcgtatggaccttgtgcgtcatcgccatcgaccgctacct
ggccatcacctctccattccgctaccagagcctgatgaccagggctcgggccaaggtcatcatctgcaccgtctgggccatct
ccgctctggtctctttcctgcccatcatgatgcactggtggcgggacgaggaccctcaggcgctcaagtgctaccaggacccg
ggctgctgcgactttgtcaccaaccgggcttacgccatcgcctcgtccatcatctccttctacatccccctcctcatcatgat
cttcgtggcgctgcgggtgtaccgggaggccaaggagcagatcaggaagatcgaccgcgctagcaagaggaagacgtcccgtg
tcatgctgatgagggaacacaaagctctgaagacattgggtatcatcatgggggtgttcaccctctgctggctccctttcttc
ttggtgaacattgtcaacgtcttcaacagagatctggtgccggactggctcttcgttgccttcaactggttgggctacgccaa
ctctgctatgaaccccatcatcctgtgccgcagcccagacttccgtaaggccttcaagaggctgctcgccttcccccgcaaag
ctgacaggcggctg caccatcaccatcaccatcaccatcatcactga
```

Thermostabilised truncated turkey Beta1AR with sfGFP-His_6-tag (Mg Ts-Delta-Beta1AR-sfGFP-His_6)
Vector: pET21a(+)
Restriction sites: non (restriction free cloning)

```
atgggagcagaattattatcacagcagtgggaggcgggcatgagcctgctgatggccctggtggtgctgctcatcgtggccgg
caacgtgctggtgatcgcggccatcgggagcacgcagcggctgcagacgctcaccaacctcttcatcacctcgctggcctgcg
ccgacctggtggtggggctgctggtggtgcctttcggggccacgctggtggtgcggggcacctggctgtggggctccttcctc
tgcgagctctggacatcgctggacgtgctttgcgtgacggcaagcgtatggaccttgtgcgtcatcgccatcgaccgctacct
ggccatcacctctccattccgctaccagagcctgatgaccagggctcgggccaaggtcatcatctgcaccgtctgggccatct
ccgctctggtctctttcctgcccatcatgatgcactggtggcgggacgaggaccctcaggcgctcaagtgctaccaggacccg
ggctgctgcgactttgtcaccaaccgggcttacgccatcgcctcgtccatcatctccttctacatccccctcctcatcatgat
cttcgtggcgctgcgggtgtaccgggaggccaaggagcagatcaggaagatcgaccgcgctagcaagaggaagacgtcccgtg
tcatgctgatgagggaacacaaagctctgaagacattgggtatcatcatgggggtgttcaccctctgctggctccctttcttc
ttggtgaacattgtcaacgtcttcaacagagatctggtgccggactggctcttcgttgccttcaactggttgggctacgccaa
ctctgctatgaaccccatcatcctgtgccgcagcccagacttccgtaaggccttcaagaggctgctcgccttcccccgcaaag
ctgacaggcggctggcaggaggcatgagcaaaggagaagaacttttcactggagttgtcccaattcttgttgaattagatggt
gatgttaatgggcacaaattttctgtccgtggagagggtgaaggtgatgctacaaacggaaaactcacccttaaatttatttg
cactactggaaaactacctgttccgtggccaacacttgtcactactctgacctatggtgttcaatgcttttcccgttatccgg
atcacatgaaacggcatgacttttcaagagtgccatgcccgaaggttatgtacaggaacgcactatatctttcaaagatgac
gggacctacaagacgcgtgctgaagtcaagtttgaaggtgataccttgttaatcgtatcgagttaaagggtattgattttaa
agaagatggaaacattcttggacacaaactcgagtacaactttaactcacacaatgtatacatcacggcagacaaacaaaaga
atggaatcaaagctaacttcaaaattcgccacaacgttgaagatggttccgttcaactagcagaccattatcaacaaaatact
ccaattggcgatggccctgtccttttaccagacaaccattacctgtcgacacaatctgtcctttcgaaagatcccaacgaaaa
gcgtgaccacatggtccttcttgagtttgtaactgctgctgggattacacatggcatggatgagctctacaaaggatcccacc
accaccaccaccactga
```

Non-stabilised truncated turkey Beta1AR with sfGFP-His_6-tag (Mg Delta-Beta1AR-sfGFP-His_6)
Vector: pET21a(+)

Restriction sites: non (restriction free cloning)

ATGGGCGATGGGTGGCTGCCGCCCGACTGCGGCCCCCACAACCGCTCCGGAGGCGGCGGGGCGACGGCGGCGCCGACCGGGAG
CCGTCAGGTGTCCGCCGAGCTGCTGTCGCAGCAGTGGGAGGCGGGCATGAGCCTGCTGATGGCCCTGGTGGTGCTGCTCATCG
TGGCCGGCAACGTGCTGGTGATCGCGGCCATCGGGCGCACGCAGCGGCTGCAGACGCTCACCAACCTCTTCATCACCTCGCTG
GCCTGCGCCGACCTGGTGATGGGGCTGCTGGTGGTGCCTTTCGGGGCCACGCTGGTGGTGCGGGGCACCTGGCTGTGGGGCTC
CTTCCTCTGCGAGTGCTGGACATCGCTGGACGTGCTTTGCGTGACGGCAAGCATCGAGACCTTGTGCGTCATCGCCATCGACC
GCTACCTGGCCATCACCTCTCCATTCCGCTACCAGAGCCTGATGACCAGGGCTCGGGCCAAGGTCATCATCTGCACCGTCTGG
GCCATCTCCGCTCTGGTCTCTTTCCTGCCCATCATGATGCACTGGTGGCGGGACGAGGACCCTCAGGCGCTCAAGTGCTACCA
GGACCCGGGCTGCTGCGACTTTGTCACCAACCGGGCTTACGCCATCGCCTCGTCCATCATCTCCTTCTACATCCCCCTCCTCA
TCATGATCTTCGTGTACCTGCGGGTGTACCGGGAGGCCAAGGAGCAGATCAGGAAGATCGACCGCTGCGAGGGCCGGTTCTAT
GGCAGCCAGGAGCAGCCGCAGCCACCCCCGCTCCCCCAACACCAGCCCATCCTCGGCAACGGCCGTGCCAGCAAGAGGAAGAC
GTCCCGTGTCATGGCCATGAGGGAACACAAAGCTCTGAAGACATTGGGTATCATCATGGGGGTGTTCACCCTCTGCTGGCTCC
CTTTCTTCTTGGTGAACATTGTCAACGTCTTCAACAGAGATCTGGTGCCGGACTGGCTCTTCGTTTTCTTCAACTGGTTGGGC
TACGCCAACTCTGCTTTCAACCCCATCATCTACTGCCGCAGCCCAGACTTCCGTAAGGCCTTCAAGAGGCTGCTCTGCTTCCC
CCGCAAAGCTGACAGGCGGCTGGCAGGAGGCATGAGCAAAGGAGAAGAACTTTTCACTGGAGTTGTCCCAATTCTTGTTGAAT
TAGATGGTGATGTTAATGGGCACAAATTTTCTGTCCGTGGAGAGGGTGAAGGTGATGCTACAAACGGAAAACTCACCCTTAAA
TTTATTTGCACTACTGGAAAACTACCTGTTCCGTGGCCAACACTTGTCACTACTCTGACCTATGGTGTTCAATGCTTTTCCCG
TTATCCGGATCACATGAAACGGCATGACTTTTTCAAGAGTGCCATGCCCGAAGGTTATGTACAGGAACGCACTATATCTTTCA
AAGATGACGGGACCTACAAGACGCGTGCTGAAGTCAAGTTTGAAGGTGATACCCTTGTTAATCGTATCGAGTTAAAGGGTATT
GATTTTAAAGAAGATGGAAACATTCTTGGACACAAACTCGAGTACAACTTTAACTCACACAATGTATACATCACGGCAGACAA
ACAAAAGAATGGAATCAAAGCTAACTTCAAAATTCGCCACAACGTTGAAGATGGTTCCGTTCAACTAGCAGACCATTATCAAC
AAAATACTCCAATTGGCGATGGCCCTGTCCTTTTACCAGACAACCATTACCTGTCGACACAATCTGTCCTTTCGAAAGATCCC
AACGAAAAGCGTGACCACATGGTCCTTCTTGAGTTTGTAACTGCTGCTGGGATTACACATGGCATGGATGAGCTCTACAAAGG
ATCCcaccaccaccaccaccactga

Thermostabilised full-length human Beta1AR with sfGFP-His$_6$-tag (Hs Ts-fl-Beta1AR-sfGFP-His$_6$)

Vector: pET21a(+)

Restriction sites: 5‘ Nde1 + 3‘ Spe1

atgaaaccatacgatggtccaggcgcgggcgtgctggtgctgggcgcgagcgaaccgggcaacctgagcagcgcggcgccgct
gccggatggcgcggcgaccgcggcgcgcctgctggtgccggcgagcccgccggcgagcctgctgccgccggcgagcgaaagcc
cggaaccgctgagccagcagtggaccgcgggcatgggcctgctgatggcgctgattgtgctgctgattgtggcgggcaacgtg
ctggtgattgtggcgattgcgagcaccccgcgcctgcagaccctgaccaacctgtttattatgagcctggcgagcgcggatct
ggtggtgggcctgctggtggtgccgtttggcgcgaccattgtggtgggggccgctgggaatatggcagctttttttgcgaac
tgtggaccagcgtggatgtgctgtgcgtgaccgcgagcgtgtggaccctgtgcgtgattgcgctggatcgctatctggcgatt
accagcccgtttcgctatcagagcctgctgacccgcgcgcgcgcgcgcggcctggtgtgcaccgtgtgggcgattagcgcgct
ggtgagctttctgccgattctgatgcattggtggcgcgcggaaagcgatgaagcgcgccgctgctataacgatccgaaatgct
gcgattttgtgaccaaccgcgcgtatgcgattgcgagcagcgtggtgagcttttatgtgccgctgtgcattatggcgtttgtg
gcgctgcgcgtgtttcgcgaagcgcagaaacaggtgaaaaaaattgatagctgcgaacgccgctttctgggcggcccggcgcg
cccgccgagcccgagcccgagcccggtgccggcgccggcgccgccgggcccgccgcgcccggcggcggcggcggcgaccg
cgccgctggcgaacggccgcgcgggcaaacgccgcccgagccgcctggtgctgctgcgcgaacagaaagcgctgaaaaccctg
ggcattattatgggcgtgtttaccctgtgctggctgccgttttttctggcgaacgtggtgaaagcgtttcatcgcgaactggt
gccggatcgcctgtttgtggcgtttaactggctgggctatgcgaacagcgcgatgaacccgattattctgtgccgcagcccgg
attttcgcaaagcgtttcagggcctgctggcggcggcgcgccgcgcggcgcgccgccgccatgcgacccatggcgatcgcccg
cgcgcgagcggctgcctggcgcgcccgggcccgccgccgagcccgggcgcggcgagcgatgatgatgatgatgatgtggtggg
cgcgaccccgccggcgcgcctgctggaaccgtgggcgggctgcaacggcggcgcggcggcggatagcgatagcagcctggatg
aaccgtgccgcccgggctttgcgagcgaaagcaaagtgggtaccAGCAAAGGAGAAGAACTTTTCACTGGAGTTGTCCCAATT
CTTGTTGAATTAGATGGTGATGTTAATGGGCACAAATTTTCTGTCCGTGGAGAGGGTGAAGGTGATGCTACAAACGGAAAACT
CACCCTTAAATTTATTTGCACTACTGGAAAACTACCTGTTCCGTGGCCAACACTTGTCACTACTCTGACCTATGGTGTTCAAT
GCTTTTCCCGTTATCCGGATCACATGAAACGGCATGACTTTTTCAAGAGTGCCATGCCCGAAGGTTATGTACAGGAACGCACT
ATATCTTTCAAAGATGACGGGACCTACAAGACGCGTGCTGAAGTCAAGTTTGAAGGTGATACCCTTGTTAATCGTATCGAGTT

AAAGGGTATTGATTTTAAAGAAGATGGAAACATTCTTGGACACAAACTCGAGTACAACTTTAACTCACACAATGTATACATCA
CGGCAGACAAACAAAAGAATGGAATCAAAGCTAACTTCAAAATTCGCCACAACGTTGAAGATGGTTCCGTTCAACTAGCAGAC
CATTATCAACAAAATACTCCAATTGGCGATGGCCCTGTCCTTTTACCAGACAACCATTACCTGTCGACACAATCTGTCCTTTC
GAAAGATCCCAACGAAAAGCGTGACCACATGGTCCTTCTTGAGTTTGTAACTGCTGCTGGGATTACACATGGCATGGATGAGC
TCTACAAActcgagcaccaccaccaccaccactga

Thermostabilised truncated human Beta1AR with sfGFP-His$_6$-tag (Hs Ts-Delta-Beta1AR-sfGFP-His$_6$)
Vector: pET21a(+)
Restriction sites: 5‘ Nde1 + 3‘ Spe1

atgaaaccatacgatggtccaagcccggaaccgctgagccagcagtggaccgcgggcatgggcctgctgatggcgctgattgt
gctgctgattgtggcgggcaacgtgctggtgattgtggcgattgcgagcaccccgcgcctgcagaccctgaccaacctgtttа
ttatgagcctggcgagcgcggatctggtggtgggcctgctggtggtgccgtttggcgcgaccattgtggtgtggggccgctgg
gaatatggcagctttttttgcgaactgtggaccagcgtggatgtgctgtgcgtgaccgcgagcgtgtggaccctgtgcgtgat
tgcgctggatcgctatctggcgattaccagcccgtttcgctatcagagcctgctgacccgcgcgcgcgcgcgcggcctggtgt
gcaccgtgtgggcgattagcgcgctggtgagctttctgccgattctgatgcattggtggcgcgcggaaagcgatgaagcgcgc
cgctgctataacgatccgaaatgctgcgattttgtgaccaaccgcgcgtatgcgattgcgagcagcgtggtgagcttttatgt
gccgctgtgcattatggcgtttgtggcgctgcgcgtgtttcgcgaagcgcagaaacaggtgaaaaaaattgatagcgcgggca
aacgccgcccgagccgcctggtgctgctgcgcgaacagaaagcgctgaaaaccctgggcattattatgggcgtgtttaccctg
tgctggctgccgtttttttctggcgaacgtggtgaaagcgtttcatcgcgaactggtgccggatcgcctgtttgtggcgtttaa
ctggctgggctatgcgaacagcgcgatgaacccgattattctgtgccgcagcccggattttcgcaaagcgtttcagggcctgc
tggcggcggagctcggtaccggtggtatgagcaaaggagaagaacttttcactggagttgtcccaattcttgttgaattagat
ggtgatgttaatgggcacaaatttttctgtccgtggagagggtgaaggtgatgctacaaacggaaaactcacccttaaatttat
ttgcactactggaaaactacctgttccgtggccaacacttgtcactactctgacctatggtgttcaatgcttttcccgttatc
cggatcacatgaaacggcatgacttttcaagagtgccatgcccgaaggttatgtacaggaacgcactatatctttcaaagat
gacgggacctacaagacgcgtgctgaagtcaagtttgaaggtgataccttgttaatcgtatcgagttaaagggtattgattt
taaagaagatggaaacattcttggacacaaactggagtacaactttaactcacacaatgtatacatcacggcagacaaacaaa
agaatggaatcaaagctaacttcaaaattcgccacaacgttgaagatggttccgttcaactagcagaccattatcaacaaaat
actccaattggcgatggccctgtccttttaccagacaaccattacctgtcgacacaatctgtcctttcgaaagatcccaacga
aaagcgtgaccacatggtccttcttgagtttgtaactgctgctgggattacacatggcatggatgagctctacaaactcgagc
atcaccatcaccatcaccatcaccatcactag

Non-stabilised truncated human Beta1AR with sfGFP-His$_6$-tag (Hs Delta-Beta1AR-sfGFP-His$_6$)
Vector: pET21a(+)
Restriction sites: 5‘ Nde1 + 3‘ Spe1

atgaaaccatacgatggtccaagcgaaagcccggaaccgctgagccagcagtggaccgcgggcatgggcctgctgatggcgct
gattgtgctgctgattgtggcgggcaacgtgctggtgattgtggcgattgcgaaaaccccgcgcctgcagaccctgaccaacc
tgtttattatgagcctggcgagcgcggatctggtgatgggcctgctggtggtgccgtttggcgcgaccattgtggtgtggggc
cgctgggaatatggcagctttttttgcgaactgtggaccagcgtggatgtgctgtgcgtgaccgcgagcattgaaaccctgtg
cgtgattgcgctggatcgctatctggcgattaccagcccgtttcgctatcagagcctgctgacccgcgcgcgcgcgcgcggcc
tggtgtgcaccgtgtgggcgattagcgcgctggtgagctttctgccgattctgatgcattggtggcgcgcggaaagcgatgaa
gcgcgccgctgctataacgatccgaaatgctgcgattttgtgaccaaccgcgcgtatgcgattgcgagcagcgtggtgagctt
ttatgtgccgctgtgcattatggcgtttgtgtatctgcgcgtgtttcgcgaagcgcagaaacaggtgaaaaaaattgatagcg
cgggcaaacgccgcccgagccgcctggtggcgctgcgcgaacagaaagcgctgaaaaccctgggcattattatgggcgtgttt
accctgtgctggctgccgtttttttctggcgaacgtggtgaaagcgtttcatcgcgaactggtgccggatcgcctgtttgtgtt
ctttaactggctgggctatgcgaacagcgcgtttaacccgattatttattgccgcagcccggattttcgcaaagcgtttcagg
gcctgctgggtaccggtggtatgagcaaaggagaagaacttttcactggagttgtcccaattcttgttgaattagatggtgat
gttaatgggcacaaatttttctgtccgtggagagggtgaaggtgatgctacaaacggaaaactcacccttaaatttatttgcac
tactggaaaactacctgttccgtggccaacacttgtcactactctgacctatggtgttcaatgcttttcccgttatccggatc
acatgaaacggcatgacttttcaagagtgccatgcccgaaggttatgtacaggaacgcactatatctttcaaagatgacggg
acctacaagacgcgtgctgaagtcaagtttgaaggtgataccttgttaatcgtatcgagttaaagggtattgattttaaaga

agatggaaacattcttggacacaaactggagtacaactttaactcacacaatgtatacatcacggcagacaaacaaaagaatg
gaatcaaagctaacttcaaaattcgccacaacgttgaagatggttccgttcaactagcagaccattatcaacaaaatactcca
attggcgatggccctgtccttttaccagacaaccattacctgtcgacacaatctgtcctttcgaaagatcccaacgaaaagcg
tgaccacatggtccttcttgagtttgtaactgctgctgggattacacatggcatggatgagctctacaaactcgagcatcacc
atcaccatcaccatcaccatcactag

human Endothelin A receptor with sfGFP-His$_6$-tag (Hs ETA-sfGFP-His$_6$)
Vector: pET21a(+)
Restriction sites: non (restriction free cloning)

atggctagcatgactggtggacagcaaatgggtcgcggatctatggaaacccttgcctcagggcatccttttggctggcact
ggttggatgtgtaatcagtgataatcctgagagatacagcacaaatctaagcaatcatgtggatgatttcaccacttttcgtg
gcacagagctcagcttcctggttaccactcatcaacccactaatttggtcctacccagcaatggctcaatgcacaactattgc
ccacagcagactaaaattacttcagctttcaaatacattaacactgtgatatcttgtactattttcatcgtgggaatggtggg
gaatgcaactctgctcaggatcatttaccagaacaaatgtatgaggaatggccccaacgcgctgatagccagtcttgcccttg
gagaccttatctatgtggtcattgatctccctatcaatgtatttaagctgctggctgggcgctggccttttgatcacaatgac
tttggcgtatttctttgcaagctgttcccctttttgcagaagtcctcggtggggatcaccgtcctcaacctctgcgctcttag
tgttgacaggtacagagcagttgcctcctggagtcgtgttcagggaattgggattcctttggtaactgccattgaaattgtct
ccatctggatcctgtcctttatcctggccattcctgaagcgattggcttcgtcatggtacccttgaatataggggtgaacag
cataaaacctgtatgctcaatgccacatcaaaattcatggagttctaccaagatgtaaaggactggtggctcttcgggttcta
tttctgtatgcccttggtgtgcactgcgatcttctacaccctcatgacttgtgagatgttgaacagaaggaatggcagcttga
gaattgccctcagtgaacatcttaagcagcgtcgagaagtggcaaaaacagttttctgcttggttgtaatttttgctctttgc
tggttccctcttcatttaagccgtatattgaagaaaactgtgtataacgagatggacaagaaccgatgtgaattacttagttt
cttactgctcatggattacatcggtattaacttggcaaccatgaattcatgtataaaccccatagctctgtattttgtgagca
agaaatttaaaaattgtttccagtcatgcctctgctgctgctgttaccagtccaaaagtctgatgacctcggtccccatgaac
ggaacaagcatccagtggaagaaccacgatcaaaacaaccacaacacagaccggagcagccataaggacagcatgAACCTCGA
GGGAACGGGCAGCAAAGGAGAAGAACTTTTCACTGGAGTTGTCCCAATTCTTGTTGAATTAGATGGTGATGTTAATGGGCACA
AATTTTCTGTCCGTGGAGAGGGTGAAGGTGATGCTACAAACGGAAAACTCACCCTTAAATTTATTTGCACTACTGGAAAACTA
CCTGTTCCGTGGCCAACACTTGTCACTACTCTGACCTATGGTGTTCAATGCTTTTCCCGTTATCCGGATCACATGAAACGGCA
TGACTTTTTCAAGAGTGCCATGCCCGAAGGTTATGTACAGGAACGCACTATATCTTTCAAAGATGACGGGACCTACAAGACGC
GTGCTGAAGTCAAGTTTGAAGGTGATACCCTTGTTAATCGTATCGAGTTAAAGGGTATTGATTTTAAAGAAGATGGAAACATT
CTTGGACACAAACTCGAGTACAACTTTAACTCACACAATGTATACATCACGGCAGACAAACAAAAGAATGGAATCAAAGCTAA
CTTCAAAATTCGCCACAACGTTGAAGATGGTTCCGTTCAACTAGCAGACCATTATCAACAAAATACTCCAATTGGCGATGGCC
CTGTCCTTTTACCAGACAACCATTACCTGTCGACACAATCTGTCCTTTCGAAAGATCCCAACGAAAAGCGTGACCACATGGTC
CTTCTTGAGTTTGTAACTGCTGCTGGGATTACACATGGCATGGATGAGCTCTACAAActcgagcaccaccaccaccaccACCA
CTAA

human Endothelin B receptor with sfGFP-His$_6$-tag (Hs ETB-sfGFP-His$_6$)
Vector: pET21a(+)
Restriction sites: non (restriction free cloning)

atggctagcatgactggtggacagcaaatgggtcgcggatccgaggagagaggcttcccgcctgacagggccactccgctttt
gcaaaccgcagagataatgacgccacccactaagaccttatggcccaagggttccaacgccagtctggcgcggtcgttggcac
ctgcggaggtgcctaaaggagacaggacggcaggatctccgccacgcaccatctcccctcccccgtgccaaggacccatcgag
atcaaggagactttcaaatacatcaacacggttgtgtcctgccttgtgttcgtgctggggatcatcgggaactccacacttct
gagaattatctacaagaacaagtgcatgcgaaacggtcccaatatcttgatcgccagcttggctctgggagacctgctgcaca
tcgtcattgacatccctatcaatgtctacaagctgctggcagaggactggccatttggagctgagatgtgtaagctggtgcct
ttcatacagaaagcctccgtgggaatcactgtgctgagtctatgtgctctgagtattgacagatatcgagctgttgcttcttg
gagtagaattaaaggaattggggttccaaaatggacagcagtagaaattgttttgatttgggtggtctctgtggttctggctg
tccctgaagccataggttttgatataattacgatggactacaaaggaagttatctgcgaatctgcttgcttcatcccgttcag
aagacagctttcatgcagttttacaagacagcaaaagattggtggctattcagtttctatttctgcttgccattggccatcac
tgcatttttttatacactaatgacctgtgaaatgttgagaaagaaaagtggcatgcagattgctttaaatgatcacctaaagc

agagacgggaagtggccaaaaccgtcttttgcctggtccttgtctttgccctctgctggcttccccttcacctcagcaggatt
ctgaagctcactctttataatcagaatgatcccaatagatgtgaacttttgagctttctgttggtattggactatattggtat
caacatggcttcactgaattcctgcattaacccaattgctctgtatttggtgagcaaaagattcaaaaactgctttaagtcat
gcttatgctgctggtgccagtcatttgaagaaaaacagtccttggaggaaaagcagtcgtgcttaaagttcaaagctaatgat
cacggatatgacaacttccgttccagtaataaatacagctcatctCTCGAGGGAACGGGCAGCAAAGGAGAAGAACTTTTCAC
TGGAGTTGTCCCAATTCTTGTTGAATTAGATGGTGATGTTAATGGGCACAAATTTTCTGTCCGTGGAGAGGGTGAAGGTGATG
CTACAAACGGAAAACTCACCCTTAAATTTATTTGCACTACTGGAAAACTACCTGTTCCGTGGCCAACACTTGTCACTACTCTG
ACCTATGGTGTTCAATGCTTTTCCCGTTATCCGGATCACATGAAACGGCATGACTTTTTCAAGAGTGCCATGCCCGAAGGTTA
TGTACAGGAACGCACTATATCTTTCAAAGATGACGGGACCTACAAGACGCGTGCTGAAGTCAAGTTTGAAGGTGATACCCTTG
TTAATCGTATCGAGTTAAAGGGTATTGATTTTAAAGAAGATGGAAACATTCTTGGACACAAACTCGAGTACAACTTTAACTCA
CACAATGTATACATCACGGCAGACAAACAAAAGAATGGAATCAAAGCTAACTTCAAAATTCGCCACAACGTTGAAGATGGTTC
CGTTCAACTAGCAGACCATTATCAACAAAATACTCCAATTGGCGATGGCCCTGTCCTTTTACCAGACAACCATTACCTGTCGA
CACAATCTGTCCTTTCGAAAGATCCCAACGAAAAGCGTGACCACATGGTCCTTCTTGAGTTTGTAACTGCTGCTGGGATTACA
CATGGCATGGATGAGCTCTACAAActcgagcaccaccaccaccaccACCACTAA

human thermostabilised truncated Endothelin B receptor with sfGFP-His_6-tag (Hs ts-ETB-DeltaC-sfGFP-His_6)

Vector: pET21a(+)

Restriction sites: 5‘ Nde1 + 3‘ Spe1

atgactggtggacagcaaatgggtcatatgaaaccatacgatggtccagaagaacgcggctttccgccggatcgcgcgacccc
tctgctgcagaccgccgaaattatgacccctccgaccaaaacgctgtggccgaaaggcagcaacgcgagcttagcgcgtagcc
tggcgccggcggaagtgccgaaaggcgatcgcaccgcgggcagcccgcctcgcaccatttcaccgcctccgtgccagggtccg
attgaaatcaaagaaaccttcaaatatattaacacggtggtgagctgcctggtgtttgtgctgggcattattggcaacagcac
cttactgtatattatctataaaaacaaatgcatgcgtaacggtccgaacattctgattgccagcctggcgttaggtgatctgc
tgcatattgtgattgcgattccgattaacgtgtataaactgctggcggaagactggccgtttggtgccgaaatgtgcaaactg
gtgccgttcattcagaaagcgagcgtgggcattaccgtgctgagcttatgcgcgctgagcattgatcgttatcgtgcggtggc
gagctggagccgtattaaaggcattggtgtgccgaaatggaccgcggtggaaattgtgctgatttgggttgtgagcgttgtgc
tggcggtgcctgaagccattggctttgatatcattaccatggattataaaggcagctatctgcgcatttgcctgctgcatcct
gtgcagaaaaccgcgtttatgcagttctatgccaccgcgaaagattggtggctgtttagcttctatttctgcttaccgctggc
gattacggcgttcttttataccctgatgacctgcgaaatgctgcgcaagaaaagcggcatgcagattgcgctgaacgatcatc
tgaaacagcgtcgcgaagtggcgaaaaccgtgttttgcctggtgctggtgtttgcgctgtgctggctgccgctgcatctggcg
cgcattctgaaactgaccctgtataaccagaacgatccgaaccgctgcgaactgctgagctttctgttagtgctggattatat
tggcattaacatggcgagcctgaacagctgcgccaacccgattgcgctgtatctggtgagcaaacgcttcaaaaacgcgttta
aaagcgcgctgggtatgagcaaaggagaagaacttttcactggagttgtcccaattcttgttgaattagatggtgatgttaat
gggcacaaattttctgtccgtggagagggtgaaggtgatgctacaaacggaaaactcacccttaaatttatttgcactactgg
aaaactacctgttccgtggccaacacttgtcactactctgacctatggtgttcaatgcttttcccgttatccggatcacatga
aacggcatgacttttcaagagtgccatgcccgaaggttatgtacaggaacgcactatatctttcaaagatgacgggacctac
aagacgcgtgctgaagtcaagtttgaaggtgataccttgttaatcgtatcgagttaaagggtattgattttaaagaagatgg
aaacattcttggacacaaactggagtacaactttaactcacacaatgtatacatcacggcagacaaacaaaagaatggaatca
aagctaacttcaaaattcgccacaacgttgaagatggttccgttcaactagcagaccattatcaacaaaatactccaattggc
gatggccctgtccttttaccagacaaccattacctgtcgacacaatctgtcctttcgaaagatcccaacgaaaagcgtgacca
catggtccttcttgagtttgtaactgctgctgggattacacatggcatggatgagctctacaaactcgagcatcaccatcacc
atcaccatcaccatcactag